

Thesis
SATH

BACULOVIRUS DIVERSITY AND ITS EFFECT ON VIRULENCE

ELIZABETH M. REDMAN

A thesis submitted in partial fulfillment of the requirements of the
University of Stirling for the degree of Doctor of Philosophy

The work was carried out in collaboration with NERC Centre for Ecology
and Hydrology, Oxford

October 2005

05/10/05

ProQuest Number: 13917102

All rights reserved

INFORMATION TO ALL USERS

The quality of this reproduction is dependent upon the quality of the copy submitted.

In the unlikely event that the author did not send a complete manuscript and there are missing pages, these will be noted. Also, if material had to be removed, a note will indicate the deletion.



ProQuest 13917102

Published by ProQuest LLC (2019). Copyright of the Dissertation is held by the Author.

All rights reserved.

This work is protected against unauthorized copying under Title 17, United States Code
Microform Edition © ProQuest LLC.

ProQuest LLC.
789 East Eisenhower Parkway
P.O. Box 1346
Ann Arbor, MI 48106 – 1346

Abstract

The baculovirus, *SpexNPV* is the biggest mortality agent of natural populations of the African armyworm, *Spodoptera exempta* and in terms of control has displayed considerable potential as a bioinsecticide in aerial spray trials undertaken by Natural Resources International (NRI). This project was charged with assessing the diversity of natural populations of *SpexNPV*, a subject of direct relevance for the development of *SpexNPV* as a bioinsecticide and about which little was known.

The genetic composition of a natural *SpexNPV* population was characterized using *in vivo* cloning techniques and RFLP analysis. Seventeen individual genotypes were isolated from the wild-type population and phylogenetic analysis was carried out to attempt to assess their potential relatedness, but no single conclusion on their shared histories could be reached. The fitness traits (pathogenicity, speed of kill and viral yield of OBs) of eight genotypes and the wild-type virus were assessed in laboratory bioassays. A nine-fold difference in pathogenicity (estimated in terms of LD₅₀) was witnessed between the different genotypes. Genotypes and wild-type virus also varied in their speed of kill and yield and although there was evidence of a trade-off between speed of kill and yield trade-off, for a number of the genotypes, this study failed to demonstrate any statistical evidence for a general trade-off between these fitness traits.

SpexNPV epizootics, from out-breaking populations of armyworm in Northern Tanzania, were sampled in 2002 and 2004. RFLP analysis was conducted on individual virus-infected larvae and revealed a high level of heterogeneity. In addition, forty percentage of all isolates analysed were identified as mixed-genotype infections by the presence of sub-molar bands in RE profiles. This genetic diversity appeared to lack any obvious population structure.

Controlled mixed-genotype inoculations were carried out to assess any change in phenotype relative to single-genotype infections. Genotypes, which were found to be equally pathogenic in single-genotype infections, were combined in equal ratio. Thirteen different dual inoculations were carried out across a range of doses. Mixed-genotype infections were found to be more pathogenic, and in general, possess longer speeds of kill relative to single genotype infections. The effect on yield varied considerably between mixtures. The inclusion of more than two genotypes within the mixtures (2-, 4-, 8-, and 16-genotype inoculations) revealed a correlation between level of diversity and pathogenicity and, to a certain extent, between level of diversity and speed of kill. This appears to suggest that mixed-infections possess higher levels of fitness than single genotype infections and that genetic diversity of *SpexNPV* should be maintained when used as a bioinsecticide.

List of presentations

Redman, E.M., Villaplana, L., Wilson, K., Cory, J.S. (2002) *Spodoptera exempta* nucleopolyhedrovirus as a natural control agent: Biology and Ecology. 1st Annual CEH conference, Nottingham.

Redman, E.M., Wilson, K.W., Cory, J.S. (2003) Persistence of African armyworm, *Spodoptera exempta* nucleopolyhedrovirus. Postgraduate Symposium, CEH Oxford.

Redman, E.M., Wilson, K.W., Cory, J.S. (2003) Vertical transmission of nucleopolyhedrovirus in *Spodoptera exempta*.. Internal seminar, CEH Oxford.

Redman, E.M., Wilson, K.W., Cory, J.S. (2003) Genotypic and phenotypic variation of *Spodoptera exempta* nucleopolyhedrovirus. XXXVI Annual Meeting of the Society for Invertebrate Pathology (SIP), Vermont, US.

Redman, E.M., Wilson, K.W., Cory, J.S. (2003) Effect of variation on ecology of the African armyworm, *Spodoptera exempta* nucleopolyhedrovirus. Internal seminar, University of Stirling.

Redman, E.M., Wilson, K.W., Cory, J.S. (2004) Diversity of the African armyworm nucleopolyhedrovirus (*SpexNPV*). Annual Symposium of the British Ecological Society, University of Lancaster.

Acknowledgements

I would like to thank my supervisors Prof. Jenny Cory and Dr Ken Wilson for giving me the opportunity to carry out this research and for their help and guidance throughout the past four years.

I would also like to thank the other collaborators on the African Armyworm project including David Grzywacz and Mark Parnell (NRI in Chatham), Charles Dewhurst and Wilfred Mushobozi (Pest Control Services in Tanzania) for helping make my fieldwork such a pleasure.

I would also like to thank Dr Lluisa Villaplana for initiating me into the strange new-world of molecular biology, Tim Carty for his unsurpassed skill at rearing insects and Dr John Burden whose unwavering kindness, considerable knowledge of all things baculovirus and dogged faith sustained me when things got tough.

I would also like to acknowledge Professor Bob Possee whose good nature, tolerance and provision of a part-time job allowed me the means to continue through a fourth year.

Finally I would like to acknowledge the unconditional love and support of my parents and big brother to whom I dedicate this thesis - more than just a pretty front cover!

Table of Contents

	Page no.
Abstract	i
List of presentations	ii
Acknowledgements	iii
Table of contents	iv
List of figures	viii
List of tables	xviii
Chapter 1 Introduction and Literature Review	1
1.1 Evolution of Virulence	1
1.2 Mixed Parasite Infections	6
1.3 The Pathogen: Baculovirus	7
1.3.1 Definition and phylogeny of Baculoviridae	7
1.3.2 Baculovirus pathogenesis and life-cycle	9
1.4 Insect-Baculovirus Interactions	10
1.5 Baculovirus Variation	15
1.5.1 Genetic variation	15
1.5.2 Generation of variation	17
1.5.3 Biological variation	19
1.5.4 Maintenance of variation	20
1.6 The Host: African armyworm, <i>Spodoptera exempta</i>	22
1.6.1 Armyworm outbreaks	22
1.6.2 Distribution of outbreaks	25
1.6.3 Pest status	26
1.6.4 Natural enemies of <i>S. exempta</i>	26
1.7 Aims of research	28
Chapter 2 Materials and Methods	30
2.1 Insect Culture	30
2.1.1 Insect rearing	30
2.1.2 Semi-synthetic diet	31
2.2 Baculovirus Techniques	31
2.2.1 Source of wild-type virus	31

2.2.2	Purification of wild-type virus	32
2.2.3	Amplification of wild-type virus	32
2.2.4	Purification of virus from single larvae	33
2.2.5	Enumeration of occlusion bodies	34
2.3	Molecular Biological Techniques	34
2.3.1	DNA extraction from wild-type virus	34
2.3.2	DNA extraction from individual viral infected larvae	36
2.3.3	Restriction endonuclease digestion of viral DNA	36
2.3.4	Agarose gel electrophoresis	36
2.3.5	Field inverted gel electrophoresis (FIGE)	37
2.3.6	Polymerase chain reaction (PCR)	38
2.3.7	Sequencing	38
2.4	Bioassay Procedures	39
2.4.1	Diet-plug contamination method	39
2.4.2	Determining cause of death	40
2.4.3	Viral yield estimation	41
2.5	Data Analysis	41
2.5.1	Analysis of sequence data	41
2.5.2	Phylogenetic analysis	42
2.5.3	Statistical analysis	42
Chapter 3	Genetic characterisation of a wild-type <i>Spodoptera exempta</i> NPV population	44
3.1	Introduction	44
3.2	Methods	49
3.2.1	<i>In vivo</i> cloning	49
3.2.2	Gene selection for phylogenetic analysis	55
3.2.3	Primer design	57
3.2.4	Amplification and sequencing of genes from <i>Spex</i> NPV genotypes	62
3.2.5	Phylogenetic analysis	64
3.3	Results	64
3.3.1	Genetic characterisation of individual genotypes	64
3.3.2	Phylogenetic analysis	69
3.4	Discussion	77
3.4.1	Cloning	77
3.4.2	Sizing genome	82
3.4.3	Phylogeny	83

Chapter 4	Biological characterisation of <i>SpexNPV</i> genotypes isolated <i>in vivo</i>	87
4.1	Introduction	87
4.2	Materials and Methods	90
4.2.1	Bioassay design	90
4.2.2	Determination of viral infection	91
4.2.3	Data Analysis	91
4.3	Results	92
4.3.1	Purity and stability of genotypes	92
4.3.2	Pathogenicity	94
4.3.3	Speed of kill	100
4.3.4	Yield	106
4.3.5	Relationship between phenotypic traits	113
4.4	Discussion	118
Chapter 5	Diversity of <i>SpexNPV</i> in natural epizootics	123
5.1	Introduction	123
5.2	Materials and Methods	128
5.2.1	Field season 2002	128
5.2.2	Field season 2004	130
5.2.3	Sampling of <i>SpexNPV</i> epizootics	134
5.2.4	Host and viral prevalence	134
5.2.5	Genetic characterisation	135
5.2.6	Measurement of diversity	136
5.2.7	Sequencing polyhedrin gene	137
5.2.8	Biological characterisation	137
5.3	Results	138
5.3.1	Field season 2002	138
5.3.2	Field season 2004	141
5.3.3	Investigation of population structure	144
5.3.4	Genetic characterisation	147
5.3.5	Phylogenetic analysis	148
5.3.6	Pathogenicity of <i>SpexNPV</i> field isolates	151
5.3.7	Speed of kill of <i>SpexNPV</i> field isolates	157
5.3.8	Yield of <i>SpexNPV</i> field isolates	160
5.4	Discussion	165
Chapter 6	Dual infections of <i>SpexNPV</i> genotypes	171
6.1	Introduction	171

6.2	Methods	173
6.2.1	Bioassay experimental design	173
6.2.2	Determination of viral pathogenicity	174
6.2.3	Calculating predicted mortality in dual infections	174
6.2.4	Determination of proportions of different genotypes in progeny virus	177
6.3	Results	178
6.3.1	Pathogenicity	178
6.3.2	Speed of kill	185
6.3.3	Viral yield	191
6.3.4	Interaction between speed of kill and yield	193
6.3.5	Proportions of different genotypes in progeny virus	204
6.4	Discussion	208
Chapter 7	Effect of diversity of <i>Spex</i>NPV infections on virulence	213
7.1	Introduction	213
7.2	Methods	214
7.2.1	Production of mixed inoculum	214
7.2.2	Replication of level of diversity	215
7.2.3	Experimental design	215
7.2.4	Yield and RFLP analysis to determine the proportion of different genotypes in progeny virus	216
7.2.5	Data analysis	217
7.2.6	Calculating predicted mortality in dual infections	217
7.2.7	Attempts to predict mortality in 4-genotype inoculations	219
7.3	Results	221
7.3.1	Effect of diversity on pathogenicity	221
7.3.2	Predicting mortality in two and four genotype infections	226
7.3.3	Speed of kill	232
7.3.4	Yield	235
7.3.5	Proportion of different genotypes in progeny virus	241
7.4	Discussion	247
Chapter 8	General Discussion	249
	References	259

List of Figures

Chapter 1		Page no.
Figure 1.1	Late instar <i>Spodoptera exempta</i> larvae in its solitary (on left) and gregarious (on right) morphs reared on wheat seedlings in the laboratory. (Photo: courtesy of K. Wilson).	24
Figure 1.2	Typical densities of <i>Spodoptera exempta</i> larvae under outbreak conditions. Densities have been reported on occasion exceeding 1000 larvae/m ² (Cheke and Tucker, 1995). Photo: courtesy of K. Wilson	24
Chapter 3		
Figure 3.1	Restriction endonuclease profiles of wild-type <i>SpexNPV</i> digested with <i>EcoRI</i> (1-2), <i>BamHI</i> (3-4), <i>HindIII</i> (5-6), <i>SalI</i> (7-8), <i>PstI</i> (9-10), <i>KpnI</i> (11-12) and <i>XhoI</i> (13-14) before (odd lane nos.) and after (even lane nos.) <i>in vivo</i> passage. Molecular weight ruler, \square - <i>HindIII</i> DNA marker (Lane 15). 0.8% agarose gel run for 24 hours at 40V.	50
Figure 3.2	Mortality (proportion dying) of <i>SpexNPV</i> isolates at the second round of <i>in vivo</i> cloning in 3 rd instar <i>S. exempta</i> larvae at a dose of 1200 occlusion bodies.	53
Figure 3.3	PCR products run on 1.2% agarose gel following amplification using consensus primers of the <i>egt</i> gene and <i>SpexNPV</i> DNA (3), <i>SpltNPV</i> DNA (4), <i>SeNPV</i> DNA (5) and <i>AcMNPV</i> DNA (6). Negative control of reaction with DNA template replaced by distilled water (lanes 2). Lane 1, Hyperladder I (Bioline).	61
Figure 3.4	Analysis of PCR products on 1.2% agarose gel following amplification using <i>SpexNPV</i> DNA as a template and using specific <i>SpexNPV</i> primers of the chitinase gene (1-3), <i>lef-8</i> gene (4-6) and the polyhedrin gene (7-9). In negative controls of reactions (lanes 3, 6 and 9) <i>SpexNPV</i> DNA template was replaced by distilled water. Lane 10, Hyperladder I (Bioline). The amplification of the correct sized PCR products was confirmed for all PCR reactions prior to any sequencing being undertaken.	63
Figure 3.5	Restriction endonuclease profiles (<i>EcoRV</i>) of 17 <i>SpexNPV</i> genotypes isolated after four rounds of <i>in vivo</i> cloning from the wildtype virus. DNA fragments separated on 0.8% agarose gel run for 24 hours at 40V. Molecular markers: M ₁ , Hyperladder I (Bioline); M ₂ , 1kb ruler (BioRad).	65
Figure 3.6	Restriction endonuclease profiles of wildtype <i>SpexNPX</i> DNA digested with <i>BamHI</i> , <i>EcoRV</i> and <i>XhoI</i> showing alphabetical labeling of bands from largest to smallest. Molecular markers: M1, \square - <i>HindIII</i> DNA marker (Bioline); M2 and M3, 1kb ruler (BioRad). 0.8% agarose gels ran for 24 hours at 40V.	66

Figure 3.7	Phylogenetic analysis of 17 <i>Spex</i> NPV genotypes and wild-type <i>Spex</i> NPV using the polyhedrin gene and a neighbour-joining algorithm. Trees rooted to <i>Ac</i> MNPV and <i>Se</i> MNPV. Numbers given at each node are percentage bootstrap values (for 1000 repetitions). Genotypes appear not to cluster together to form any groups at a bootstrap value of 100 using <i>polyhedrin</i> .	70
Figure 3.8	Phylogenetic analysis of 17 <i>Spex</i> NPV genotypes and wild-type <i>Spex</i> NPV using the chitinase gene and a neighbour-joining algorithm. Trees rooted to <i>Sex</i> MNPV and <i>Ac</i> MNPV. Numbers given at each node are percentage bootstrap values (for 1000 repetitions). Genotypes appear to cluster together at a bootstrap value of 100 to form two main groups.	71
Figure 3.9	Phylogenetic analysis of 17 <i>Spex</i> NPV genotypes and wild-type <i>Spex</i> NPV using the <i>lef-8</i> gene and a neighbour-joining algorithm. Trees rooted to <i>Ac</i> MNPV and <i>Sex</i> MNPV. Numbers given at each node are percentage bootstrap values (for 1000 repetitions). Genotypes appear to cluster together to form two main groups at a bootstrap value of 100.	72
Figure 3.10	Phylogenetic analysis of 17 <i>Spex</i> NPV genotypes and wild-type <i>Spex</i> NPV using the <i>egt</i> gene and a neighbour-joining algorithm. Trees rooted to <i>Sex</i> MNPV and <i>Ac</i> MNPV. Numbers given at each node are percentage bootstrap values (for 1000 repetitions). Genotypes appear to cluster together at a bootstrap value of 100 to form two main groups.	73
Chapter 4		
Figure 4.1	<i>Eco</i> RV restriction endonuclease profiles of <i>Spex</i> NPV genotypes A-H and wild-type virus after <i>in vivo</i> passage in bioassay. Lanes: 1-3, (C); 4-7, (B); 8-11, (A); 12-15, (wild-type virus); 16-19, (H); 20-23, (G); 24-27, (F); 28-31, (E); 32-35, (D). Molecular marker (M), hyperladder I (Bioline). 0.8% agarose gels run at 40V for 24 hour.	93
Figure 4.2	LD ₅₀ estimates ($\pm 95\%$ confidence intervals) for genotypic clones A-H of <i>Spex</i> NPV and wild-type parent virus in 3 rd instar <i>Spodoptera exempta</i> larvae.	95
Figure 4.3	Dose-mortality curves of genotypic clones (A-H) and WT <i>Spex</i> NPV in 3 rd instar <i>Spodoptera exempta</i> larvae. Fitted lines represent minimal adequate model fitted by ANCOVA: genotype A (intercept = -5.886), genotype B (intercept = -4.884), genotype C (intercept = -5.85), genotype D (intercept = 5.557), genotype E (intercept = -5.557), genotype F (intercept = -5.762) genotype G (intercept = -4.995), genotype H (intercept = -4.636) and WT (intercept = -4.356). Gradient of all lines = 0.774. Symbols represent mean observed values.	96

- Figure 4.4** Dose-mortality curves of grouped genotypic clones (A-H) and wild type *SpexMNPV* in 3rd instar *Spodoptera exempta* larvae. Fitted lines: WT virus, $\text{logit}(\text{mortality}) = -5.14 + 0.69(\ln(\text{dose}))$; A,C,D,E and F, $\text{logit}(\text{mortality}) = -5.72 + 0.91(\ln(\text{dose}))$; B,G and H, $\text{logit}(\text{mortality}) = -5.21 + 0.90(\ln(\text{dose}))$. Symbols represent group mean of observed values. 98
- Figure 4.5** LD₅₀ estimates ($\pm 95\%$ confidence intervals) for genotypic clones A-H and wild type virus grouped on the basis of analysis of covariance with dose. 99
- Figure 4.6** Speed of kill-dose relationship of *SpexNPV* genotypes, A-H and wild type virus in 3rd instar *S. exempta* larvae. Symbols represent the mean speed of kill for each genotype at each dose. Standard error bars are not shown to improve clarity. Fitted lines: wild type virus, $\text{speed of kill}^2 = 12190 + (1362.8(\ln(\text{dose})) - (161(\ln(\text{dose})^2))$; A, $\text{speed of kill}^2 = 3444 + (2208(\ln(\text{dose})) - (161(\ln(\text{dose})^2))$; B, $\text{speed of kill}^2 = 4856 + (2095(\ln(\text{dose})) - (161(\ln(\text{dose})^2))$; C, $\text{speed of kill}^2 = 5981 + (1911(\ln(\text{dose})) - (161(\ln(\text{dose})^2))$; D, $\text{speed of kill}^2 = 7292 + (2005(\ln(\text{dose})) - (161(\ln(\text{dose})^2))$; E, $\text{speed of kill}^2 = 4326 + (2385(\ln(\text{dose})) - (161(\ln(\text{dose})^2))$; F, $\text{speed of kill}^2 = 1492 + (2657(\ln(\text{dose})) - (161(\ln(\text{dose})^2))$; G, $\text{speed of kill}^2 = 6202 + (2128(\ln(\text{dose})) - (161(\ln(\text{dose})^2))$; H, $\text{speed of kill}^2 = 6058 + (2205(\ln(\text{dose})) - (161(\ln(\text{dose})^2))$. 101
- Figure 4.7** Back transformed mean speed of kill (hrs) of *SpexNPV* virus genotypes A-H and wild type virus at doses of 50 000 OBs and 500 OBs (± 1 SE) in third instar *S. exempta*. 103
- Figure 4.8** Speed of kill-dose relationship of *SpexNPV* genotypes, A-H and wild type virus infecting 3rd instar *S. exempta* larvae. Symbols represent the mean speed of kill for each genotype at each dose. Standard error bars are not shown to improve clarity. Fitted lines: wild type virus, $\text{speed of kill}^2 = 12252 + (1348.2(\ln(\text{dose})) - (160.2(\ln(\text{dose})^2))$; ABC, $\text{speed of kill}^2 = 4820 + (2059(\ln(\text{dose})) - (160.2(\ln(\text{dose})^2))$; DEFGH, $\text{speed of kill}^2 = 5463 + (2228.3(\ln(\text{dose})) - (160.2(\ln(\text{dose})^2))$. 104
- Figure 4.9** Back transformed mean speed of kill (hrs) of virus genotypes and wild type virus grouped according to analysis of covariance, at a high (50 000 OBs) and low dose (500 OBs) (± 1 SE). 105
- Figure 4.10** Back transformed mean yield of OBs (± 1 SE) per larva at doses of 1000 and 10000 OBs and at a fast (82 hrs) and a slower speed of kill (156 hrs) for genotypes A-H and the wild type *SpexNPV*. 108
- Figure 4.11** Speed of kill-yield relationship. Symbols represent mean yields of 3rd instar *S. exempta* larvae infected with individual *SpexNPV* genotypes 109

(A-H) and the wild type virus at a dose of 10000 OBs. Fitted lines represent minimal adequate model fitted by ANCOVA.

Figure 4.12	Influence of virus dose and speed of kill on yield for (a) genotype B and (b) genotype F.	111
Figure 4.13	Fitted lines for dose-yield relationship of 3 rd instar <i>S. exempta</i> larvae infected with individual <i>SpexNPV</i> genotypes (A-H) and the wild-type virus at a single speed of kill, (a) 82 hours and (b) 156 hours.	112
Figure 4.14	Estimates of pathogenicity, measured in terms of LD ₅₀ ($\pm 95\%$ confidence intervals) and mean speed of kill ($\pm 1SE$) produced from analysis of covariance with ln(dose) at a dose of 5000 OBs.	114
Figure 4.15	Estimates of pathogenicity, measured in terms of LD ₅₀ and mean yield of OBs ($\pm 1SE$) produced from analysis of covariance with ln(dose) at a dose of (a) 5000 OBs and (b) 500 OBs.	116
Figure 4.16	Estimates of mean speed of kill ($\pm 1SE$) and yield of OBs ($\pm 1SE$) produced from analysis of covariance with ln(dose) at a dose of 5000 OBs.	117
 Chapter 5		
Figure 5.1	Relief maps of Arusha, Northern Tanzania highlighting locations PCS and other fieldsites: Meringa Coffee Estate and Lucky Lucky Farm Estate (epizootic sampled 25 th -28 th Febuary 2002) and Tengeru (epizootic sampled 21 st -22 nd Febuary 2004).	127
Figure 5.2	Diversity of <i>SpexNPV</i> isolates (individual cadavers) collected from two geographically distinct field sites within the same armyworm outbreak Arusha, Northern Tanzania, 2002 estimated using (a) the proportion of mixed infections ($\pm 1SE$), (b) the number of variants identified and (c) Adjusted Simpson's Diversity Index ($\pm 1SE$).	140
Figure 5.3	Relationship between <i>S. exempta</i> density and viral prevalence. Fitted line: $\sqrt{\text{viral prevalence}} = 2.199 + (0.0101 \times \text{host density})$. Symbols represent observed values.	142
Figure 5.4	The effect of <i>S. exempta</i> host density on the proportion of mixed <i>SpexNPV</i> infections Fitted line: $\% \text{ mixed infections} = -1.137 + (0.00226 * \text{host density})$. Symbols represent observed values.	143
Figure 5.5	Mean adjusted Simpsons' Diversity Index ($\pm 1SE$) at the 25m ² scale for each of the four 2 ha field sites at Tengeru, 2004.	145
Figure 5.6	Comparison of diversity of <i>SpexNPV</i> isolates (individual cadavers) from 8ha field site at Tengeru (2004) estimated using the Adjusted Simpson's Diversity Index ($\pm 1SE$) from different spatial scales.	146

- Figure 5.7** Eighteen *Spex*NPV field isolates (named FS1-FS18) characterised using *EcoRV* and chosen for further sequencing analysis and biological characterisation. DNA fragments separated by electrophoresis on 0.8% agarose gel at 40V for 24 hours. Molecular markers: M₁, 1kb ruler (Biorad); M₂, λ -*EcoRI* DNA marker (Bioline) 147
- Figure 5.8** Phylogenetic analysis of the *polh* gene for *Spex*NPV wild-type, 18 isolates of *Spex*NPV collected from Tengeru, Northern Tanzania in 2004, and other related species of nucleopolyhedroviruses using a neighbour-joining algorithm. Differential colouring of field isolates represent the apparent clustering into three main groups. The numbers given at each node are percentage bootstrap values (for 1000 repetitions). 149
- Figure 5.9** Phylogenetic analysis of 18 *Spex*NPV field isolates, collected from Tengeru, Northern Tanzania (2004), 17 *EcoRV* *in vivo* cloned genotypes from *Spex*NPV wild-type, wild-type *Spex*NPV and other related species of nucleopolyhedroviruses using the polyhedrin gene and a neighbour-joining algorithm. Numbers given at each node are percentage bootstrap values (for 1000 repetitions). 150
- Figure 5.10** LD₅₀ estimates ($\pm 95\%$ confidence intervals) for 18 field samples of *Spex*NPV and wild-type virus i.e. viral dose required to kill 50% of 3rd instar *Spodoptera exempta* larvae. Stripped bars represent estimates produced through extrapolation of model beyond dose range of bioassay (FS17, LD₅₀ = 33,324,386 OBs and FS18, LD₅₀ = 25,892 OBs). 152
- Figure 5.11** Dose-mortality curves of *Spex*NPV field isolates and wild-type virus. Fitted lines represent minimal adequate models fitted by ANCOVA. Observed values omitted to improve clarity. 153
- Figure 5.12** Dose-mortality curves of *Spex*NPV field isolates and wild-type virus, grouped according to dose-response relationship. Fitted lines: gp1 (field samples: 1, 2, 4, 6, 8 and wild-type virus), logit (mortality) = $-2.977 + (0.607 \times \ln(\text{dose}))$; gp2 (field samples: 3 and 7), logit (mortality) = $-2.975 + (0.768 \times \ln(\text{dose}))$; gp3 (field samples: 5, 9, 11, 12, 13, 15 and 16), logit (mortality) = $-6.539 + (0.885 \times \ln(\text{dose}))$; gp4 (field samples: 10, 14 and 18), logit (mortality) = $-3.937 + (0.453 \times \ln(\text{dose}))$; gp5 (field sample 17), logit (mortality) = $-11.086 + (1.018 \times \ln(\text{dose}))$. Symbols are observed values. 155
- Figure 5.13** LD₅₀ estimates ($\pm 95\%$ confidence intervals) for field samples and wild-type *Spex*NPV of 3rd instar *Spodoptera exempta* larvae grouped according to dose-response relationship. Stripped bar represent estimates produced through extrapolation of model beyond dose range of bioassay (gp5 (FS17): LD₅₀ = 38744524 OBs). 156

- Figure 5.14** Estimated speed of kill (± 1 SE) of *Spex*NPV field isolates at doses of 10000 OBs and 100 OBs. Sample sizes (10000 OBs, 100 OBs) = FS1, (21, 9); FS2, (19, 11); FS3, (15, 7); FS4, (20, 5); FS5, (23, 13); FS6, (21, 16), FS7, (22, 10); FS8, (23, 5); FS9, (22, 7); FS10, (9,7); FS11, (19, 8); FS12, (19, 7); FS13, (21, 6); FS14, (11, 7); FS15, (15, 8); FS16, (16, 6); FS17, (4, 7); FS18, (10, 10); WT, (20, 18). 158
- Figure 5.15** Estimated speed of kill (± 1 SE) of *Spex*NPV field isolates at a dose of 10000 OBs and 100 OBs grouped according to dose-speed of kill relationship. 159
- Figure 5.16** Speed of kill-yield relationship. Symbols represent yield of 3rd instar *S. exempta* larvae infected with individual *Spex*NPV field isolates (FS1-12) and wild-type virus at a dose of 10000 OBs. Fitted lines represent minimal adequate model fitted by ANCOVA. 161
- Figure 5.17** Estimated mean yield of OBs per *S. exempta* larva (± 1 SE) at doses of 100 and 10000 OBs for *Spex*NPV field samples 1-12 and the wild type virus. Sample sizes = 30 larvae for each isolate (15 larvae at each dose). 163
- Figure 5.18** Speed of kill-yield relationship. Symbols represent yield of 3rd instar *S. exempta* larvae infected with individual field isolates and wild-type virus at a dose of 10000 OBs grouped according statistical similarity. Fitted lines: Gp1 (FS2 and 3) yield = $1.19e+^9 - (5.3e+^{12} * (1/(\text{speed of kill}^2))) - (4.4e+^7 * \text{Indose}) + (2.74e+^{11} * (1/(\text{speed of kill}^2)*\text{Indose}))$; gp2 (FS1, 5 and 6), yield = $8.48e+^8 - (3.6e+^{12} * (1/(\text{speed of kill}^2))) - (4.4e+^7 * \text{Indose}) + (2.74e+^{11} * (1/(\text{speed of kill}^2)*\text{Indose}))$; gp3 (FS4, 10 and 12), yield = $7.51e+^8 - (3.7e+^{12} * (1/(\text{speed of kill}^2))) - (4.4e+^7 * \text{Indose}) + (2.74e+^{11} * (1/(\text{speed of kill}^2)*\text{Indose}))$; gp 4 (FS7, 8, 9 and 11), yield = $5.64e+^8 - (2.7e+^{12} * (1/(\text{speed of kill}^2))) - (4.4e+^7 * \text{Indose}) + (2.74e+^{11} * (1/(\text{speed of kill}^2)*\text{Indose}))$; gp5 (WT virus), yield = $1.65e+^9 - (1.1e+^{13} * (1/(\text{speed of kill}^2))) - (4.4e+^7 * \text{Indose}) + (2.74e+^{11} * (1/(\text{speed of kill}^2)*\text{Indose}))$. 164
- Chapter 6**
- Figure 6.1** Schematic representation for predicting the proportionate mortality of a dual infection (XY) at a dose of 10000 OBs using the fitted values of single genotype infections (X and Y) at 5000 OBs. 176
- Figure 6.2** Dose-mortality curves of *Spex*NPV genotypes A and F in single (blue) and mixed (red) infections. Fitted lines: A/F mixed infection, $\text{logit}(\text{mortality}) = -8.187 + 1.032(\ln(\text{dose}))$; A and F single infections grouped according to level of virulence $\text{logit}(\text{mortality}) = -7.22 + 1.032(\ln(\text{dose}))$. Symbols represent observed values. Similar results were observed for DF, CF, EF, BG and BH dual infections (not shown). 181

Figure 6.3	Dose-mortality curves of <i>Spex</i> NPV single and mixed infections. (a) Genotypes A and C, fitted lines: AC mixed infection, $\text{logit}(\text{mortality}) = -6.867 + 0.8426(\ln(\text{dose}))$; A and C single infections (grouped), $\text{logit}(\text{mortality}) = -13.499 + 1.664(\ln(\text{dose}))$. (b) Genotypes H and G, fitted lines: HG mixed infection, $\text{logit}(\text{mortality}) = -13.51 + 1.74(\ln(\text{dose}))$; H and G single infections (grouped), $\text{logit}(\text{mortality}) = -6.55 + 0.968(\ln(\text{dose}))$. Symbols represent observed values.	182
Figure 6.4	Difference between observed and predicted mortality for dual infections of <i>Spex</i> NPV genotypes using fitted mortality values for single genotype infections obtained from this experiment.	184
Figure 6.5	Speed of kill-viral dose relationship for single and dual infections of <i>Spex</i> NPV genotypes A and C. Fitted lines: AC mix infection, $1/(\text{speed of kill})^2 = 3.686 \cdot 10^{-5} + (5.628 \cdot 10^{-6} * \ln(\text{dose}))$ and single A and C infections grouped according to speed of kill, $1/(\text{speed of kill})^2 = 7.247 \cdot 10^{-5} + (5.628 \cdot 10^{-6} * \ln(\text{dose}))$. Symbols represent observed values.	187
Figure 6.6	Increase in time to death (hrs) of dual infections of <i>Spex</i> NPV genotypes relative to corresponding single infections at a dose of 10000 OBs.	189
Figure 6.7	Back-transformed speed of kill (hrs) (\pm 1SE) of <i>Spex</i> NPV genotypes BH and HG dual infections and their corresponding single infections at a dose of 10000 OBs.	190
Figure 6.8	Estimated mean yield (\pm 1SE) of <i>Spex</i> NPV genotypes D and F in single and dual infection at a range of infectivity levels.	194
Figure 6.9	Estimated mean yield (\pm 1SE) of <i>Spex</i> NPV genotypes A and F in single and dual infection at a range of infectivity levels and a dose of 10000 OBs.	195
Figure 6.10	Estimated mean yield (\pm 1SE) from single and dual infections with <i>Spex</i> NPV genotypes A and E at LD ₅₀ .	196
Figure 6.11	Speed of kill-yield relationship for <i>Spex</i> NPV genotypes A and E in single and dual infections at a dose of 10000 OBs. Symbols represent observed data and fitted lines: A, $\ln(\text{yield}) = 18.77 + (0.00758 * \text{speed of kill})$; E, $\ln(\text{yield}) = 18.43 + (0.00758 * \text{speed of kill})$; AE, $\ln(\text{yield}) = 18.61 + (0.00758 * \text{speed of kill})$.	197
Figure 6.12	Estimated mean yield (\pm 1SE) of <i>Spex</i> NPV genotypes C and E in single and dual infection at a range of infectivity levels.	199
Figure 6.13	Estimated mean yield (\pm 1SE) of <i>Spex</i> NPV genotypes A and C in single and dual infection at a range of infectivity levels.	200

Figure 6.14	Estimated mean yield (\pm 1SE) of <i>SpexNPV</i> genotypes B and G in single and dual infection at a range of infectivity levels and a dose of 10000 OBs.	202
Figure 6.15	<i>EcoRV</i> profiles of DNA from virus deaths from dual inoculation with <i>SpexNPV</i> genotypes A and C at dose 10000 OBs in 3 rd instar <i>S. exempta</i> larvae. Lanes 1, 3 and 4 show genotype A dominating the infection, lanes 2 and 5 shows genotype C dominating the infection and lane 6 shows a profile characteristic of a mixed infection indicated by the presence of novel bands (c, j and p) belonging to genotype C. Lane 7 molecular marker, 1Kb ruler (BioRad).	205
Figure 6.16	Proportion of genotypes and mixed infections resulting form dual inoculation of <i>SpexNPV</i> genotypes in a ratio of 1:1 at a dose of 10000 OBs. Labelling of genotypes in legend follows order of genotypes in dual infections on y-axis.	207
Chapter 7		
Figure 7.1	Schematic representation for predicting the proportionate mortality of a dual infection (XY) at a dose of 10000 OBs using the fitted values of single genotype infections (X and Y) at 5000 OBs.	218
Figure 7.2	The influence of <i>SpexNPV</i> genotype diversity on fatal infection in third instar <i>S. exempta</i> larvae at a dose of 5000 OBs. a) Backtransformed model mean proportionate mortality (\pm 1 SE) of 1, 2, 4, 8 and 16 genotypes compared with the mixed parent wild type virus.	223
Figure 7.3	Influence of infection diversity of <i>SpexNPV</i> in 3 rd instar larvae at a dose of 5000 OBs on proportional mortality. Fitted mortality curves: linear, $\text{logit}(\text{mortality}) = 1.064 + (0.0785 * \text{diversity})$. Triangular symbols represent mean observed values (\pm 1SE) and diamond symbol represents the estimated number of genotypes in the wildtype virus extrapolated from linear model using observed $\text{logit}(\text{mortality})$.	224
Figure 7.4	Comparison of two different statistical models which represent the influence of <i>SpexNPV</i> genotype diversity on fatal infection in third instar <i>S. exempta</i> larvae at a dose of 5000 OBs. Back transformed mean mortality (\pm 1 SE) estimated by assigning level of diversity as a factor or as a covariate.	225
Figure 7.5	Fitted dose-response curves of <i>SpexNPV</i> genotypes and wild-type virus in 3 rd instar <i>S. exempta</i> larvae.	227

Figure 7.6	Difference between observed and predicted mortality for dual genotype infections using fitted mortality values for single genotype infections obtained from baseline bioassays (chapter 4) and this experiment.	228
Figure 7.7	Difference between observed and predicted mortality for 4-genotype infections using fitted mortality values for single genotype infections obtained from baseline bioassays (chapter 4) and this experiment.	231
Figure 7.8	Back transformed mean speed of kill (\pm 1SE) for (a) single genotype infections, wild type virus and mixed infections at various levels of diversity and (b) virus treatment grouped according to speed of kill represented by differential colouring of bars.	233
Figure 7.9	Speed of kill of mixed infections in relation to its level of diversity. Symbols represent observed mean speed of kill (\pm 1SE) at each level of diversity tested. Fitted lines: $(1/\text{speed of kill}^2) = 9.264\text{e-}5 + (-3.910\text{e-}6 * \text{diversity}) + (2.112\text{e-}7 * \text{diversity}^2)$.	234
Figure 7.10	Yield-speed of kill relationship for mixed infections. Fitted lines: 1 genotype, $\sqrt{\text{yield}} = 17287 + (-69665104 * (1/\text{speed of kill}^2))$; 2 genotypes, $\sqrt{\text{yield}} = 17217.9 + (-69665104 * (1/\text{speed of kill}^2))$; 4 genotypes, $\sqrt{\text{yield}} = 17015.3 + (-69665104 * (1/\text{speed of kill}^2))$; 8 genotypes, $\sqrt{\text{yield}} = 14975 + (-69665104 * (1/\text{speed of kill}^2))$; 16 genotype, $\sqrt{\text{yield}} = 14911 + (-69665104 * (1/\text{speed of kill}^2))$; WT virus, $\sqrt{\text{yield}} = 14611 + (-69665104 * (1/\text{speed of kill}^2))$. Symbols represent observed values.	236
Figure 7.11	Yield-speed of kill relationship for mixed infections. Fitted lines: 1, 2, 4 genotypes, $\sqrt{\text{yield}} = 17099 + (-68589144 * (1/\text{speed of kill}^2))$; WT, 8, 16 genotypes, $\sqrt{\text{yield}} = 14745 + (-68589144 * (1/\text{speed of kill}^2))$. Symbols represent observed values.	237
Figure 7.12	Influence of virus level of diversity and speed of kill on yield for <i>Spex</i> NPV infection of 3 rd instar <i>S.exempta</i> larvae at a dose of 5000 OBs.	239
Figure 7.13	Comparison of two different statistical models which represent the influence of <i>Spex</i> NPV genotype diversity on yield (OBs per cadaver) in third instar <i>S. exempta</i> larvae at a dose of 5000 OBs. Back-transformed mean yield (\pm 1 SE) estimated by assigning level of diversity as a factor or as a covariate.	240
Figure 7.14	<i>EcoRV</i> profiles of DNA from virus deaths resulting from dual inoculation with <i>Spex</i> NPV genotypes A and C at dose of 5000 OBs in 3 rd instar <i>S. exempta</i> larva. Lanes 1, 3 and 4 show genotype A dominating the infection, lanes 2 and 5 shows genotype C dominating the infection and lane 6 shows a profile characteristic of a mixed infection indicated by the presence of novel bands (c, j and p) belonging to genotype C. Lane 7 molecular marker, 1Kb ruler (BioRad).	242

- Figure 7.15** Proportion of genotypes and mixed infections resulting from dual inoculation of *SpexNPV* genotypes in a ratio of 1:1 at a dose of 5000 OBs. Labelling of genotypes in legend follows order of genotypes in dual infections on y-axis. 243
- Figure 7.16** Proportion of mixed infections resulting from inoculation with four *SpexNPV* genotypes in equal ratios, at a dose of 5000 OBs per insect. 244
- Figure 7.17** Proportion of mixtures detected in virus-killed larvae using REN analysis after inoculation with mixed *SpexNPV* variant inoculations, modelled against level of diversity within the inoculum. Fitted line is the back transformation of the minimal adequate model fitted by ANCOVA, $\text{logit}(\text{proportion of mixed infections}) = -2.608 + (0.191 * \text{mix})$ when $\text{logit} = \ln(p/(1-p))$, p = proportion of mixed infections and mix = the number of genotypes in the inoculation. Symbols represent mean observed values (\pm 1SE). 246

List of Tables

Chapter 3	Page no.
Table 3.1	Restriction enzymes used to differentiate single <i>SpexNPV</i> genotypes after each round of <i>in vivo</i> cloning of wild-type <i>SpexNPV</i> . 54
Table 3.2	Number of single <i>SpexNPV</i> genotypes initially identified from wild-type <i>SpexNPV</i> together with the number of single genotypes which subsequently remained pure through additional rounds of <i>in vivo</i> cloning. 54
Table 3.3	Alignment of <i>egt</i> gene sequences. 58
Table 3.4	Specific and consensus primers designed and used for PCR and sequencing of targeted genes to allow phylogenetic analysis of <i>SpexNPV</i> genotypes. 60
Table 3.5	Mean size estimates of <i>SpexNPV</i> DNA fragments (kbp) produced after digestion with the restriction endonucleases, <i>EcoRV</i> , <i>BamHI</i> and <i>XhoI</i> . Means calculated from estimates gained from between 3 and 5 different gels. 67
Table 3.6	Mean genome size estimates (kbp) of <i>in vivo</i> cloned <i>SpexNPV</i> genotypes. 68
Table 3.7	Summary of maximum sequence divergence observed between different species of nucleopolyhedroviruses and between different genotypes of <i>SpexMNPV</i> following phylogenetic analysis with a range of genes (<i>polyhedrin</i> , <i>chitinase</i> , <i>lef-8</i> and <i>egt</i>). 74
Table 3.8	Summary of groupings at a bootstrap value of 100 (for 1000 repetitions) of <i>SpexNPV</i> genotypes and wildtype following single-gene phylogenetic analysis using partial sequences of the chitinase, <i>egt</i> , <i>lef-8</i> and <i>polyhedrin</i> gene and a neighbour-joining algorithm. Trees rooted to <i>AcMNPV</i> and <i>SeMNPV</i> . 76
Chapter 5	
Table 5.1	Sampling regime for armyworm cadavers infected by virus followed in 2002. 129
Table 5.2	Sampling regime for infected <i>S. exempta</i> larvae at the 2 hectare scale at Tengeru, 2004. 131
Table 5.3	Sampling regime for infected <i>S. exempta</i> larvae at the 25m ² scale at Tengeru, 2004. 132

Table 5.4	Sampling regime for infected armyworm larvae at the 0.5 x 0.5 m quadrat scale at Tengeru, 2004.	133
Table 5.5	<i>S. exempta</i> density and <i>SpexNPV</i> prevalence data from two field sites (sample size = 10 quadrats per site).	139
Chapter 6		
Table 6.1	Summary of analysis of observed pathogenicity of <i>SpexNPV</i> dual infections against corresponding single infections and predicted values. Each genotype is only paired with another genotype from within its pathogenicity group (see Chapter 4). For calculation of the predicted values see section 6.2.2.	180
Table 6.2	Speed of kill (hrs) for single and dual infections of <i>SpexNPV</i> genotypes, calculated using corresponding models at a viral dose of 10 000 OBs.	186
Table 6.3	Outcome of dual infection of <i>SpexNPV</i> genotypes on yield of OBs per <i>S.exempta</i> larva at a dose equivalent to an LD ₅₀ relative to single infection.	192
Table 6.4	Summary of the effects of dual infection of <i>SpexNPV</i> genotypes on phenotypic fitness traits.	203
Table 6.5	Summary of characteristic novel bands in restriction endonuclease profiles used to identify mixed infections resulting from dual inoculation of <i>SpexNPV</i> genotypes at 10 000 OBs. For nomenclature of bands see chapter 3.	206
Chapter 7		
Table 7.1	Number of replicates per block at each level of diversity of mixed variant <i>SpexNPV</i> inoculations used to infect 3 rd instar <i>S. exempta</i> larvae.	215
Table 7.2	Formulae used to calculate predicted mortality of 4-genotype inoculation (CDEF) at a dose of 5000 OBs, when genotypes are present in equal ratio. Proportionate mortality (X) is the sum of: mortality resulting from 4-genotype mixed infections, (P); mortality resulting from 3-genotype mixed infections, (Q); mortality resulting from dual infections, (S); and also mortality resulting from single genotype infections, (U).	220
Table 7.3	Estimated mortality of single genotype infections, at a dose of 1250 OBs, used to predict mortality of 4-genotype infection, CDEF when present in equal ratio.	229

Table 7.4	Predicted mortality of the 4-genotype infection (X), of CDEF, estimated using formula derived from the mass action hypothesis (Set-out in Table 7.2). Mortality estimates of single infections (dose = 1250 OBs) from this experiment and from chapter 4 experiments (Summarised for CDEF in Table 7.3) were used.	230
Table 7.5	Summary of characteristic novel bands in restriction endonuclease profiles used to identify mixed infections resulting from dual inoculation of <i>Spex</i> NPV genotypes at 10 000 OBs. For nomenclature of bands see chapter 3.	241

Chapter One

Introduction and Literature Review

Chapter 1: Introduction and literature review

1.1 Evolution of virulence

The desire of researchers to understand the why parasites cause harm to their hosts' remains unrelenting. For some parasites virulence has been interpreted simply as the coincidental cross-over of a parasite into an atypical environment or host and therefore is unrelated to fitness (Bull, 1994; Levin and Bull, 1994; Weiss, 2002). The vast majority of work though, has interpreted virulence as an evolutionary adaptation that results from the trade-off between parasite traits, in particular between parasite transmissibility and virulence. Although there lacks considerable multi-discipline consensus of opinion on the correct definition and usage of the term virulence, for the majority of researchers who view virulence from this evolutionary perspective, it can be defined as a reduction of fitness of the host as a result of the presence of the parasite (Ewald, 1994; Bull, 1994; Ebert and Herre, 1996; Ganusov, 2003).

For much of the last century conventional wisdom (May and Anderson, 1983) stated that a well adapted parasite evolves over time to reduce the negative impact of virulence on transmission to become more benign. Anecdotal observations that many harmful parasites typically result from more recent host-parasite associations and arguments based on group selection were used in support of this view (Palmieri, 1982; Levin and Pimentel, 1981). Herre (1993) conducted a ten year comparative study of the relationship between nematode parasites and the fig wasps of Panama and concluded that the easier it is for a species of nematode to find a new host the more virulent the

nematodes appeared to be (Herre, 1993). This appeared to offer important new ecological evidence to spear-head an opposing school of thought which placed individual selection at the heart of their arguments (Herre, 1993; Ewald, 1994). They argued that within a parasite population, natural selection should favour whichever level of virulence optimises reproductive rates (R_0 : number of secondary infections produced by an infected host), in light of the trade-off between transmission and virulence (Lenski and May, 1994; Anderson and May, 1982) and consequently should promote prudent host exploitation within a single genotype infection. This forms the basis for the “adaptive trade-off hypothesis” (Ewald, 1994). Ewald compared the natural history of human and many other diseases and argued that there was significant evidence to support the trade-off hypothesis citing the high virulence of HIV and the 1918 influenza pandemic as good examples where high host densities and consequently high rates of transmission had evolved alongside high levels of virulence (Ewald 1994). Correlative evidence in support of this hypothesis was obtained from a study investigating temporal changes in virulence and resistance in the interaction between rabbits and myxomavirus in Australia, for which parasite populations appeared to evolve towards an intermediate level of virulence (Fenner and Radcliffe, 1965). It was found that the infectious period of the virus was shortened for extremely virulent forms, because the rabbits died before they could pass on the virus, and also for relatively benign strains, because they could be successfully suppressed by the rabbit’s immune response. Therefore it was argued that the parasites had evolved towards an optimum level of virulence which maximized the period of infectiousness and thus transmission, consistent with the adaptive trade-off hypothesis (Anderson & May 1982; May and

Anderson, 1983). Since then direct evidence for a positive relationship between transmission rate and virulence among natural pathogen isolates has been found for trypanosomes in mice (Turner *et al.*, 1995), microsporidia in *Daphnia* (Ebert, 1994) and malaria in mice (Mackinnon and Read, 1999). Indirect evidence has been found from experimental evolution studies (Bull *et al.*, 1991; Ebert and Mangin, 1997; Turner *et al.*, 1998; Mackinnon and Read, 1999b; Messenger *et al.*, 1999). Other studies though have also yielded evidence which begins to question the generality of the adaptive trade-off hypothesis for all parasites (Lipsitch and Moxon, 1997; Weiss, 2002).

The use of epidemiological models to investigate the within-host dynamics of parasite infections has generated a large body of theoretical work which suggests that multiple infections can promote the evolution of increased parasite virulence (through intra-host competition) above that considered optimal for a “prudent” parasite, as predicted by the adaptive trade-off hypothesis, within a single parasite infection (Levin and Pimentel, 1981; Anita *et al.*, 1994; Bonhoeffer and Nowak, 1994; Nowak and May, 1994; May and Nowak, 1995; van Baalen and Sabelis, 1995; Frank, 1996). In the competitive situation of a mixed infection, parasites which slowly exploit host resources are expected to be out-competed by those exploiting hosts more rapidly. Thus, short-term selection driven by within host competition is predicted to lead to increased levels of virulence, with greatly reduced transmission. This phenomenon has been termed as short-sighted evolution by Levin and Bull (1994).

Theory also seems to predict that the nature of the intra-host competition is important in determining the evolutionary outcome of a mixed infection. Models designed to simulate “superinfection” (Nowak and May, 1994; Levin and Pimentel, 1981) within mixed infections tend to predict that despite the transmission of only the most virulent strains, virulence polymorphisms will still be generated and maintained. In contrast, models designed to simulate “coinfection” assume no direct competition between genotypes. Although the host exploitation strategy and transmission of each genotype is not affected by the presence of other genotypes, host death promotes an advantage for the parasite to reproduce earlier in the infection at the population level (May and Nowak, 1995). The simulation of coinfection appears to limit the maintenance of virulence polymorphisms so only strains of very similar phenotypes are expected to persist (Frank, 1996). Theoretical investigations of the effect of mixed infection upon infection characteristics appear to have out-paced empirical studies and direct testing of the key assumptions which appear to underpin these theoretical models. One of the key assumptions is that virulence is an unavoidable consequence of parasite exploitation and thus a faster replicating parasite is more virulent. Another is that selection, imposed by host death, produces an advantage in mixed infections to genotypes that have a faster host resource use. Recently though this balance is beginning to be re-addressed. Single and mixed infection studies of the rodent malarial parasite, *Plasmodium chabaudi*, used as a model system for the highly virulent human malaria, *P. falciparum*, have demonstrated that mixed infections possess increased levels of virulence (Taylor *et al.*, 1997 and 1998). In addition increased virulence and reproductive rate of mixed

schistosome infections of snails were also found to correlate positively with the increasing heterogeneity of the infection (Davies *et al.*, 1999 and 2002). Although these two studies appear to provide evidence in support of the theoretical predictions they fail to elucidate the exact mechanism for the observed elevation of virulence and the action of intra-host competition. Both authors do though postulate that the increased virulence probably has more to do with strain-specific immunity and the hosts reduced ability to clear genetically diverse infections rather than resource limitation (Taylor *et al.*, 1998; Davies *et al.*, 2002). In order to prove the existence of intraspecific competition, evidence, that per capita parasite fitness is reduced by the presence of another strain, is needed. Gower and Webster (2005) have demonstrated very recently this for genetic strains of *Schistosoma mansoni* and their intermediate snail host, *Biomphalaria glabrata* using strain-specific quantitative real-time PCR. Similar technology was used by De Roode (2005b) who demonstrated that parasite strains that inhabit very similar niches inside their host compete with each other. The relative importance of resource limitation and strain-specific immunity has yet to be elucidated. The inability to detect intra-host competition between co-infecting strains of the trypanosome *Crithidia bombi* in bumblebees has been ascribed to strains inhabiting completely different niches inside their host and consequently the complete absence of ecological niche overlap (Imhoof & Schmid-Hempel, 1998; Schmid-Hempel *et al.*, 1999). Other studies have struggled to predict the phenotypic traits of mixed infections from single-genotype infections (Nakamura *et al.*, 1992; Weeds *et al.*, 2000; Cox, 2001; Hodgson *et al.*, 2004). Residency has also been suggested to be an important determinant of within-host competition; prior colonization by *Silene latifolia* flowers by a strain of the anther-smut

pathogen prevented coloinisation of competitors (Hood, 2003). In addition the host genotype has also been shown to play an important role (Willie *et al.*, 2002; de Roode *et al.*, 2004). It is now being realized that the theoretical predictions of mixed infections depend entirely on the biological details of the host-parasite interaction (Chao *et al.*, 2000; Brown *et al.*, 2002).

1.2 Mixed parasite infections

Mixed infections, defined as the concomitant infection by two or more genetically distinct parasites of the same host (Cox, 2001) have long been acknowledged as the probable rule not the exception for the host-parasite relationship. It is only recently though, with the advancement of molecular techniques and the ability to accurately distinguish between individual pathogen genotypes, that evidence in support of the ubiquitous nature of mixed infections has grown. Evidence of mixed infections from a range of host-parasite systems include malaria parasites of humans and rodents (Day *et al.* 1992; Snounou *et al.*, 1992; Paul *et al.*, 1999), trypanosomes of tsetse fly (Woolhouse *et al.*, 1996), African horse sickness in zebra (Lord *et al.*, 1997), HIV (Holmes *et al.*, 1992) of humans, schistosomes of snails (Davies *et al.*, 1999, 2002) as well as baculoviruses (Cooper *et al.*, 2003a; Cory *et al.*, 2005). While some mixed infections can be the result of infection by more than one genotype, as have often been observed for malaria parasites (Day *et al.*, 1992) and some baculoviruses (Cooper *et al.*, 2003a; Cory *et al.*, 2005), within-host diversity of the human immunodeficiency virus (HIV) is believed to be generated mostly through mutations of a single infection where the

creation of antigenic diversity allows the parasite to escape the host's immune response over time.

1.3 The pathogen: Baculovirus

1.3.1 Definition and phylogeny of Baculoviridae

Baculoviruses are by far the most extensively studied group of insect viruses and their long association with Lepidopteran host species can be traced back 2000 years to early accounts of the disease “jaundice” of the silk-worm, *Bombyx mori* (Benz, 1986). The Baculoviridae is a large family of arthropod-specific viruses which have primarily been isolated from insects (Matthews, 1992; Volkman *et al.*, 1995). They have been recorded from more than 400 species, mainly lepidopteran and some hymenopteran and dipteran hosts (Granados and Federici, 1986). Host range can vary: some isolates can infect several species from within one Order (Bishop *et al.*, 1995), whereas the majority of isolates appear to infect only a small number of species, in some cases only one (Richards *et al.*, 1999; Cory *et al.*, 2000). The restricted host range of baculoviruses renders them attractive alternatives to current methods of chemical pest control as they have no detrimental effects on the environment and limited effects on non-target organisms (Payne, 1982). Compared to the number of insect viruses to have been identified, relatively few baculoviruses have been extensively studied and successfully exploited as control agents (Black *et al.*, 1997). Recent advances in genetic manipulation have led to the possibility of modifying them in order to improve their speed of kill and increase commercial viability (Cory *et al.*, 1994; Burden *et al.*, 2000; Hernandez-Crespo *et al.*, 2001).

Baculoviruses are currently divided into two genera according to structural criteria (Murphy *et al.*, 1995); the nucleopolyhedrovirus (NPV's) and granuloviruses (GVs'). The NPVs possess two morphological types and may package virus particles containing single nucleocapsids (SNPV) or multiple nucleocapsids (MNPV) within the occlusion body. GVs generally only contain a single virus particle. Phylogenetic analysis clusters lepidopteran baculoviruses into three groups, the GVs, Group 1 NPVs and Group II NPVs. Hymenopteran and dipteran NPVs fall outside these three groups (Herniou *et al.*, 2001, 2003; Zanotto *et al.*, 1993). The genome of nucleopolyhedroviruses is generally large, between 80-170KB in size (Francki *et al.*, 1991). It consists of a single molecule of super-coiled circular DNA which can have the potential to encode more than 150 proteins (Ahrens *et al.*, 1997). The nucleic acid is embedded within rod-shaped capsid proteins to produce nucleocapsids. Virions (or virus particles) are produced as a result of packaging these nucleocapsids within a lipoprotein membrane. Virions are themselves subsequently occluded within a crystalline matrix of the 29kDa protein, polyhedrin to form occlusion bodies (OBs). OBs can contain anything upto 100 virions (Harrap, 1972) and can range in size from between 1 to 5µm in diameter. This structure endows them with a degree of environmental persistence. They can survive for months, or even years, if protected from ultraviolet irradiation, but can be broken down in hours in strong sunlight (Ignoffo *et al.*, 1989).

1.3.2 Baculovirus pathogenesis and life-cycle

Baculoviruses are transmitted by two routes; the most common route is via horizontal transmission where susceptible larvae ingest sufficient virus occlusion bodies from the environment to cause death. Other routes of horizontal transmission include cannibalism (Chapman *et al.*, 1999), regurgitation and defaecation (Vasconcelos, 1996). Transmission can also occur via vertical transmission from adult to offspring, either through the contamination of the egg surface (transovum) (e.g. Hamm and Young, 1974) or within the egg (transovarial) (Cory *et al.*, 1997; Kukan, 1999; Burden *et al.*, 2002).

The life-cycle of baculoviruses is bi-phasic (Volkman and Keddie, 1990) and involves the production of two virus forms: the occluded virus (OBs) which facilitates host-host transmission, and the budded virus (BVs), which spreads the infection within the host (Miller, 1997). NPVs are primarily horizontally transmitted to susceptible larvae by the ingestion of OB-contaminated plant foliage. OBs rapidly dissolve in the alkaline (pH 10) digestive juices of the mid-gut where enzymes and proteases aid the release of virions. Differentiating and mature mid-gut columnar epithelial cells provide the primary sites for virion attachment and entry (Engelhard *et al.*, 1994; Flipsen *et al.*, 1995; Washburn *et al.*, 1995). Infection begins when the virions or occlusion derived virus (ODV) cross the peritrophic membrane (Volkman, 1997). The envelopes of the ODV fuse with the microvillar membrane of mid-gut columnar cells allowing the nucleocapsid to enter the host cell's cytoplasm (Engelhard *et al.*, 1994). DNA is transported to the nucleus where replication occurs amongst the virogenic stroma.

Within 8 hours of infection (8 h.p.i) of the midgut cells, virions bud primarily as single nucleocapsids, through the nuclei membrane acquiring a lipid envelope. The envelope, which contains a viral-encoded protein, GP64 or GP67, is temporarily lost on passage through the cytoplasm but regained for final budding out of the cell at approximately 12 h.p.i. and is reportedly important for the infection of neighbouring host cells and tissues (Monsma *et al.*, 1996). Once the BV is in the haemocoel in addition to fat body and nerve cells, cells of the tracheal system offer important primary targets for infection. The tracheal matrix is also believed to provide the virus with a rapid transport system to access other host tissues around the body (Engelhard *et al.*, 1994). In these secondary sites of infection, viral replication and particle *de novo* synthesis takes place generating large numbers of polyhedra. The death of the larvae involves tissue deterioration and cell lysis which results in liquefaction. Liquefaction only occurs after systemic infection of all major host tissue including the epidermis which characteristically turns creamy (Granados and Williams, 1986). Lysis of the infected larvae releases OBs into the environment (Volkman, 1997) in quantities of anything up to 10^9 OB per cadaver in a final instar noctuid (Evans, 1986; 1982; Kunimi *et al.*, 1996).

1.4 Insect-baculovirus interaction

The theoretical relationships of host-parasite dynamics of insects have received considerable attention. Anderson and May were the first to integrate the disciplines of parasitology and population biology to demonstrate, in a series of papers which suggested that parasites may operate in a density-dependent fashion to regulate a host population (Anderson and May, 1980, 1981). Using a theoretical framework they were

able to identify the conditions in which a pathogen could stabilise an insect population or generate cyclic or chaotic changes in insect abundance. They postulated that the combination of high parasite-induced mortality, large pathogen yields, long-lived resting spores and relatively low rates of host population growth as seen in some insect-baculovirus interactions, can produce population cycles. The four main parameters upon which the basic theoretical framework of insect-parasite interactions is based are persistence, transmission between hosts, yield of pathogen from the infected host and duration of infection. Transmission depends on the interactions between infected and susceptible host larvae and the rate at which contacts result in a new infection. Therefore the majority of models predict that transmission is a density-dependent process (Anderson and May, 1981), combining a per capita transmission coefficient, β , the number of susceptible hosts, S , and the number of infected hosts, I (βSI). Experimental studies have shown that baculovirus transmission is greatly influenced by the variation that exists within natural systems. Experimental studies to estimate the transmission coefficient for baculovirus infection in insect populations have identified a negative correlation with increasing inoculum densities (e.g. D'Amico *et al.*, 1996; Beisner and Myers, 1999; Knell *et al.*, 1998). Beisner and Myers (1999) have also found that transmission was more efficient at low host densities and that group size influenced infection levels by increasing the between group movement and thus virus spread. Incorporation of the concept of meta-populations into the model suggested that small-scale transmission was able to drive large-scale epizootics (Fenton *et al.*, 2002). Transmission could also vary if the susceptibility of larvae altered at high host density. Wilson and Reesson (1998) identified a 10-fold difference in susceptibility to NPV

between solitary *S. exempta* larvae and larvae reared in crowded conditions. The authors postulated that due to the increased risk of exposure to pathogens at higher densities, insects respond physiologically and invest more in resistance mechanisms (density-dependent prophylaxis). By comparing *Spex*NPV transmission on maize plants using solitary or gregarious larvae, virus transmission was found to be lower in larvae previously reared gregariously (Reeson *et al.*, 2000).

In addition to differences in transmission parameter *per se* the spatial distribution and persistence of the virus also influences insect-host dynamics. The distribution of virus on the plant or in the soil is likely to have a significant impact on transmission at the local scale (Cory and Myers, 2003). Experimental studies which varied the size and location of inoculum found that the number of viral patches (virus-infected cadavers) upon a plant is likely to have a greater influence on virus transmission rather than patch size itself (Hails *et al.*, 2002). Viral persistence is highly contingent on the location of the virus in the environment. Reservoirs of virus have been reported to be a major influence on NPV epizootics (Fuxa, 2004). In forest systems virus can remain viable for upto forty-one years in soil (Thompson *et al.*, 1981) and upto to five years in agricultural systems (Jacques, 1967). A positive correlation has been reported between NPV density in the soil and NPV infection of insect hosts feeding on pasture (Fuxa and Gaegham, 1983). Fuxa and Richter (2001) though, have shown that baculovirus movement from soil to plants is very low and depends on rainfall. Acquisition of virus from reservoirs can be influenced by host behaviour. Dwyer (1991) found that the virus transmission in sedentary third instar Douglas Fir Tussock moth, *Orgyia*

pseudotsugata, was highly affected by virus location upon the host plant, whereas in the later more mobile instars, location of virus was not such a factor and viral transmission was higher. Early instars of the vapourer moth, *Orgyia antiqua*, balloon off trees into the lower vegetation canopy where they pick-up virus from a lower reservoir of NPV. As they move back up the tree, the NPV is transmitted to other susceptible larvae (Richards *et al.*, 1999). An upward migration of infected larvae just prior to death has been observed in other systems including *Mamestra brassicae* larvae infected with NPV (Goulson, 1997). It is assumed that this facilitates the dissemination of the virus over the food-plant as the cadaver decomposes (Bonning and Hammock, 1996).

Heterogeneity in larval susceptibility is also an important factor when considering horizontal transmission. Stage dependent heterogeneity was investigated by Goulson *et al* (1995). They found that despite eating more food, and thereby increasing the likelihood of ingesting more virus, later instars were less susceptible to baculovirus infection. A similar phenomenon was observed in *S. frugiperda* where median lethal doses for fourth instar larvae were ten thousand times higher than the dose required for infection in first instar larvae. A number of models now consider heterogeneity of larval susceptibility and is believed to influence host outbreak densities (Dwyer and Elkington, 1993; Dwyer *et al.*, 1997; Dwyer *et al.*, 2000).

Although baculoviruses are thought to be primarily transmitted horizontally host to host via OBs' they can also be transmitted vertically from parent to offspring (Kukan, 1999

and Myers *et al.*, 2000). This can either be achieved through egg surface contamination (transovum) or containment within the egg (transovarial). Evidence is growing to suggest baculoviruses can exist as persistent infections. The use of reverse transcriptase polymerase chain reaction (RT-PCR) technology has enabled detection of replicating virus at extremely low titre. A persistent baculovirus infection has been detected in both laboratory cultures (Hughes *et al.*, 1993 and 1997) and field populations of *Mamestra brassicae* (Burden *et al.*, 2003 and 2005). Challenge to the persistently infected larvae with either the closely related *Panolis flammea* NPV (*Pnfl*NPV) or the distantly related *Autographa californica* NPV (*AcMNPV*), “triggered” fully blown overt, lethal infections (Hughes *et al.*, 1993) clearly demonstrating the ability of persistent infections to retain horizontal transmission capabilities. In addition, Cooper *et al.* (2003b) used an NPV from the western tent caterpillar, *Malacosoma californicum pluviale* to “trigger” a genetically distinct NPV from field stocks of the forest tent caterpillar, *M. disstria*. Other “stressors” may include overcrowding, malnutrition, high relative humidity and temperature shock but none have yet proved consistently reliable. Although the role of vertical transmission plays in the virus-host dynamics of the field is not clear. It has been suggested that asymptomatic persistent infections in natural environments represent an important mechanism for persistence in host populations when densities are low and when hosts are migratory in nature. In natural populations of the African armyworm which is both a seasonal and a migratory pest, high levels of persistent *Spex*NPV infections have been detected, using RT-PCR technology (L. Vilaplana *et al.*, unpublished data).

Since the seminal papers by Anderson and May, models have attempted to include additional biological realism by including factors which allow for vertical transmission (Vezina and Peterman, 1985), non-linear transmission (Liu *et al.*, 1986; Hochberg, 1991), host-stage structure (Briggs and Godfray, 1995), sub-lethal and persistent infections (Boots and Norman, 2000; Bonsall *et al.*, 2005) and discrete generations and seasonal host reproduction (Dwyer *et al.*, 2000; Briggs and Godfray, 1996). However, development of mathematical models has progressed at a far faster rate than it has been possible to gather field data and it must be remembered that a large number of the assumptions and models still remain untested.

1.5 Baculovirus variation

1.5.1 Genetic Variation

The evolution of baculoviruses, as with any organism requires the presence of genetic variation. Variation can be created and maintained in different ways but has to be present before natural selection or genetic drift can act (Futuyama, 1998). Restriction endonuclease (RE) profiles of baculovirus DNA are commonly used for genetic characterisation purposes and their comparison has shown baculoviruses to be highly variable. Virus isolates from the same host species are frequently found to vary from region to region. This geographical variation has been identified for NPVs (e.g. Gettig and McCarthy, 1982; Shapiro *et al.*, 1991; Takatsuka *et al.*, 2003), GVs (Crook *et al.*, 1985; Vickers *et al.*, 1991; Parnell *et al.*, 2002) and also for baculoviruses of sawflies (Brown, 1982). Baculoviruses have also been shown to vary genetically between isolates collected locally within the same field site or agricultural field (Shapiro *et al.*, 1991;

Cooper *et al.*, 2003a; Graham, *et al.*, 2004). Studies to critically examine variation in the field at the ecologically important scale of the individual infected larvae, (Cory and Myers, 2003) without amplification of the virus prior to analysis, are rare. The value of this approach is now beginning to be appreciated, and has been used to survey the variation of the NPV of the western tent caterpillar, *Malacosoma californicum pluviale*. This study was able to highlight a hierarchical spatial structure of epizootics within host populations at low densities, with isolates within a family group more likely to be the same. Isolates within a population were also found more likely to be the same than isolates collected from different populations (Cooper *et al.*, 2003a). Nucleopolyhedrovirus populations of the winter moth (*Opbu*NPV), from spatially separated heather moorland sites in Orkney, have also been studied using individual virus-infected cadavers. This study revealed populations were often dominated by individual genotypes (Graham *et al.*, 2004). Baculoviruses can also vary within the same host, and this variation can be identified by the detection of sub-molar bands within a RE profile, indicating the presence of more than one genotype within the isolate. The prevalence of mixed-genotype infections was found to be much higher in natural populations of the western tent caterpillar NPV in comparison to populations of *Opbu*NPV in which they represented less than 1% of the population. Mixed-genotype NPVs can be separated using *in vitro* (Crozier and Ribeiro, 1992; Stiles and Himmerich, 1998) or *in vivo* techniques (Smith and Crook, 1988; Munoz *et al.*, 1998; Cory *et al.*, 2005). The number of genotypes within an individual infected larvae have been shown to be surprisingly high with a total of 24 different genotypes were isolated *in vivo* from a single infected caterpillar of the pine beauty moth (Cory *et al.*, 2005).

Separation of the individual genotypes from wild-type *S. exigua* NPV isolates have also revealed the presence of deletion mutants which were not capable of initiating viral infection alone (Munoz *et al.*, 1998). These mutants were found to be relatively prevalent in wild-type isolates but reduced the pathogenicity of the virus population as a whole suggesting that they may well act as parasitic genotypes (Munoz and Caballero, 2000). Plaque purification of wild-type *S.littoralis* NPV has also yielded virus genotypes with a 4.5kb deletion which related to the loss of expression of a specific gene responsible for the viruses ability to infect *per os* (*pif*) (Kikhno *et al.*, 2002).

1.5.2 Generation of variation

There are several different ways new genotypes can be created these include point mutations, gene duplication and DNA insertions and deletions. *De novo* mutations can be incorporated due to DNA replication errors. In addition, environmental factors such as chemicals and UV can also damage DNA. Baculovirus DNA is particularly susceptible to UV light when the occlusion bodies are exposed in the environment. Ramoska *et al* (1975) found that the longer viruses were exposed to sunlight between infection cycles the less virulent they became. Cory *et al* (1997) also argues that the need for higher doses of ‘weathered’ virus implied that a large portion of the natural virus population is inactivated through the accumulation of mutations. Recombination between nucleic sequences of viruses allows the shuffling of genotypes through the re-assorting of genes and alleles. Such exchange of genetic material is known to occur among baculoviruses. Heterologous recombination can take place between different

strains of baculoviruses from the same population, infecting the same cell, and has been reported to occur *in vivo* at very high frequencies (Crozier *et al.*, 1988; Crozier and Ribeiro, 1992; Hajos *et al.*, 2000). It can also take place though between closely related viruses such as *AcMNPV* and *BmNPV* which normally infect different host species but can be forced to co-infect the same cell (Kondo and Maeda, 1991). New genotypes can also arise through the acquisition of host DNA. The Ted gypsy retrotransposon and the IFP2 transposon from *Trichoplusia ni* are able to spontaneously insert themselves in the genome of *AcMNPV* in cell culture (Fraser *et al.*, 1995; Friesen and Nissen, 1990). Similarly lepidopteran Tc1-like transposable elements have been found to jump into the genome of *CpGV* (Jehle *et al.*, 1998; Arends *et al.*, 2002). Recombination within the same genome is responsible for the presence of sequence duplications and represents another mechanism through which new genotypes can arise. Duplication gives rise to the presence of tandem repeats and gene families. Homologous regions (*hrs*) represent the main class of repeated sequences in baculovirus and are dispersed along the genome (Hayakawa *et al.*, 2000) and may represent recombinational ‘hotspots’ within the genome (Cory and Myers, 2003). In addition *hrs* also contains repeated motifs the number of which varies between strains of the same virus (Chen *et al.*, 2002). Baculoviruses contain two main gene families, *iap* and *bro*. The *iap* gene family is similar to the anti-apoptotic genes of eukaryotes for which some viruses contain upto four gene copies (Ahrens *et al.*, 1997). The *bro* gene family is the baculovirus repeated ORFs’ whose copy number varies considerably between viral genomes (Kuzio *et al.*, 1999) and between different virus strains (Lopez-Ferber *et al.*, 2001). Finally homologous recombination is a natural mechanism in baculovirus infected cells which

has been utilised to great effect for the genetic engineering of these viruses. Recombination requires co-infection of the same cell and studies using *AcMNPV* show that the frequency of multiple infection of single cells *in vivo* is surprisingly high (Bull *et al.*, 2001, 2003; Godfray *et al.*, 1997). In addition studies have also demonstrated that genetically distinguishable NPVs can be packaged within a single OB (Bull *et al.*, 2001). Thus it is highly likely that recombination *in vivo* is a major source of variation driving the evolution of virulence and host range (Cory and Myers, 2003).

1.5.3 Biological variation

Whether this genetic variation in baculoviruses carries any biological relevance which could possibly impact upon the host-virus dynamics and evolution depends on whether phenotypic variation can also be identified in baculovirus populations. Biological traits such as pathogenicity, speed of kill and yield of occlusion bodies correlate with virus fitness and are frequently estimated in laboratory bioassays. Isolates collected from the same species, but in different locations, have been found to vary in their degree of pathogenicity (Allaway and Payne, 1983; Ebling and Kaupp, 1995; Hatfield and Entwistle, 1988) and their speed of kill (Hughes *et al.*, 1983). Biological comparison of individual genotypes following *in vitro* or *in vivo* cloning has also revealed that genotypes can also possess very different pathogenicities (Lynn *et al.*, 1993; Ribeiro *et al.*, 1997; Stiles and Himmerich, 1998; Munoz *et al.*, 1999; Hodgson *et al.*, 2001a; Cory *et al.*, 2005). One particular study which estimated and compared the biological activity of four *in vivo* cloned *Panolis flammea* NPV genotypes from an individual virus infected host revealed up to a seven-fold difference in LD₅₀ and a 36

hour difference in speed of kill between the genotypes (Hodgson *et al.*, 2001a). Other biologically important traits such as degree of liquefaction and size of OB are also highly likely to influence baculovirus transmission and persistence in the wild and have been investigated in some baculovirus species (e.g. Hamm and Styer, 1985).

1.5.4 Maintenance of variation

Although the persistence of genetic variation in natural NPV-lepidopteran systems suggests that heterogeneity is important to virus survival, little is known of how this variation is generated or maintained (Hodgson *et al.*, 2001a and 2001b). There are numerous potential mechanisms that may be involved. For example, baculovirus diversity may be maintained by differential selection where individual variants possess a fitness advantage under different ecological or environmental conditions. For baculoviruses, which infect more than one host species and possess different levels of virulence in each, this may indicate that variants have higher fitness in different hosts. The virulence of *Panolis flammea* NPV genotypes were found to vary depending on the host species they infected (Cory *et al.*, 2005). Another possibility is that host food plant influences baculovirus ecology and phenotype. Preliminary evidence that *Panolis flammea* NPV genotypes also possess different phenotypes (pathogenicity and speed of kill) depending on whether larvae are fed on *P. sylvestris* and *P. contorta* (Hodgson *et al.*, 2002). Further evidence for the impact of host-plant has come from a study of isolates of the western tent caterpillar NPV which found that isolates had the fastest speeds of kill on the host plant from which they were isolated. This appears to suggest that isolates to be adapted to the locally abundant host plant (Cory and Myers, 2004).

Another mechanism through which diversity may be maintained is through frequency dependent selection, which may in theory, allow smaller sized genotypes to be maintained as a polymorphism in the population at the mutation/selection equilibrium, because of a trade-off between genome size and replication rate. Although a model by Godfray *et al* (1997) predicted that the ‘few-polyhedra’ (FP) phenotype possessed very little, if any fitness advantage in pure infections, it has been shown that a FP phenotype is able to persist as a stable polymorphism with the wild-type via a process of frequency dependent selection (Bull *et al.*, 2003). It has been argued that the morphology of co-occlusion of NPVs may also make baculoviruses especially prone to the harbouring of defective genotypes and increasing the equilibrium frequency of defective mutants (Hodgson *et al.*, 2001b). Another mechanism through which diversity of *Spex*NPV infections could be maintained is through the correlation of life-history traits. A negative trade-off between speed of kill and virus yield may theoretically promote the co-existence, within a population, of fast-killing/ low yielding genotypes alongside equally fit genotypes with slow speeds of kill and high yields (Hodgson *et al.*, 2001b). Another possibility is that multiple infection, as commonly witnessed in natural baculovirus populations, may be ‘fitter’ than single-genotype infections. Conventional theory predicts that mixed infections should be more virulent, as multiple genotypes will increase the rate of host exploitation (Frank, 1996). Comparison of two equally infective variants of *P. flammea* in single and dual infections have been shown to result in increased pathogenicity though, unexpectedly this was not accompanied by a more rapid speed of kill and reduction of yield (Hodgson *et al.*, 2004). Although differential immunity has been implicated as the most possible reason for the observed elevation of

host exploitation rate in mixed malaria infections of rodents (Taylor *et al.*, 1998), because of the non-specificity of the insects immune system, other mechanisms such as variable tissue tropisms seem more likely. Co-infection has been shown to have a major influence on the infection characteristics and fitness traits of baculoviruses and this has important implications on the host-parasite dynamics and the application of genetically diverse bioinsecticides (Cory and Myers, 2003).

1.6 The Host: The African Armyworm, *Spodoptera exempta*

1.6.1 Armyworm out-breaks

The African armyworm, *Spodoptera exempta* (Walker; 1856) (Lepidoptera: Noctuidae) is distributed throughout the old-world tropics from parts of Western Arabia and Australia to various countries of South-East Asia and the Pacific islands. Its prevalence though, is highest in sub-Saharan Africa where its status as a pest species is second only to that of the locust (Rose *et al.*, 2000). Like the desert locust, (*Schistocerca gregaria*, Ophthoptera: Acrididae), *S. exempta* is a migratory pest which exhibits density-dependent phase polyphenism, an adaptive response resulting in two distinct larval morphs, a black, crowded or gregarious form and a green, solitary form, depending on the population density during larval development (Penner and Yerushalmi, 1998; Gunn, 1988). It is the gregarious form which causes the crop damage. Extremely high numbers of adults can appear almost spontaneously in out-break populations and can infest many hundreds of square kilometres at any one time (Figure 1.2). The distribution of outbreaks varies both temporally and spatially, but usually follows the breaking of drought conditions with the onset of the wet season,

when grasslands produce new growth and cereal crops are planted. The gregaria phase is physiologically and behaviourally adapted for the accelerated larval development required to exploit such seasonal grasslands. The black, melanised cuticle absorbs solar radiation, which in turn increases larval body temperature and rates of metabolism, resulting in elevated development rates. Larvae of the solitary phase are extremely sluggish in demeanour, cryptically coloured, (green, brown or pink) and are usually found at low host densities, typically spending their days in hiding at the base of host plants and only coming out to feed at night (Figure 1.1).



Figure 1.1 Late instar *Spodoptera exempta* larvae in its solitary (on left) and gregarious (on right) morphs reared on wheat seedlings in the laboratory. (Photo: courtesy of K. Wilson).



Figure 1.2 Typical densities of *Spodoptera exempta* larvae under outbreak conditions. Densities have been reported on occasion exceeding 1000 larvae/m² (Cheke and Tucker, 1995). Photo: courtesy of K. Wilson.

1.6.2 Distribution of out-breaks

Historically countries along the eastern seaboard of the African continent have borne the brunt of this migratory pest from Somalia, Sudan and Ethiopia in the North through equatorial Africa (Kenya, Tanzania, Uganda) and into South Africa and Botswana (Haggis, 1986). Recent records of outbreak occurrence, however, are beginning to show a widening of the prevalence of this pest to more Central and Western African countries, such as, Senegal, The Gambia, Guinea, Sierra Leone, Ghana and Nigeria, where previously armyworm had rarely been seen (Rose *et al.*, 2000; Wilfred Mushobozi, personal communication).

In Equatorial Africa, larval populations are able to persist during the dry “off-season” (July- December) as the *solitaria* form, either in the highlands, where lower temperatures prolong development, or more commonly in coastal regions. The on-set of the short-rains initiates “primary” outbreaks in central or northern Tanzania or south-east Kenya from these low-density populations (Odiyo, 1981). In turn, these primary outbreaks initiate the on-set of secondary outbreaks. These subsequently spread westwards and later, following the movement of the Inter-Tropical Convergence Zone (ITCZ), which is the meeting of the north-easterly and south-easterly tropical wind systems, northwards through Kenya and southwards into Malawi and Mozambique (Odiyo, 1981 and 1984; Pedgley *et al.*, 1989; Rose *et al.*, 1985; Tucker, 1993). Outbreak distribution is also strongly influenced by inland topography with outbreaks rarely seen higher than 2200m above sea level (Haggis, 1986).

1.6.3 Pest status

Larvae of the African armyworm are oligophagous feeders of a wide-range of graminaceous (grasses) and cyperaceaeous (sedges) species, including cereal crops such as maize, millet, wheat and sorghum (Rose *et al.*, 2000). There have also been occasional reports of larvae feeding on non-host crop plants such as tobacco, cotton, tea and coconut seedlings, this though is rare and will only occur when available host plants in the locality have been exhausted (Brown and Dewhurst, 1975). The economic impact of an outbreak is strongly correlated, not only to the susceptibility of crop stage and the timing of attack, but also to the control measures available to the farmer. For many subsistence farmers without the means to protect his crop with chemicals or to re-plant, complete crop failure is a very real possibility. Pastureland is also extremely vulnerable to decimation during an outbreak, with larvae preferentially feeding on what are commonly called “sweet” annual and perennial pasture grasses, such as *Cynodon dactylon*, *Eleusine indica*, *Pennisetum* and *Urochloa* species. Some researchers also speculate that elevated levels of cyanide, found in the fresh growing shoots of cyanogenic species following armyworm outbreaks, are directly responsible for the cyanide poisoning of cattle (Wilson, unpubl.). If this proved to be the case such cattle losses could also be indirectly attributable to armyworm outbreaks.

1.6.4 Natural enemies of *S. exempta*

The migratory nature of *S. exempta*, coupled with its rapid generation time, means that although a great variety of parasitoids can attack all life-stages of the pest, they rarely

reach high enough numbers to reduce host populations. Infestation levels of greater than 70% have only been recorded in areas attacked by several successive outbreaks in a season (Merrett, 1986). Generalist predators include invertebrates such as thrips, ants, beetles and spiders which are able to destroy eggs and early instar larvae. In addition, at the larger end of the spectrum, impressive flocks of storks, crows and kites can often be seen feasting on the bountiful and readily available protein source an outbreak offers (E. Redman, personal observation) and can on occasion result in complete decimation at the local scale (Merrett, 1986). *S.exempta* is attacked by an extremely lethal and highly infectious nucleopolyhedrovirus (*SpexNPV*) which represents the most important natural cause of mortality in armyworm outbreaks. Although the disease had been reported since the 1930s it was not until 1965 that Brown and Swaine identified the mortality agent as a nucleopolyhderovirus (Brown and Swaine, 1965). The data available on *SpexNPV* is only very limited. Initial biological characterisation of an isolate of *SpexNPV* was undertaken by Odindo (1981) who produced estimates of pathogenicity and speed of kill. In addition Swaine identified vertical transmission of *SpexNPV* in laboratory cultures (Swaine, 1966) and high levels of persistent infections have been identified in natural populations of *S. exempta* larvae (L.Vilaplana *et al.*, unpublished data). Evidently this represents a considerable lack of even baseline biological data and one which needs to be addressed if *SpexNPV* is to be developed into a successful bioinsecticide.

1.7 Aims of project

The potential of *Spex*NPV as a bioinsecticide for control of African armyworm is considerable. Baculoviruses in general yield few, if any non-target effects, which is a very desirable characteristic for any insecticide. *Spex*NPV, in addition possesses an extremely rapid speed of kill, even for a NPV, with the first viral induced mortality recorded in less than 72 hours (Odindo, 1981; D. Grzywacz *et al.*, unpublished data). In African armyworm outbreaks cause agricultural losses which affect the economies of not only small subsistence farmers, who represent 95% of the total population in East Africa (Rose *et al.*, 2000), but also at the nation level, through the defoliation of cash crops such as sugar cane and cereals. Resource-poor smallholder farmers are, particularly vulnerable to severe economic losses due to their insufficient resources to cope with armyworm invasions. They do not have the equipment, pesticide or funds to enable them to control infestation in time. Although in some countries, like Tanzania, whilst armyworm control has been the responsibility of the government, in reality economic and logistical constraints have limited the amount of assistance available to farmers. This situation is likely to deteriorate even more in the next year or so as international aid to African countries continues to decrease and the legislation concerning chemical pesticides and their correct usage begin to encompass the developing world (Charles Dewhurst, personal communication). Research undertaken by Natural Resources International (NRI) has shown that aerial spray application of *Spex*NPV formulations, are able to significantly reduce Armyworm populations. Further research has recently been funded to in order to optimize production, formulation and application methods (D. Grzywacz, personal communication). My

research project was undertaken, alongside the aforementioned applied research program, and was charged firstly with the investigation of the diversity of *Spex*NPV within natural populations of armyworm and secondly to investigate the effect diversity had on the virulence of *Spex*NPV, a subject of direct relevance for the development of *Spex*NPV as a bioinsecticide and about which very little was known.

The aims of the research were specifically to:

- Characterise and quantify the genetic and biological variation found in natural NPV epizootics of the African Armyworm in Northern Tanzania.
- Use cloning techniques to separate individual genotypes from the wild-type *Spex*NPV and characterise them genetically.
- Characterise the phenotype of individual genotypes in terms of a range of fitness traits.
- Investigate the dynamics of mixed *Spex*NPV infections and the interaction between co-infecting genotypes

Chapter Two

Materials and Methods

Chapter 2 Materials and Methods

2.1 Insect culture

An original culture of *Spodoptera exempta* (Lepidoptera: Noctuidae) has been maintained in the insectary at the NERC Centre for Ecology and Hydrology (C.E.H.) in Oxford since it was originally obtained from the Natural Resources Institute, Chatham in July 1997. It was used for the initial amplification of virus and *in-vivo* cloning of *Spex*NPV genotypes (Chapter 3). In February 2002, a new culture of *S. exempta* was initiated to replace the old one, which was beginning to suffer from low fecundity and in-breeding depression. Pupae were bought back from Arusha, Northern Tanzania and reared in quarantine at the University of Stirling for 6 generations on wheat seedlings, with no signs of overt virus infection. The culture was then transferred to the insectary at C.E.H. in Oxford where it was fed on artificial diet (see below) for ease of maintenance. This culture was used for all other experimental work (Chapters 4-7).

2.1.1 Insect rearing

S. exempta cultures maintained in the C.E.H.-Oxford insectary were reared on a semi-synthetic diet at 28°C with an 10:14 h light:dark cycle. At each generation eggs were surface sterilised in 1% hypochlorite for 10 min and then in 5% formalin for 30 min, in order to ensure removal of any potential pathogen contamination prior to hatching. To prevent cannibalism in later instars, newly moulted 2nd instar larvae were separated for rearing on individually in polypots. The lids of the polypot were scored to allow adequate ventilation and a single layer of tissue paper was placed underneath the lids to

soak up excess moisture and to increase probability of successful pupation. Pupae were sexed and placed in groups of 90-100, of approximately 50:50 ratio, in cylindrical rearing cages (25cm diameter * 35cm height = 960cm²). Adults were fed with a 10% honey solution and allowed to lay their eggs on strips of filter paper.

2.1.2 Semi-synthetic diet

The semi-synthetic diet used for insect rearing was a modification of Hoffmans' tobacco hornworm diet (Smith, 1966). The diet consisted of 288g wheatgerm, 132g casein, 177g sugar, 70g agar, 57g dried brewers yeast, 37.5g Wessons salts, 6g sorbic acid, 3.75g cholesterol, 3.75g methyl-4-hydroxybenzoate to which 2750ml of water was added and autoclaved for 25 min at 20psi. The diet was allowed to cool to approximately 70°C before the antibiotics (2g streptomycin, 18g aureomycin, 40g ascorbic acid), vitamins (5g nicotinic acid, 5g calcium pantothenate, 2.5g riboflavin, 1.25g aneurine hydrochloride (B1), 1.25g pyridoxine hydrochloride (B5), 1.25g folic acid, 0.1g, D-biotin, 0.001g cyanocobalamin (B12)) and 3.75g of choline chloride were added.

2.2 Baculovirus techniques

2.2.1 Source of wild-type virus

The wild-type *Spex*NPV virus used throughout this research project originated from a natural *Spex*NPV epizootic in Tanzania in 1977. The infected cadavers were frozen at -20°C in the C.E.H. – Oxford virus collection where it remained unpurified until the start of the period of research.

2.2.2 Purification of wild-type virus

Wild-type virus was purified from insect larvae following a modified method described by King and Possee (1992). Cadavers were macerated in 0.1% SDS using an electric stomacher (Colworth 400) in order to release the occlusion bodies (OBs) from the body tissue. The crushed cadavers were then filtered through a double thickness of muslin on ice and centrifuged at 1000 rpm for 10 min. to pellet the unwanted larval debris. The supernatant was then spun at a higher speed (4000 rpm) for 20 min to pellet the OBs (Centrifuge 5810 R, Eppendorf). The OBs were re-suspended in a minimal amount of water and layered on to a 50%:60% (w/w) discontinuous sucrose gradient and centrifuged for 90 min at 25 000 rpm at a temperature of 4°C (Optima L-100 XP Ultracentrifuge, Beckman Coulter). The resulting band of virus was harvested from between the sucrose layers using a Pasteur pipette and the excess sucrose was washed out of the viral suspension with several 10 min spins at 5000rpm with deionised water (Centrifuge 5810 R, Eppendorf). The OBs were finally re-suspended in water, counted (section 2.2.5), aliquotted and stored at -20°C until required.

2.2.3 Amplification of wild-type virus

In order to produce an ample amount of stock virus for working with throughout the entire period of research the virus isolate from the culture collection was amplified by passaging through larvae. 'Butter-tubs' (volume = 252cm²; Just Plastics), containing a thin layer of diet, were brushed with the wild-type virus at concentrations of 1 x 10⁴ OB/μl using a paintbrush. Ten newly moulted 4th instar larvae were introduced per tub

and left to feed at 28°C. The resulting viral deaths were harvested, pooled, purified (see section 2.2.4), counted (see section 2.2.5) and stored at -20°C in aliquots until required.

2.2.4 Purification of virus from single larvae

Pelleting method

Single infected larvae were homogenised individually using a method adapted from Hunter-Fujita *et al.* (1998) using pellet pestles in 1.5 ml micro-tubes in the presence of 250µl 0.1% SDS. Larval debris was separated from the OB-containing supernatant by centrifugation at 6000 rpm for 15 seconds (Centrifuge 5417 C, Eppendorf). Repetition of this process was required using fresh 0.1% SDS until the resulting supernatant became clear, indicating that all the OBs had been collected. Spinning the pooled OB-containing supernatants at 13 000 rpm for 3 minutes produced a viral pellet which was then washed once in 750µl sterile Milli-Q water and finally re-suspended in a volume of 150µl.

Small muslin filter method

For some of the virus samples collected directly from the field an alternative method of purification was adopted. For although care was taken to avoid grass and soil contamination, the presence of such debris, in many of the samples warranted the inclusion an additional level of purification and the use of a sucrose cushion. The protocol started with the homogenisation of single cadavers using pestle pellets in the presence of 0.1% SDS. The homogenate though was then loaded into a small muslin filter constructed within the 1.5 ml micro-tube and spun for 1 min (6 000 rpm). The

resulting filtrate was then passed through a 30 % (w/w) sucrose cushion with a 5 min spin (13 000 rpm). The OBs were then washed with 1ml of water to remove any excess sucrose and finally re-suspended in a volume of 150 μ l.

2.2.5 Enumeration of occlusion bodies

In order to determine the concentration of viral occlusion bodies (OBs) in a viral sample, a haemocytometer was used. A thick specially designed cover-slip was pressed firmly in position on a 0.1mm Improved Neubauer haemocytometer until Newton's rings appeared. A sub-sample of the viral suspension to be counted, diluted either 1 in 10 or 1 in 100 with water, was placed into the counting chamber of the haemocytometer and left to settle for 15 mins. OBs were visualised and counted using a phase-contrast microscope at a magnification of x 400. OBs present within or touching the upper or left-hand wall of five squares of the haemocytometer grid were counted. The concentration of the original suspension could then be estimated using the equation: number of OBs x 5 x 10⁴ x dilution factor. In order to increase the accuracy of the estimation five separate counts of four sub-samples of the original viral suspension were made.

2.3 Molecular biological techniques

2.3.1 DNA extraction from wild type virus

Viral DNA was extracted using a method adapted from Hunter-Fujita *et. al* (1998). An OB suspension was diluted to give a concentration of 5*10⁸ OB/ml in a volume of 500 μ l. 100 μ l of 0.5M EDTA and 10 μ l Proteinase K (25mg/ml) were added to the viral

suspension and tubes were occasionally inverted during a 90 min incubation period at 37°C to ensure thorough. A weak alkali, in the form of sodium carbonate (67µl), was then added to facilitate the release of the virus particles from the occlusion bodies, which could be visualised by the clearing of the suspension after incubation at 37°C for a further 90 min. The addition of a surfactant to the suspension (10 µl 10% SDS), followed by a further incubation period of 15 min, preceded removal of the unwanted debris from the suspension by centrifugation (13 000 rpm for 3 min). The resulting supernatant was placed in new tubes and the DNA was further purified with a phenol/chloroform wash. An equal volume of phenol/chloroform (1:1) was added to the sample and mixed gently by inversion for 5 min before centrifuging at 13,000 rpm for 10 min. The aqueous phase was collected in to a new tube and care was taken not to disturb the phenol/chloroform layer, which was discarded at this point. This extraction step was repeated twice more, once using phenol/chloroform and once with chloroform/isoamyl (24:1), in order to remove any excess phenol. The final aqueous phase was transferred to a dialysis chamber consisting of the top section and lid of a plastic 1.5ml microfuge tube having been removed using a sharp blade. The DNA was placed in the upturned lid and covered with a single layer of dialysis tubing which was held securely in position by the top section of microtube. The dialysis chamber was then placed in dialysis buffer (10mM TRIS, 1mM EDTA in 1 litre water) at 4°C for at least 24 h with constant stirring and three changes of buffer.

2.3.2 DNA extraction from individual, virally-infected cadavers

Occlusion bodies purified from a single cadaver were suspended in a volume of 150µl of water, 75µl of which were used for the extraction of DNA. Viral DNA was extracted using a scaled-down version of the previous method for the DNA extraction from the wild-type virus (section 2.3.1). The viral suspension was incubated with 15µl 0.5M EDTA and 1.5µl Proteinase K at 37°C for 90 min with occasional inversion. Sodium carbonate was then added to the sample (15µl 1M NaCO₃) was then added to the sample and incubated at 37°C for 90 min or until the sample cleared. Upon clearing, 10µl 10% SDS was added and the sample was returned to the 37°C water bath for a further 15 min. The sample was centrifuged at 13 000 rpm for 30 sec. The DNA was then extracted twice using phenol/chloroform and once using chloroform/isoamyl and dialysed as previously described (section 2.2.6).

2.3.3 Restriction endonuclease digestion of viral DNA

Purified DNA was digested with 5U of restriction endonuclease and the appropriate buffer in volumes of 10-20µl, for a minimum of 6 hours at the prescribed temperature for optimal cutting efficiency for the chosen enzyme i.e. 37°C for *EcoRV* (New England Biolabs). Bovine Serum Albumen was added to the samples at a final concentration of 0.1mg/ml to facilitate optimum restriction. Following digestion loading buffer was added to a final concentration of 1 * (0.025% bromophenol blue, xylene cyanol, 2.5% Ficoll) and samples were then stored at -20°C until required.

2.3.4 Agarose gel electrophoresis

Nucleic acid samples were routinely fractionated in high-gelling temperature agarose, submerged in 1 x TBE (90mM Tris Borate, pH 8.0, 2mM EDTA) in horizontal gel tanks (BioRad). Agarose concentrations of between 0.8% and 1.2% were used depending on the size of the DNA fragments to be separated. Electrophoresis of digested total viral DNA usually required 24 h with samples initially run at 100V for 2 h. The voltage was then lowered to 40-60V and the orientation of the current flow was reversed for 15 minutes in every 2 hours to ensure greater separation of the bands. For visualisation purposes the gels were either stained with SYBR Gold (Molecular Probes) (0.1µl/ml) or ethidium bromide (0.5µg/ml). A VersaDoc Imaging System Model 3000, running Quantity One software version 4.2 (Bio-Rad), was used to capture and analyse the image. Fragment molarity and molecular weight were estimated by comparison with known molecular markers: Hyperladder I (10kb to 0.2kb), Hyperladder VI (48.5kb to 10.09kb) (Bioline) and 1kb Molecular ruler (15kb to 1kb) (Bio-Rad).

2.3.5 Field Inverted Gel Electrophoresis (FIGE)

This method was carried out to establish accurate sizing of larger DNA fragments. Agarose gels were made as 1% solutions (w/v) of pulse-field grade agarose powder boiled in 0.5 x T.B.E. buffer. Nucleic acid samples were loaded onto the gel and a FIGE Mapper Field Inversion System (BioRad) was then connected to the tank. A suitable run condition was selected from the pre-programmed system protocols, depending on the size of the DNA to be separated. Visualisation and analysis of the gel was carried out as above.

2.3.6 Polymerase Chain Reaction (PCR)

The supplied freeze dried pellets of oligonucleotides, synthesised by MWG-Biotech, were re-suspended in distilled Milli-Q water to achieve a stock concentration of 100pmol/ μ l and stored at -20°C. Working concentrations were diluted from this. Reactions were performed either using either Robocycler (Gradient 40, Stratagene) or PCR Sprint (Touchdown Thermal Cycler, Hybaid) machines. The reaction mixture consisted of 50pmol of each of the forward and reverse primers, with approximately 10ng of template DNA, 10mM dNTPs, 1.25 μ l BSA (20mg/ml) and 1U Taq DNA polymerase together with its supplied buffer (Sigma), in a total volume of 50 μ l. The preparation of reaction mixes were carried out on ice and in a laminar flow hood under sterile conditions using filter pipette tips. All PCR amplifications included a negative control, where the template DNA was replaced by distilled Milli-Q water, and a positive control (*SpexNPV* DNA). The amplification reaction comprised 1 cycle 95°C for 5 min, 52°C for 1 min and 72°C for 1 min, followed by 28 cycles of 95°C for 1 min, 52°C for 1min and 72°C for 1 min and a final cycle of 5min at 72°C. PCR products (5 μ l) were visualised by electrophoresis on 1.1% agarose gels which were stained with ethidium bromide.

2.3.7 Sequencing

Sequencing was carried out using the dideoxy chain-termination method (Sanger *et al.*, 1977) in an Applied Biosystems Incorporated (ABI) 3730XL DNA Analyzer. Approximately 200ng DNA was added to 1pM of the required primer (MWG-Biotech)

and 1µl dye terminator mix (BigDye 3.1, ABI) in a final volume of 5 or 10µl. The reaction solution was gently mixed and placed in a PCR cycler (ThermoHybaid) and run for 25, 30 second cycles at 96°C, a single cycle of 15 seconds at 50°C and a final 4 min incubation at 60°C. On completion of the PCR reaction the DNA was fractionated through G-50 sephadex columns. The columns were first prepared by adding G-50 sephadex (washed and suspended in two parts T.E. buffer) to 96-well plates and centrifuging at 3000 rpm, 20°C for 2 min (Beckman GS-15R bench top centrifuge) to extract the excess moisture from the column. The plates were then positioned on 96-well microtitre plates to collect the flow through. The DNA was loaded carefully in to the centre of the column, which was further centrifuged at 3000 rpm, 20°C for 2 min and the resulting DNA fraction was collected. The DNA was subsequently transferred to a 0.5ml microtube and placed with the lid open in a condensation trap for 45 min. The pellet was then stored at -20°C prior to sequencing. The DNA was allowed to thaw on ice before 10-30µl Hi-Di Formamide (ABI) was added, the samples were centrifuged and loaded into the gel of the DNA Analyzer.

2.4 Bioassay procedures

2.4.1 Diet-plug contamination method

There are several methods for inoculating insects with known amounts of viral OBs. One of these is the diet plug method in which insects are given a small amount of food contaminated with a known number of viral OBs. Insects that had eaten all of the diet are then known to have ingested an exact, known amount of virus. Small diet plugs of approximately 1mm² were made using a diet-plug making pump and positioned into

square 25-well petri-dishes. Several layers of moistened paper towel were positioned firmly under the lid of the Petri-dishes to ensure the diet-plugs did not dry-out too quickly. The petri-dishes could then be kept at 4°C, for a limited period of time until needed without the diet-plug drying out and becoming unpalatable. Serial dilutions were made to give known doses of virus per 1µl of suspension. These were then pipetted onto each diet-plug. Newly moulted third instar larvae that had been starved for the previous 12 h were then introduced into the wells and allowed to eat. After 24 h only the larvae that had successfully eaten all of their allocated diet-plug, and thus ingested the required dose of virus, were transferred to individual polypots (12ml) containing artificial diet (section 2.2). The larvae were kept at 28°C and checked initially after 24 h for handling deaths, which were eliminated from the data set, and subsequently every 8-12 h for viral mortality, until death or pupation. At approximately the 5th instar, paper towel was positioned under the polypot lid to reduce the proportion of larvae that failed to pupate. Upon death the cadavers were transferred to 1.5ml eppendorf tubes and kept at -20°C for later yield and RFLP profile analysis. Larval deaths not displaying obvious symptoms of viral infection were also kept to establish cause of death.

2.4.2 Determining cause of death

The diagnosis of viral mortality, or more commonly the determination of the presence of OBs in a mixed infection where obvious viral symptoms were lacking, was through staining smeared cadavers with Gurr's Improved R66 Geimsa Stain (BDH) and

visualising by light microscope with oil immersion under phase contrast. The presence of high numbers of occlusion bodies was interpreted as viral-induced mortality. In this scenario, even though virus was not seen as the obvious cause of death because of the lack of symptoms, the virus was present at high enough levels to increase susceptibility to secondary infections, such as bacteria, to which the larvae could otherwise be able to withstand. Consequently viral-induced mortality was included in all mortality analysis. When only a very few occlusion bodies were found upon staining, deaths were considered non-viral and discarded from the dataset.

2.4.3 Viral yield estimation

One method of establishing the pathogenicity or virulence of a baculovirus is to determine how much virus is produced from each cadaver (i.e. viral yield). To establish this, only cadavers that could be transferred whole from the rearing containers were used for yield analysis. Each dead larva was macerated in 1ml of sterilised water with a plastic pestle and vortexed thoroughly. A small amount of the macerate (10 μ l) was diluted 1 in 10 with sterile water. Occlusion bodies from two sub-samples were then counted using a haemocytometer and a light microscope, as described above (section 2.2.5).

2.5 Data Analysis

2.5.1 Analysis of DNA sequence data

Sequenced data were assembled and analysed using PreGap4 (Staden) and Gap4 (Staden). Raw ABI files were first imported into PreGap4 and reformatted into the

appropriate configuration for alignment in Gap4. Gap4 was used to align the data, produce consensus sequences which were saved in *fasta* format for exportation and further use in other programs.

2.5.2 Phylogenetic analysis

Phylogenetic analysis was carried out using the ClustalX 1.81 (Thompson *et al.*, 1997) and Mega2 (Kumar *et al.*, 2001) packages. ClustalX created a multiple alignment which was used to calculate a distance matrix with all pair-wise distances between the nucleotide sequences. This was saved as an alignment file, which was opened in Mega2. Phylogenetic trees were constructed using the neighbour-joining (NJ) algorithm which involved progressively clustering sequences that were close to each other. The distances (percent divergence) between all pairs of sequence from the multiple alignment were calculated and applied to the NJ method of the distance matrix. A NJ tree with bootstrap values was then created. Bootstrapping uses a method for deriving confidence intervals for the groupings in a tree and involves the production of N random samples of sites from the alignments (N was set at 1000) to allow the drawing of 1000 trees. The number of times groupings from the original tree occurred in the sample trees determined its confidence intervals. The appropriate trees were constructed to determine phylogenies.

2.5.3 Statistical analysis

The data were analysed using a generalised linear modelling program (GLIM version 3.77, 1985 Royal Statistical Society). The maximal model was initially created by

fitting all explanatory variables and their interactions. Each term was then progressively removed from the model to test the significance of its individual contribution. Non-significant terms were removed until the minimal adequate model was obtained which contained only significant terms. Proportional mortality and the proportion of mixed infections was modelled using binomial errors, with adjustment of the scale parameter to allow for the over dispersion of the dataset if required. Speed of kill and yield data were transformed, if necessary, for analysis assuming a normal error structure.

Chapter Three

Genetic characterisation of a wild-type

***Spodoptera exempta* NPV population**

Chapter 3:

Genetic characterisation of a wild type *Spodoptera* *exempta* NPV population

3.1 Introduction

Before the recent advances in molecular techniques, the characterisation of baculovirus diversity relied exclusively on their immunology (Knell *et al.*, 1983), structure and protein composition (Francki *et al.*, 1991) and degree of genomic hybridization (Kislev *et al.*, 1985). The discovery and widespread availability of restriction endonucleases (RE) revolutionized studies of baculoviruses by providing strain-specific genotypic markers. Fragments of viral DNA produced after digestion with the RE are separated by gel electrophoresis to produce specific banding patterns. The comparison of the banding patterns from different virus isolates is called restriction fragment length polymorphism (RFLP) analysis and is now the most commonly used technique to characterise and identify different viruses (Gettig & McCarthy, 1982; Cherry and Summers, 1985; Shapiro *et al.*, 1991; Vickers *et al.*, 1991; Parnell *et al.*, 2002; Cooper *et al.*, 2003a; Graham, *et al.*, 2004; Cory *et al.*, 2005). The RE analysis of viruses collected from individual caterpillars in the field has shown that baculoviruses can exhibit a high degree of genotypic diversity (Cooper *et al.*, 2003a; Graham, *et al.*, 2004; Cory *et al.*, 2005). Genotypic heterogeneity has been identified between isolates from different countries and between isolates collected from the same agricultural field. Genotypic

heterogeneity can also be identified by the detection of sub-molar bands within a RE profile, a common phenomenon among baculoviruses, indicating the presence of more than one genotype within the isolate.

Sequence data can also be used to study the diversity of baculoviruses (Shapiro *et al.*, 1991; Cooper *et al.*, 2003b; Graham *et al.*, 2004; Burden *et al.*, 2005) and for species whose entire genome has been sequenced, gene order and gene composition can also be utilised to reconstruct phylogenies and infer relatedness. Such comparative genomic techniques, by utilizing the complete genetic makeup of the species, can consequently yield much more robust phylogenetic inferences than the use of just sequence data alone. This was first adopted for the study of mitochondrial genomes but recently has been employed in the study of larger much more closely related genomes such as herpesviruses and baculoviruses (Herniou *et al.*, 2001). Such whole genome approaches though, are restricted to completely sequenced genomes. Consequently only sequence data from individual genes will be used for the phylogenetic analyses of *SpexNPV* in this study.

The wild-type *Spodoptera exempta* nucleopolyhedrovirus (*SpexNPV*) isolate selected for this study originated from the pooling of numerous virus-infected larvae collected from a natural epizootic in Tanzania in 1977. Preliminary restriction endonuclease digestion of this pooled (wild-type) *SpexNPV* DNA revealed several fainter bands within the restriction profile, indicating that the wild-type virus represented a heterogeneous population of genotypes.

Study of the genetic diversity of this wildtype population required the isolation of the individual genotypes from the mixture. This has been successfully achieved in some nucleopolyhedroviruses, for which permissive cell lines are available, by plaque purification. This technique was first used to clone numerous genotypically distinguishable variants from a single *Autographa californica* NPV infected larva (Lee and Miller, 1978; Stiles and Himmerich, 1998) and has since proved effective for other nucleopolyhedroviruses. These include *S. frugiperda* NPV (Knell and Summers, 1981; Maruniak, *et al.*, 1984), *Lymantria dispar* NPV (Lynn *et al.*, 1993), *S. litura* NPV (Maeda *et al.*, 1990) and *S. littoralis* NPV (Cherry and Summers, 1985). Many of these viruses infect host species that are closely related to *Spodoptera exempta*. Consequently the probability of *Spex*NPV propagating successfully in cell culture was considered high, and thus offered one way of isolating the individual genotypes from the mixed population.

An alternative method of cloning, which involves the infection of larvae at low doses where mortality is low and infection is assumed to initiate from a single virus particle (Van Beek *et al.*, 1988), is dilution or *in vivo* cloning and was first developed by Smith and Crook (1988) to purify eight genotypic variants present in wild type cabbage white butterfly, *Pieris rapae*, GV. The isolation of individual genotypes, following just a single *in vivo* passage, indicated that a low-mortality infection could theoretically result from the uptake and replication of a single occlusion body. In the same study a similar technique was employed to attempt to purify genotypes from the MNPV of the gypsy

moth, *Lymantria dispar*. The multicapsid nature of MNPVs, and thus the possibility of co-enveloping more than one genotype within the same occlusion body, failed to preclude the successful separation of three genotypes using this methodology (Smith and Crook, 1988). The authors did postulate, however, that the co-occlusion of multiple genotypes may have accounted for the recovery of fewer *LdMNPV* genotypes in comparison to *ArGV3* genotypes following infections at similar mortality levels (Smith and Crook, 1988).

For the cloning of wildtype *SpexNPV*, the *in vivo* method was chosen in preference to the *in vitro* method mainly because of the artificial nature of serial passage through cell culture. Cell culture could, in theory, select for certain genotypes and thus distort the true picture of the genetic diversity of the wildtype population. In addition, there is good evidence that passage of baculoviruses in cell culture can generate variants with sizeable deletions in their genome (Pijlman *et al.*, 2001).

Modifications of Smith and Crook's (1988) technique have been used successfully to *in vivo* clone genotypes from other mixed nucleopolyhedrovirus populations, including *S. exigua* NPV (Munoz and Caballero, 2000) and *Panolis flammea* NPV, for which a total of 24 different genotypes were isolated from a single virus infected larva (Cory *et al.*, 2005). While many studies have shown the ubiquity of baculovirus variation, few have gone on to investigate how related a virus population is.

In this chapter the aims were to isolate different genotypes from the mixed genotype *Spex*NPV wildtype using *in vivo* cloning techniques; to conduct RFLP analysis to assess genetic diversity and estimate the size of their genomes; and to determine the genetic relatedness of the genotypes through the use of phylogenetic analyses of individual genes.

3.2 Methods

3.2.1 *In vivo* cloning

For the *in vivo* cloning of wild type *SpexNPV*, a low dose capable of causing approximately 10% viral mortality (LD₁₀) was required. Before initiating the first bioassay the literature was scoured to find an estimation of the dose required to produce this level of mortality. Reeson *et al* (1998) estimated an LD₅₀ of 3082 OBs for *S. exempta* larvae reared individually from 24 hrs after hatching (referred to as 'black solitaires' by Reeson *et al.*). A viral dose able to cause approximately 10% mortality was estimated from the dose-response curve, and for the purposes of this experiment, was taken to be 1200 OBs.

In order to select enzymes best suited for the genetic characterisation of *SpexNPV* isolates and, in particular for the identification individual genotypes, a range of restriction enzymes were screened. Figure 3.1 represents just one of the agarose gels produced, showing the distinctive banding patterns obtained for seven of the more common enzymes available (sections 2.3.3 and 2.3.4). Enzymes were selected on the basis of producing enough bands to yield variation but not so many that they became difficult to separate clearly. The restriction enzymes *XhoI*, *EcoRV* and *BamHI* were selected for the purposes of distinguishing *SpexNPV* genotypes.

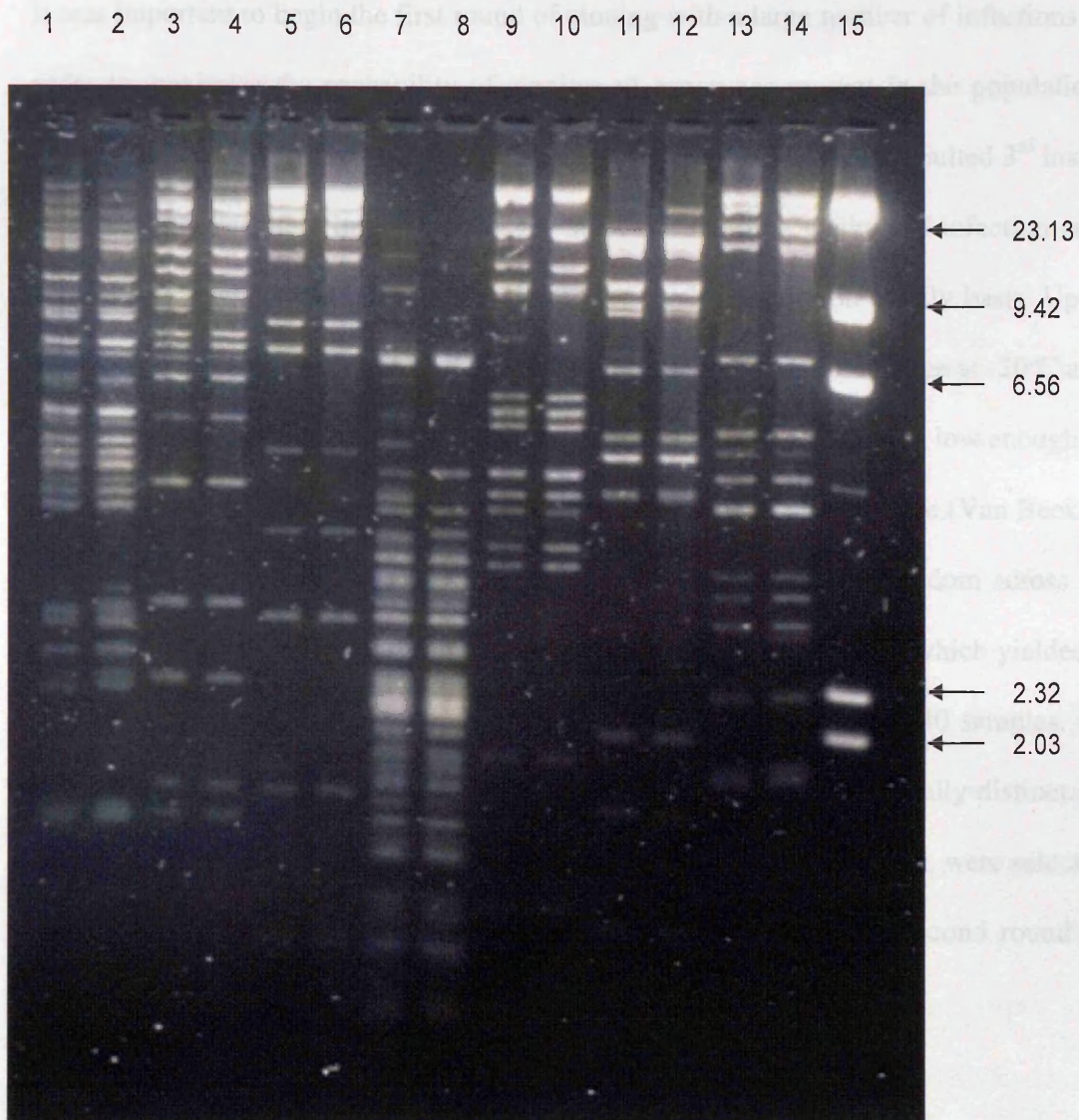


Figure 3.1 Restriction endonuclease profiles of wild-type *SpexNPV* DNA digested with *EcoRI* (1-2), *BamHI* (3-4), *HindIII* (5-6), *SalI* (7-8), *PstI* (9-10), *KpnI* (11-12) and *XhoI* (13-14) before (odd lane nos.) and after (even lane nos.) *in vivo* passage. Molecular weight ruler, \square -*HindIII* DNA marker (Lane 15). 0.8% agarose gel run for 24 hours at 40V.

It was important to begin the first round of cloning with a large number of infections in order to maximize the probability of cloning all genotypes present in the population, even those present at only low levels. Therefore a batch of 600 newly moulted 3rd instar *S. exempta* larvae were infected using the standard diet-plug method of infection (see section 2.4.1) with 1200 OBs and monitored for viral mortality on a daily basis. Upon death, viral cadavers were transferred to individual micro-tubes for storage at -20°C and later analysis. A total mortality of 18% was achieved and was considered low enough to ensure that infection by single viral particles had theoretically taken place (Van Beek *et al.*, 1988). From the 112 viral deaths, 40 cadavers were selected at random across all time-points for RE analysis. The restriction digestion enzyme *EcoRV*, which yielded a clear and useful diagnostic banding pattern, was used to profile these 40 samples. Of these 40 isolates, 12 lacked sub-molar bands and thus appeared genetically distinct. In addition, a further ten isolates, possessing the occasional sub-molar band, were selected along with the genetically distinct isolates and taken forward for a second round of cloning.

The 22 isolates identified at this stage were used to infect small batches ($n = 35$) of newly-moulted 3rd instar larvae, at a dose equivalent to a LD₁₀ for the wild-type virus (1200 OBs). Figure 3.2 shows the proportionate mortality for each isolate infected at this dose. From this second round of cloning, all viral deaths (maximum of three per isolate) were selected for RE analysis (total = 60). Ten out of 12 potential clones from the first round remained pure, producing no obvious sub-molar bands in all 3

replicates analysed. The remaining two potential clones did produce profiles with sub-molar bands and were thus discarded at this point. Therefore, after just a single low dilution passage of wildtype *SpexNPV* ten single genotypes had been isolated and remained stable after an additional *in vivo* passage.

In addition to the single genotype profiles ten mixed genotype isolates (identified in the first round) were passaged through a second round of cloning and the progeny isolates were analysed with *EcoRV* to identify an additional nine genetic profiles. These 9 isolates (potential clones), along with the ten already identified, were used to infect small batches ($n = 35$) of newly-moulted 3rd instar larvae at a low dose equivalent to a LD₁₀ for the wildtype virus (1200 OBs). A maximum of three viral deaths per isolate were profiled. From this third *in vivo* passage, all viral profiles were found to be free of sub-molar bands when their *EcoRV* profiles were studied, with the exception of isolate 39 which still yielded profiles with obvious signs of mixtures. Therefore, after three rounds of *in vivo* cloning a total of 18 single genotypes had been isolated using *EcoRV*, ten of which had remained stable for two passages and eight had remained stable after one passage. These 18 *EcoRV* genotypes were subjected to further restriction enzyme analysis using both *BamHI* and *XhoI*. The profile of one of the isolates produced sub-molar bands when analysed with *BamHI* and thus was discarded at this point. A fourth *in vivo* passage of the remaining 17 single genotypes was conducted to ensure the stability of the purified genotypes and to amplify the amount of each genotype available (Table 3.2).

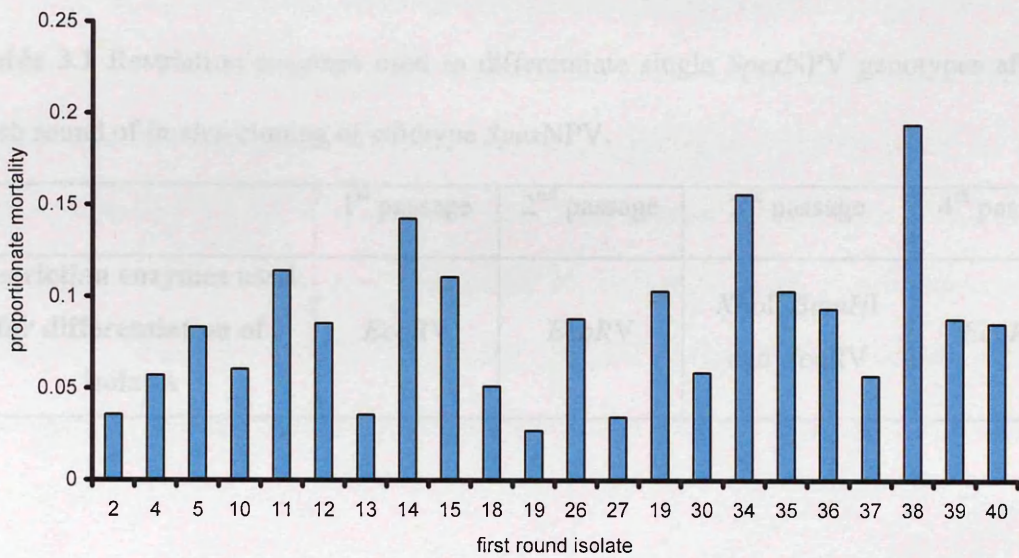


Figure 3.2 Mortality (proportion dying) of *SpexNPV* isolates at the second round of *in vivo* cloning in 3rd instar *S. exempta* larvae at a dose of 1200 occlusion bodies.

	No. of single genotypes identified after 1 st or 2 nd passage	No. of single genotypes to remain pure after 4 th passage
1 st passage	12	10
2 nd passage	9	7
Total no. of single genotypes identified after four rounds of <i>in vivo</i> cloning		17

Table 3.1 Restriction enzymes used to differentiate single *SpexNPV* genotypes after each round of *in vivo* cloning of wildtype *SpexNPV*.

	1 st passage	2 nd passage	3 rd passage	4 th passage
Restriction enzymes used for differentiation of isolates	<i>EcoRV</i>	<i>EcoRV</i>	<i>XhoI</i> , <i>BamHI</i> and <i>EcoRV</i>	<i>EcoRV</i>

Table 3.2 Number of single *SpexNPV* genotypes initially identified from wild-type *SpexNPV* together with the number of single genotypes which subsequently remained pure through additional rounds of *in vivo* cloning.

	No. of single genotypes identified after 1 st or 2 nd passage	No. of single genotypes to remain pure after 4 th passage
1 st passage	12	10
2 nd passage	9	7
Total no. of single genotypes identified after four rounds of <i>in vivo</i> cloning		17

3.2.2 Gene selection for phylogenetic analysis

A number of different genes, were selected for this phylogenetic analysis. Genes vary in their ability to resolve phylogenetic relationships on the basis of their size, degree of conservation and their function. Ideally the sequence should be relatively conserved but retain sufficient variation to allow meaningful comparisons. Much baculovirus phylogenetic analysis has been conducted on occlusion body protein sequences (polyhedrin: Zanotto *et al*, 1993; granulins: Bideshi *et al*, 2000). Because of the abundance of the data for these proteins the polyhedrin gene was selected as the first gene to be used in this study.

Late and very late baculovirus gene expression utilises a host RNA polymerase II, which is a large four-sub-unit enzyme encoded by *lef-8*, *lef-4*, *lef-9* and *p47* which are all considered essential genes (Guarino *et al.*, 1998). It has been postulated that baculoviruses have evolved this enzyme for the efficient transcription of viral genes in preference to host genes during the post-replication phase (Titterton *et al.*, 2003). A study which investigated the value of individual baculovirus genes for phylogenetic analysis highlighted *lef-8* as one of the few genes to produce a strong phylogenetic signal (Herniou *et al*, 2001) and consequently was also selected for the investigation of relatedness of *Spex*NPV genotypes.

Other genes that have also been used for phylogenetic analysis include the gene *gp41* (Liu *et al*, 1999) which encodes the structural glycoprotein required for egress of nucleocapsids out of the nucleus of infected cells to form budded virus and genes

involved in viral replication such DNA polymerase (Bulach *et al*, 1999; Nielsen *et al*, 2002) and *lef-2* (Chen *et al*, 1999). Despite the non-essential nature of auxillary genes several have also proved useful in phylogenetic studies. These include the gene *egt* (Chen *et al*, 1997; Clarke *et al*, 1996) and the chitinase and cathepsin genes (Kang *et al*, 1998). Viral chitinase (*chiA*) and cathepsin (*cath*) genes are expressed late in the infection cycle (Hawtin, *et al.*, 1995). There is evidence that the enzymes that they encode act synergistically to degrade the cuticle integrity of the larvae post-death (Samuels and Patterson, 1995; Slack *et al.*, 1995; Thomas *et al.*, 2000; Hom and Volkman, 2000; Hom *et al.*, 2002). Thus the chitinase gene is important for the dissemination of OBs and horizontal transmission.

The ecdysteroid UDP-Glucosyltransferase (*egt*) gene encodes the insect hormone, EGT and is expressed through-out infection. This protein is secreted into the insects' haemocoel, where it accumulates and inactivates circulating ecdysteroids, by catalyzing their conjugation with glucose or galactose. This sugar conjugation suppresses host molting and therefore also prevents the cessation of feeding usually associated with moulting (O'Reilly and Miller, 1989; Burand and Park, 1992; Eldridge *et al.*, 1992). The biological significance for the virus of *egt* is unclear for, although the delay of host death obviously delays OB transmission, there will also undoubtedly be more host biomass being converted to virus because of a longer speed of kill. The identification of *egt* homologues in a large number of baculovirus genomes, including representatives of both baculovirus sub-groups does suggest that it is an ancestral gene which has co-evolved with the viruses, suggesting an important role in the biology of baculoviruses

(Clarke *et al*, 1996; O'Reilly, 1995). Consequently the *egt* and *chitinase* genes were selected, alongside *polyhedrin* and *lef-8* for the phylogenetic analysis of *Spex*NPV genotypes in this study.

3.2.3 Primer design

Oligonucleotide primers were designed for the PCR amplification of each of the four genes for *Spex*NPV. The complete genome of *Spex*NPV has yet to be fully sequenced but several genes have been partially sequenced and were therefore available for the design of specific primers for the amplification of regions of the polyhedrin, *lef-8* (sequences obtained from Elizabeth Herniou, unpubl.) and the chitinase gene (sequence obtained from Bill Tyne, unpubl.). The conserved region of the *polh* gene was used to generate a 295bp product and partial sequences of *lef-8* and chitinase genes were used to generate a 514bp and 566bp products respectively. The complete absence of even a partial sequence of the *egt* gene for *Spex*NPV necessitated the design of consensus primers. Consensus primers were designed on the basis of the cluster analysis of known sequences of other closely related NPVs obtained from Genbank, namely *Spodoptera littoralis* (*Splt*NPV; AF527603; protein ID, AAM93421.1), *S. exigua* (*Sex*NPV; NC002169; gene ID, 2715779), and *S. frugiperda* (*Sf*NPV; AY250076; protein ID AAP79109.1) (Table 3.3). Primers were designed to generate a 639bp product.

Table 3.3 Alignment of *egt* gene sequences

	5'- 3'
<i>Sf</i> NPV	ATCCGGTTTTTCGATAACAATC
<i>Splt</i> NPV	ATCCAGTGTTTCGACAACAATC
<i>Se</i> NPV	ATCCCGTTTTTCGACAACAATC
	799 820
Consensus egt5'	ATCC GGT TTTT CGA ACAATC
<i>Sf</i> NPV	CAAGGCAATTTGGTACACGG
<i>Splt</i> NPV	GAAGGCCGTCTGGTATACGG
<i>Se</i> NPV	CAAGGCGGTGTGGTACACGG
	CAAGGCAGTTTGGTACACGG
	GTTCCGTCAAACCATGTGCC
	1417 1438
Consensus egt3'	CCG TGT ACCAA ACT GCCTTG

Egt consensus primers were used to amplify a product of the *Spex*NPV *egt* gene using total *Spex*NPV wildtype, *S. littoralis* NPV, *S. exigua* NPV and AcMNPV DNA as a template (section 2.3.6). A band of approximately the correct size was successfully amplified for all four NPVs tested. Multiple bands though were observed for *Splt*NPV and *Se*MNPV DNA demonstrating the lack of specificity of the reaction for these NPVs. The PCR of *Spex*NPV DNA yielded a single band with extremely strong signal

(Figure 3.3). This band was excised from the agarose gel and a gel extraction kit (Qiagen) was used to extract the DNA fragment, which was then purified and sequenced in triplicate (section 2.3.7). The resulting consensus sequence generated after alignment (section 2.5.1) was used for the design of specific *Spex*NPV primers for the amplification of the *egt* gene (Table 3.4). Primers were designed to generate a 590bp product. The specificity of the new primers was confirmed through the failure to amplify *Split*MNPV, *Se*MNPV and *Ac*MNPV DNA while successfully amplifying *Spex*NPV DNA (gel not shown).

Table 3.4 Specific and consensus primers designed and used for PCR and sequencing of targeted genes to allow phylogenetic analysis of *SpexNPV* genotypes.

Gene	Type of primers	Name of primer	Oligonucleotide sequence (5' to 3') and position on gene	Product size (bp)
<i>Polyhedrin</i>	Specific	<i>Spexpolh1</i> (forward)	97 117	295
			AGC GGC AAA GAG TTT CTC AG	
		<i>SpexPolh2</i> (reverse)	GGT GTA CTC GGA ATG CAG GT	
			372 392	
<i>Lef-8</i>	Specific	<i>Spexl8f</i> (forward)	10 30	512
			CAT GGT GAA ATG ACT GTG GC	
		<i>Spexl8r</i> (reverse)	GGC GAA CAT TGA AAG ATG GT	
			502 522	
<i>Chitinase</i>	Specific	<i>Spexchit1</i> (forward)	29 50	566
			TCG CAT GTG TTG TAT GGA TTC	
		<i>Spexchit2</i> (reverse)	GAC GGC TAT TTT ATC GTT TCC	
			574 595	
<i>Egt</i>	Consensus	<i>Conegt1</i> (forward)	799 820	639
			ATC CGG TTT TCG ACA ACA ATC	
		<i>Conegt2</i> (reverse)	CCG TGT ACC AAA CTG CCT TG	
			1417 1438	
	Specific	<i>Spexegt1</i> (forward)	828 849	590
			ATC CGG TTT TCG ACA ACA ATC	
		<i>Spexegt2</i> (reverse)	CCG TGT ACC AAA CTG CCT TG	
			1398 1418	

kb

1 2 3 4 5 6

0.8 →
0.6 →
0.4 →

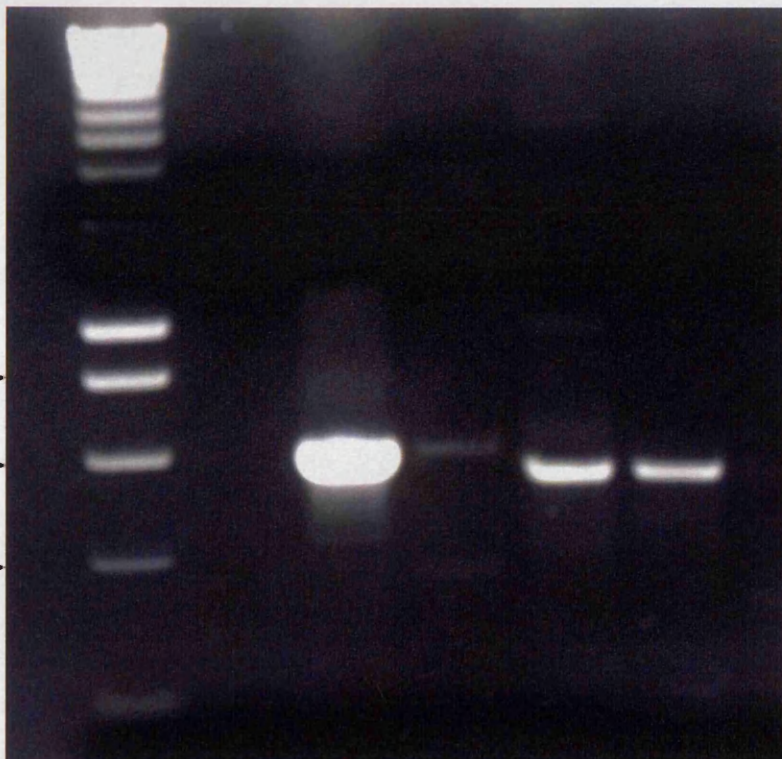


Figure 3.3 Analysis of PCR products on 1.2% agarose gel following amplification using consensus primers of the *egt* gene and *Spex*NPV DNA (3), *Splt*NPV DNA (4), *Se*NPV DNA (5) and *Ac*MNPV DNA (6). Negative control of reaction with DNA template replaced by distilled water (lanes 2). Lane 1, Hyperladder I (Bioline).

3.2.4 Amplification and sequencing of genes from *Spex*NPV genotypes

Total DNA was extracted from all 17 *Spex*NPV genotypes and wildtype virus (section 2.3.1). This DNA was used as a template for the amplification of fragments of each of the four genes (section 2.3.6) using the specific primers (Table 3.4). The specificity of the *Spex*NPV primers was confirmed by the failure to amplify *SpIt*MNPV, *Se*MNPV and *Ac*MNPV DNA while successfully amplifying *Spex*NPV DNA (gels not shown). Successful amplification was confirmed by analysing 5µl of the PCR product on a 1.2% agarose gel alongside the molecular marker, Hyperladder I (BioRad) as set out in section 2.3.4. The gel was stained with ethidium bromide (0.5µg/ml) and visualized using a UV imaging system in the usual way (section 2.3.4). Figure 3.4 shows the successful amplification of partial DNA sequences using the specific primers for the genes *lef-8*, *polyhedrin* and *chitinase* using *Spex*NPV DNA as a template. The lack of signal in the control reactions indicate the reactions were uncontaminated.

The resultant PCR products were purified using a PCR Purification Kit (Qiagen) and were sequenced by direct cycle sequencing (section 2.3.7). A total of six reactions (3 per strand) were set-up for each of the 17 genotypes and the wildtype virus to ensure a three-fold coverage of the consensus sequence. The sequence data were aligned and a consensus sequence generated for each PCR product (section 2.5.1).

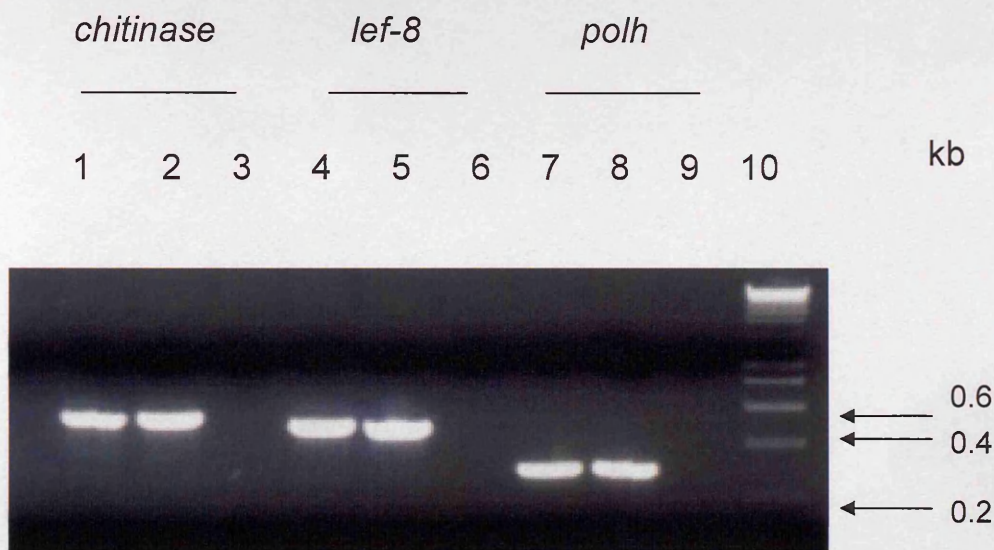


Figure 3.4 Analysis of PCR products on 1.2% agarose gel following amplification using *Spex*NPV DNA as a template and using specific *Spex*NPV primers of the chitinase gene (1-3), *lef-8* gene (4-6) and the polyhedrin gene (7-9). In negative controls of reactions (lanes 3, 6 and 9) *Spex*NPV DNA template was replaced by distilled water. Lane 10, Hyperladder I (Bioline). The amplification of the correct sized PCR products was confirmed for all PCR reactions of all genotypes and the wild-type virus prior to any sequencing being undertaken.

3.2.5 Phylogenetic analysis

The relationships between the sequences were represented as neighbour joining (NJ) rooted trees (section 2.5.2) using sequences from both *AcMNPV* and *SeMNPV* as out-groups. The robustness of the tree topology was estimated by 1000 bootstrap replicates using the program MEGA 2.1. Separate trees were constructed for *polyhedrin*, *lef-8*, *chitinase* and *egt* sequences to allow comparison of the phylogenies generated by the different genes.

3.3 Results

3.3.1 Genetic characterisation of individual genotypes

The DNA fragments produced from restriction enzyme digestion of the wildtype *SpexNPV* were designated alphabetically starting with A for the largest fragment for each enzyme digest (Figure 3.6), as proposed by Vlak and Smith (1982). A number of gels of various agarose concentrations (0.6-1.2%) were used to obtain estimates of the fragment sizes. Field Inverted Gel Electrophoresis (FIGE; section 2.3.5) was also carried out in order to gain more precise size estimates of the larger fragments. The sizing estimates for all three enzymes (*XhoI*, *BamHI* and *EcoRV*) were calculated as means from several different gels (Table 3.5). Molarity investigations of the single *SpexNPV* genotypes revealed that no bands co-migrated. Estimates of total genome size were taken as the mean size estimated using each enzyme (Table 3.6).

1 2 3 4 5 6 7 8 9 10 11 12 13 14 15 16 17 M₁ M₂

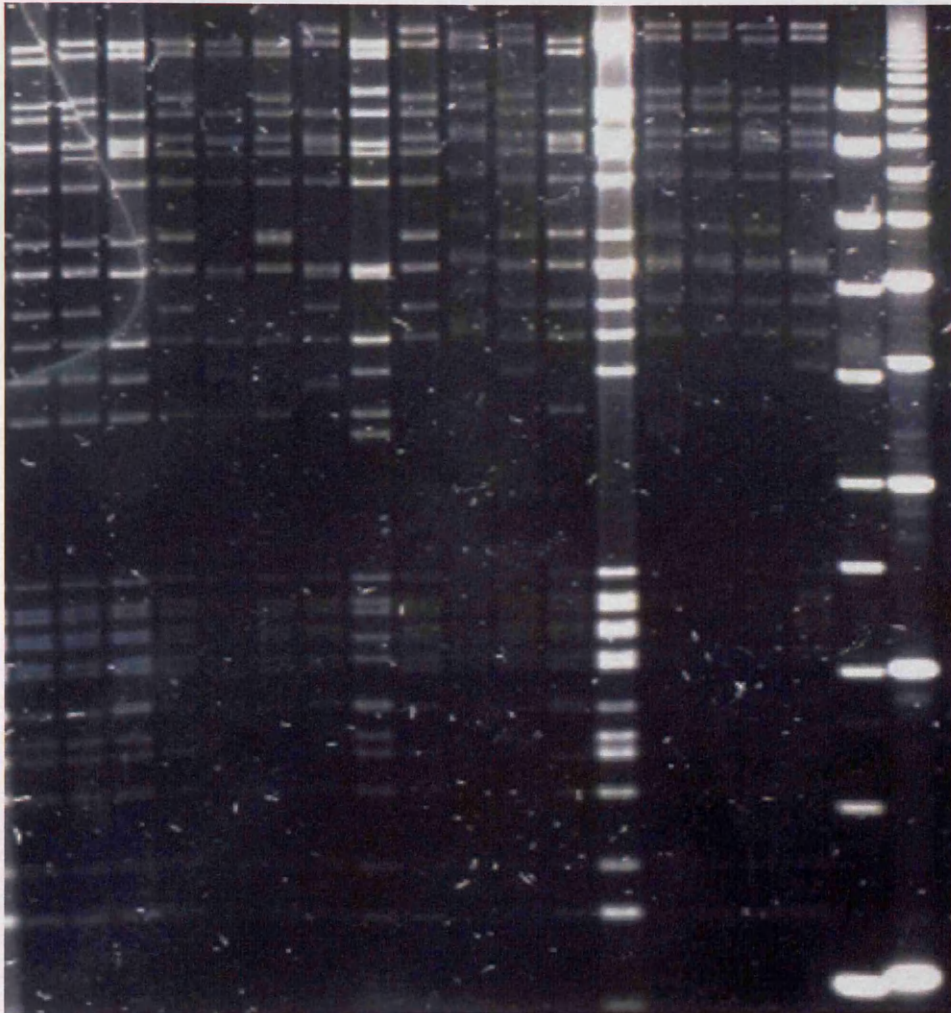


Figure 3.5 Restriction endonuclease profiles (*EcoRV*) of 17 *SpexNPV* genotypes isolated after four rounds of *in vivo* cloning from the wildtype virus. DNA fragments separated on 0.8% agarose gel run for 24 hours at 40V. Molecular markers: M₁, Hyperladder I (Bioline); M₂, 1kb ruler (BioRad).

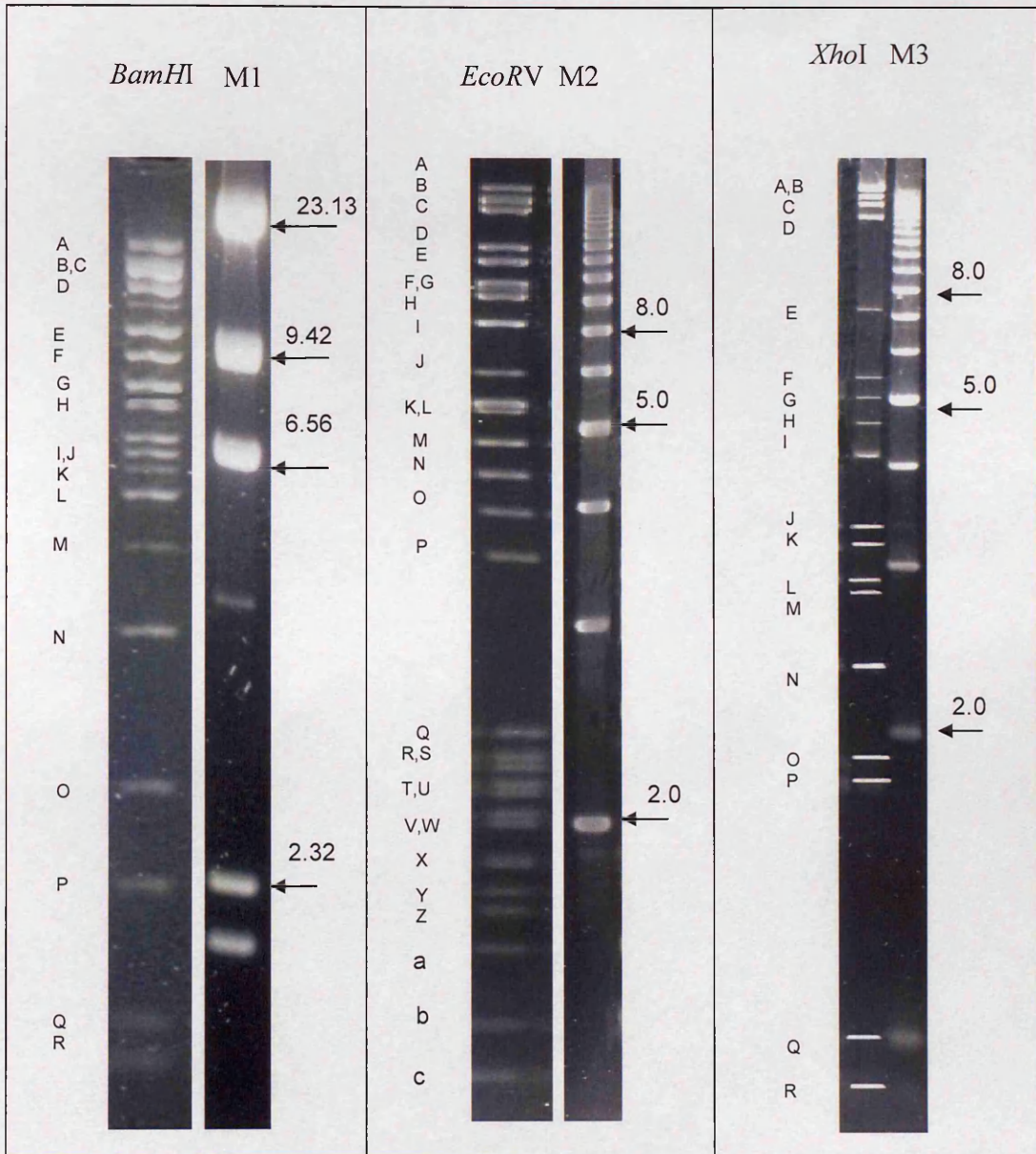


Figure 3.6 Restriction endonuclease profiles of wildtype *SpexNPX* DNA digested with *Bam*HI, *Eco*RV and *Xho*I showing alphabetical labeling of bands from largest to smallest. Molecular markers: M1, \square -*Hind*III DNA marker (Bioline); M2 and M3, 1kb ruler (BioRad). 0.8% agarose gels ran for 24 hours at 40V

Table 3.5 Mean size estimates of *Spex*NPV DNA fragments (kbp) produced after digestion with the restriction endonucleases, *EcoRV*, *BamHI* and *XhoI*. Means calculated from estimates gained from between 3 and 5 different gels.

Restriction enzyme	<i>EcoRV</i>	<i>BamHI</i>	<i>XhoI</i>
No. of gels used to calculate mean estimates	5	3	4
A	18.56	17.87	22.59
B	16.01	16.54	21.4
C	14.38	15.2	18.74
D	10.53	14.08	16.21
E	9.57	12.82	7.3
F	8.4	11.53	5.47
G	8.25	10.16	5.08
H	7.96	9.29	4.63
I	7.06	8.53	4.25
J	5.86	8.1	3.43
K	5.25	7.56	3.25
L	5.12	6.58	3.01
M	4.76	5.63	2.95
N	4.34	4.46	2.46
O	3.96	2.98	1.94
P	3.6	2.31	1.83
Q	2.5	1.68	1.03
R	2.36	1.55	0.94
S	2.32		
T	2.26		
U	2.2		
V	2.1		
W	2.07		
X	1.88		
Y	1.67		
Z	1.56		
a	1.33		
b	0.84		
c	0.61		

Table 3.6 Mean genome size estimates (kbp) of *in vivo* cloned *SpexNPV* genotypes

Genotype	<i>EcoRV</i>	<i>BamHI</i>	<i>XhoI</i>	Mean size of genotype (± 1 SE)
1	125.22	117.14	123.56	121.97 \pm 2.46
2	159.2	155.05	144.02	152.76 \pm 4.53
3	129.01	121.1	118.48	122.86 \pm 3.17
4	123.19	118.64	118.48	119.94 \pm 1.63
5	140.13	133.34	137.34	136.94 \pm 1.97
6	117.47	117.4	115.05	116.56 \pm 0.75
7	131.08	139.84	135.51	135.48 \pm 2.53
8	118.52	122.3	115.05	118.63 \pm 2.09
9	120.33	127.43	118.48	122.08 \pm 2.73
10	118.65	127.43	118.48	121.52 \pm 2.96
11	122.58	122.3	115.05	119.98 \pm 2.46
12	114.99	116.33	116.88	116.07 \pm 0.56
13	109.35	117.14	118.48	114.98 \pm 2.84
14	124.87	122.3	122.73	123.30 \pm 0.79
15	118.56	122.3	118.48	119.78 \pm 1.26
16	130.5	126.67	115.05	124.07 \pm 4.65
17	117.42	126.67	188.48	120.86 \pm 2.92

3.3.2 Phylogenetic analysis

Neighbour-Joining trees were generated for each gene sequenced and were rooted on the appropriate Genbank sequences from *AcMNPV* and *SeMNPV* (Figure 3.7-3.10). For all the genes investigated *SeMNPV* appears to be much more closely related to *SpexMNPV* than to *AcMNPV* with the exception of *lef-8* for which *SeMNPV* appears marginally more similar to *AcMNPV* than *SpexMNPV*. The level of variation witnessed between wildtype *SpexNPV* and these other related species of nucleopolyhedroviruses varies between genes with as little of 13% variation estimated for the highly conserved polyhedrin gene and as much as 39% for the much more variable *egt*. The level of sequence conservation between species is indicated for each gene in table 3.6. The level of variation seen between the *SpexMNPV* genotypes is very low with between 1.5% and 3% variation (Table 3.7).

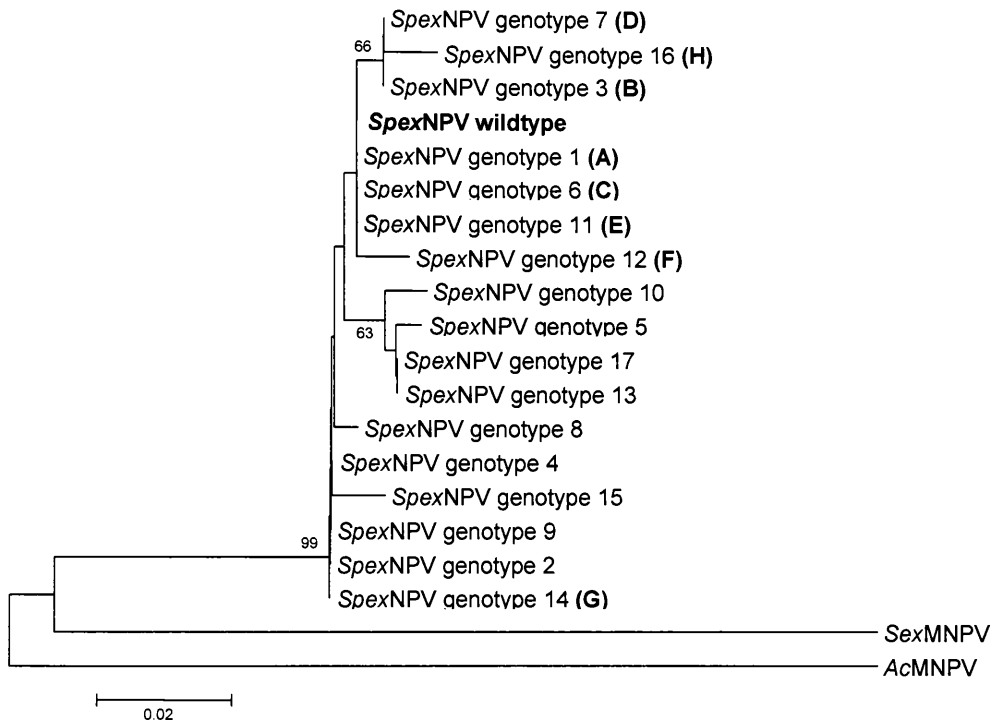


Figure 3.7 Phylogenetic analysis of 17 *SpexNPV* genotypes and wild-type *SpexNPV* using the polyhedrin gene and a neighbour-joining algorithm. Letters in brackets refers to *SpexNPV* genotypes chosen for biological characterisation (chapter 4). Trees rooted to *AcMNPV* and *SeMNPV*. Numbers given at each node are percentage bootstrap values (for 1000 repetitions). Genotypes appear not to cluster together to form any groups at a bootstrap value of 100 using polyhedrin.

Figure 3.8 Phylogenetic analysis of 17 *SpexNPV* genotypes and wild-type *SpexNPV* using the **chitinase** gene and a neighbour-joining algorithm. Letters in brackets refers to *SpexNPV* genotypes chosen for biological characterisation (chapter 4). Trees rooted to *SexMNPV* and *AcMNPV*. Numbers given at each node are percentage bootstrap values (for 1000 repetitions). Genotypes appear to cluster together at a bootstrap value of 100 to form two main groups.

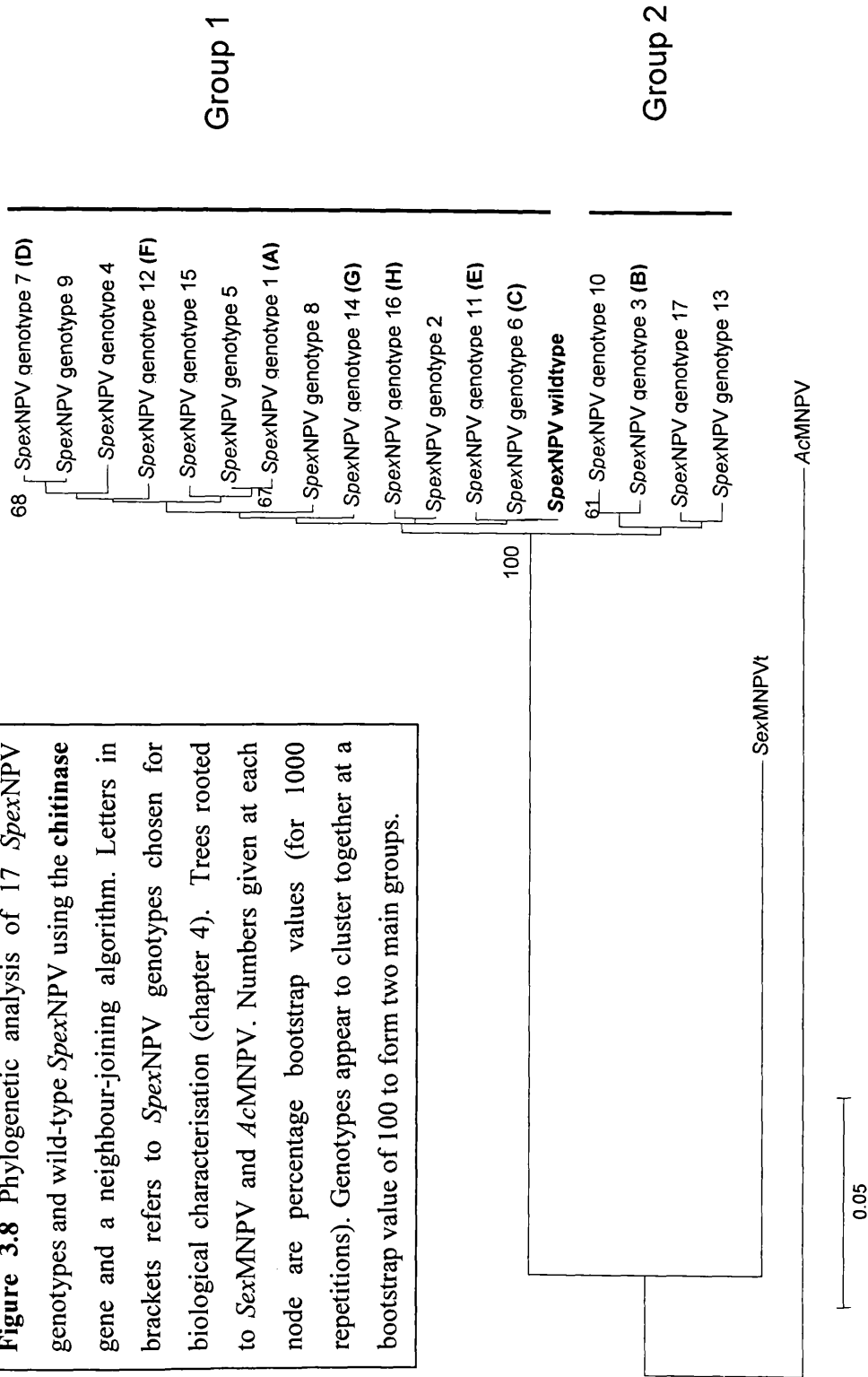
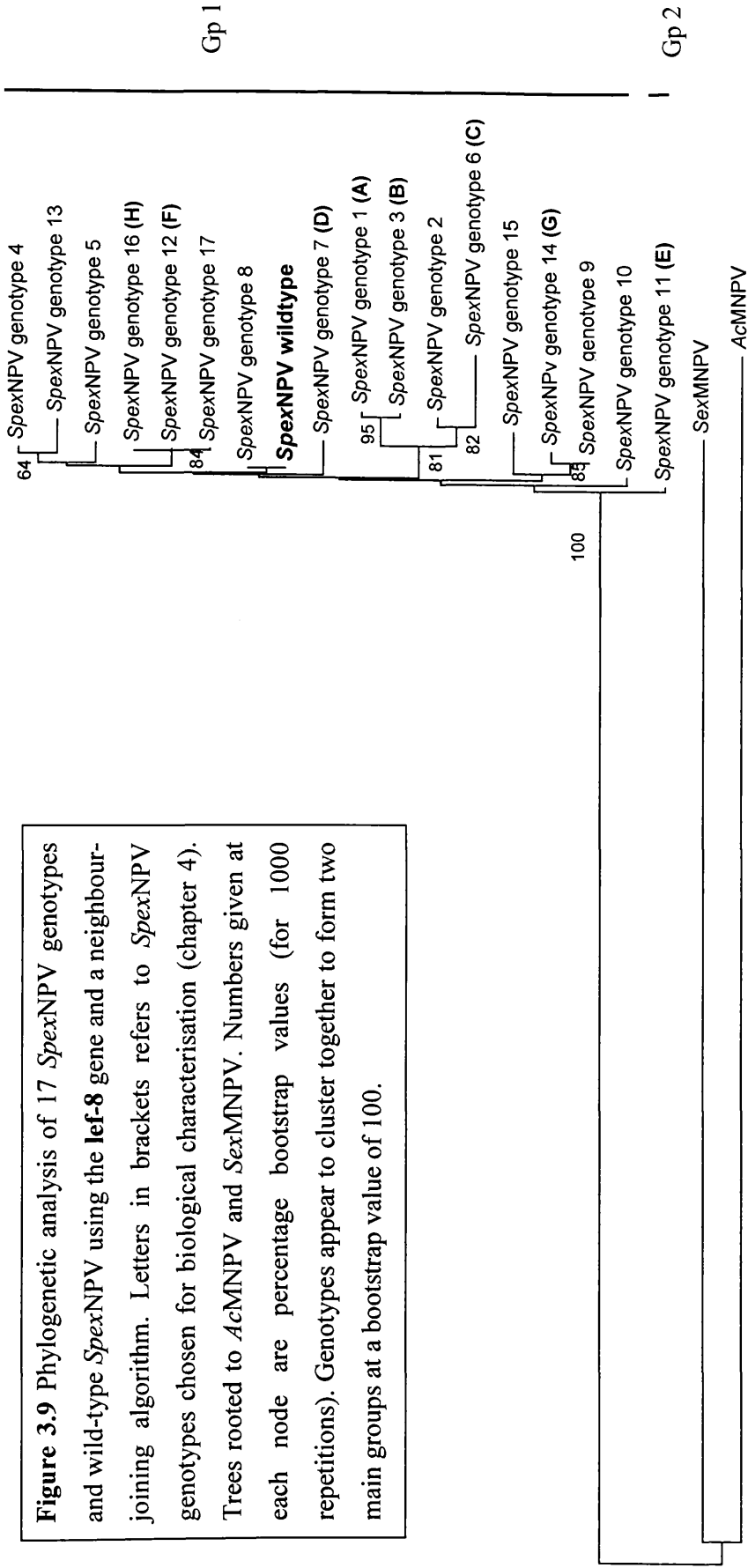


Figure 3.9 Phylogenetic analysis of 17 *Spex*NPV genotypes and wild-type *Spex*NPV using the *lef-8* gene and a neighbour-joining algorithm. Letters in brackets refers to *Spex*NPV genotypes chosen for biological characterisation (chapter 4). Trees rooted to *AcMNPV* and *SexMNPV*. Numbers given at each node are percentage bootstrap values (for 1000 repetitions). Genotypes appear to cluster together to form two main groups at a bootstrap value of 100.



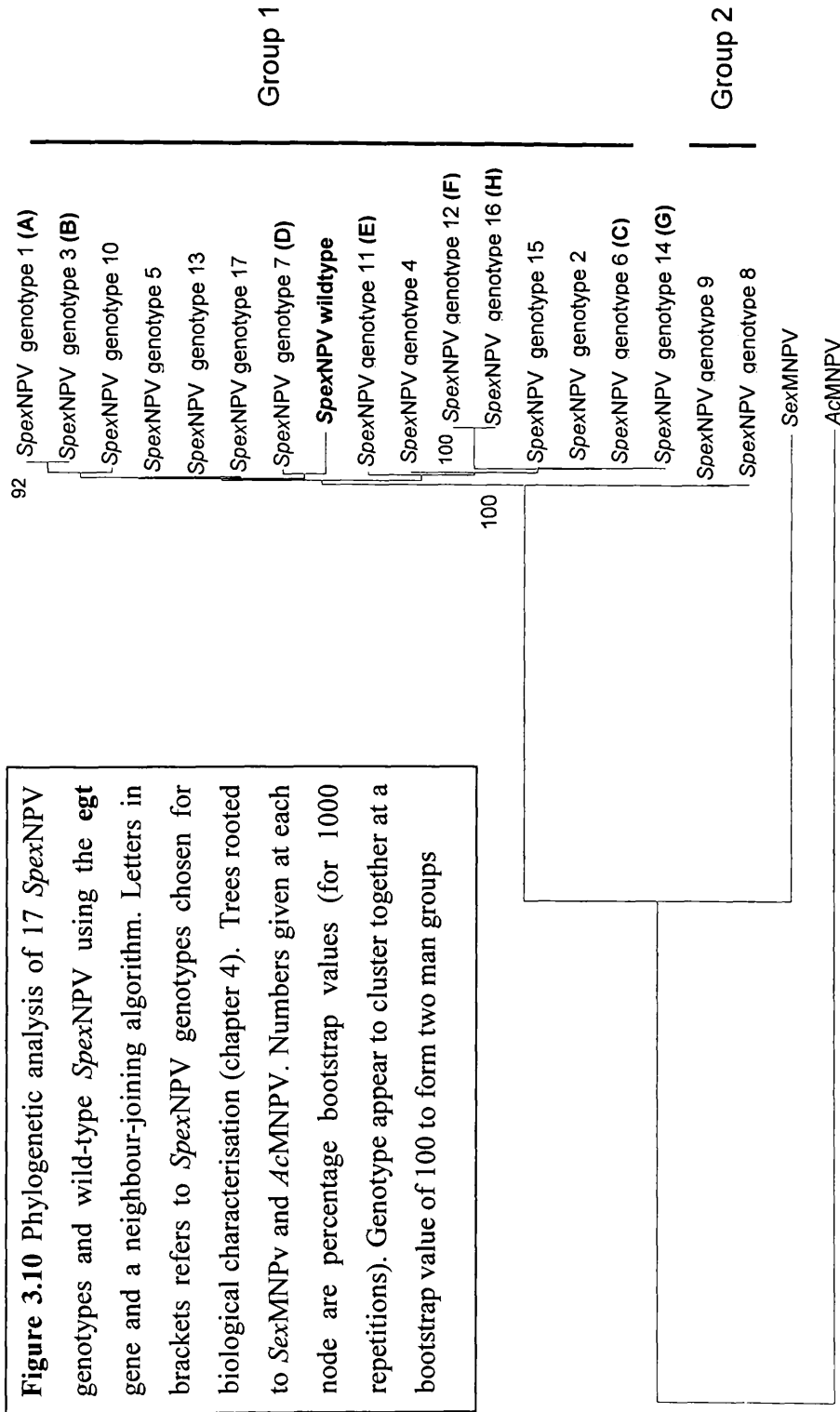


Table 3.7 Summary of maximum sequence divergence observed between different species of nucleopolyhedroviruses and between different genotypes of *SpexMNPV* following phylogenetic analysis with a range of genes (*polyhedrin*, *chitinase*, *lef-8* and *egt*).

Gene	Maximum inter-species variation (sequence divergence between <i>AcMNPV</i> , <i>SeMNPV</i> and wildtype <i>SpexMNPV</i>)	Maximum intra-species variation (sequence divergence between <i>SpexNPV</i> genotypes)
<i>polyhedrin</i>	13%	1.5%
<i>chitinase</i>	22%	1.6%
<i>lef-8</i>	29%	3%
<i>egt</i>	39%	2%

Bootstrap values are used to measure the robustness of certain branches when conducting phylogenetic analysis, and therefore indicates the confidence one can place in the relative position of an isolate in a tree. The high degree of conservation among the genotypes necessitated the use of the maximum bootstrap value (100) in order to investigate the exact relationship between the *SpexMNPV* genotypes. For the *chitinase*, *lef-8* and the *egt* genes, there is some evidence that certain genotypes are much more similar and therefore can be clustered together to produce groups. The groups are indicated on the phylogenies (Figure 3.8-3.10) and also summarized in table 3.8. Comparison of the *polyhedrin* sequences though, at a bootstrap value of 100, produced no apparent clustering (Figure 3.7). The groupings of the genotypes produced for the different genes were then compared to see if any general trend could be identified. The genotypes appeared to fall into completely different groupings depending on which gene was used for the analysis and therefore suggested that no clear conclusions could be made about the evolution and thus relatedness of the genotypes using single gene phylogenetic analysis except that they were very highly conserved (Table 3.8).

Table 3.8 Summary of groupings at a bootstrap value of 100 (for 1000 repetitions) of *Spex*NPV genotypes and wildtype following single-gene phylogenetic analysis using partial sequences of the chitinase, *egt*, *lef-8* and polyhedrin gene and a neighbour-joining algorithm. Trees rooted to *Ac*MNPV and *Se*MNPV.

Genotype	<i>chitinase</i>	<i>egt</i>	<i>lef-8</i>	<i>polyhedrin</i>
1	1	1	1	1
2	1	1	1	1
3	2	1	1	1
4	1	1	1	1
5	1	1	1	1
6	1	1	1	1
7	1	1	1	1
8	1	2	1	1
9	1	2	1	1
10	2	1	1	1
11	1	1	2	1
12	1	1	1	1
13	2	1	1	1
14	1	1	1	1
15	1	1	1	1
16	1	1	1	1
17	2	1	1	1
Wild type	1	1	1	1

3.4 Discussion

3.4.1 Cloning

Seventeen genotypes were successfully isolated from the wildtype *Spex*NPV virus. Although the number of larvae originally inoculated in the first round was kept deliberately high in order to increase the probability of detecting rarer genotypes, it is likely, that these genotypes simply represent a proportion of the total number of genotypes actually present in the wildtype virus. Only 35% of the progeny isolates produced after the initial low dilution inoculation were selected for RE analysis. The characterisation of the remaining first round isolates, and the elucidation of all discarded mixtures, would likely yield additional genotypes. This would have represented a massive logistical undertaking and was beyond the scope of this project.

The wildtype *Spex*NPV virus used in this study represents numerous infected cadavers and, theoretically, a much larger source of genotypic variation than just a single infected cadaver. *In vivo* cloning techniques have shown that a single *Panolis flamea* larva can be infected with as many as 24 different *Pf*MNPV genotypes at the same time (Cory *et al.*, 2005). Consequently, there is every reason to believe that many more genotypes have yet to be identified from the *Spex*NPV wildtype virus.

Although *in vivo* cloning is a relatively simple, if laborious, technique by which to isolate genotypes from mixed populations, care must be taken when interpreting results for multiple occluded NPVs as different genotypes could still be co-occluded in a single

OB and even a single virus particle and mixed infections can theoretically still result from infection by a single OB (Bull *et al.*, 2001). Plaque purification has been used to purify several genotypically distinct variants of *S. littoralis* NPV from what appeared to be a single *in vivo* cloned genotype, lacking any obvious sub-molar bands in RE profile (Cherry and Summers, 1985). Plaque purification requires permissive cell lines and for many baculovirus species this is prohibitive. A pilot study has shown that *Spex*NPV will propagate successfully in both *Sf9* and *Sf21* cell lines (E. Redman, unpublished data). Therefore, *in vitro* cloning offers a potential method to check the purity of the 17 *in vivo* produced *Spex*NPV genotypes.

Similarly, Hitchman (2002) used the recently developed BAC cloning techniques to reveal the presence of a second *PafI*NPV genotype from what was believed to be a single genotype isolated again by *in vivo* cloning (Cory *et al.*, 2005). Such examples clearly demonstrate the limitations of *in vivo* cloning as a technique to purify absolutely all genotypes present within mixed isolates, and the danger of categorically classifying genotypes as “clones”. By maximizing the number of passages used in the cloning process, as well as the number of different restriction enzymes used to screen for mixtures, the probability of isolating single genotypes is increased. However, its importance depends on the nature of the study. Genetic and biological characterisation can still be carried out on what is certainly the predominant genotype. Clonal purity would be considered a necessity in evolutionary experiments designed to assess mutation or recombination rate.

Another way to increase the likelihood of producing single genotypes is through the use of haemolymph containing budded virus which contain singly enveloped nucleocapsids, rather than OBs. This modification of Smith and Crooks' (1988) original method was utilized by Munoz *et al* (1998) to isolate seven distinct genotypes from a wildtype NPV isolate of *Spodoptera exigua* (Se-US2). Two of the seven genotypes, US2C and US2E were found to possess major deletions of 21kb and 14 kb respectively. Although these genotypes were abundant in the wildtype virus they were found to be completely noninfectious to 2nd and 4th instar larvae when administered *per os*. Their presence reduced the pathogenicity of the wildtype population by 3.6-fold, suggesting that they appear to act as parasitic genotypes in the virus population (Munoz and Caballero, 2000).

In my study because *in vivo* cloning was used which relies on *per os* infectivity, natural deletion-mutant genotypes, lacking *pif* gene expression, were not expected to be detected in the *Spex*NPV wild-type. Deletion mutants and parasitic genotypes increase the heterogeneity of virus isolates. The very fact that such minority genotypes are not eliminated is increasingly taken to indicate that these variants play an important functional role in virus persistence (Simon *et al.*, 2005). Restriction analysis of a naturally occurring deletion mutant, identified by plaque purification of *S. littoralis* NPV (strain M2), revealed a 4.5kb deletion within the *NotI* D fragment. The deletion mutant while retaining the ability to be infectious upon injection was unable to infect larvae *per os* (Kikhno *et al*, 2002). This biological phenotype was mapped to the deleted fragment by rescue experiments. Sequencing demonstrated that the fragment

was homologous to ORF19 of *AcMNPV* whose product is an occlusion body derived virion structural protein, necessary for the first stages of larval infection within the mid-gut (*per os infectivity factor, pif*) (Kikhno *et al.*, 2002). Mixed infection experiments of the *pif*-negative genotype and single complete genotypes resulted in enhanced levels of pathogenicity above single genotypes alones in contrast to the previous study (Simon *et al.*, 2005). The authors interpret this as an example of a synergistic relationship between the co-infecting genotypes with the mutant conferring a fitness advantage through increased mortality and thus, in theory, increased transmission.

Another approach which involved the alternate use of larvae and cells for the cloning of *SeMNPV*, was adopted by Dai *et al.* (2000) to generate a deletion mutant, SeXD1 which lacked a 10593bp region of its genome and the genes, p10, chiA, v-cath, egt, gp37 and ptp2 (Ijkel, 1999). The deletion mutant retained the ability to replicate both *in vitro* and *in vivo* and possessed a superior speed of kill to the wildtype virus (25% lower ST₅₀). This has not only important implications for the development of *SeMNPV* bioinsecticides but also offers a procedure that balances the *in vivo* and *in vitro* selective forces and therefore offers the most realistic approach for the isolation of the full range of genotypes in wild type populations, be they fully functional or helper-virus dependent.

The presence of persistent baculovirus infections in many laboratory and field populations of larvae (Hughes *et al.*, 1993, 1997) also needs to be considered when virus is passaged through larvae. The *Spodoptera exempta* insect stock used for the *in*

vivo cloning of this study has been shown, through the use of RT-PCR technology, to harbour a low level *Spex*NPV infection (Vilaplana, L, *et al.* unpublished). The expression or recombination of the persistent virus with the isolate being passaged may produce a distorted representation of the parent population under study. However, continued monitoring of progeny virus significantly reduces the possibility of contamination from this source.

One method, which circumvents both the problems created by the artificial selective forces generated *in vitro* and also the highlighted drawbacks of *in vivo* cloning, is BAC cloning. BAC cloning is the linearization and ligation of a complete genome into a bacterial artificial chromosome (Hitchman, 2002). The first stage of this process involves the identification of a restriction enzyme to digest the genome of interest at a single site. The digested genome is then cloned directly into a BAC vector by and is then propagated in *E. coli* cells of which individual plaques, in theory, represent individual genotypes. There remain several issues that still need resolving with this approach. The first is the identification of a single cutting enzyme. For many species whose whole genome has yet to be sequenced this represents a singularly laborious screening procedure. In addition, the ability to recover cloned genotypes has yet to be successfully demonstrated and there is some evidence that genotypes of different sizes are cloned differentially with smaller ones being more easily cloned than the larger genotypes. Although this technology is in its infancy it offers a powerful tool for the future to allow the isolation of single genotypes without having to negotiate the problems associated with the established methodologies. A considerable number of

restriction enzymes (approx. 60) were screened for their single-site cutting potential of *Spex*NPV DNA which would have allowed this procedure of cloning to be carried out for *Spex*NPV. Unfortunately no such enzyme was identified and consequently the *in vivo* cloning approach was adopted instead for this study.

3.4.2 Sizing genome

The molecular size of the genomes of the individual genotypes was estimated from restriction digestion and, for the majority of the genotypes, was approximately 120 kbp in size (mean = 123.99 kbp, n = 17 genomes). This is comparable to other NPV genomes which have either been estimated using the construction of physical maps from restriction digestion or directly through sequencing of the complete genome. The genome of *Ac*MNPV was estimated as 133.9 kbp (Ayres *et al.*, 1994), *Mamestra configurata* B MNPV as 155.0 kbp (Li *et al.*, 2002), *Spodoptera exigua* NPV as 135.6 kbp (Ijkel *et al.*, 1999) and *Spodoptera litura* NPV as 139.4 kbp (Pang *et al.*, 2001). The size of the genotypes varied from the largest estimated as 152 kbp (genotype 2) to the smallest which was estimated as 114.98 kbp (genotype 13). This differential genome size is quite considerable and warrants further study. The precise nature of the genomic variation could be mapped in order to identify the deletions and insertions to have taken place. Large genomic deletions have been mapped in other studies to specific genes known to produce significant alterations of the biology of the virus. For example, a 4.5 kb deletion of *S. littoralis* MNPV has been mapped to the *pif* gene which is responsible for infectivity of the baculovirus *per os* (Kikho *et al.*, 2002) as discussed above.

3.4.3 Phylogeny

Single-gene phylogenetic analysis was carried out to investigate the relatedness of the *in vivo* cloned genotypes isolated from a natural *Spex*NPV population. Each of the four genes used generated similar tree topologies but the clustering of the genotypes into groups exhibited marked heterogeneity. A high level of heterogeneity was also observed between trees when 30 separate single-gene analyses were carried out to compare 13 baculovirus genomes, for which their complete genomes were available, with no two single-gene analyses giving the same tree (Herniou *et al.*, 2003). The production of heterogeneous tree topologies coupled with the inability to resolve branches with high statistical support could reflect differences in the phylogeny of individual genes due to recombination. Alternatively, such variation may simply be the result of using genes with differential rates of evolution or using gene sequences possessing weak phylogenetic signals (Herniou *et al.*, 2001).

Recombination is known to occur between co-infecting baculoviruses (Crozier and Ribeiro, 1992; Kondo and Maeda, 1991) and baculoviruses and their hosts (Wang *et al.*, 1989). The influence such gene exchange may have had on shaping baculovirus evolution is unclear. For other viruses where horizontal gene exchange has long been acknowledged as a strong evolutionary driver (Holmes *et al.*, 1999) the ability of phylogenetic trees to represent evolutionary history has been brought into question (Doolittle, 1999).

By using genes with such a divergent range of biological functions, which have presumably been exposed to differential selection pressures, it is quite conceivable that the variation in tree topologies could simply reflect differing rates of evolution of the genes. *Polyhedrin* and *lef-8* are both essential genes and as such are in theory, under extremely strong selection pressure. *Egt* and chitinase genes on the other hand, are auxillary genes and are not directly involved in the infection process. Although they offer some selective advantage to the virus through the facilitation of OB dissemination (*chitinase*), and through the delaying of host death and the optimization of productivity (*egt*) they are under considerably less selection pressure and presumably possess slower rates of evolution.

Genes with weak phylogenetic signal have also been cited as the reason for conflicting phylogenetic trees. The polyhedrin gene offers a case in point and has often produced erroneous evolutionary inferences (Herniou *et al.*, 2001; Bulach *et al.*, 1999). Thus the choice of sequence is vital. Large DNA polymerase genes have been used to create phylogenies with strong resolution (Bulach *et al.*, 1999; Nielsen *et al.*, 2002) and *lef-8*, encoding a large sub-unit of RNA polymerase II, has been used to successfully identify the ancient co-evolution of baculoviruses and their hosts (Herniou *et al.*, 2004).

Although single-gene analysis produced a range of different trees a majority rule consensus tree was generated from the 30 separate single gene analyses in the study by Herniou *et al.* (2003) and demonstrated that certain divisions could be supported by the majority of genes. The separation of *Cumi*NPV from the lepidopteran viruses, the

division of GVs' and NPVs' and the division among Group 1 NPVs were all resolved. However, the branches within Group II NPVs and GVs' possessed only low percentage values demonstrating that even the use of 30 genes to generate a consensus tree failed to find agreement between genes on the relationships of these baculoviruses (Herniou *et al.*, 2003).

Combination of all the gene alignments allows a single analysis to be conducted of all the sequence data at the same time. This reduces sampling error and has been shown to increase the strength of the phylogenetic signal of single-gene datasets. This approach was used successfully for the phylogenetic analysis of metazoans based on mitochondrial genomes (Nikaido *et al.*, 2001), for the phylogeny of herpesviruses (McGeoch *et al.*, 2000), the large scale analysis of prokaryotic genomes (Sicheritz-Ponten and Andersson, 2001) and also for the phylogeny of baculoviruses (Herniou *et al.*, 2003). This potentially could circumvent the problems encountered with the single-gene approach adopted in this study and resolve the actual phylogenetic relationships of the *Spex*NPV genotypes.

To date very little data exists on the nature of the evolutionary history of single genotypes from the same species. Although trees (dendograms) have been constructed to represent the similarity of individual genotypes of the same species, they have been based on RFLP analysis not sequence data and therefore have not attempted to address the question of relatedness.

In the only other study to investigate the phylogeny of individual genotypes of the same species, single cadaver field isolates of winter moth NPV (*OphuNPV*) were collected from heather moorland in Orkney from spatially separate field sites in an attempt to correlate relatedness to spatial distribution. Sequence data of the polyhedrin gene was generated from a total of 26 isolates, which appeared to represent just single distinct genotypes, and used to construct a phylogenetic tree. Although the study provided evidence for the clustering together of the genotypes to produce three separate groups (high bootstrap values) these did not relate to spatial distribution of the virus (Graham *et al*, 2004). In addition, the phylogeny was based on just a single gene and a gene whose usefulness in these types of studies, as previously discussed, has been brought into question.

Chapter Four

Biological characterisation of *Spex*NPV genotypes isolated *in vivo*

Chapter 4: Biological characterisation of *Spex*NPV

genotypes isolated *in vivo*

4.1 Introduction

Although the isolation of 17 individual constituent genotypes from the wildtype *Spex*NPV isolate confirms the anticipated heterogeneity of natural populations it is unclear whether this variation is neutral or carries biological significance. Therefore phenotypic characterisation of the individual *Spex*NPV genotypes was required to ascertain whether variation at the molecular level actually conferred biological differences which could potentially impact host-virus evolution and dynamics. Natural selection is defined as the process by which, genotypes in a population that are better adapted (fitter) in a certain environment, increase in frequency relative to less well-adapted genotypes. Consequently, the presence of variance of individual phenotypic traits believed to directly contribute to fitness, is essential for selection to occur (Fairbairn and Reeve, 2001).

Fitness is a difficult parameter to measure especially for microparasites but for NPVs' it is a function of both the rate of degradation of transmission stages (OBs) and the rate of uptake of OBs by susceptible hosts (Cory *et al.*, 1997). The estimation of transmission parameters and degradation rates requires large field trials and is a large logistical undertaking and therefore has not been attempted in this study though the transmission

parameter has been estimated previously for *SpexNPV* at different larval rearing densities (Reeson *et al.*, 2000) who found that transmission was significantly higher among larvae reared in isolation than among those reared in crowds.

Numerous biological traits contribute to the transmission and persistence and consequently, to the overall fitness of a virus isolate. These include the duration of infection, pathogenicity, the ability to liquefy ones host to facilitate efficient horizontal transmission, the yield of OBs produced upon death as well as the ability to produce structurally robust occlusion bodies for the enhancement of persistence in the environment. The standard procedure for the biological characterisation of genotypes in the laboratory is through the challenge of homogenous stock insect populations with a range of doses of the virus isolate under investigation. From such biological assays estimates of three commonly studied life-history traits, can be simultaneously obtained namely pathogenicity, speed of kill and yield of occlusion bodies.

Pathogenicity, defined as the capacity of the nucleopolyhedrovirus to cause lethal infection in the host, is traditionally described using estimates of LD₅₀, which is the dose required to kill 50% of the hosts being challenged. Pathogenicity will correlate positively with fitness because infection is required for replication. The speed of kill is equivalent to the duration of infection of the virus and is measured from initial infection to the time the host dies. A fast speed of kill is assumed in other host-parasite systems to confer a positive fitness advantage to the virus when competing alongside other

isolates or microparasites within the same host (Frank, 1996). Yield describes the number of occlusion bodies produced upon death. NPVs tend to convert the bulk of the hosts' internal tissue before lysing the cuticle and therefore the larger the larvae the greater the yield.

Biological organisms evolve and develop as integrated units and consequently any given morphological, behavioural, or physiological phenotypic trait can be potentially correlated with many other traits (Fairbairn and Revve, 2001). In order to understand evolutionary responses to selection and to test adaptive hypothesis it is vital to study the correlation between fitness traits. The study of phenotypic trait relationships is also useful for the identification of trade-offs between fitness traits. The theory of life history evolution is dominated by the premise that combinations of trait values are constrained by trade-offs between the two traits (Roff, 2002). Many trade-offs are believed to result from the partitioning of finite resources among the various needs of the organism (James, 1974; Riska, 1986; Houle, 1991). For baculoviruses, a larva represents a finite resource and there is growing evidence for an important trade-off between speed of kill and virus yield in several nucleopolyhedrovirus-host systems (Burden *et al.*, 2000, Hernandez-Crespo *et al.*, 2001, Wilson *et al.*, 2000). Speed of kill clearly affects yield by altering the absolute host tissue available for conversion into progeny occlusion bodies. This and any other possible relationships between traits have been investigated in a biological study of four genotype variants of *Panolis flamea* NPV (Hodgson *et al.*, 2001) using fitted values produced following their estimation in bioassay. Although inter-genotypic trade-offs were not identified in this study it was

postulated that this most likely simply reflected the low sample size available in the study.

Therefore a series of large scale bioassays were conducted on eight of the *EcoRV* genotypes (A-H) and the wildtype isolate in order to gain accurate estimates of pathogenicity, speed of kill and yield. The relationships between the traits were examined using regression coefficients with a sample size of eight which was hoped would increase the sensitivity of the analysis.

4.2 Materials and methods

4.2.1 Bioassay design

In order to gain an accurate biological profile of the individual 8 genotypes they were bioassayed against the parent wild type (WT) virus. Newly moulted third instar larvae were challenged with a range of five doses (50 000, 10 000, 5 000, 1 000, 500 OBs per larva) using the diet-plug inoculation method (see section 2.4.1). Twenty five larvae were infected per dose, except for the lowest two doses for which 50 larvae were used in order to produce sufficient numbers of cadavers for yield and time to death analysis. An additional 25 larvae were dosed with sterile distilled water to act as controls. Treatment was replicated within the experiment (2 reps) and the entire bioassay was also repeated (2 blocks, two weeks apart) using new aliquots of the same viral stocks and a lower dose range (5000, 1000, 500, 100 and 50 OBs) because too many died at the higher doses. Virus mortality was confirmed using geisma staining (see section 2.4.2) and the insects were monitored every 8-16 hours to produce estimates of

pathogenicity and speed of kill until death or pupation. Speed of kill was calculated from the time larvae were first introduced into the dosing arena to the time death. This method may have produced an overestimate of actual time to death but will have been consistent across treatment. Ten cadavers per dose for each virus treatment were randomly selected for yield analysis across a range of timepoints in order to estimate the number of progeny OBs produced at death (see section 2.4.3). In addition, four cadavers from each genotype treatment were randomly selected to confirm that the genetic identity of the virus remained constant after bioassay using RFLP profiling with the endonuclease *EcoRV* (see section 2.3.3).

4.2.2 Determination of viral infection

None of the control larvae died of virus, demonstrating the absence of contamination in the experiment. Non-viral deaths, predominantly bacterial, did occur but only at a very low level (< 5%) late in the assay and resulted in death, often while the insects were attempting to pupate. Geisma staining (see section 2.4.2) of these cadavers was carried out to ascertain whether a mixed infection could be involved i.e. virus induced mortality. The lack of OBs and the fact that such deaths were seen in both control and treatment larvae meant that such non-viral deaths could be justifiably removed from the dataset.

4.2.3 Data analysis

For the analysis of viral mortality the data were logit transformed ($\text{logit} = \ln(p/(1-p))$, when p = proportional mortality) and modelled assuming a binary error structure.

Deviances were adjusted via the scale parameter to allow for over dispersion of the data. Speed of kill and yield data were transformed (speed of kill² and sqrt(yield)) and analysed using a normal error structure. In all analyses, block, and genotype were assigned as factors and dose was treated as a covariate in the full model. Yield analysis also included speed of kill as a second covariate. All transformations and error structures satisfied model-checking procedures (GLIM version 3.77, 1985 Royal Statistical Society)

4.3 Results

4.3.1 Purity and stability of genotypes

All *SpexNPV* virus genotypes produced at the end of the infection cycle matched that of the dosing virus, demonstrating the stability of the single genotypes (Figure 4.1). As expected, the RFLP profile of the progeny virus from the WT treatment produced a variety of profiles.

1 2 3 4 5 6 7 8 9 10 11 M M 12 13 14 15 16 17 18 19 20 21 22 23 24 25 26 27 28 29 M M 30 31 32 33 34 35

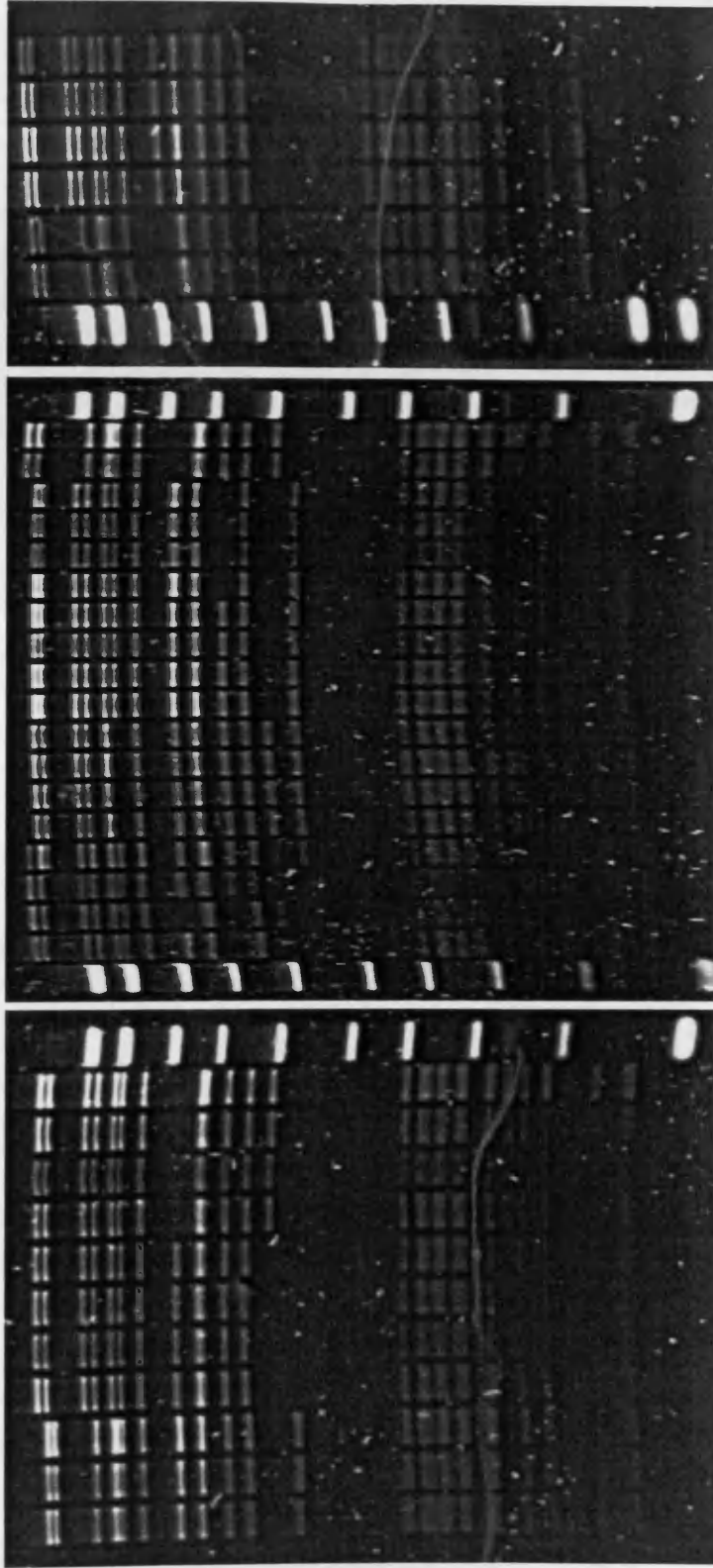


Figure 4.1 *EcoRV* restriction endonuclease profiles of *SpexNPV* genotypes A-H and wild-type virus after *in vivo* passage in bioassay. Lanes: 1-3, (C); 4-7, (B); 8-11, (A); 12-15, (wild-type virus); 16-19, (H); 20-23, (G); 24-27, (F); 28-31, (E); 32-35, (D). Molecular marker (M), hyperladder I (Bioline). 0.8% agarose gels run at 40V for 24 hour.

4.3.2 Pathogenicity

The LD₅₀ estimates for the *Spex*NPV genotypes spanned an impressive range, with genotype H more than seven times more pathogenic than genotype A (Figure 4.2). The WT virus proved to be more pathogenic than any of the clones derived from it with at least a 2-fold difference and at most a 9-fold difference between its LD₅₀ value and genotype H and genotype A, respectively. Genotypes B, G and H appeared to be similarly pathogenic and caused a much higher level of mortality than genotypes A, C, D, E and F, which also appeared to share a similar level of pathogenicity.

Although LD₅₀ estimates are a useful summary statistic at times they may offer an oversimplified perspective of pathogenicity, particularly in instances where different pathogen isolates do not respond in the same way to dose. Therefore, an analysis of covariance was also carried out to explore how pathogenicity (mortality) altered with virus dose. Block ($\chi^2_1 = 0.62$, $P = 0.431$) and repetition ($\chi^2_1 = 0.38$, $P = 0.538$) were both found to be insignificant terms and were thus removed from the model. As expected, virus dose had a considerable influence on pathogenicity ($\chi^2_1 = 668.4$, $P < 0.001$) with higher mortality seen at the higher doses. Although genotype proved to be a significant predictor of mortality ($\chi^2_2 = 79.1$, $P < 0.001$), all the genotypes along with the WT virus, responded in a similar fashion to virus dose (genotype*dose: $\chi^2_8 = 11.02$, $P = 0.201$; Figure 4.3).

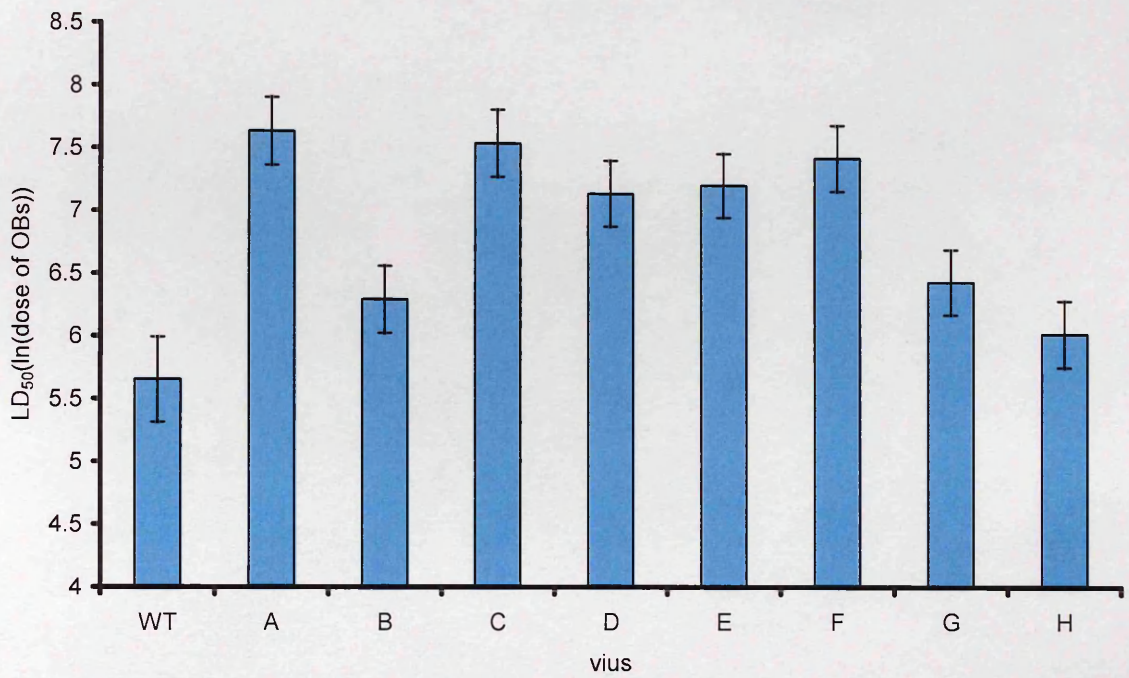


Figure 4.2 LD₅₀ estimates ($\pm 95\%$ confidence intervals) for genotypic clones A-H of *SpexNPV* and wild type parent virus in 3rd instar *Spodoptera exempta* larvae.

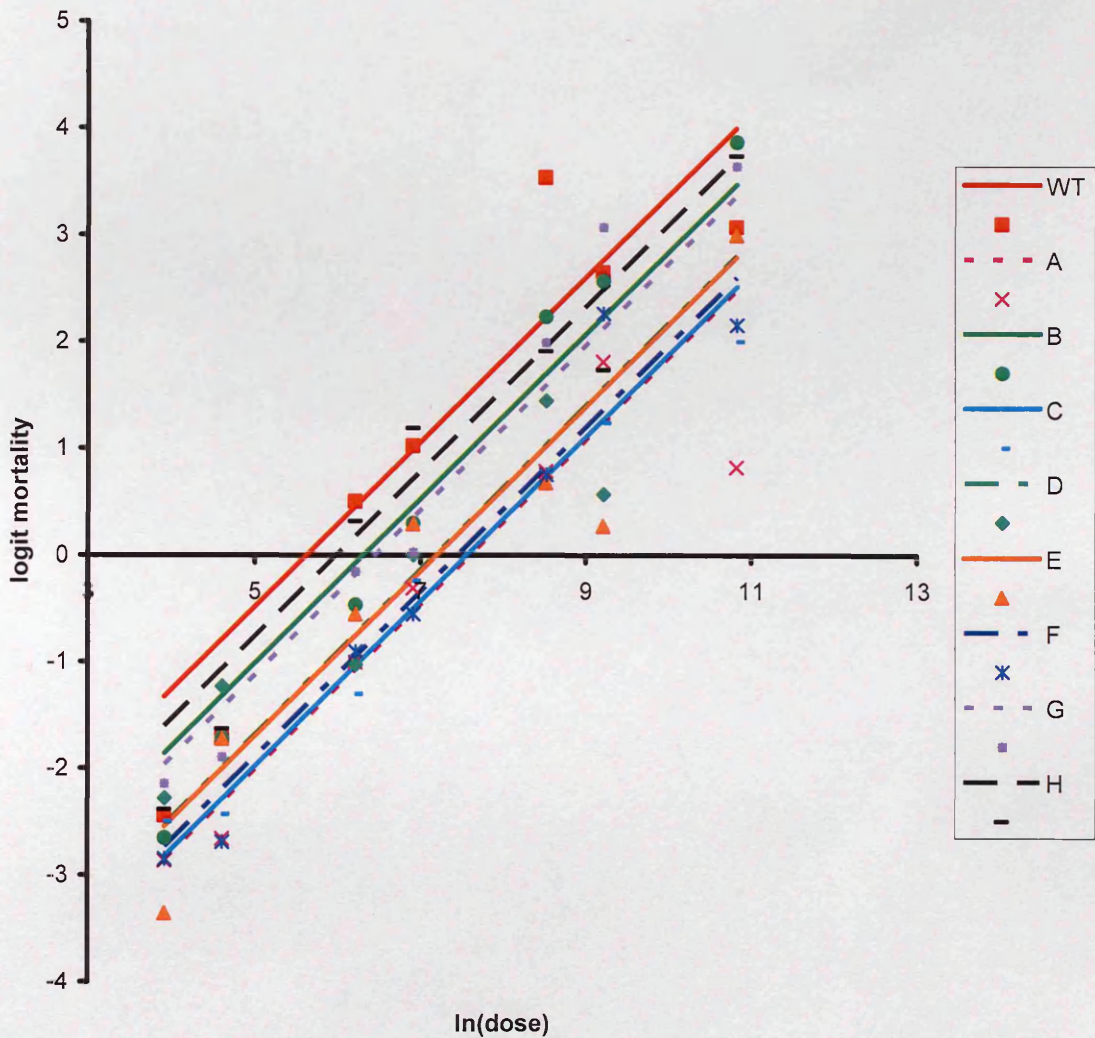


Figure 4.3 Dose-mortality curves of genotypic clones (A-H) and WT *SpexNPV* in 3rd instar *Spodoptera exempta* larvae. Fitted lines represent minimal adequate model fitted by ANCOVA: genotype A (intercept = -5.886), genotype B (intercept = -4.884), genotype C (intercept = -5.85), genotype D (intercept = 5.557), genotype E (intercept = -5.557), genotype F (intercept = -5.762) genotype G (intercept = -4.995), genotype H (intercept = -4.636) and WT (intercept = -4.356). Gradient of all lines = 0.774. Symbols represent mean observed values.

It was evident from inspection of Figure 4.3 and the estimates from the statistical model that several of the variants were similar and thus it might be possible to group them without a significant increase in residual deviance. The genotypes were clustered into three groups (ACDEF, BGH, WT). This change in deviance and change in degrees of freedom between the two models was tested for significance and produced a non-significant increase in residual deviance ($F_{6,165} = 0.9228$, $P = 0.48$). This was taken to be the simplest and best model to explain the dataset. Grouping the genotypes, however, produced a significant interaction between virus genotype and dose, resulting in the ACDEF grouping having a shallower response to increasing dose than the other viruses ($\chi^2_2 = 7.39$, $P < 0.03$; Figure 4.4).

Figure 4.5 shows the back transformed LD_{50} estimates of the genotypes and the wildtype virus after statistical grouping on the basis of analysis of covariance with dose.

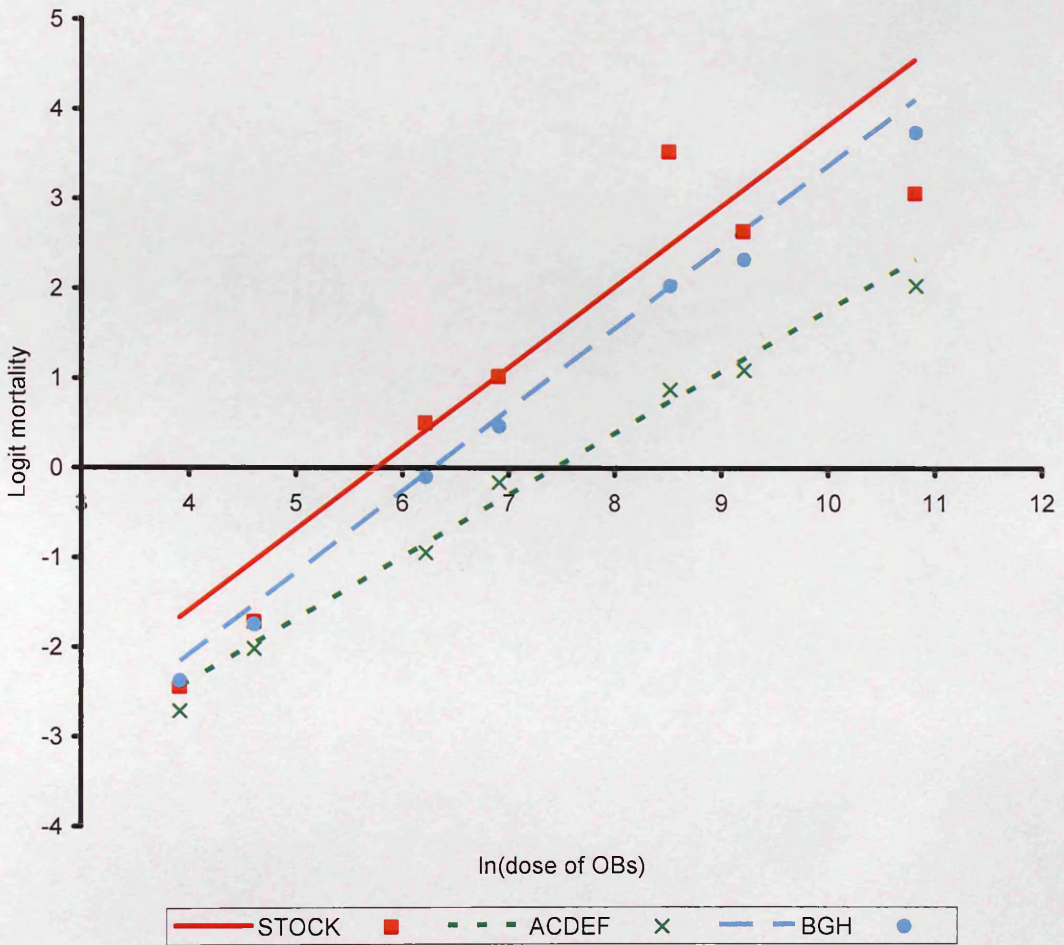


Figure 4.4 Dose-mortality curves of grouped genotypic clones (A-H) and wild type *SpexMNPV* in 3rd instar *Spodoptera exempta* larvae. Fitted lines: WT virus, $\text{logit}(\text{mortality}) = -5.14 + 0.69(\ln(\text{dose}))$; A,C,D,E and F, $\text{logit}(\text{mortality}) = -5.72 + 0.91(\ln(\text{dose}))$; B,G and H, $\text{logit}(\text{mortality}) = -5.21 + 0.90(\ln(\text{dose}))$. Symbols represent group mean of observed values.

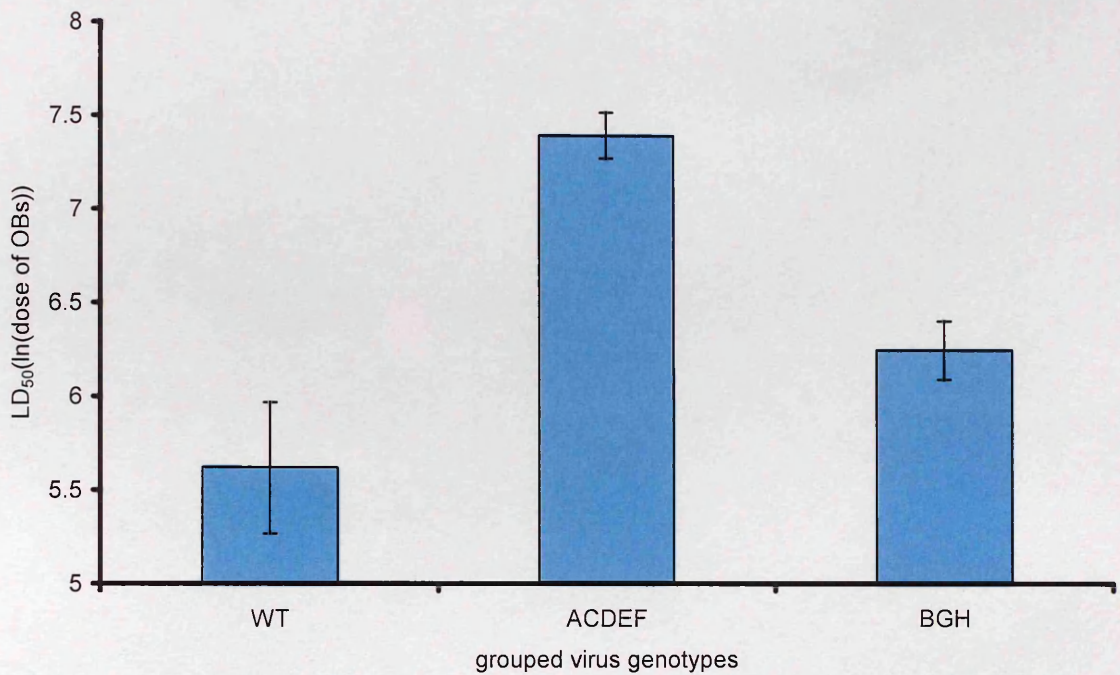


Figure 4.5 LD₅₀ estimates ($\pm 95\%$ confidence intervals) for genotypic clones A-H and wild type virus grouped on the basis of analysis of covariance with dose.

4.3.3 Speed of kill

Comparison of the frequency distributions for the speed of kill data revealed significant differences between the mean speeds of kill of the two blocks and as a consequence a bimodal distribution when the two blocks were combined. Transformation of the combined data failed to produce normality and allow analysis of the blocks together. Block 1, because of its higher dose range, produced many more data points for speed of kill which covered a much larger range, than block 2 and consequently was used in preference to block 2, for analysis of covariance with dose.

The data were transformed (x^2) and analysed using a normal error structure. Genotype was treated as a factor and the natural log (ln) of dose was assigned as a covariate both as a linear and a quadratic term. Genotype was found to be an important indicator of speed of kill although the genotypes responded differently to dose (genotype*dose, $F_{8,1519} = 4.07$, $P < 0.001$; Figure 4.6). Increasing virus dose clearly produces a faster speed of kill for most *SpexNPV* genotypes, the exception being genotype F whose speed of kill remains unchanged irrespective of dose. The speed of kill of the WT virus appeared to alter the most with dose. Although lower doses lengthened speed of kill, the contribution of dose as a quadratic covariate produced a plateau at lower doses for the genotypes (but not the wild type) ($F_{1,1519} = 14.7$, $P < 0.0001$; Figure 4.6), suggesting that they possess a minimum dose below which speed of kill is unaffected by initial dose. For the WT virus, which is more pathogenic than the single genotypes (lower LD_{50}), no plateau is apparent at lower doses.

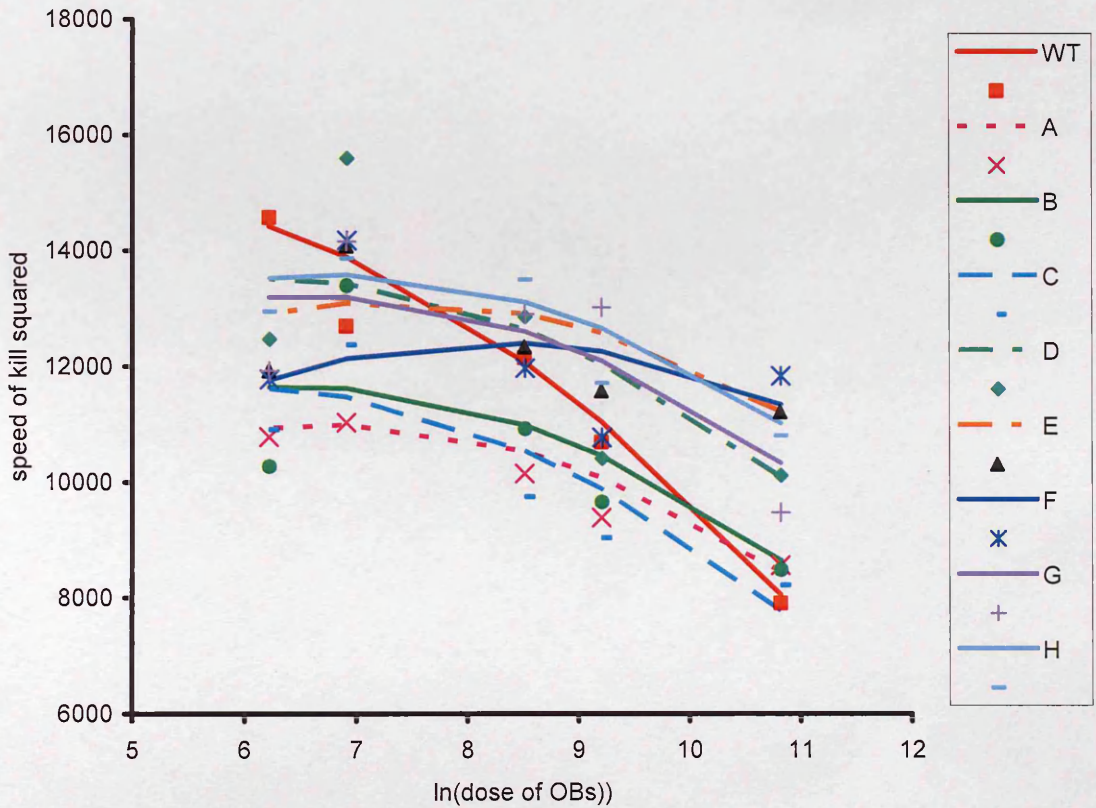


Figure 4.6 Speed of kill-dose relationship of *SpexNPV* genotypes, A-H and wild type virus in 3rd instar *S.exempta* larvae. Symbols represent the mean speed of kill for each genotype at each dose. Standard error bars are not shown to improve clarity. Fitted lines: wild type virus, speed of kill² = 12190 + (1362.8(lndose)) - (161(lndose²)); A, speed of kill² = 3444 + (2208(lndose)) - (161(lndose²)); B, speed of kill² = 4856 + (2095(lndose)) - (161(lndose²)); C, speed of kill² = 5981 + (1911(lndose)) - (161(lndose²)); D, speed of kill² = 7292 + (2005(lndose)) - (161(lndose²)) ; E, speed of kill² = 4326 + (2385(lndose)) - (161(lndose²)); F, speed of kill² = 1492 + (2657(lndose)) - (161(lndose²)). ; G, speed of kill² = 6202 + (2128(lndose)) - (161(lndose²)); H, speed of kill² = 6058 + (2205(lndose)) - (161(lndose²)).

Comparison of the back transformed mean speed of kill showed differences of approximately 12hrs and 15hrs between the fastest killing genotype (A) and the slowest killing genotype (D) and the WT virus respectively, at the low dose of 500 OBs. At the higher dose of 50 000 OBs, genotype C became the fastest genotype and genotype F had the slowest speed of kill. The difference between them, however, was still approximately 15hrs. The variation between the viruses of dose response has again been highlighted in Figure 4.7 which shows speed of kill to remain the same at the low (500 OBs) and the high dose of 50000 OBs for genotype F while for the wildtype virus and for genotype C time to death at 50000 OBs is lengthened by anything upto 30 hours (25%) or 20hours (20%) respectively (Figure 4.7).

Genotypes which appeared similar were clustered into three groups (WT, ABC, DEFGH) without significantly increasing the residual deviance ($F_{8,1520} = 0.55$, $P = 0.819$; Figure 4.8). Figure 4.9 shows the back transformed speed of kill of the genotypes and wild type virus after statistical grouping on the basis of dose response analysis for a high dose of 50 000 OBs and a lower dose of 500 OBs.

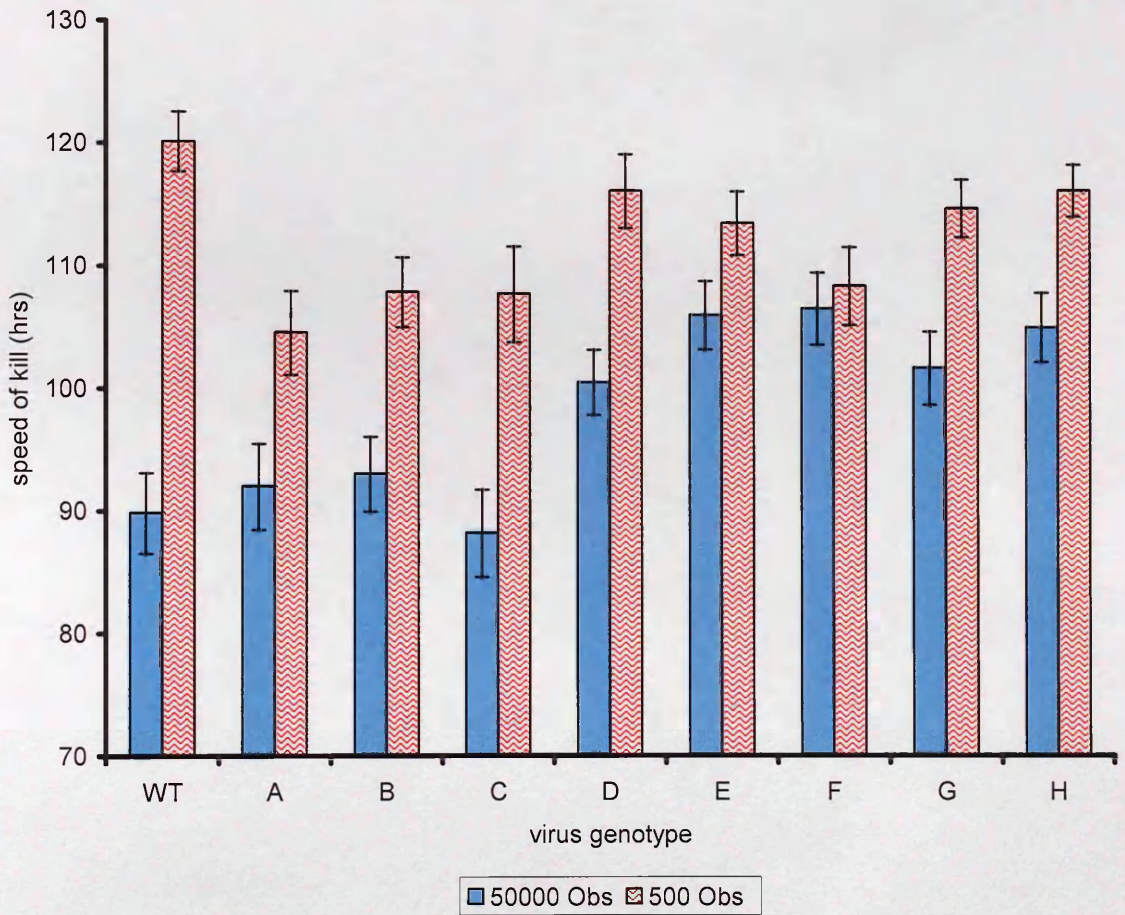


Figure 4.7 Back transformed mean speed of kill (hrs) of *SpexNPV* virus genotypes A-H and wild type virus at doses of 50 000 OBs and 500 OBs (± 1 SE) in third instar *S. exempta*.

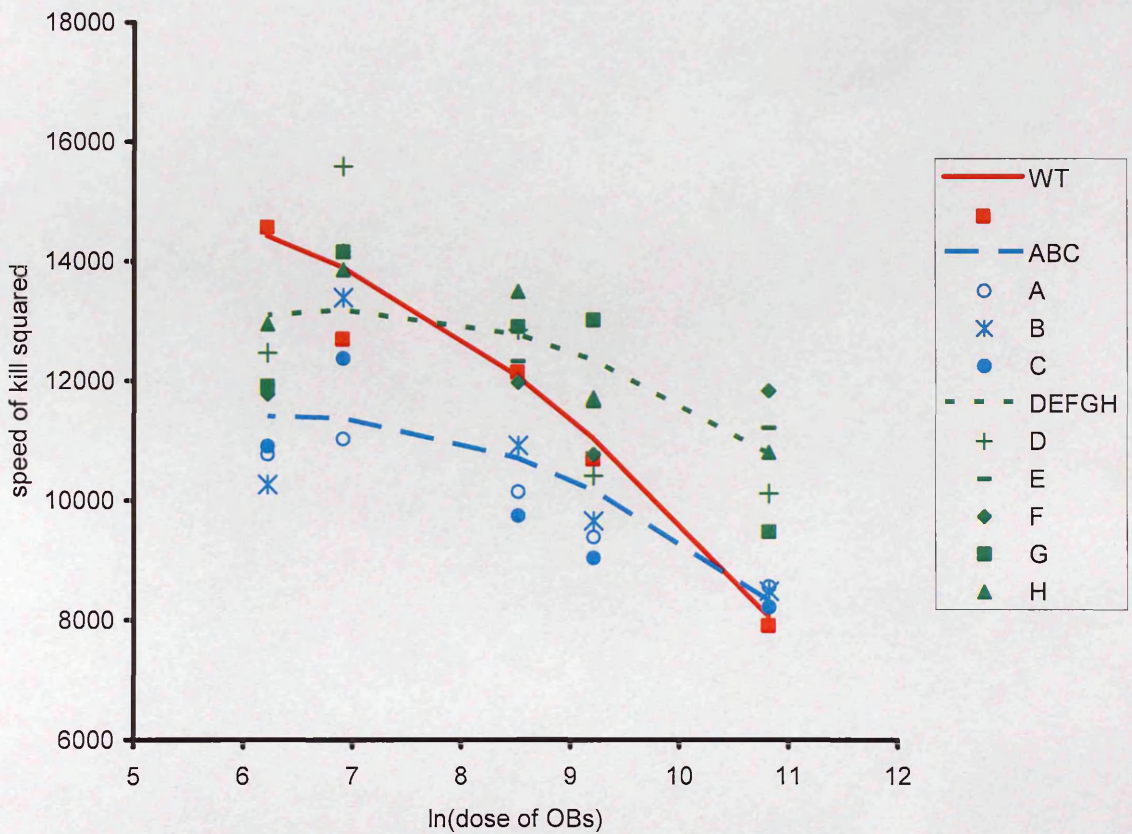


Figure 4.8 Speed of kill-dose relationship of *SpexNPV* genotypes, A-H and wild type virus infecting 3rd instar *S.exempta* larvae. Symbols represent the mean speed of kill for each genotype at each dose. Standard error bars are not shown to improve clarity. Fitted lines: wild type virus, speed of kill² = 12252 + (1348.2*(ln dose)) - (160.2(ln dose²)); ABC, speed of kill² = 4820 + (2059(ln dose)) - (160.2(ln dose²)); DEFGH, speed of kill² = 5463 + (2228.3(ln dose)) - (160.2(ln dose²)).

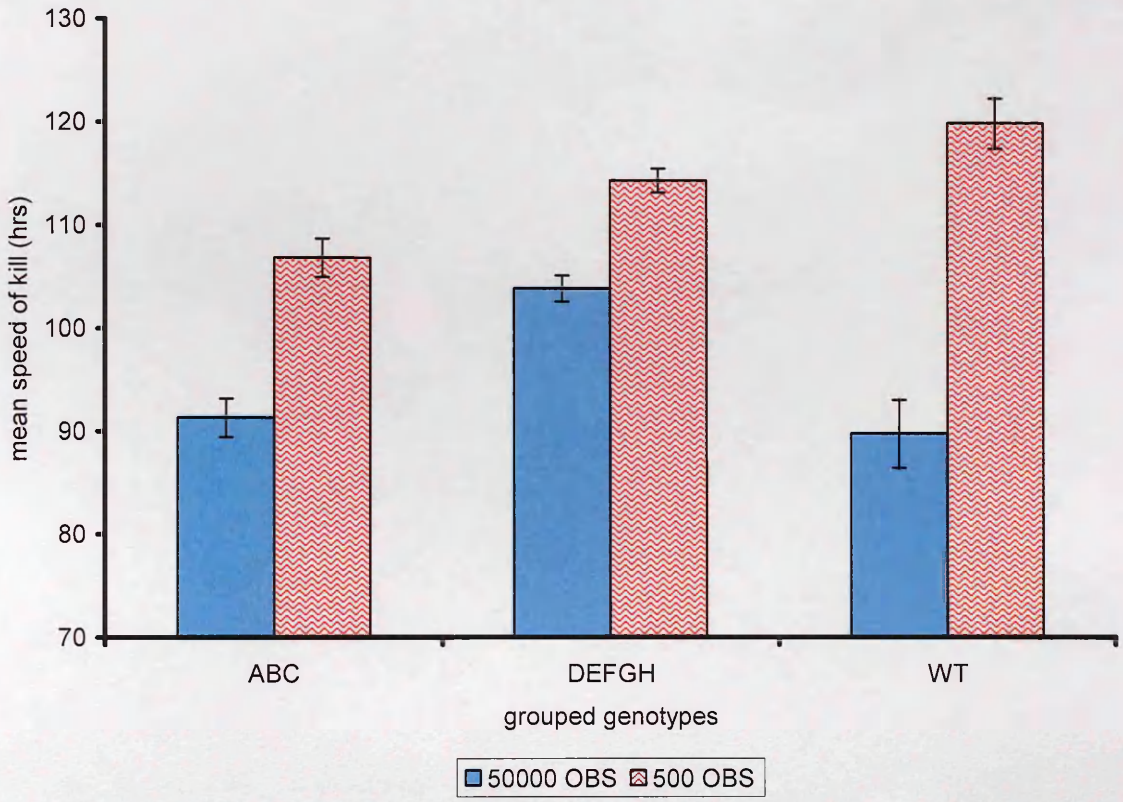


Figure 4.9 Back transformed mean speed of kill (hrs) of virus genotypes and wild type virus grouped according to analysis of covariance, at a high (50 000 OBS) and low dose (500 OBS) (± 1 SE).

4.3.4 Yield

Yield data were transformed (sqrt) and modelled with a normal error structure with genotype as a factor and virus dose as a covariate. Yield differed significantly between genotypes and there was also an interaction with the natural log of dose (genotype*ln(dose); $F_{7,156} = 2.2$, $P = 0.037$). Speed of kill (x^2) was then introduced into the model as a second covariate. The interaction between dose and speed of kill was converted into a factor (Indose * speed of kill = inter) and included in the maximum model to allow analysis of two covariates at the same time. This interaction though was found not to be significant and was therefore removed from the model ($F_{1,147} = 0.24$, $P = 0.0.624$).

The inclusion of speed of kill resulted in a significant reduction in residual deviance ($F_{8,156} = 4.07$, $P = 0.0002$) and therefore better explained the data set. The relative contributions that speed of kill and dose had on yield clearly varied between virus genotype. This becomes apparent when the mean yield at fast and slow speeds of kill and high and low doses are compared against each other for each virus (Figure 4.10). For the WT virus and genotype H speed of kill appears to influence yield to a far larger extent than dose with a 10-fold difference between yield produced at fast and slow speed of kill. Yet yields at 1000 OBs and 10000 OBs are not significantly different. For all the other genotypes, with the exception of genotype E which appears unresponsive to both, speed of kill and dose both influence yield produced.

Yield increased with increasing time to death, however this relationship varied between genotypes (genotype * speed of kill; $F_{7,133} = 3.060$, $P = 0.0051$). The production of lower yields at fast speed of kill was mirrored in all genotypes but to various degrees depending on the steepness of the fitted curve. Genotype H and the wild type virus possessed extremely steep curves in comparison to the other genotypes, showing that speed of kill, at least for these viruses, is a major predictor of yield. However, genotype E which possessed an almost horizontal line yield, irrespective of speed of kill, remained relatively constant (Figure 4.11).

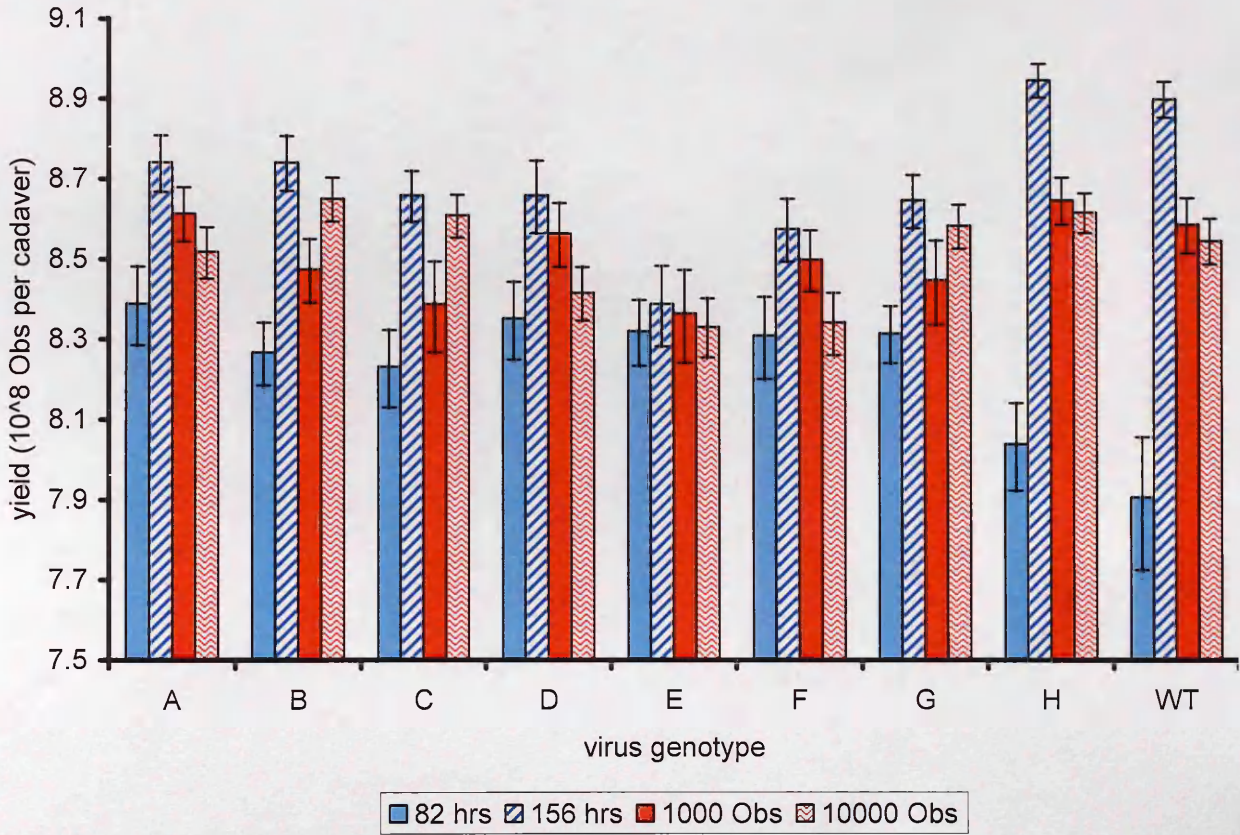


Figure 4.10 Back transformed mean yield of OBs (± 1 SE) per larva at doses of 1000 and 10000 OBs and at a fast (82 hrs) and a slower speed of kill (156 hrs) for genotypes A-H and the wild type *SpexNPV*.

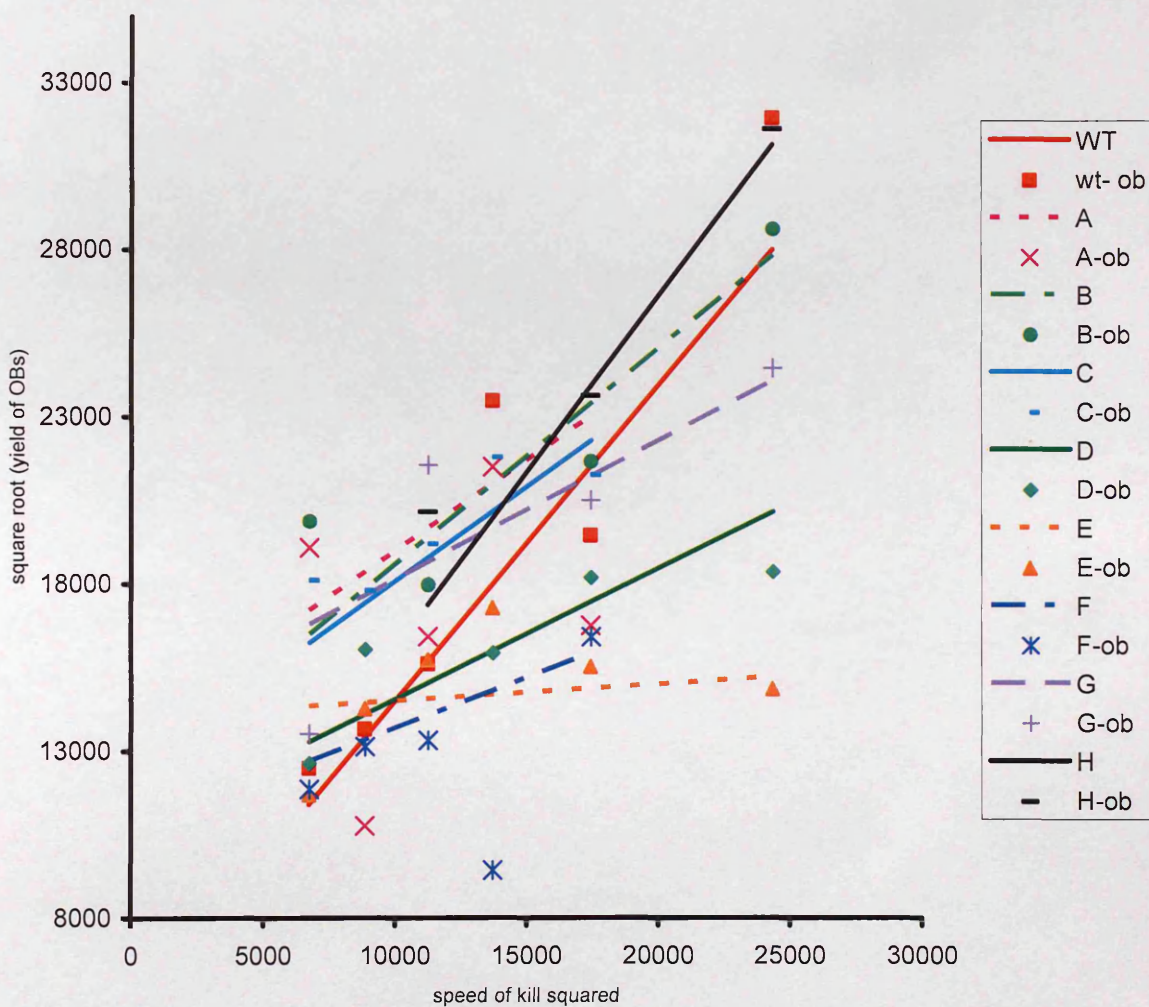


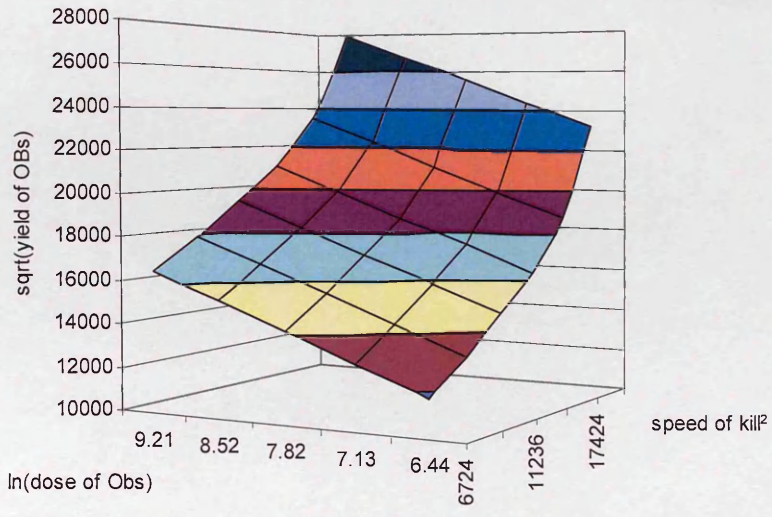
Figure 4.11 Speed of kill-yield relationship. Symbols represent mean yields of 3rd instar *S. exempta* larvae infected with individual *SpexNPV* genotypes (A-H) and the wild type virus at a dose of 10000 OBs. Fitted lines represent minimal adequate model fitted by ANCOVA.

Virus dose influenced yield and this also varied depending on virus genotype (genotype*dose: $F_{7,133} = 2.476$, $P = 0.020$). For genotypes B, C and G there was a positive relationship between dose and yield, with higher yields being produced at higher virus doses. Figure 4.12a shows the response surface for this relationship for genotype B which proved representative of similar relationships found for genotype C and G. In complete contrast genotypes A, D, E, F and H all exhibited a negative relationship between dose and yield, with high doses producing lower yield. This is visualised by the response surface generated for genotype F (Figure 4.12b).

Examination of the fitted dose-genotype curves for the genotypes and the wild type virus at each speed of kill revealed that the direction of the response of yield to dose was maintained across the range of speeds of kill for all genotypes (Figure 4.13).

Genotypes appear to not only vary in the direction of the response to yield but also on the strength of the response as shown by the slope of the lines (Figure 4.13). This goes some way to explain the inability to group any of the genotypes on the basis of yield and reaffirms the importance of using a full suite of fitness traits for biological characterisation.

(a)



b)

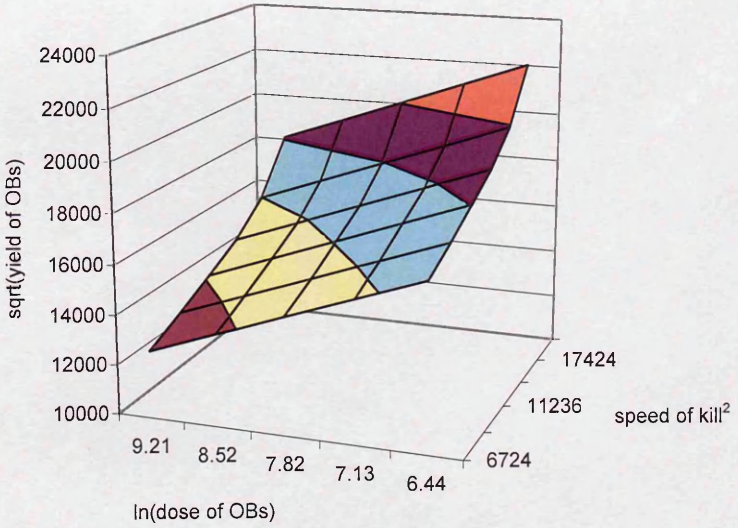
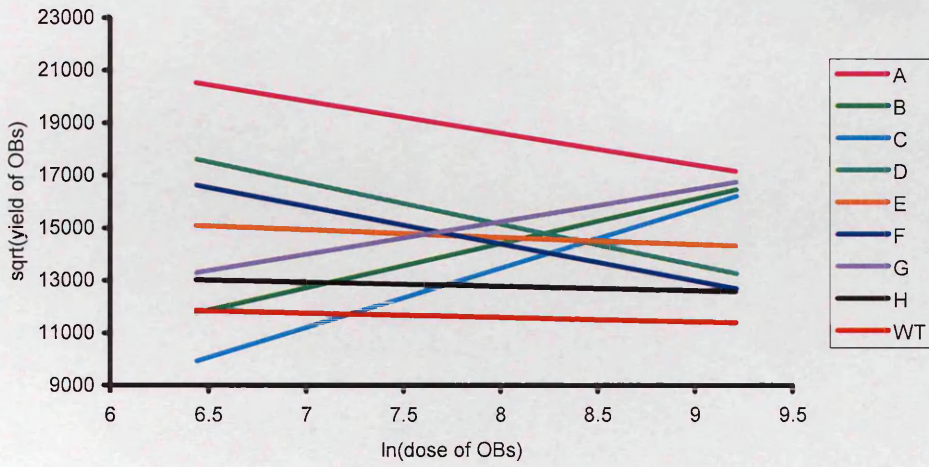


Figure 4.12 Influence of virus dose and speed of kill on yield for (a) genotype B and (b) genotype F.

(a)



(b)

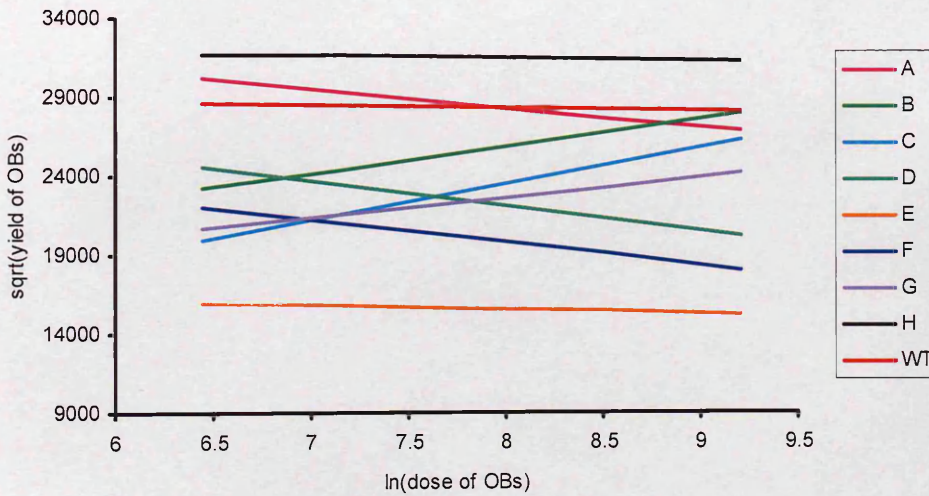


Figure 4.13 Fitted lines for dose-yield relationship of 3rd instar *S. exempta* larvae infected with individual *Spex*NPV genotypes (A-H) and the wildtype virus at a single speed of kill, (a) 82hours and (b) 156 hours.

4.3.5 Relationships between phenotypic traits

The estimation of several biologically relevant traits (pathogenicity, speed of kill and virus yield) for each genotype allowed the investigation of the potential relationships between the traits as a whole. Such analysis was hoped to give a valuable insight into any possible trade-off relationships that may drive viral fitness and the maintenance of genetic diversity in baculovirus populations. The intra-genotypic relationships between dose, speed of kill and virus yield were taken into account by calculating mean speed of kill and mean virus yield at a standard dose for each genotype. Mean speed of kill was calculated at a dose of 5000 OBs using the previously generated analysis of covariance relating genotype and dose. Mean yield at a dose of 5000 OBs was calculated using the analysis of covariance relating genotype and dose without the inclusion of speed of kill as a covariate to ensure independence of the data-sets.

LD₅₀, as an indicator of pathogenicity, correlated very poorly with speed of kill (Pearson's correlation coefficient, $r = -0.416$, $P = 0.305$; Figure 4.14). A similar result was obtained when the same analysis was carried out at 500 OBs (Pearson's correlation coefficient, $r = -0.538$, $P = 0.169$; data not shown).

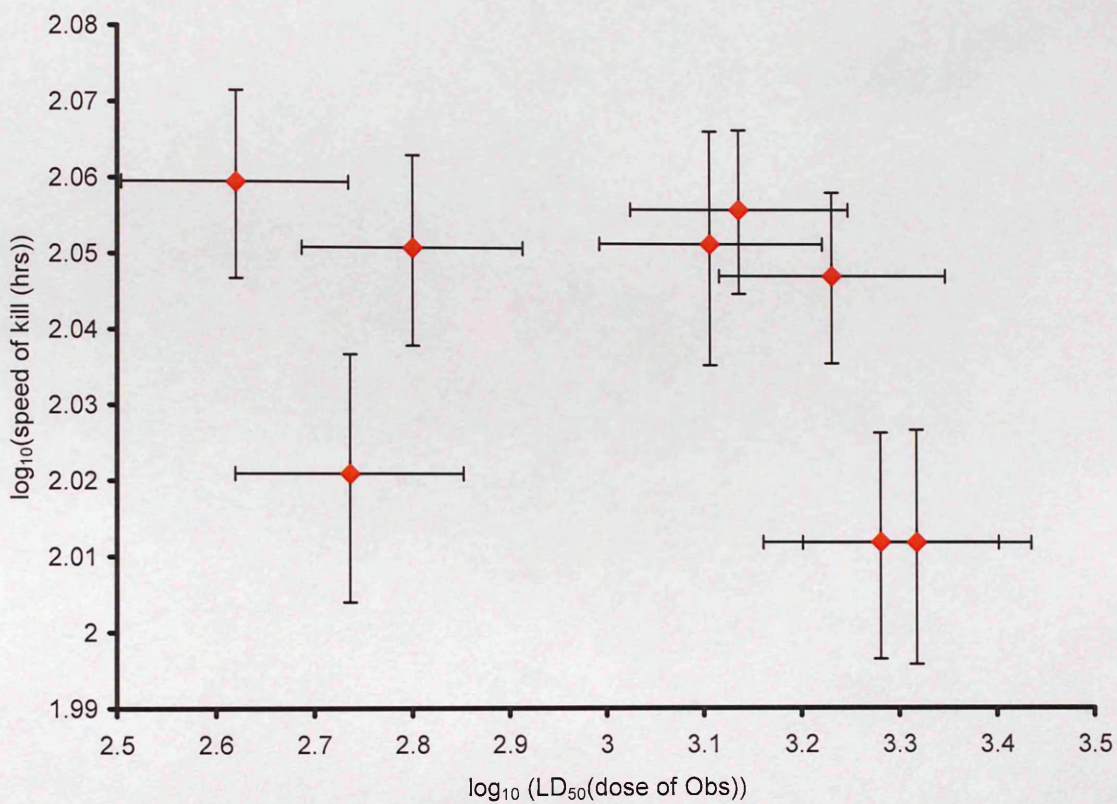
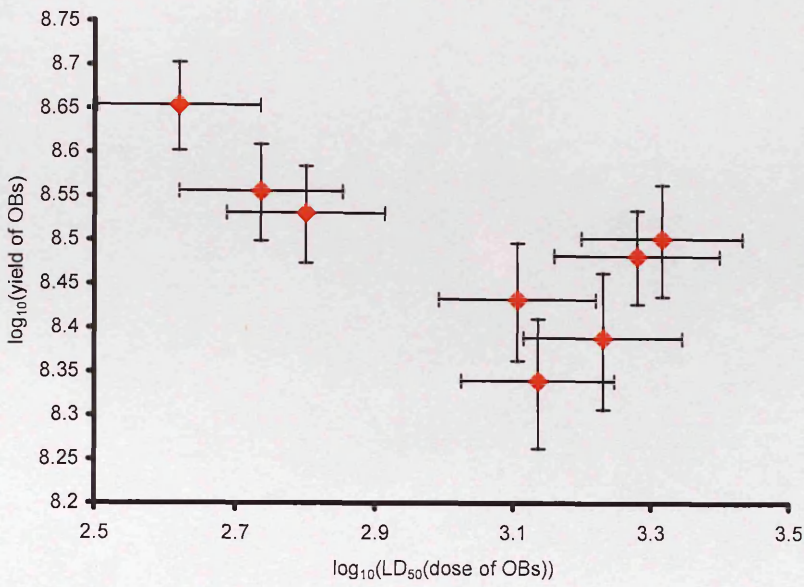


Figure 4.14 Estimates of pathogenicity, measured in terms of LD₅₀ ($\pm 95\%$ confidence intervals) and mean speed of kill ($\pm 1SE$) produced from analysis of covariance with $\ln(\text{dose})$ at a dose of 5000 OBs.

A negative correlation was identified between LD_{50} and mean yield ($r = -0.715$, $P = 0.046$; Figure 4.15a) revealing that increasing levels of pathogenicity produce higher yields at least at a dose of 5000 OBs. This relationship was not significant when the same analysis was repeated at the lower dose of 500 OBs ($r = -0.127$, $P = 0.764$; Figure 4.15b).

Speed of kill and mean yield, which had a strong relationship at the within-genotype scale for all genotypes, did not correlate at the between genotype scale at 5000 OBs ($r = -0.121$, $P = 0.776$; Figure 4.16) or at the lower dose of 500 OBs ($r = 0.294$, $P = 0.479$; Figure not shown).

(a)



(b)

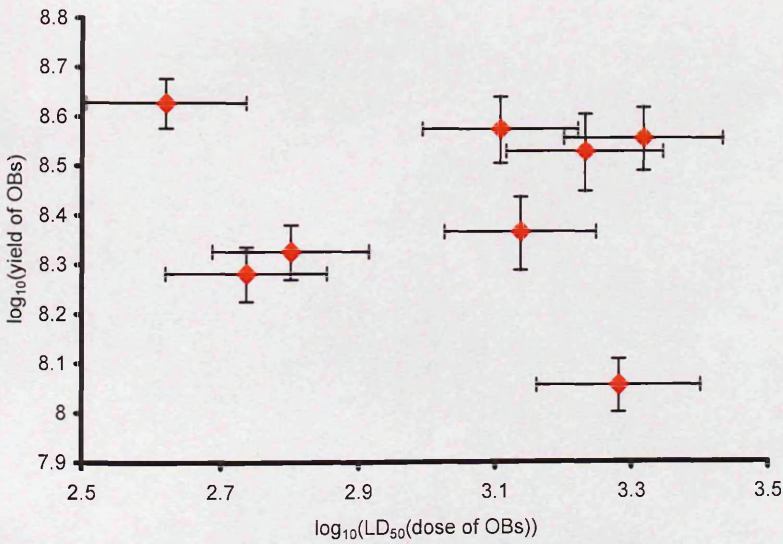


Figure 4.15 Estimates of pathogenicity, measured in terms of LD₅₀ and mean yield of OBs (± 1 SE) produced from analysis of covariance with $\ln(\text{dose})$ at a dose of (a) 5000 OBs and (b) 500 OBs.

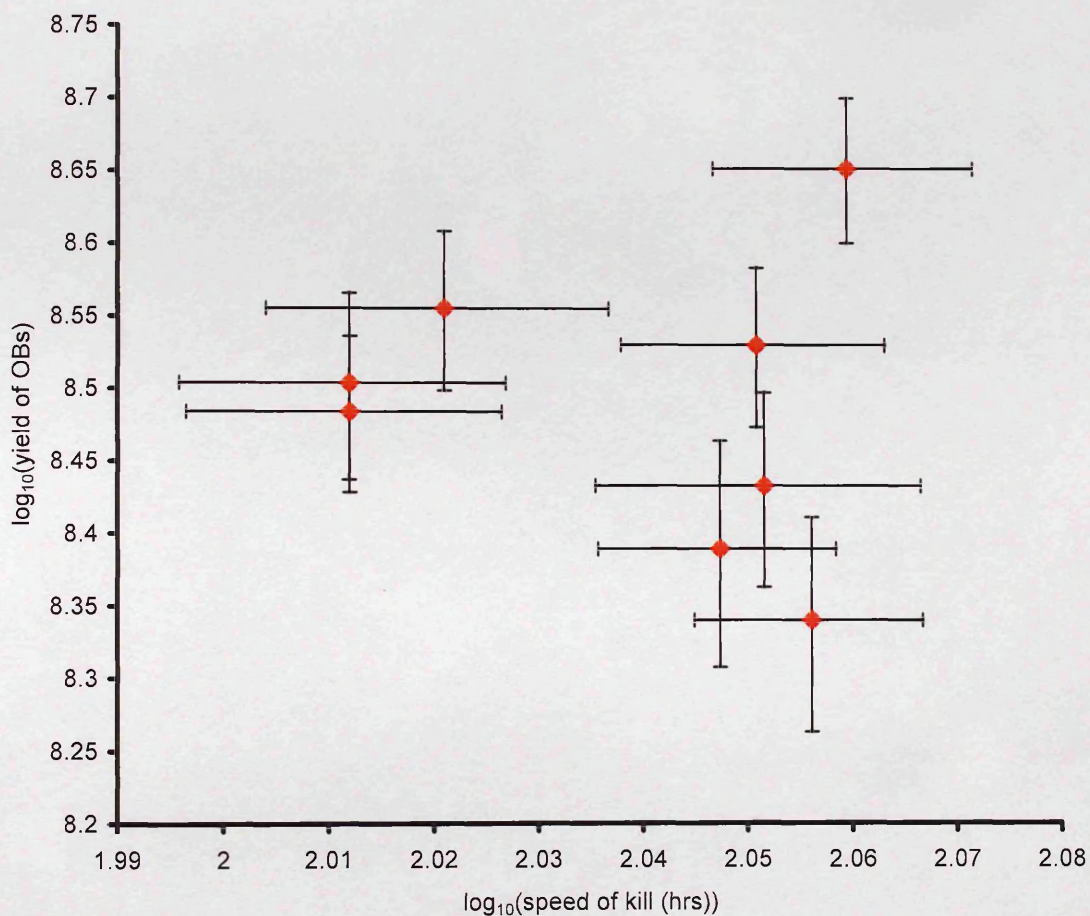


Figure 4.16 Estimates of mean speed of kill (± 1 SE) and yield of OBs (± 1 SE) produced from analysis of covariance with $\ln(\text{dose})$ at a dose of 5000 OBs.

4.4 Discussion

To fully characterise the biology of different genotypes, an array of different life-history traits was estimated in bioassay under ideal conditions and using a homogenous insect stock population. Striking differences in absolute pathogenicity, and more subtle differences in dose-dependent pathogenicity, were seen, not only between genotypes, but also between the genotypes and the wild-type virus, with approximately a 9-fold difference in LD_{50} estimates between the least and the most pathogenic variant. The wild-type virus proved consistently more pathogenic and possessed the slowest speed of kill than all single genotypes. Differences in speed of kill and productivity (yield of OBs) were also identified. The speed of kill of variants varied by approximately 20% and estimation of yields revealed productivity of the variants varied by approximately 10%. Other studies to investigate the biological characteristics of cloned baculovirus variants isolated *in vitro* and *in vivo*, have also demonstrated considerable differences in pathogenicity, speed of kill and yield (Lynn *et al.*, 1993; Ribeiro *et al.*, 1997; Simon *et al.*, 2004; Stiles and Himmerich, 1998; Hodgson *et al.*, 2001; Cory *et al.*, 2005). Two other studies have estimated pathogenicity of *Spex*NPV isolates in *S. exempta* larvae. The first also used third instar larvae and reared their larvae on maize plants. They produced an LD_{50} of just 48 OBs (Odindo, 1980). This represents an extremely pathogenic isolate, but is comparable to the LD_{50} (270 OBs) obtained for the wild-type virus used in this study. The second study was concerned with the differential resistance of the gregarious and solitary morphs and found a 10-fold difference between the LD_{50} of solitary (1325 OBs) and gregarious (14188 OBs) larvae (Reeson *et al.*,

1998). In our bioassays, larvae were reared individually from third instar and as expected our LD₅₀ estimate is closer to what would be expected for solitary larvae.

The *Spex*NPV genotypes varied considerably in pathogenicity, speed of kill and yield and thus genotypic differences between the variants must account for much of this biological variation. Much more work though would be required to map these differences and link them directly to biological function. Although baculovirus genomes are relatively small, they contain many genes known to control many different aspects of the infection cycle. For example, the regulation of 100 or more open reading frames is required to accomplish productive infection by *Se*MNPV; this is highly complex and involves sequential and coordinated expression of immediately early, early, late and very late genes (Lu and Miller, 1997). The disruption of genes involved in the initial infection process such as *p35* and *iap* have been shown to alter pathogenicity and host range of *A. californica* (Griffiths *et al.*, 1999). Other recent studies to investigate the genetic determinants of host cell specificity and pathogenicity have revealed that cell entry, and the primary virus infection cycle are not the only, or the major determinants, for *Se*MNPV infection of heterologous Spodoptera species (Simon *et al.*, 2004).

Above and beyond the influence of gene expression, pathogenicity is also determined by viral dose, with elevated levels of virulence seen at higher doses. Under certain conditions, such as epizootics the effect of dose may be negated by extreme viral abundance in the environment. Genotypes with lower LD₅₀ will be selectively favoured

under non-epizootic conditions when lower doses are more commonplace. Genotypes with steep dose-response curves could theoretically possess a selective advantage under conditions of changing viral abundance (which could itself be interpreted as a fitness trait). The overall level of viral pathogenicity, seen within a mixed-genotype infection, as well as within an epizootic, will be determined by the relative proportions of each of these genotypes and their corresponding phenotypes, found in natural environments.

Earlier studies have shown a trade-off usually occurs between the time required for insect death and the resulting yield of OBs, such that earlier death results in fewer infectious OBs' being produced (Hernandez-Crespo *et al.*, 2001; Hodgson *et al.*, 2001). We found that rapid speed of kill was accompanied by reduced virus productivity for all *SpexNPV* genotypes, though the strength of the correlation proved genotype dependent, for example genotype E possessed an extremely flat speed of kill-yield response curve. This genotype differential in productivity can largely be attributed to the manner in which individual genotypes responded to dose, with several of the genotypes producing decreasing yield with increasing dose. The mechanisms behind these differences are as yet unclear. Insects killed by higher virus dose usually die more rapidly and this might be expected to result in a lower virus yield. Other studies have shown that virus yield is often increased at higher doses, despite being combined with a more rapid speed of kill (Cory *et al.*, 2004). This highlights the complexity of the dose-response relationship.

Historically, epidemiological models have assumed that infection rate is simply the product of the concentration of the hosts and the parasites and is the result of *mass action* (Hamer, 1906, cited in Regose *et al.*, 2001). Dose-dependence has been found to affect the mortality, speed of kill and productivity of *Spex*NPV genotypes. Similar results have been identified in many other micro-parasitic infection experiments (Diffley *et al.*, 1987; Hochberg, 1991; Agnew and Koella, 1999; Little and Ebert, 2000). Infection of *Daphnia magna* with the microparasitic bacterium *Pasteuria ramose* and the fungus *Metschnikowiella biscuspidata*, for example, showed strong dose dependences of host mortality and fecundity, parasite reproduction within the host and infection rate (Ebert *et al.*, 2000). For most macro and micro parasites, where dose-dependence has been identified, infection rate has been found to be an increasing function of the parasite dose, which is usually sigmoidal.

The presence of trade-offs between competing phenotypic traits for a limited amount of energy is a well-documented phenomenon in nature. It has been argued that trade-offs prevent species from evolving as “Darwinian demons”: that is to say a species that develops rapidly, reproduces continuously and does not age. By restricting the investment in life-history traits against ecological competitive ability, multiple species or strains are allowed to co-exist (Stearns, 1992). A commonly cited trade-off for higher organisms is the differential allocation of resources available for reproduction, which affects the quality and quantity of offspring (Crawley, 1997, plants; Smith *et al.*, 1989, great tits; Sinervo *et al.*, 1992, lizards). Another trade-off which has often been identified between phenotypic traits in higher organisms, is between generation time

and fecundity (Reed and Bryant, 2004, housefly). It may be possible to relate this particular trade-off to the relationship in baculoviruses between speed of kill (infection duration) and yield. Although a negative correlation between speed of kill and yield was anticipated for *Spex*NPV genotypes, no evidence for a trade-off between these two traits was identified in this study. From the speed of kill-yield fitted response curves there appeared to be a positive relationship, with faster speeds producing lower yields and vice versa for the majority of genotypes. Genotype E though appeared to possess an almost horizontal fitted curve and was found to produce similar yields at all speeds of kill. Removal of genotype E from the analysis may alter the result and produce a significant correlation between speed of kill and yield of OBs. A positive correlation was identified between pathogenicity and yield of OBs. This suggests that less pathogenic genotypes also produce lower yields. Although there is no obvious biological reasoning to underpin this correlation, both these traits are clearly equally important for the optimisation of genotypic fitness. This correlation was only significant at the higher dose of 5000 OBs though and then only just ($p = 0.045$). Consequently more work needs to be done to try to understand the biological relationships between these two traits before any definite conclusion can be drawn. Another possible trade-off for baculoviruses is the relationship between OB persistence in the environment and host-to-host transmission. Studies investigating trade-offs between parasite infection traits have focused on the correlation between parasite transmission and infection virulence. Mackinnon and Read (1999) found positive genetic correlations between malaria pathogenicity in rodent hosts and both within-host growth and transmission stage production but not between the latter two.

Chapter Five

Diversity of *SpexNPV* in natural epizootics

Chapter 5: Diversity of *Spex*NPV in natural epizootics

5.1 Introduction

Genetic differences have been identified within numerous species of baculoviruses, at a range of spatial scales (Cherry and Summers, 1985; Gettig and McCarthy, 1982; Shapiro *et al.*, 1991; Laitinen, 1996; Vickers *et al.*, 1991; Parnell *et al.*, 2002). At the large regional scale, Vickers *et al.*, (1991) compared 8 different *geographic* isolates of the granulovirus (PMT GV) attacking the Potato tuberworm (*Phthorimaea operculella*) and identified three *genetically* distinguishable isolates. However, they found little correlation between the genetic differences and the region of origin, with the Peruvian isolate producing identical endonuclease profiles to the isolate from India when digested with *Sma*I. Regional variation has been identified in epizootics of both forest and agricultural pests. A study to compare wild geographically-distinct NPV isolates of the Douglas Fir Tussock moth (*Orgyia pseudotsugata*), a forest pest in British Columbia, found that although 8 genotypes were identified, two of which appeared to dominate prevalence, their frequency varied considerably between sites (Laitinen *et al.*, 1996). Gelernter and Federici (1990) investigated *Spodoptera exigua* NPV during viral epizootics of this agricultural pest, over a three year period in California and found that although genotypic variants were identified, prevalence was dominated by a single genotype. The same variants were similarly found in natural *S. exigua* populations in Spain over a several year period (Caballero *et al.*, 1992).

In an effort to assess and compare the level of variation identified between and within a region, Parnell *et al.*, (2002) studied GV of Diamond Back moth of Kenya and Taiwanese isolates and found that variation in banding patterns between isolates from Taiwan and Kenya was no greater than the variation identified between all Kenyan isolates studied. A more systematic approach to the study of spatial variation was adopted by Shapiro *et al* (1991) who used RFLP analysis to compare the similarity of 22 isolates of *S. frugiperda* NPV and sequence divergence to assess the relatedness of the isolates. Isolates were collected from Georgia (USA), Columbia, Venezuela, Mexico, as well as Louisiana (USA). Isolates collected within Louisiana were found to be much more similar to each other relative to isolates collected outside Louisiana. Isolates were also compared at the much smaller ecological scale, within individual fields, where considerable genetic variation was identified (though this was not found to be related to host plant or to possess any discernible structure).

The ability to extract only small amounts of viral DNA from individual cadavers has meant few of the aforementioned studies have examined RFLP variation of baculoviruses at this single larva scale. The majority of studies have *in vivo* amplified the virus prior to analysis, or used multiple-cadaver isolates, resulting from pooling in an attempt to produce sufficient quantities of DNA for molecular analysis. This may have yielded distorted representations of the genetic composition of natural baculovirus populations. The value of using individual cadavers from the field without passaging through larvae was highlighted by Cory *et al* (1997) who argued that “the individual

host represents a distinct patch of resource and is therefore the most critical scale at which to study host-parasite interactions”.

One of the recent studies to adopt this approach investigated genetic variation of wild populations of the NPV to attack the Western Tent caterpillar, *Malacosoma californicum pluviale* (*Mcp*NPV). This study examined viral prevalence and the cyclic dynamics of host abundance (Cooper *et al.*, 2003a) in an attempt to relate genetic variation to observed host ecology and dynamics. Another detailed study of the temporal and spatial distribution of genetic variation within natural baculovirus epizootics, which also analysed single viral cadavers direct from the field, was undertaken within NPV epizootics occurring in spatially separate populations of Winter moth, *Operophtera brumata* nucleopolyhedrovirus (*Opbu*NPV) in Orkney (Graham, *et al.*, 2004).

In this chapter, there were three main aims. Firstly, to use RFLP analysis to characterise genetic variation of natural *Spex*NPV epizootics in Northern Tanzania and to use these data to compare virus isolates at different spatial scales in an attempt to discern population sub-structuring. Secondly, to attempt to relate the observed genotypic differences in the virus to phenotypic differences, through the use of laboratory bioassays estimating biologically important fitness traits, such as pathogenicity, speed of kill and productivity (yield of occlusion bodies). The final aim of this chapter was to assess the degree of relatedness between the different genotypes, via phylogenetic analysis of sequence data of the polyhedrin gene.

Fieldwork for this study formed a small part of a much larger project investigating the potential to develop *Spex*NPV as a bioinsecticide for the strategic control of African armyworm, undertaken by colleagues at Natural Resources International (NRI) in the UK and Pest Control Services (PCS) in Tanzania, under the direction of Wilfred Mushobozi. PCS is based close to Arusha, Northern Tanzania, where armyworm outbreaks occur almost every year, and is a government-funded body established to monitor, forecast and control armyworm outbreaks throughout Tanzania. Although armyworm outbreaks occurred in 2002 and 2004, few were observed during 2003 and consequently only two years of field data were obtained for this study.

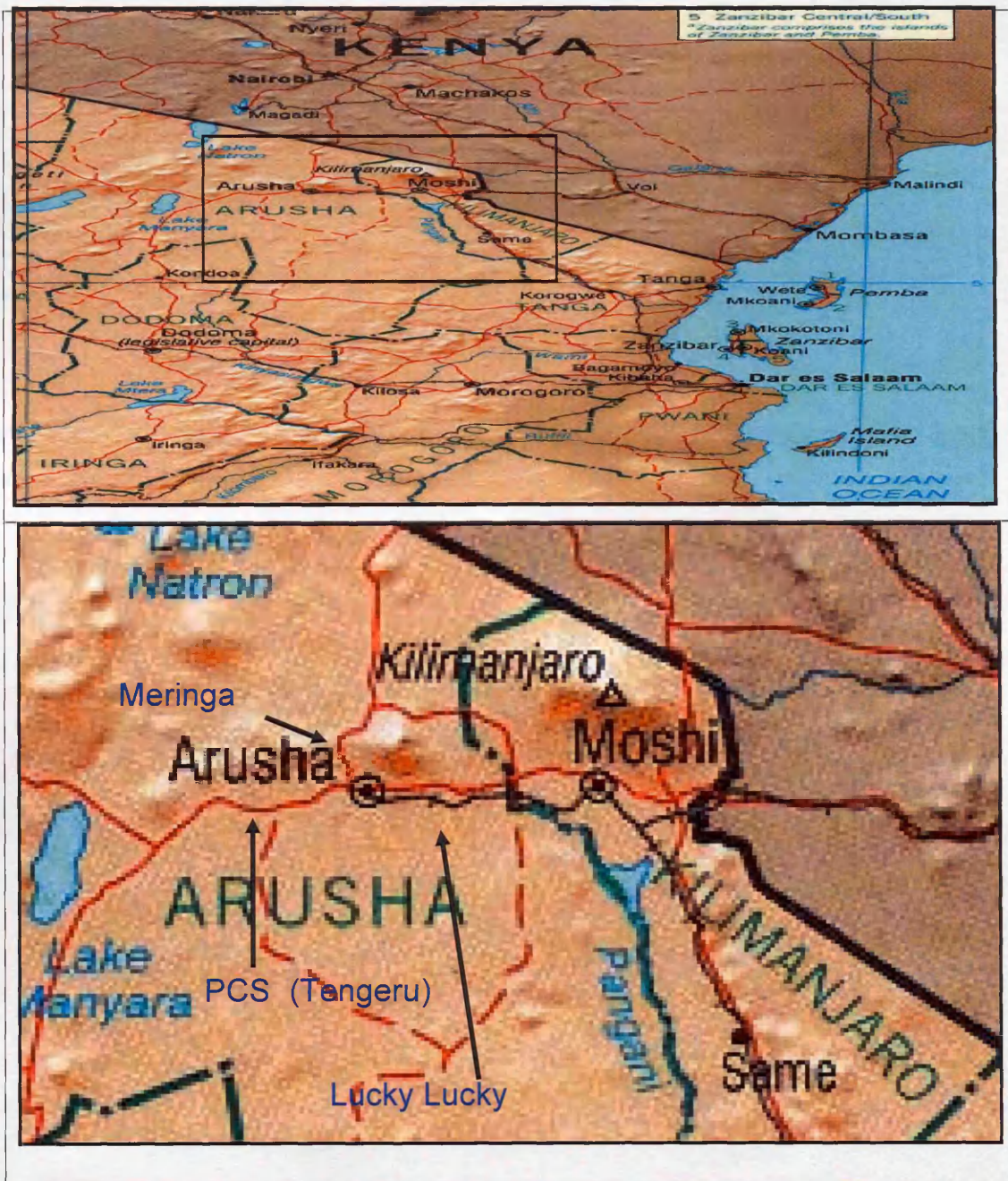


Figure 5.1 Relief maps of Arusha, Northern Tanzania highlighting locations PCS and other fieldsites: Meringa Coffee Estate and Lucky Lucky Farm Estate (epizootic sampled 25th-28th February 2002) and Tengeru (epizootic sampled, 21st-22nd February 2004).

5.2 Methods

5.2.1 Field season 2002

Sampling of viral epizootics of armyworm outbreaks during 2002 was based in Arusha, Northern Tanzania. Because of its vicinity to the Mount Meru, Arusha and its surrounding locality is extremely lush and fertile and, consequently, much of it is under cultivation. Two geographically separate field sites infested with large numbers of young (L1-L3) larvae were identified for the possible sampling of naturally occurring virus. Both areas consisted of perennial pastureland and were of approximately equal size (2 ha). After negotiation with the owners, no chemical or biological insecticides were used on the field sites. The first was within the M'ringa Coffee Estate on the Moshi Road, about 5km from Arusha (Figure 5.1). The pasture was relatively short (20cm tall) but was extremely lush following recent irrigation and thus offered a prime site for armyworm infestation. The second site consisted of much taller, flowering pastureland (approx. 80cm tall) on the Lucky Lucky Farm Estate on the Nairobi Road, approximately 3km from Arusha (Figure 5.1).

Within each field site, three non-overlapping blocks (25m x 25m) were designated and 16 naturally occurring overt viral deaths were randomly collected per block (Table 5.1).

Table 5.1 Sampling regime for armyworm cadavers infected by virus followed in 2002.

Site	Area of site	No. of blocks within site	Size of block	No. cadavers collected per block	Total no. cadavers collected
M'ringa Coffee Estate	2ha, short lush pasture	3	25m ²	16	48
Lucky Lucky Farm	2ha, tall flowering pasture	3	25m ²	16	48

5.2.2 Field season 2004

Late 2003 through to May 2004 proved an extremely good season for armyworm outbreaks in Eastern Africa. The armyworm reached Northern Tanzania in late February / early March and produced extraordinarily high larval densities (≥ 1000 larvae per m^2). In addition, the region was bombarded by several waves of moths over a period of many weeks, resulting in an extension of the outbreak period. Due to time and logistical constraints, the 2004 field season was limited to just 2 weeks. In addition, due to the delay in the appearance of the viral epizootic in the host armyworm population, the opportunity to sample overt viral infections in the field was also limited to just a 3 day period (24th - 26th March 2004).

Sampling of *Spex*NPV epizootics took place during the 2003/2004 field season at Tengeru, just outside Arusha (Figure 5.1). Tengeru is a government compound containing an agricultural college, offices for the Ministry of Agriculture and International development initiatives and PCS, as well as a substantial area of pasture and cultivated land for the employees there to farm. Several hundred viral cadavers were collected from within approximately 8 hectares of grassland and pasture following the structured sampling regime set out in Tables 5.2 - 5.4. The sampling regime was designed to minimise the bias of sample size when analysing diversity between spatial scales by attempting to collect the same number of cadavers at each ecological scale.

Table 5.2 Sampling regime for infected *S. exempta* larvae at the 2 hectare scale at Tengeru, 2004.

Site	Area of site	No. of blocks within site	Size of block	No. cadavers collected randomly per block	Total no. cadavers collected
Tengeru	8ha	4	2ha	16	64

Table 5.3 Sampling regime for infected *S. exempta* larvae at the 25m² scale at Tengeru, 2004.

Site	Area of site	No. of blocks within site	Size of block	No. cadavers collected randomly per block	Total no. cadavers collected
Chicken pen	2ha	3	25m ²	16	48
Top Paddock	2ha	3	25m ²	16	48
Bottom Paddock	2ha	3	25m ²	16	48
Pasture	2ha	3	25m ²	16	48

Table 5.4 Sampling regime for infected armyworm larvae at the 0.5 x 0.5 m quadrat scale at Tengeru, 2004.

Site	Area of site	No. of blocks within site	Size of Block	No. cadavers collected per block	Total no. cadavers collected
Maize field	25m ²	6	Individual Plants	5	30
Bottom paddock	25m ²	6	1/4 m ² quadrat (<i>Cynodon</i>)	6	36
	25m ²	6	1/4 m ² quadrat (<i>Setaria</i>)	6	36
Paddock	25m ²	1	1/4 m ² quadrat (<i>Pennisetum</i>)	16	16

5.2.3 Sampling of *Spex*NPV Epizootics

Armyworm populations were sampled for overt *Spex*NPV infections at a number of field sites. Virally-infected cadavers were collected and placed in individual, clearly labelled 1.5ml micro-tubes. The lack of easily accessible freezing facilities meant that, in an attempt to minimise bacterial contamination, the lids of the micro-tubes were left open to allow the virus to completely dry-out in a cool, shaded environment for 24 hours before storage, firstly at 4°C in Tanzania and later at -20°C in England.

5.2.4 Host and viral prevalence

Estimates of *S. exempta* density and *Spex*NPV prevalence were taken for each field site by counting the total number of larvae and the number of viral cadavers respectively, within 10 randomly-positioned quadrats. Diligence and care was required to maintain count accuracy at high host densities and to ensure all overt infections, however small, were recorded. One person (E. Redman) took all observations to ensure consistency. However, the use of quadrat counts most likely produced an underestimate of actual viral prevalence in the field. Ideally, if the locally available facilities in Tanzania had allowed, viral prevalence would have been estimated by collecting larvae randomly from the quadrats, rearing them on individually and monitoring them for viral mortality to give a much more accurate estimate.

5.2.5 Genetic characterisation

Occlusion bodies from individual cadavers were purified using a small muslin filter followed by a sucrose cushion (see section 2.2.4) and re-suspended in 150µl of sterile water. Viral DNA was extracted from 75µl of the viral suspension (see section 2.3.2) while the remainder was returned to storage at -20°C. The viral DNA was quantified by comparing band intensities produced after running 5µl on a 0.8% agarose gel against known quantity standards. The restriction endonuclease, *EcoRV* was then used to digest 75-100ng viral DNA (see section 2.3.3). The resultant DNA fragments were separated by gel electrophoresis and visualised using SYBR Gold stain (see section 2.3.4) to gain RE profiles for each individual viral death.

Each individual viral death was recorded as having resulted from either a single or a mixed infection, depending on whether sub-molar bands were present in the RE profile. The profile of mixed infections was represented by the dominant banding pattern. The fainter sub-molar bands were ignored for the purposes of this analysis. All novel banding patterns were recorded. In addition to the proportion of mixed infections and the number of different variants counted per block, a measure of diversity, which took into account the frequency distributions of each of the variants, was also calculated (Simpsons' Diversity Index, see below).

5.2.6 Measurement of diversity

The Simpson's Diversity Index was used to estimate genetic diversity of the *Spex*NPV populations. For the purposes of this analysis all novel variants, whether in single or mixed infections, were considered equally likely to exist.

$$\text{Simpson's Diversity Index, } D = 1 - \sum_{i=1}^S P_i^2$$

when P_i = proportion each variant contributes to the total

S = total number of variants in sample

$$\text{Equitability, } E_D = \frac{1}{\sum_{i=1}^S P_i^2} \times \frac{1}{S}$$

Although attempts were made to use uniform sample sizes, the inability to produce clear identifiable RFLP banding patterns from all samples collected (actual success rate, 92%), required an adjustment of the diversity index to account for this heterogeneity of sample size. Converting the diversity index into a proportion of the total diversity possible at a particular sample size (when $E = 1$) allowed the comparison of diversity irrespective of the number of viral infections used to calculate that diversity.

$$\text{Adjusted Diversity Index, } AdjD = D / D_{(E=1)}$$

5.2.7 Sequencing of polyhedrin gene

Eighteen genetically distinct isolates (FS1-FS18), were chosen for more detailed molecular characterisation through the sequencing of the polyhedrin gene. Polymerase Chain Reactions for each of the 18 field isolates were set-up using specific primers (*Spexpolh1* and *Spexpolh2*) designed for the amplification of a segment of the polyhedrin gene of *SpexNPV* using 2µl of viral DNA template (see section 2.3.6). The resultant PCR extension products were then “cleaned-up” using a PCR Purification Kit (Qiagen) and the purified PCR products were then sequenced (see section 2.3.7). A total of six reactions (3 per strand) were set-up for each of the 18 isolates to order to minimise any sequencing errors.

5.2.8 Biological characterisation

Biological investigation of the 18 field isolates (FS1-FS18) was carried out against the wild-type virus in laboratory bioassays designed to estimate fitness parameters such as pathogenicity, speed of kill and yield of OBs produced upon death (see section 2.4.3). Newly moulted third instar larvae were challenged with a range of 5 doses (10 000, 5 000, 1 000, 500 and 100 OBs per larvae) using the diet-plug inoculation method (see section 2.4.1). Twenty five larvae were infected per dose, except for the lowest two doses for which 50 larvae were used in order to produce sufficient numbers of cadavers for yield and time to death analysis. An additional 25 larvae were dosed with sterile distilled water to act as controls. Insects were monitored every 8-16 hours to produce estimates of pathogenicity and speed of kill until death or pupation. Viral mortality was

confirmed where necessary using geimsa staining (see section 2.4.2). Speed of kill was measured at intervals of between 8 and 16 hours. Yield analysis was carried out only for field samples 1 - 12 by selecting ten cadavers per dose for each viral treatment across a range time points, in order to gain estimates of the number of progeny OBs produced upon death (see section 2.4.3).

5.3 Results

5.3.1 2002

Although the grass at Lucky Lucky was much taller, and consequently offered a much larger volume of available grass to feed-on per quadrat, M'ringa possessed much higher armyworm densities (Table 5.5). Such local variation in larval prevalence is common and is largely dictated by local wind patterns and topography (Haggis, 1986). High host numbers at M'ringa may also reflect the extreme lushness of the vegetation and a possible ovipreference of female moths for vegetation of this type. Viral prevalence was also approximately four times lower at Lucky Lucky than at M'ringa (Table 5.5).

Out of the total number of cadavers profiled (88), 43 different *EcoRV* variants were identified, 35 of which appeared to be single genotype infections. Sub-molar bands were detected in the remaining eight novel banding profiles which were thus considered mixed infections. The proportion of mixed infections varied between the two sites ($\chi^2_1 = 4.6$, $P = 0.032$; Figure 5.2a) with approximately 1 in 3 of all isolates being mixed at

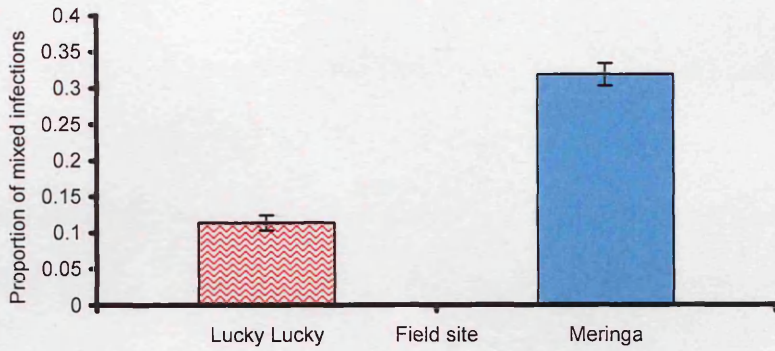
M'ringa but only 1 in 8 at Lucky Lucky. The total number of variants per block also varied between sites ($F_{1,4} = 16$, $P = 0.016$; Figure 5.2b).

The adjusted diversity index data were analysed with a normal error structure. Differences could be explained by field site ($F_{1,4} = 16.30$, $P = 0.016$) with higher levels of diversity at the M'ringa site than at Lucky Lucky (Figure 5.2c).

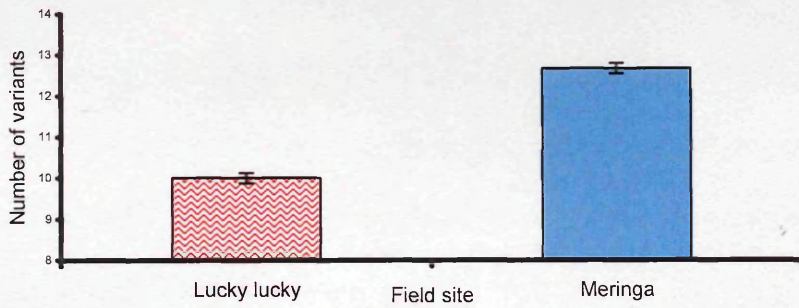
Table 5.5 *S. exempta* density and *SpexNPV* prevalence data from two field sites (sample size = 10 quadrats per site)

Field site	<i>S. exempta</i> density larvae/m² (± 1 SE)	<i>SpexNPV</i> % prevalence (± 1 SE)
M'ringa	246 (± 14.3)	7 (± 0.84)
Lucky Lucky	101 (± 14.3)	1.78 (± 0.39)

(a)



(b)



(c)

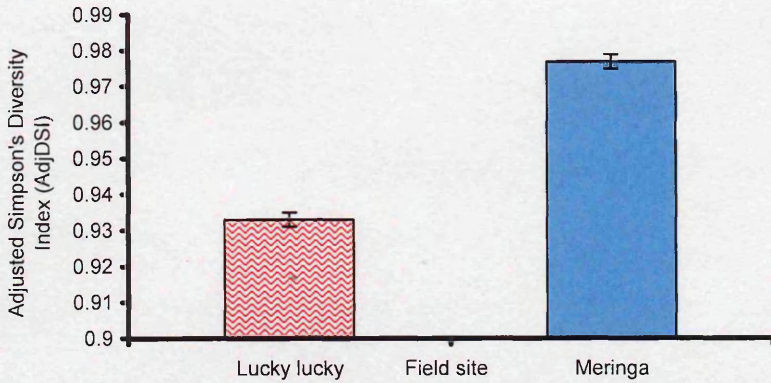


Figure 5.2 Diversity of *Spex*NPV isolates (individual cadavers) collected from two geographically distinct field sites within the same armyworm outbreak Arusha, Northern Tanzania, 2002 estimated using (a) the proportion of mixed infections (\pm 1SE), (b) the number of variants identified and (c) Adjusted Simpson's Diversity Index (\pm 1SE).

5.3.2 2004

Viral prevalence data (cadavers/ m²) collected for each 2 ha site were combined and transformed (square-root) for analysis with a normal error structure with host density as a covariate. Host density proved a major linear predictor of viral prevalence ($F_{1,43} = 440.8$, $P < 0.001$; Figure 5.3) with high levels of viral prevalence seen at high host densities.

Out of the total number of cadavers profiled in 2004 (343), 137 different *EcoRV* variants were identified, 82 of which were single-genotype infections. Where sub-molar bands were detected in DNA banding profiles, infections were considered as mixed. Mixed infections made up 40% of the total number of cadavers profiled.

The proportion of mixed infections at the 25m² block scale was analysed with a binomial error structure with field site treated as a factor and viral prevalence as a covariate. The proportion of mixed infections was positively related to viral prevalence ($\chi^2_1 = 6.63$, $P = 0.01$; Figure 5.4), irrespective of field site ($\chi^2_1 = 2.15$, $P = 0.34$). Introduction of host density into the model as a new covariate removed the effect of viral prevalence on proportion of mixed infections ($\chi^2_1 = 0.455$, $P = 0.5$) due to correlations between viral prevalence and host density (Figure 5.3).

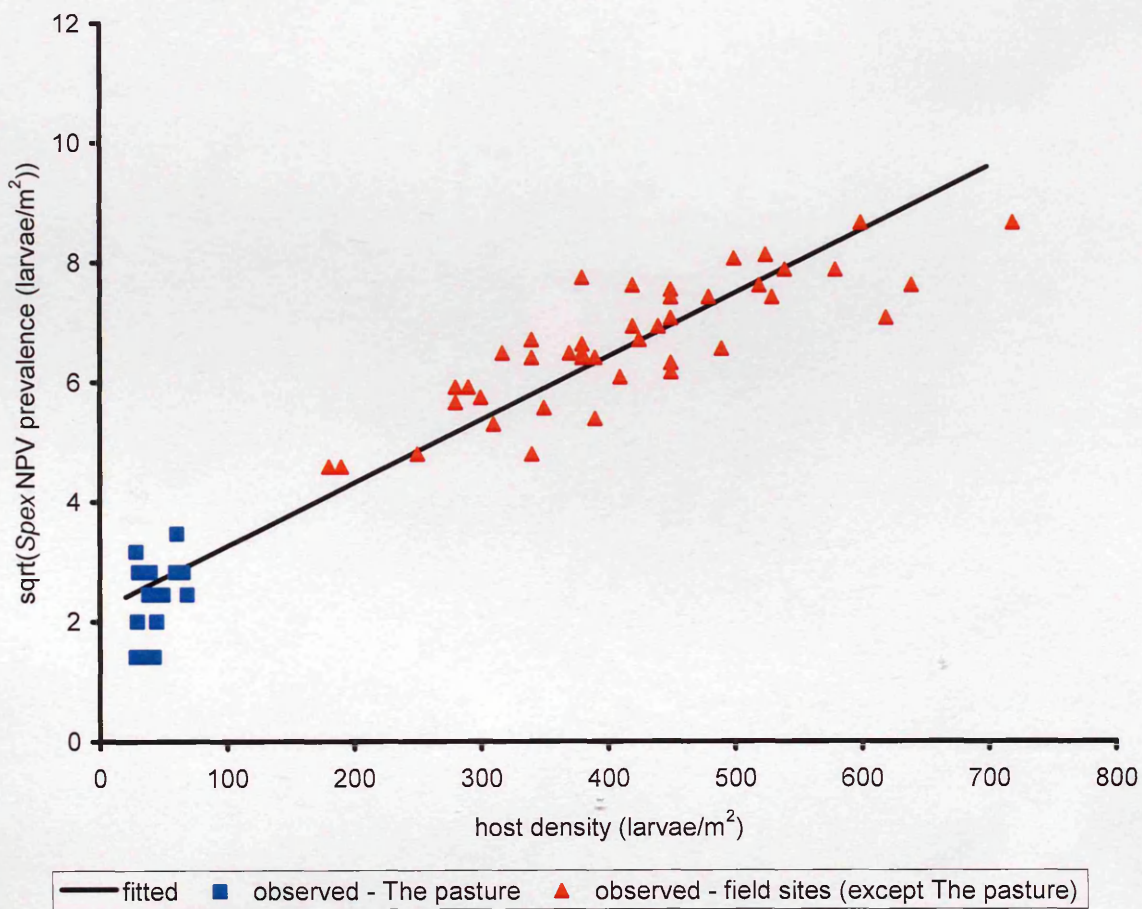


Figure 5.3 Relationship between *S. exempta* density and viral prevalence. Fitted line: $\text{sqrt}(\text{viral prevalence}) = 2.199 + (0.0101 \times \text{host density})$. Symbols represent observed values.

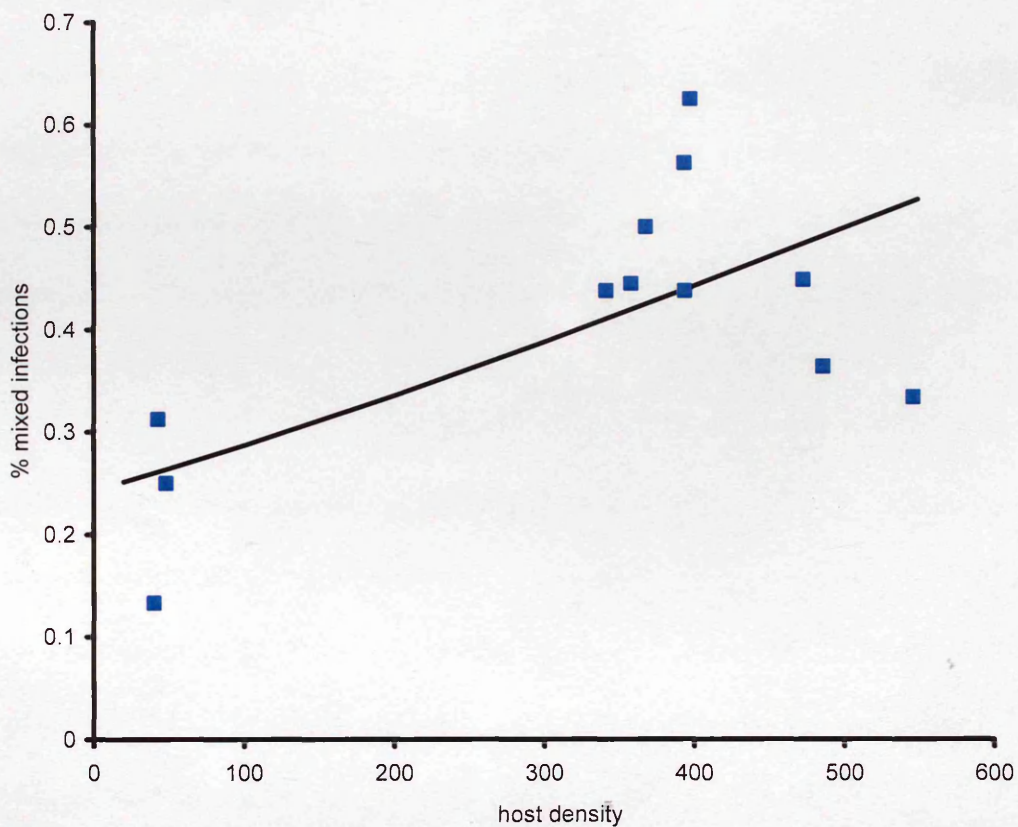


Figure 5.4 The effect of *S. exempta* host density on the proportion of mixed *SpexNPV* infections Fitted line: % mixed infections = -1.137 + (0.00226 * host density). Symbols represent observed values.

5.3.3 Investigation of population structure

To establish the presence of any possible population structure within the epizootic at Tengeru (2004), the genetic variation, quantified in terms of the Simpsons Diversity Index (adjusted for variable sample size), was analysed at several different spatial scales to test the null hypothesis that isolates are randomly distributed. Figure 5.5 illustrates how genetic diversity varied between field sites at the 25m² scale.

The diversity at three separate spatial scales, namely 2ha, 25m² and 1/4m² quadrat scale was estimated with an adjustment for number of larvae sampled, and analysed with a normal error structure with spatial scale as a factor. Scale of sampling failed to explain significant levels of variation of the data ($F_{2,32} = 2.467$, $P = 0.1$). After combination of the higher two spatial scales (i.e. 25m² and 2ha), and re-analysis, spatial scale did prove to be a significant term in the model ($F_{1,33} = 5.083$, $P = 0.031$; Figure 5.6). Although extremely high levels of diversity of *Spex*NPV are seen at all spatial scales, the lowest level (i.e. within 1/4m²) appears to have slightly less variation using this method of estimation.

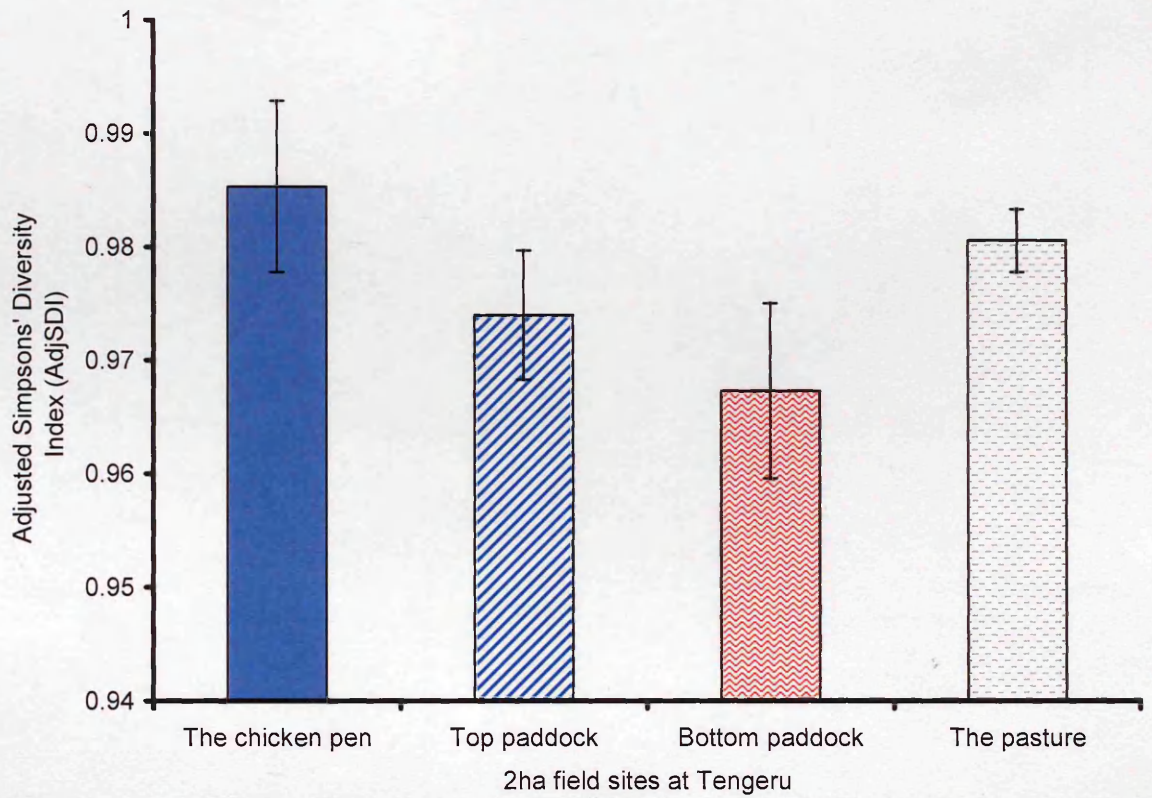


Figure 5.5 Mean Adjusted Simpsons' Diversity Index ($\pm 1SE$) at the $25m^2$ scale for each of the four 2 ha field sites at Tengeru, 2004.

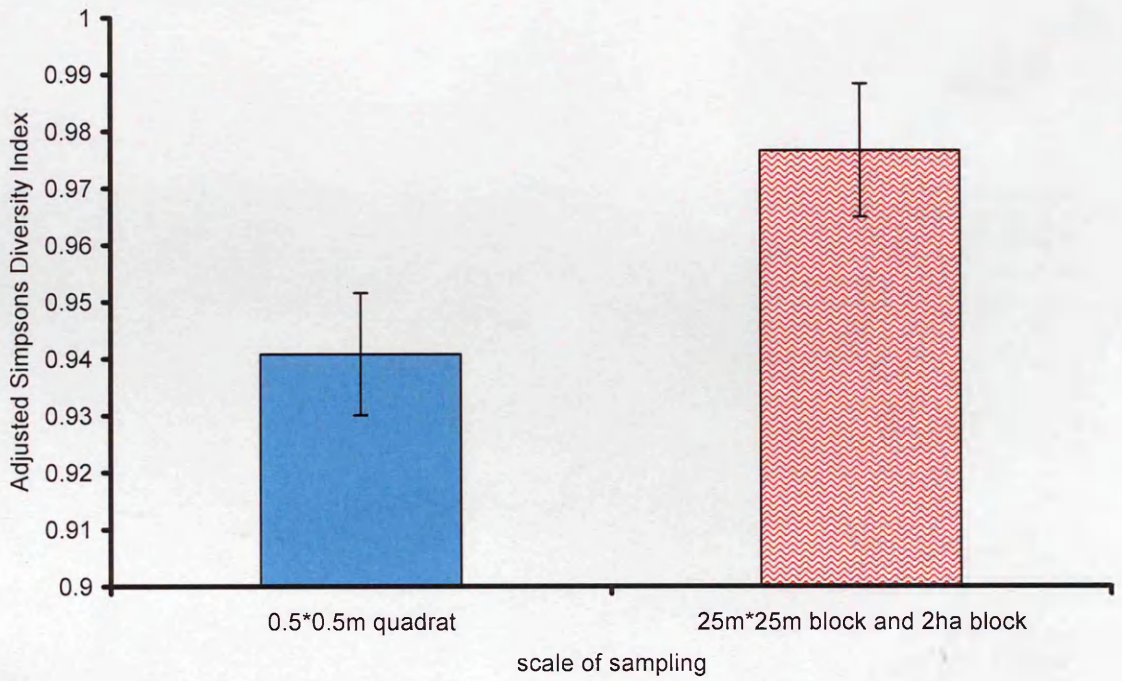


Figure 5.6 Comparison of diversity of *SpexNPV* isolates (individual cadavers) from 8ha field site at Tengeru (2004) estimated using the Adjusted Simpson's Diversity Index ($\pm 1SE$) from different spatial scales.

5.3.4 Genetic Characterisation

M₁ M₂ 1 2 3 4 5 6 7 8 9 10 11 12 13 14 15 16 M₂ 17 18 M₂ M₁

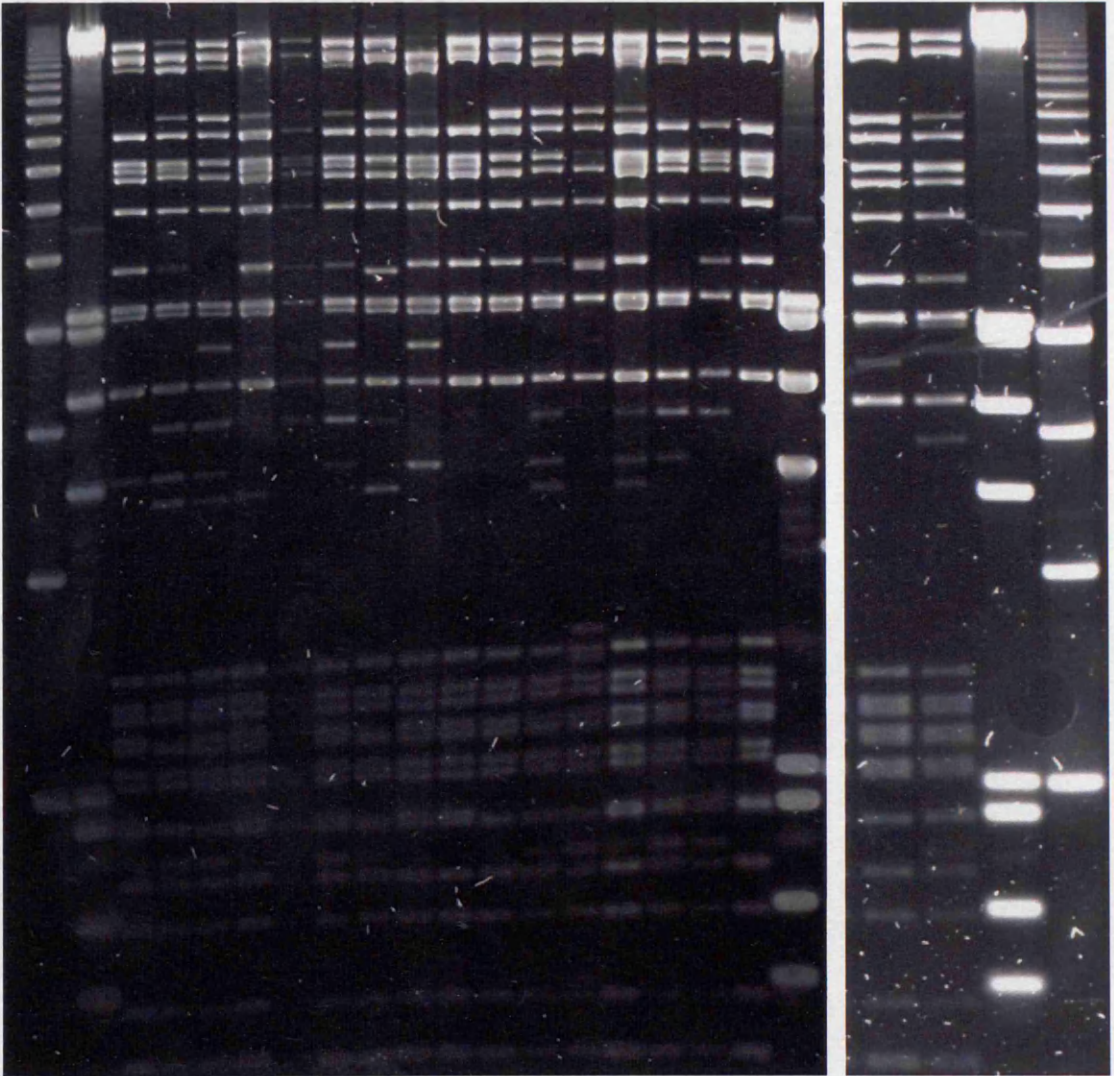


Figure 5.7 Eighteen *Spex*NPV field isolates (named FS1-FS18) characterised using *EcoRV* and chosen for further sequencing analysis and biological characterisation. DNA fragments separated by electrophoresis on 0.8% agarose gel at 40V for 24 hours. Molecular markers: M₁, 1kb ruler (Biorad); M₂, λ -*EcoRI* DNA marker (Bioline).

5.3.5 Phylogenetic Analysis

Phylogenetic analysis of the field isolates using the polyhedrin gene (295bp) appeared to highlight three main groups on the basis of percentage bootstrap values greater than 60 (for 1000 repetitions). The bootstrap value of each node represents the confidence one can place in the positioning of a particular branch. Therefore, nodes with values of less than 60 are considered much less likely to stand up to further scrutiny. Thus, a value of 100 demonstrates that, in all cases, the field isolate known as FS11 always separated out from all the other field isolates and the wild-type. A value of 64 supports the splitting FS9 and FS10 off into a third group from the remaining isolates (Figure 5.8). Further down the tree the grouping of FS6, 12 and 18 is well-supported with a bootstrap value of 82 and a value of 87 which further separates FS6 from FS18. In addition there is evidence to support the clustering of FS7, 13 and 14 (bootstrap value, 57) and a grouping of FS13 and FS14 (bootstrap value, 76).

Inclusion of the 17 variants cloned *in vivo* from the wild-type virus (chapter 3) into the phylogenetic analysis appears not to alter the three main groupings, with the bootstrap values for FS9, FS10 and FS11 remaining high. The grouping of FS6, FS12 and FS18, also remains well supported. The cloned variants are mainly attached to the FS5, FS8 and FS15 group, the FS1, FS16 and FS17 group and the wild type group (Figure 5.9).

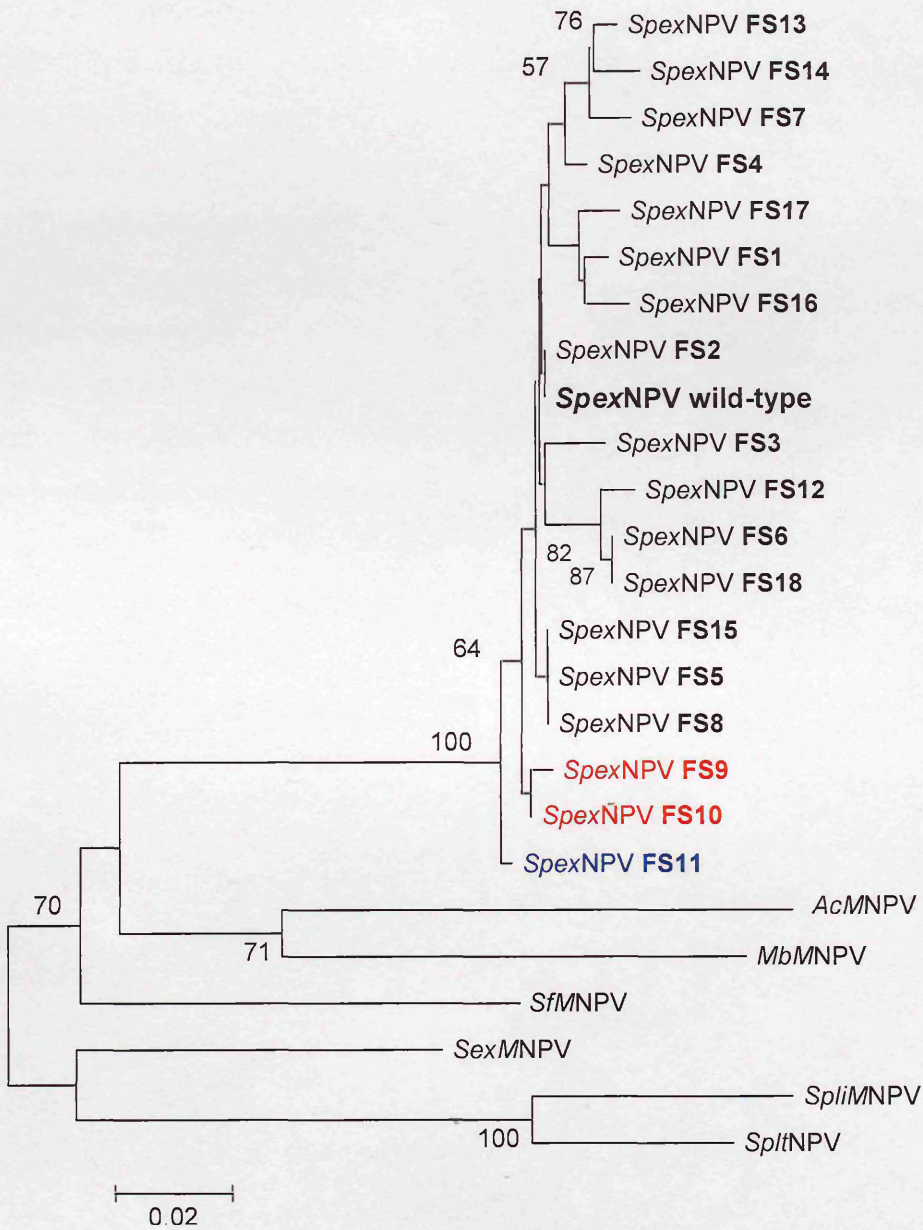
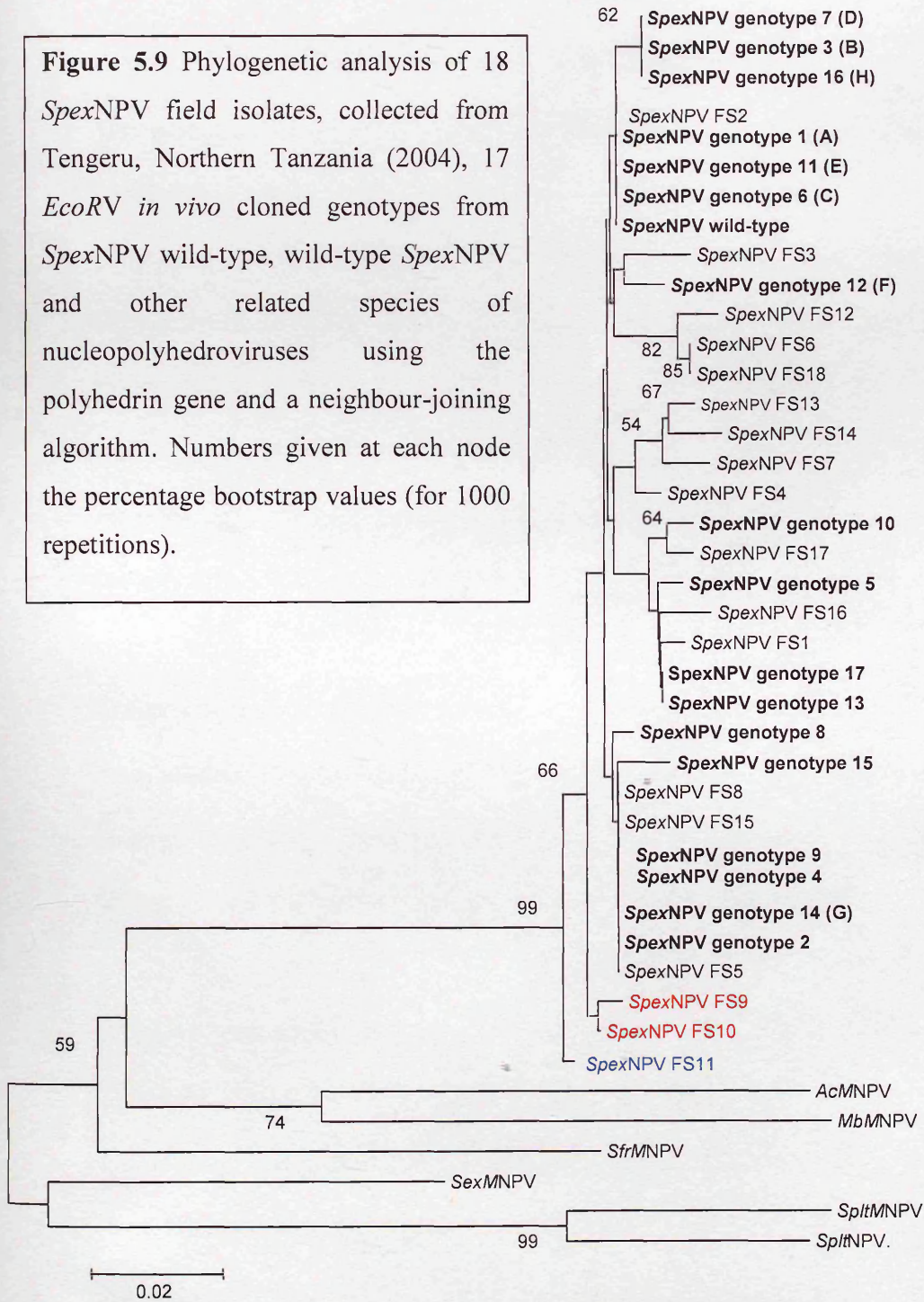


Figure 5.8 Phylogenetic analysis of the *polh* gene for *SpexNPV* wild-type, 18 isolates of *SpexNPV* collected from Tengeru, Northern Tanzania in 2004, and other related species of nucleopolyhedroviruses using a neighbour-joining algorithm. Differential colouring of field isolates represent the apparent clustering into three main groups. The numbers given at each node the percentage bootstrap values (for 1000 repetitions).

Figure 5.9 Phylogenetic analysis of 18 *SpexNPV* field isolates, collected from Tengeru, Northern Tanzania (2004), 17 *EcoRV* *in vivo* cloned genotypes from *SpexNPV* wild-type, wild-type *SpexNPV* and other related species of nucleopolyhedroviruses using the polyhedrin gene and a neighbour-joining algorithm. Numbers given at each node the percentage bootstrap values (for 1000 repetitions).



5.3.6 Pathogenicity of *Spex*NPV field isolates

The pathogenicity of field isolates, estimated in terms of LD₅₀ values, spanned a considerable range, with approximately a 100-fold difference between the most pathogenic isolate (FS3: LD₅₀ = 87 OBs/larva) and the least pathogenic (FS14: 8,864 OBs/larva). In addition, the LD₅₀ estimates produced for two of the field isolates proved extremely large (FS17 = 33,324,386 OBs and FS18 = 25,892 OBs; Figure 5.10), laying well beyond the actual dose range of the bioassay. Although these extrapolated LD₅₀ estimates are technically not valid, they do serve to highlight, for comparative purposes, the very different levels of pathogenicity found in natural populations.

The lack of replication of the bioassay demands caution when dealing with such results, but confidence in the validity of the assay, is given by the consistency of the LD₅₀ estimate for the wild-type virus (168 OBs), which lies within the confidence intervals estimated from the baseline bioassay chapter (see chapter 4).

In order to gain a more detailed picture of how pathogenicity of the field isolates altered with dose, the mortality data were logit-link transformed and analysis of covariance with ln(dose) was carried out using a binomial error structure. Deviances were adjusted using the scale parameter to allow for over dispersion of the data. As expected, dose had a considerable influence on mortality, with higher mortality at the higher doses, but the effect of dose altered with isolate (ln(dose) * isolate; $\chi^2_{18} = 48.19$, $P < 0.001$) (Figure 5.11).

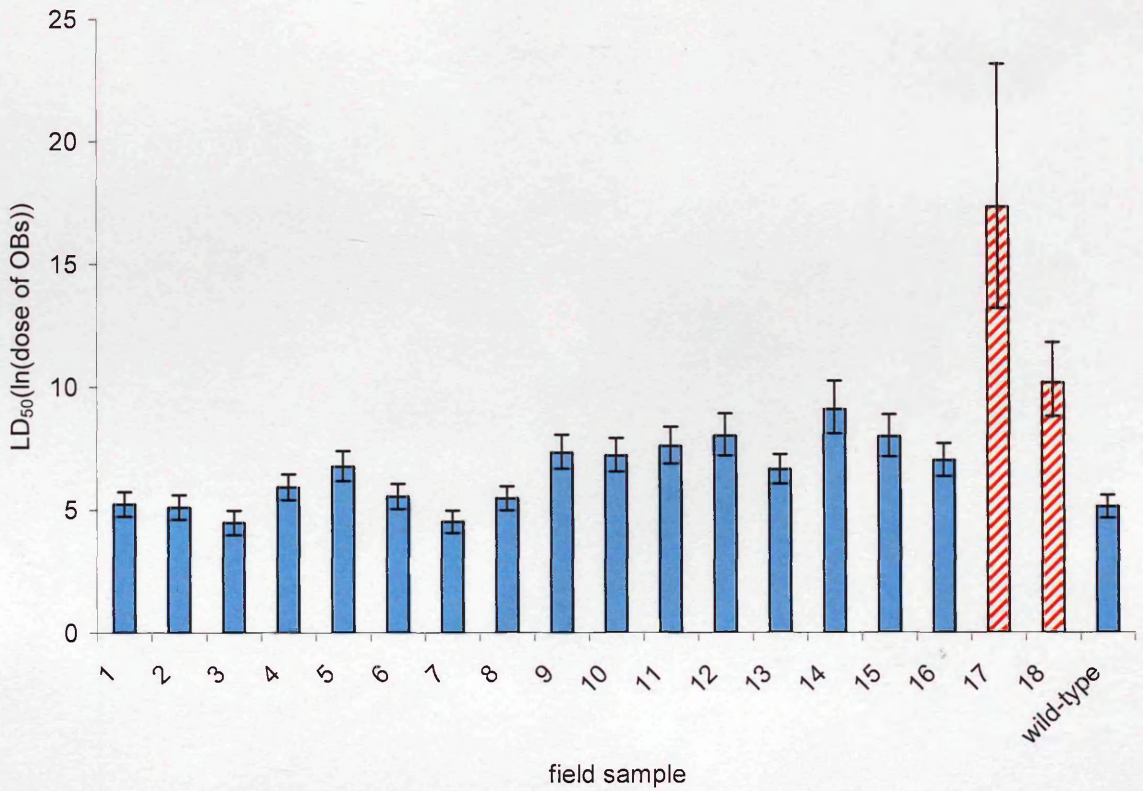


Figure 5.10 LD₅₀ estimates ($\pm 95\%$ confidence intervals) for 18 field samples of *SpexNPV* and wild-type virus i.e. viral dose required to kill 50% of 3rd instar *Spodoptera exempta* larvae. Stripped bars represent estimates produced through extrapolation of model beyond dose range of bioassay (FS17, LD₅₀ = 33,324,386 OBs and FS18, LD₅₀ = 25,892 OBs).

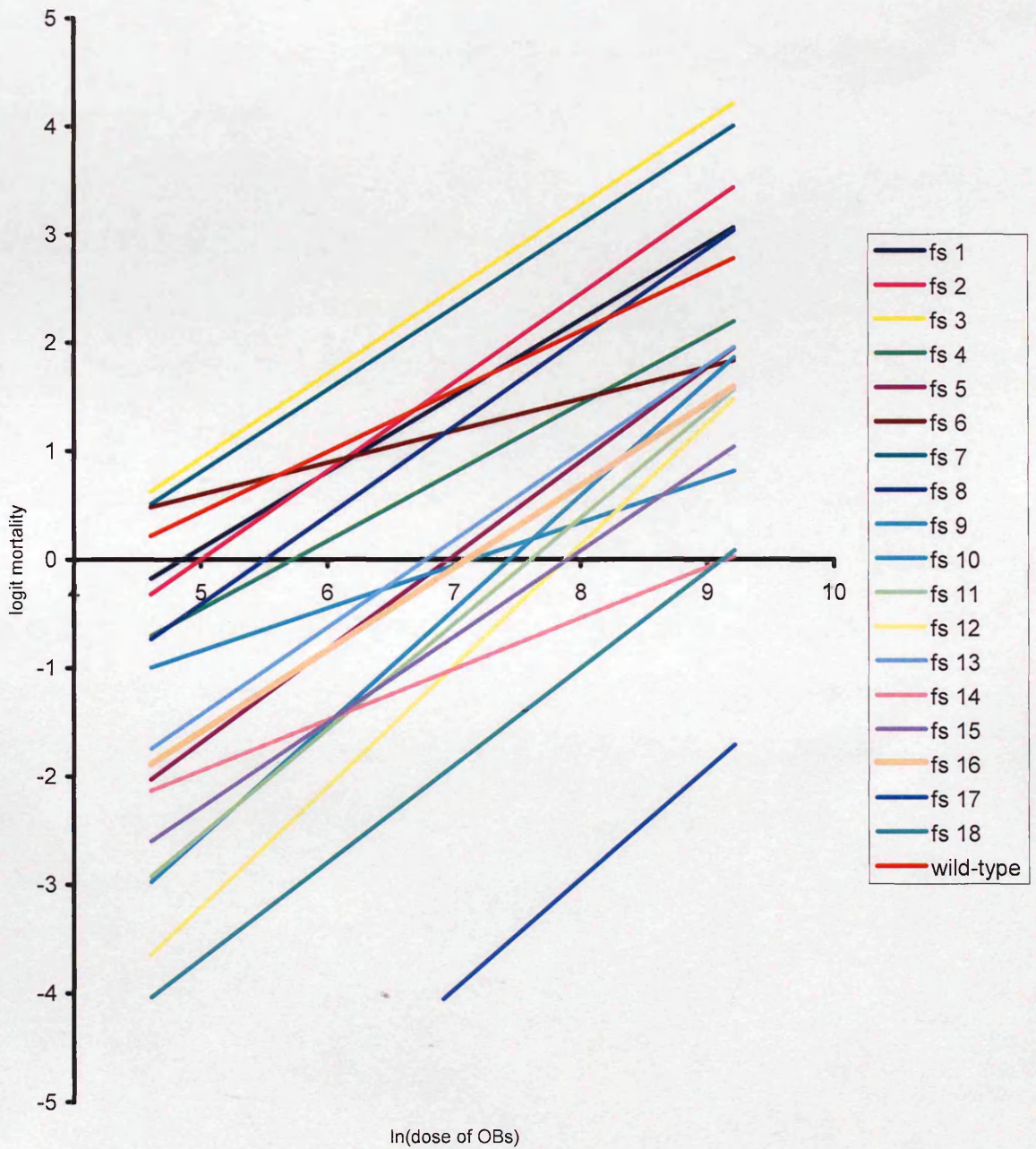


Figure 5.11 Dose-mortality curves of *SpexNPV* field isolates and wild-type virus. Fitted lines represent minimal adequate models fitted by ANCOVA. Observed values omitted to improve clarity.

From inspection of figure 5.11, several of the isolates appeared to be very similar and could be grouped without a significant increase in residual deviance. The field isolates were clustered into 5 groups (gp1: FS1, FS2, FS4, FS6, FS8 and WT; gp2: FS3 and FS7; gp3: FS5, FS9, FS11, FS12, FS13, FS15 and FS16; gp4: FS10, FS14 and FS18; gp5: FS17) without producing a significant increase in residual deviance ($F_{28,57} = 0.83$, $P = 0.69$; Figure 5.12).

Combining field sample 18 with FS10 and FS14 to produce group 4 produced an LD_{50} estimate of 5219 OBs which lies within the dose range of the assay. Field sample 17, on the other hand, which solely constitutes group 5, produced an LD_{50} estimate well beyond the upper dose of the bioassay and is represented by the striped bar in Figure 5.13. This still gives an approximately 60-fold difference between the least pathogenic group, gp4 (5219 OBs/larva), and the most pathogenic group, gp2 (87 OBs), not including group 5.

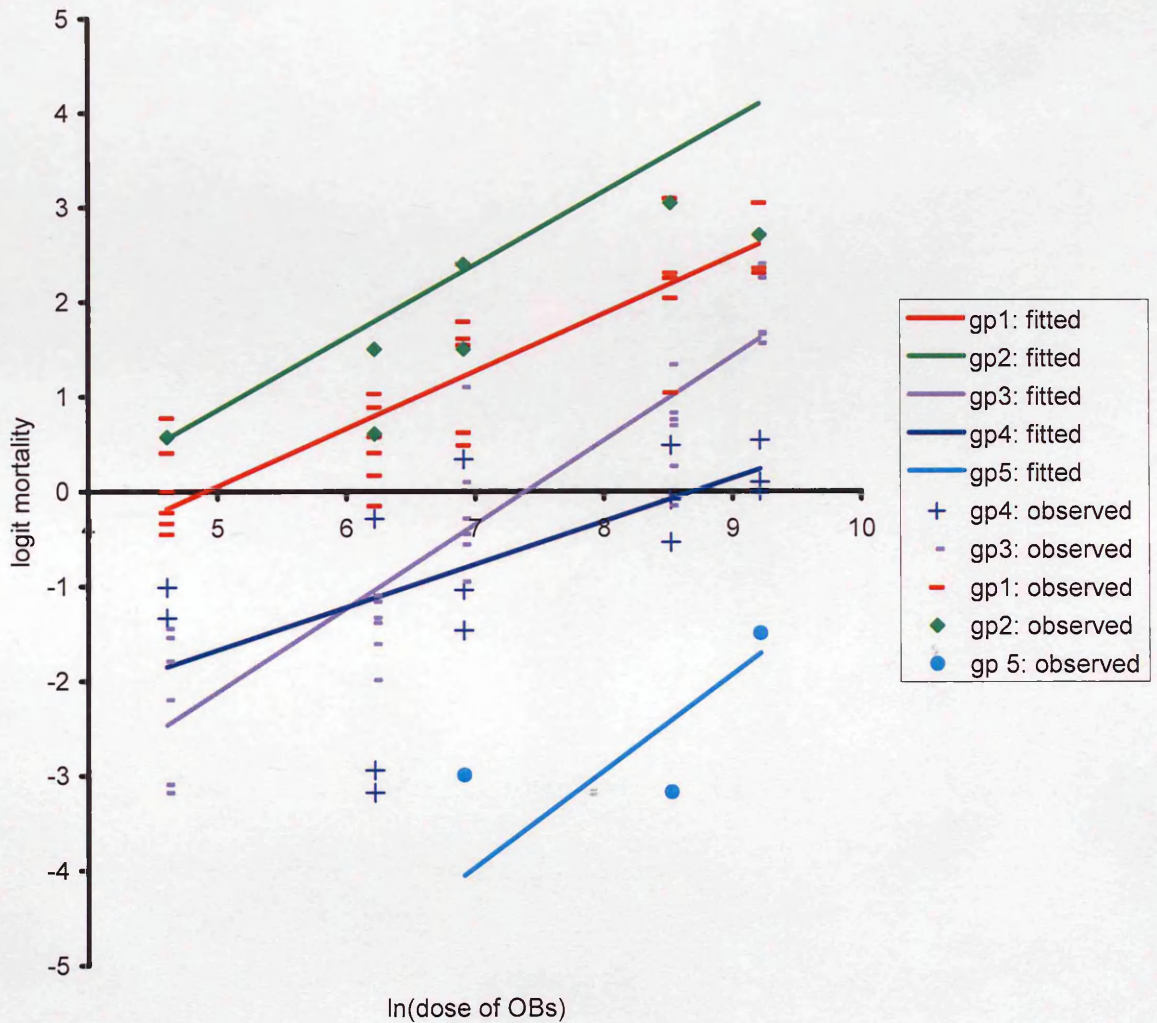


Figure 5.12 Dose-mortality curves of *SpexNPV* field isolates and wild-type virus, grouped according to dose-response relationship. Fitted lines: gp1 (field samples: 1, 2, 4, 6, 8 and wild-type virus), $\text{logit (mortality)} = -2.977 + (0.607 \times \ln(\text{dose}))$; gp2 (field samples: 3 and 7), $\text{logit (mortality)} = -2.975 + (0.768 \times \ln(\text{dose}))$; gp3 (field samples: 5, 9, 11, 12, 13, 15 and 16), $\text{logit (mortality)} = -6.539 + (0.885 \times \ln(\text{dose}))$; gp4 (field samples: 10, 14 and 18), $\text{logit (mortality)} = -3.937 + (0.453 \times \ln(\text{dose}))$; gp5 (field sample 17), $\text{logit (mortality)} = -11.086 + (1.018 \times \ln(\text{dose}))$. Symbols are observed values.

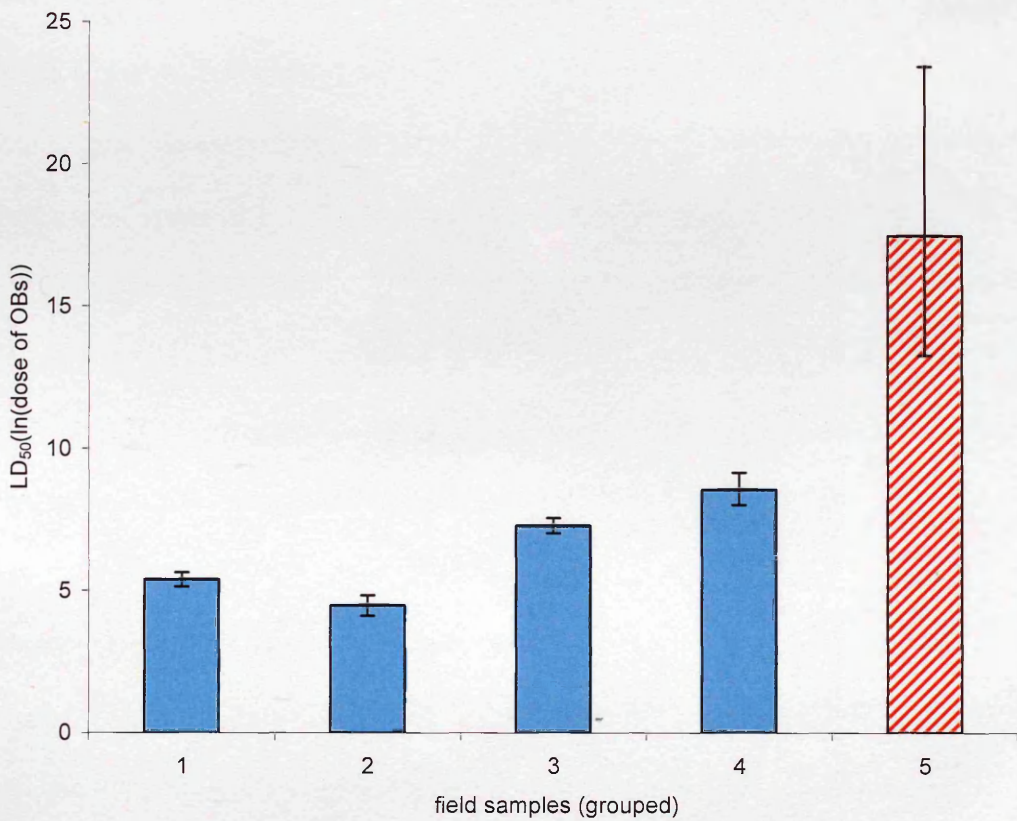


Figure 5.13 LD₅₀ estimates ($\pm 95\%$ confidence intervals) for field samples and wild-type *Spex*NPV of 3rd instar *Spodoptera exempta* larvae grouped according to dose-response relationship. Stripped bar represent estimates produced through extrapolation of model beyond dose range of bioassay (gp5 (FS17): LD₅₀ = 38744524 OBs).

5.3.7 Speed of kill of *Spex*NPV field isolates

Speed of kill data were transformed ($1/x^2$) and analysed with a normal error structure with $\ln(\text{dose})$ as a covariate and isolate as a factor. Isolate was found to be an important indicator of speed of kill, with differences of approximately 24hrs between the fastest killing isolate (FS1) and the wildtype virus, which possessed the slowest speed of kill ($F_{18,658} = 11.04$, $P < 0.001$; Figure 5.14). Dose also influenced speed of kill ($F_{1,658} = 35.77$, $P < 0.001$), irrespective of isolate (isolate * dose; $F_{1,642} = 1.22$, $P < 0.025$), with time to death decreasing with increasing dose (Figure 5.14).

On the basis of the analysis of covariance with dose, several of the isolates appeared similar and could be clustered into four groups without significantly increasing the residual deviance of the model ($F_{15,658} = 1.349$, $P = 0.167$; Figure 5.15).

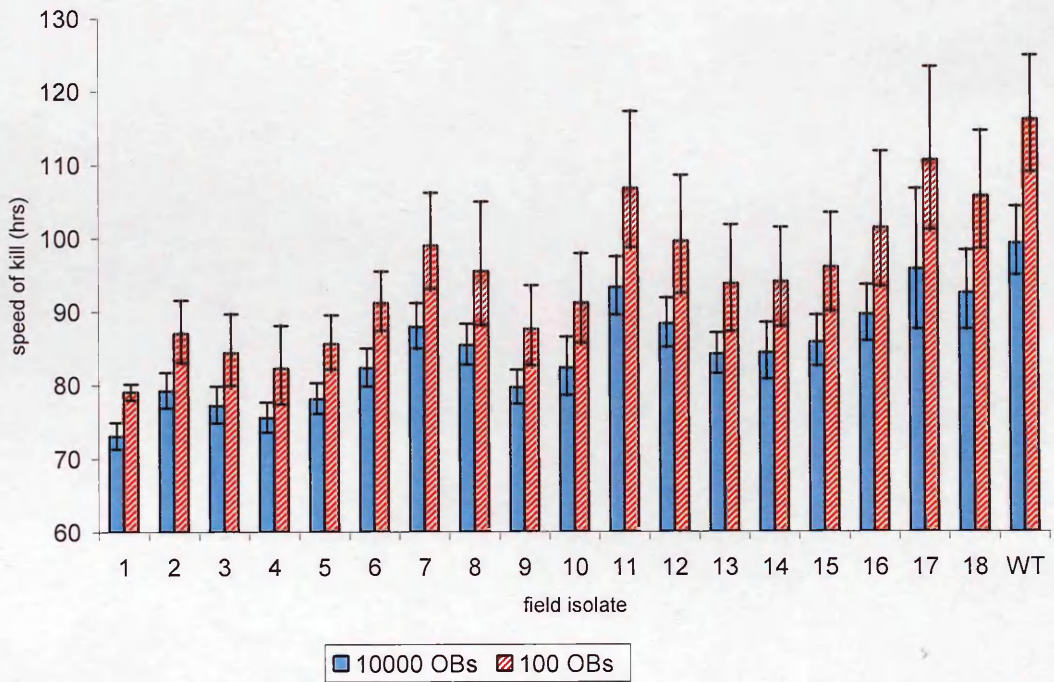


Figure 5.14 Estimated speed of kill ($\pm 1SE$) of *SpexNPV* field isolates at doses of 10000 OBs and 100 OBs. Sample sizes (10000 OBs, 100 OBs) = FS1, (21, 9); FS2, (19, 11); FS3, (15, 7); FS4, (20, 5); FS5, (23, 13); FS6, (21, 16), FS7, (22, 10); FS8, (23, 5); FS9, (22, 7); FS10, (9,7); FS11, (19, 8); FS12, (19, 7); FS13, (21, 6); FS14, (11, 7); FS15, (15, 8); FS16, (16, 6); FS17, (4, 7); FS18, (10, 10); WT, (20, 18).

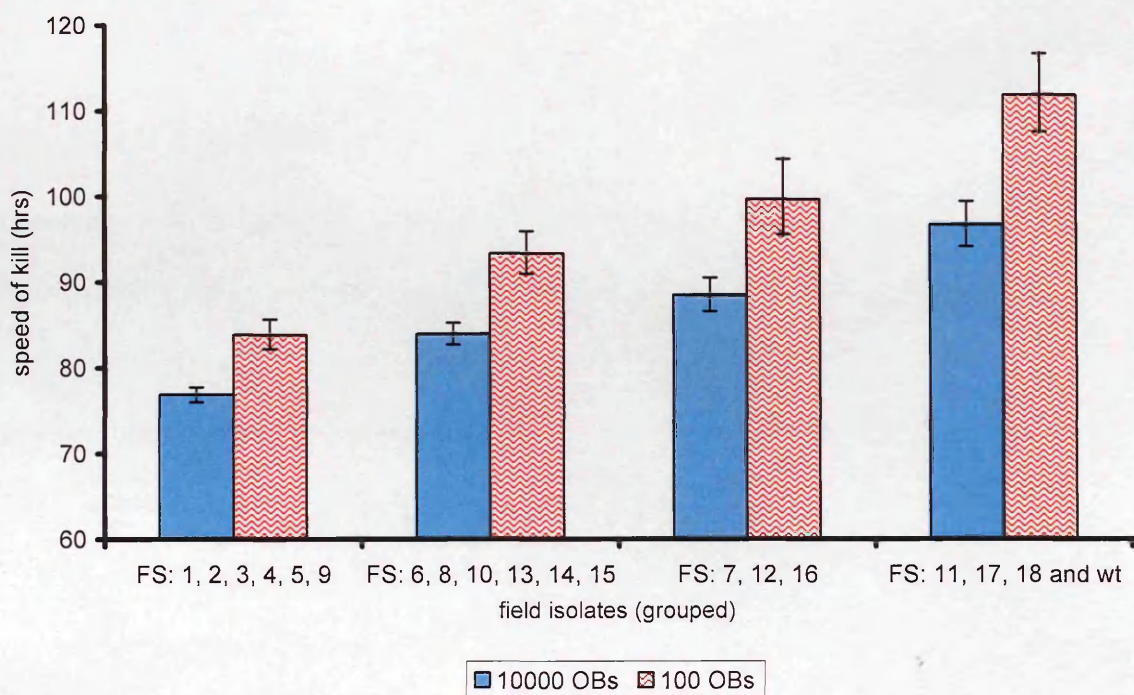


Figure 5.15 Estimated speed of kill ($\pm 1SE$) of *SpexNPV* field isolates at a dose of 10000 OBs and 100 OBs grouped according to dose-speed of kill relationship.

5.3.8 Yield of *Spex*NPV field isolates

The normality of the yield data meant that analysis of covariance could be carried out with a normal error structure without transforming the data. Isolate was assigned as a factor and $\ln(\text{dose})$ and transformed speed of kill ($1/x^2$) were treated as covariates. The interaction between dose and speed of kill was converted into a factor to allow analysis of two covariates in the model at the same time. Yield increased with lengthening time to death, however this relationship varied between genotypes, signified by the presence of an interaction term (genotype * speed of kill) in the model ($F_{11,147} = 3.333$, $P = 0.0004$). The production of lower yields at fast speed of kill was mirrored in all but one isolate but to various degrees depending on the steepness of the fitted curve. The wild-type virus and FS2 possessed extremely steep curves in comparison to the other isolates, showing that speed of kill at least for these viruses is a major predictor of yield, whereas for FS8, which possessed an almost horizontal line yield, speed of kill, remained relatively constant (Figure 5.16). Field isolate 11 proved to be the exception to this general pattern with yield for this isolate inversely correlated to speed of kill, producing lower yields at longer time to death. Interestingly, field isolate 11 also differentiated itself from all the other field isolates and the wild-type virus at the molecular level following phylogenetic analysis of the polyhedrin gene (previous section).

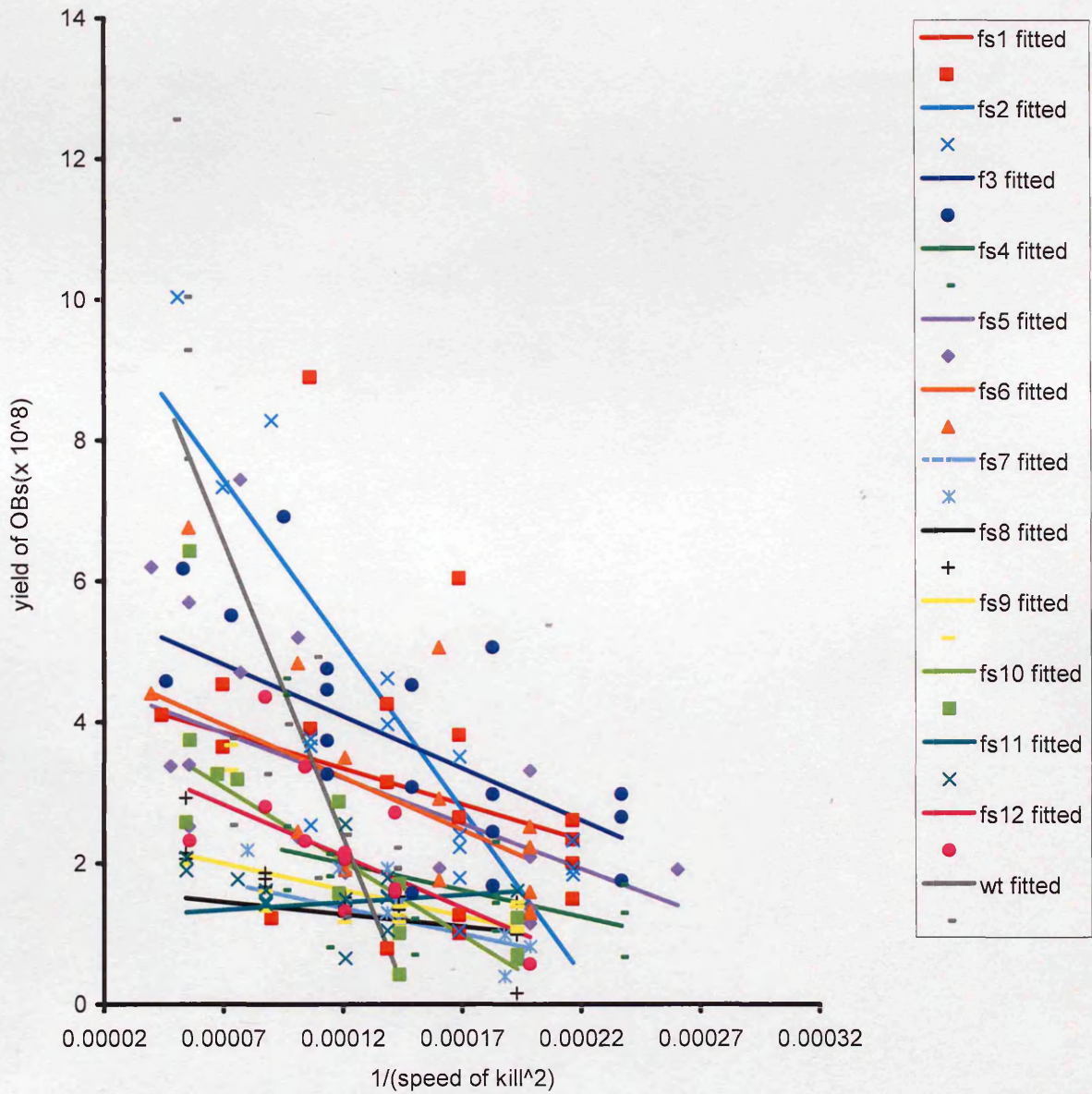


Figure 5.16 Speed of kill-yield relationship. Symbols represent yield of 3rd instar *S. exempta* larvae infected with individual *Spex*NPV field isolates (FS1-12) and wild-type virus at a dose of 10000 OBs. Fitted lines represent minimal adequate model fitted by ANCOVA.

In addition to the interaction between isolate and speed of kill, the interaction between speed of kill and dose also proved significant ($F_{1,147} = 4.799$, $P = 0.03$; Figure 5.17). Higher doses consistently produced lower yields for all isolates and wild-type virus over and above speed of kill.

Several isolates appeared very similar, based on inspection of their speed of kill-yield relationship, and could be statistically clustered in to 5 groups ($F_{16,172} = 1.305$, $P = 0.19$; Figure 5.18).

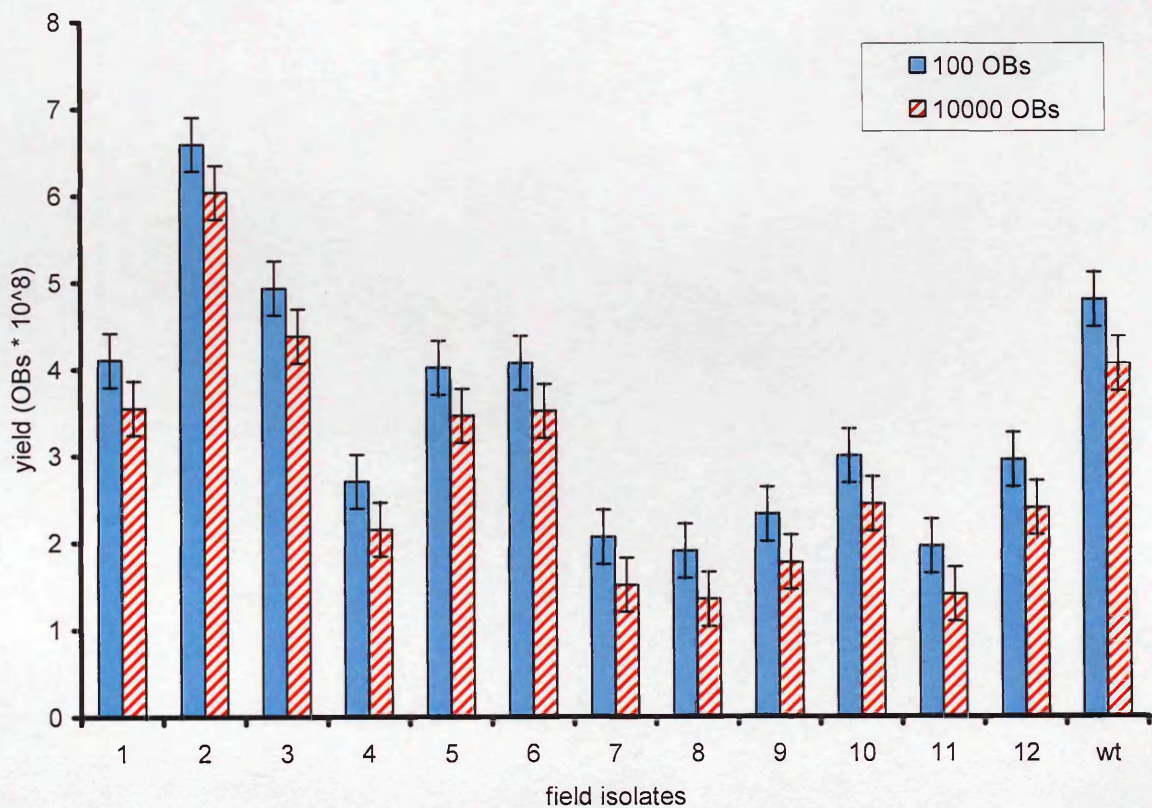


Figure 5.17 Estimated mean yield of OBs per *S. exempta* larva (± 1 SE) at doses of 100 and 10000 OBs for *SpexNPV* field samples 1-12 and the wild type virus. Sample sizes = 30 larvae for each isolate (15 larvae at each dose).

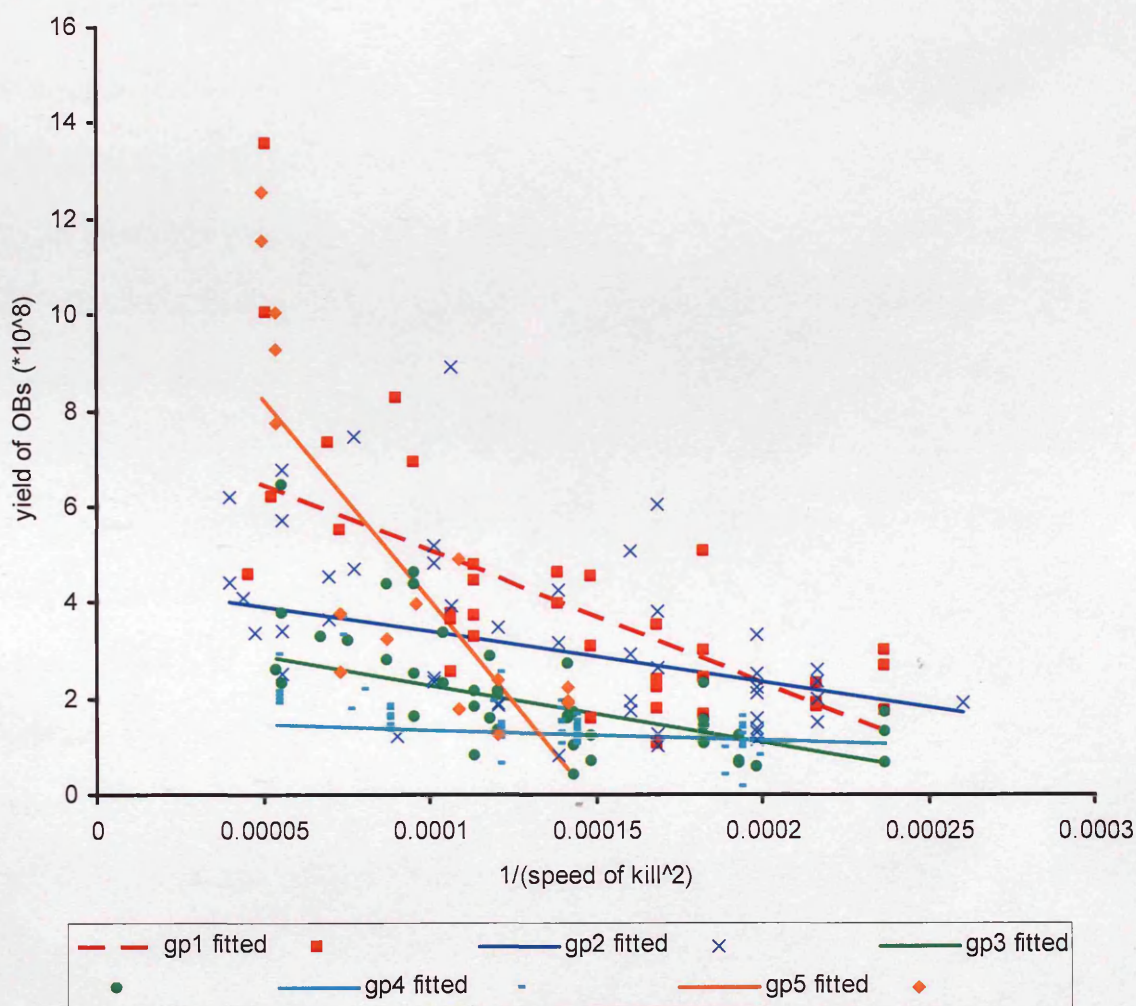


Figure 5.18 Speed of kill-yield relationship. Symbols represent yield of 3rd instar *S. exempta* larvae infected with individual field isolates and wild-type virus at a dose of 10000 OBs grouped according statistical similarity. Fitted lines: Gp1 (FS2 and 3) yield = $1.19e+9 - (5.3e+^{12} * (1/(\text{speed of kill}^2)) - (4.4e+^7 * \text{Indose}) + (2.74e+^{11} * (1/(\text{speed of kill}^2)*\text{Indose})))$; gp2 (FS1, 5 and 6), yield = $8.48e+^8 - (3.6e+^{12} * (1/(\text{speed of kill}^2)) - (4.4e+^7 * \text{Indose}) + (2.74e+^{11} * (1/(\text{speed of kill}^2)*\text{Indose})))$; gp3 (FS4, 10 and 12), yield = $7.51e+^8 - (3.7e+^{12} * (1/(\text{speed of kill}^2)) - (4.4e+^7 * \text{Indose}) + (2.74e+^{11} * (1/(\text{speed of kill}^2)*\text{Indose})))$; gp 4 (FS7, 8, 9 and 11), yield = $5.64e+^8 - (2.7e+^{12} * (1/(\text{speed of kill}^2)) - (4.4e+^7 * \text{Indose}) + (2.74e+^{11} * (1/(\text{speed of kill}^2)*\text{Indose})))$; gp5 (wt virus), yield = $1.65e+^9 - (1.1e+^{13} * (1/(\text{speed of kill}^2)) - (4.4e+^7 * \text{Indose}) + (2.74e+^{11} * (1/(\text{speed of kill}^2)*\text{Indose})))$.

5.4 Discussion

Spodoptera exempta is a migratory outbreak pest and therefore experiences enormous fluctuations in population densities. For this study African armyworm populations were only sampled during periods of extremely high host densities and from different field sites in 2002 and 2004, and therefore only offers a snapshot of the potential relationship between host density, viral prevalence and genetic diversity. The heightened potential for horizontal viral transmission at high host densities could in theory increase the prevalence of *Spex*NPV. Epizootics of *Spex*NPV have often been observed during periods of high host densities (Odindo, 1983; E. Redman, personal observation) but a thorough testing of the link between host density and viral prevalence has not previously been undertaken. The limited data obtained here appears to suggest a positive correlation between the two. Epizootics of viral disease in other species experiencing high host densities appears to suggest that these pathogens may play a role in regulating insect dynamics (Anderson and May, 1980; Cory *et al.*, 1997). Population cycles of forest Lepidoptera have provided the main focus of studies examining the long-term interactions between NPVs and their host. The ability to completely defoliate any area of vegetation, or pasture within a generation necessitates the establishment of each subsequent armyworm generation, in a completely new area. This has meant that Armyworm has evolved a migratory habit, which makes it difficult to envisage *Spex*NPV reaching high enough levels in a population, capable of exerting a similar dynamic influence on its host, as that witnessed within a relatively stable forest environment. However *Spex*NPV persists during long periods of extremely low host densities in tropical or equatorial regions, where UV levels are commonly very

high. *Spex*NPV is often reported during armyworm outbreaks and has been credited with local population collapses (see: Rose *et al.*, 2000). This clearly demonstrates that *Spex*NPV is a highly effective and well-adapted mortality agent of African armyworm, whose ecology and mechanisms of persistence have yet to be fully elucidated.

Two very different scenarios of how high host density may influence virus diversity have been generated. The first involves the dominance of the epizootic by a particularly virulent or well-adapted variant, through a process of frequency-dependent selection. Although other low-frequency genotypes will be maintained in the population, the population would possess, on the whole a reduced diversity. The dominance by a single genotype has been demonstrated within several natural baculovirus populations (Brown *et al.*, 1985; Gelernter and Federici, 1990; Laitinen *et al.*, 1996; Munoz *et al.*, 1998; Stiles and Himmerich, 1998; Graham *et al.*, 2004). Natural populations of *Spex*NPV though, did not appear to be dominated by just one or two genotypes. On the contrary the level of genetic diversity identified was immense with more than one in every three of the isolates collected representing novel genotypic variants. The apparent correlation, witnessed in this study appears to support the second of the two possible effects of host density which is the elevation of diversity.

Host density can influence viral diversity directly by alternating the selection pressures on the viral population. During armyworm outbreaks when host densities can reach in excess of 800 larvae per m², (Cheke and Tucker, 1995) the selection pressure exerted on viral genotypes for high pathogenicity and yield, as well as slow degradation outside

the host, is in theory relaxed and will therefore allow the co-existence of genotypes with varying different phenotypes. In addition, host densities can also affect the genetic composition of the viral population indirectly, through a positive correlation between host density and viral prevalence. Something that, as discussed earlier, the preliminary data presented here offers support for. It is postulated that the increased viral prevalence associated with high host densities, increases the opportunities for the expression of different virus variants, through simply the presence of higher absolute levels of virus in the environment facilitating the re-emergence of rarer variants. In addition, elevated virus prevalence increases the probability for mixed infections, and consequently the opportunities for recombination between co-infecting genotypes. 40% of the total number of isolates sampled in this study represented multi-genotype infections, based on RFLP analysis. Although mixed infections were identified in a study which investigated the genetic variation of the Western Tent caterpillar, *Malacosoma californicum pluviale* (*Mcp*NPV) (Cooper *et al.*, 2003), no attempt was made to quantify them. In the only other study to have investigated genetic variation using individual virus-infected larvae direct from the field, an individual genotype dominated prevalence and an extremely low number of mixed infections (<1%) within natural populations of Winter moth, *Operophtera brumata* NPV in Orkney were found (Graham, 2004). The identification of relatively low levels of diversity, coupled with an extremely rare incidence of mixed infection for *Opbu*NPV, appears to represent the complete opposite to that observed here for *Spex*NPV, of extremely high levels of diversity and co-infection.

The sampling and genetic analysis of the 2004 *Spex*NPV epizootic at Tengeru, Northern Tanzania revealed some evidence for a positive correlation between host density and proportion of mixed infections in support of the theory. There was no evidence though for a link between host density and level of diversity between the four main field sites sampled within the same outbreak at Tengeru. This does not mean a link between the two does not exist. The host densities of the sites were all relatively high, as expected during an outbreak. In order to increase the probability of detecting a link between host density and genetic diversity a much larger range of densities, including those witnessed during the non-outbreak periods need to be included in the sampling regime.

In an effort to elucidate if the high genetic variance of *Spex*NPV populations possessed sub-structure the level of diversity was compared at a range of spatial scales from a 0.25m² quadrat to a 2ha field-site. By using the adjusted Simpson's Diversity Index differences between sample sizes could be taken into account. Although diversity appeared a little lower at the lowest ecological scale (quadrat) the reduction was only slight and on the whole there appeared no apparent genetic structuring to the *Spex*NPV population at high host densities. Confirmation of the apparent randomness of the genetic variation could be achieved through the application of Wright's F-statistics (Wright, 1978), which measures the partitioning of genetic diversity within and among possible sub-populations. This technique, which also takes into account the potential bias of differential sample sizes, was used in a study of the genetic variation of the Western Tent caterpillar, *Malacosoma californicum pluviale* (*Mcp*NPV) (Cooper *et al.*,

2003). Cooper *et al.*, (2003) found that variants were more likely to be the same within a family group than isolates compared among populations. In addition, virus variants from within populations were more likely to be the same than isolates collected from tent caterpillar populations on different islands. This demonstrated a hierarchical spatial structure of the NPV population and indicated the degree of mixing of the population was potentially limited at low host densities. As a result, it was argued would allow the virus to become locally adapted to host populations at different sites. Unlike Western Tent caterpillars *S. exempta* does not live in the relative isolation of family groups. Larvae are highly mobile creatures whose need to consume large amounts of food in a limited space of time forces them to “march” considerable distances in search of fresh food sources. The distribution of larvae during an outbreak therefore appears to simply reflect the present availability of edible vegetation and the obvious preference *S. exempta* displays for certain host species e.g. *Cynodon dactylon* (L.) Pers. (E. Redman, personal observation). Considering the lack of structure in the host population it is hardly surprising that we found no apparent sub-structuring of *Spex*NPV populations within an outbreak. In order to elucidate how the genetic composition of *Spex*NPV populations alters over time, a much larger investigation needs to be undertaken which characterises *Spex*NPV epizootics at each generation through the season, starting in the primary outbreak sites near the coast and finishing with the final outbreaks in Northern Kenya. In this way, the diversity between outbreaks could be estimated. *Spex*NPV could also be characterised from solitaria larvae during the “off-season”, both as overt infections, if they exist, and from persistent infections in order to see if the diversity is maintained during the periods of low host density. Such investigations would allow

important insights into the extent environmental reservoirs of OBs and the triggering of persistent infections contribute in the establishment of epizootics.

Chapter Six

Dual infections of *Spex*NPV genotypes

Chapter 6: Dual infections of *Spex*NPV genotypes

6.1 Introduction

The presence of mixed genotype infections are becoming increasingly more apparent in nature from a range of host-parasite systems including malaria parasites of humans and rodents (Day *et al.* 1992; Snounou *et al.*, 1992; Paul *et al.*, 1999); trypanosomes of tsetse fly (Woolhouse *et al.*, 1996), African horse sickness in zebra (Lord *et al.*, 1997), HIV (Holmes *et al.*, 1992) of humans, schistosomes of snails (Davies *et al.*, 1999) as well as baculoviruses (Cooper *et al.*, 2003a; Cory *et al.*, 2005). We have shown that multiple-genotype infections are ubiquitous in natural epizootics of the nucleopolyhedrovirus of *Spodoptera exempta* (*Spex*NPV), with a prevalence of mixed infections of at least 40% (see Chapter 5). An overt NPV infection commonly utilises all the tissue of its host during infection. Consequently, within a mixed-genotype infection the host represents a limited resource and it has been postulated that intra-specific competition between co-infecting genotypes will undoubtedly play a crucial role in the host-parasite dynamic (Hodgson *et al.*, 2004). Epidemiological models of within-host dynamics tend to assume that the optimal level of prudent host exploitation, seen within a single genotype infection, is invalidated within a mixture due to the effect of increasing exploitation rates of competing genotypes for limited host resources (Levin and Bull, 1994; May and Nowak, 1995; Bremermann and Pickering, 1983; van Baalen and Sabelis, 1995; Frank, 1996). In the competitive situation of a mixed infection, parasites which slowly exploit host resources are expected to be out-competed by parasites able to exploit the host more rapidly. Thus, short-term selection, driven by within host competition is predicted to lead to increased levels of virulence, with reduced

transmission. Central to the prediction that mixed-genotype infections will raise virulence above that seen in single-genotype infections is the assumed trade-off between virulence and transmission. It has been termed the “adaptive trade-off hypothesis” and forms the basis of the majority of models generated to help understand the evolution of virulence. It states that increased parasite virulence, measured as host mortality, reduces the infectious period of the host and thereby reduces parasite transmission (Ewald, 1994). For obligate-killing baculoviruses the “cost” of increased virulence is measured in terms of speed of kill not mortality rate which, due to the trade-off between speed of kill and yield lowers the yield of progeny OBs produced, thus lowering parasite fitness (Ebert and Weisser, 1997; Hodgson *et al.*, 2004). Thus, theory predicts that single-genotype NPV infections observe a prudent strategy of exploitation which has evolved an optimum speed of kill in order to maximise occlusion body yield, and thus transmission. However, due to the theory of selection the adaptive trade-off is invalidated by intra-specific competition which raises virulence (faster speeds of kill) above that which is optimum for maximum parasite fitness and transmission within a multi-NPV genotype infection (Levin and Bull, 1994). Several studies have been carried out in order to test the prediction of a correlation between genotypic diversity and virulence experimentally, including malaria parasites (Taylor *et al.*, 1998), schistosome infections of snails (Davies *et al.*, 2002) and trypanosomes in bumblebees (Imhoof and Schmid-Hempel, 1998) with variable results.

In this chapter, we compare the virulence measured in terms of pathogenicity and speed of kill of single and dual *Spex*NPV genotype infections in *S. exempta* larvae in order to

test the adaptive trade-off prediction that mixed infection results in increased virulence. Thus, we predict that, in mixed infections, competition between competing genotypes will lead to an increase in the speed of kill (i.e. the infection duration will shorten) and, as a consequence, the transmission potential of the virus (i.e. the yield of occlusion bodies) will reduce.

6.2 Methods

6.2.1 Bioassay experimental design

Occlusion bodies of individual *SpexNPV* genotypes possessing similar levels of virulence and dose-responses in single-genotype infections (Chapter 4) were combined in equal numbers to produce mixed viral suspensions. These two-clone mixtures, as well as each of the individual clones, were used to challenge newly-moulted 3rd instar *S. exempta* larvae at a range of 5 doubling doses (10000, 5000, 2500, 1250 and 625 OBs per larvae) using the diet-plug inoculation technique (section 2.4.1). Twenty five larvae were used per dose, except for the lowest two doses for which 50 larvae were used in order to produce sufficient numbers of cadavers for yield and time to death analysis. Additional larvae were dosed with sterile distilled water to act as controls (3 replicates x 25 larvae = 75 larvae). Larval mortality due to *SpexNPV* was monitored every 8-12 hours to produce estimates of viral pathogenicity and speed of kill. Data analysis was via generalized linear modelling with either normal errors (speed of kill and yield) or binomial errors and logit link (mortality) using GLIM (section 2.5.3).

6.2.2 Determination of viral pathogenicity

Viral deaths were identified via examination of gross pathology, except when the cause of death was unclear, in which case the presence of viral OBs was tested via Geimsa staining (section 2.4.2). None of the control larvae died of virus, indicating the absence of contamination in the experiment. Non-viral deaths were removed from the dataset.

Estimates of the number of virus OBs produced upon death (i.e. viral yield) were estimated using standard methods (section 2.4.3). In order to identify whether the infections were by a single viral genotype or were mixed infections, the DNA from 8 cadavers from the highest dose of each treatment was extracted and digested with *EcoRV* endonuclease, and the RFLP was visualised by gel electrophoresis (section 2.3.3).

6.2.3 Calculating predicted mortality in dual infections

We attempted to predict the expected mortality rate when larvae are exposed to a dual infection clones in 1:1 ratio, by combining the mortality rates caused by the two clones when they infected *S. exempta* larvae singly. Thus, in order to estimate mortality at a combined dose of 10 000 OBs (5000 OBs from clone X and 5000 OBs from clone Y) we used the fitted values of mortality for each of the single infections at a dose of 5000 OBs each.

If the mortality rate for clone X at 5000 OBs is x (say, 0.7) and for clone Y is y (say, 0.6) then the mortality rate from mixed infections of both X and Y is equal to xy (i.e.

$0.7 \times 0.6 = 0.42$). Under this scenario, the proportion of larvae dying from clone X only would then equal $x - xy$ (i.e. $0.7 - 0.42 = 0.28$) and the proportion of larvae dying from clone Y only would equal $y - xy$ (i.e. $0.6 - 0.42 = 0.18$). Therefore, dual infection at 10 000 OBs would produce a predicted mortality of the sum of all three possible outcomes (i.e. $0.42 + 0.28 + 0.18 = 0.88$) (see Figure 6.1). The same logic can be used to calculate the predicted mortality resulting from dual infection at total doses of 5000, 2500 1250 and 625 OBs. Chi-squared analyses were used to compare observed mortality rates against these predicted values for all dual infections where differences were observed.

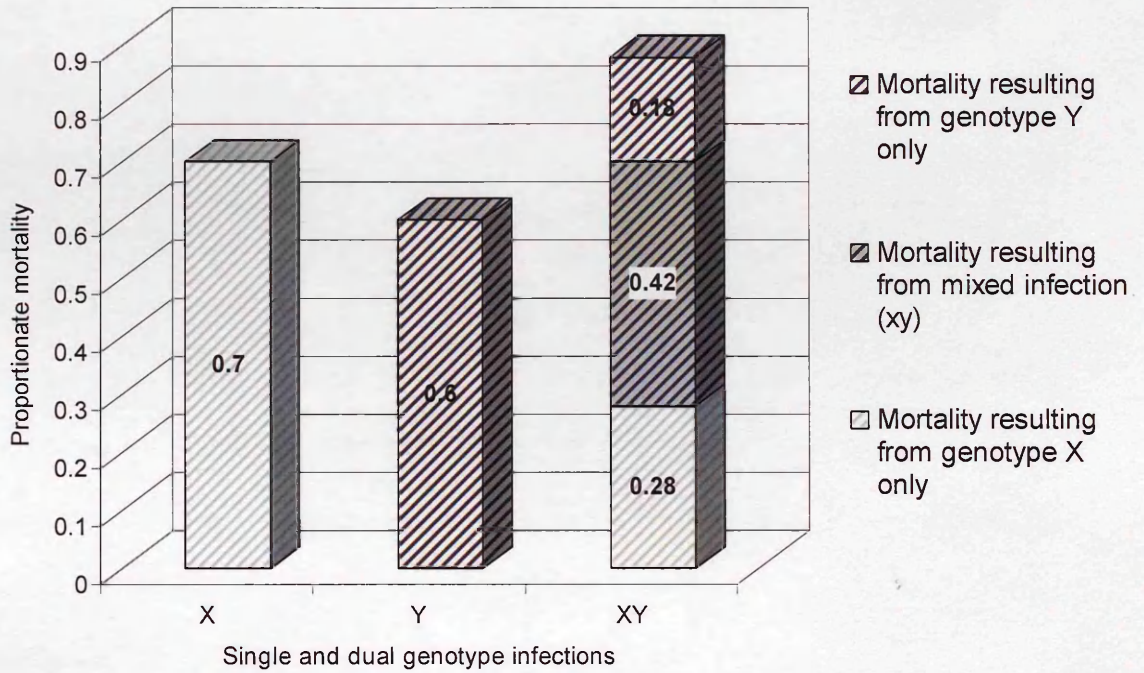


Figure 6.1 Schematic representation for predicting the proportionate mortality of a dual infection (XY) at a dose of 10000 OBs using the fitted values of single genotype infections (X and Y) at 5000 OBs.

6.2.4 Determination of proportions of different genotypes in progeny virus

In order to determine what proportion of caterpillars inoculated with two viral clones harboured mixed viral infections, DNA from ten progeny cadavers resulting from the highest dose (10000 OBs) for each of the dual infections was extracted and digested with the restriction endonuclease, *EcoRV*. The resultant bands were visualised by gel electrophoresis and subsequent staining with SybR Gold[®] in order to assess the actual proportions of mixed infections and single genotypes achieved in dual inoculation. Novel bands, for the characterisation of mixed infections were identified by comparing restriction endonuclease profiles of individual genotypes combined in dual inoculations.

6.3 Results

6.3.1 Pathogenicity

Mortality data were analysed with dose as a covariate. A binary error structure was assumed with the number of genotypes in the viral mixture (*mix*) assigned as a factor with two levels. Deviances were adjusted via the scale parameter to allow for over dispersion of the data. When all dual and single infections were analysed *en masse*, viral dose ($\ln(\text{dose})$) was found to be the only statistically significant predictor of mortality ($\chi^2_1 = 166.7$, $P < 0.001$). There were no interaction between *mix* and $\ln(\text{dose})$ ($\chi^2_1 = 0.121$, $P > 0.72$) and *mix* was also found to be statistically non-significant ($\chi^2_1 = 0.14$, $P > 0.24$). Thus, using this approach, it was not possible to detect any gross difference in mortality rates between single and mixed-clone infections, above and beyond between-genotype variation.

Therefore, a second approach was taken in which the mortality rate of each 2-clone mixture was compared to the mortality rates from the corresponding single-clone infections (e.g. the mortality rate of insects infected with mixture A/C was compared that of insects infected with either genotype A or C). In the statistical model, this was achieved by including viral treatment as a factor with three levels, namely the first single genotype, the second single genotype and the dual infection of genotypes one and two.

Viral treatment affected pathogenicity in 8 out of the 12 dual infections investigated (Table 6.1). In all these cases, the two single genotypes produced similar mortality

levels and could be grouped together without altering the model significantly and, for the majority the pathogenicity of the mixture was elevated above single infections across all doses. The dose-mortality curves of the AF bioassay are shown in Figure 6.2 to demonstrate this relationship. Similar patterns of increased pathogenicity were also observed for DF, CF, EF, BG and BH dual infections (figures not shown).

This pattern was not observed in all mixtures, however. For AC and HG dual infections, there were significant interactions between mixture and dose (Figure 6.2). However, the nature of this interaction varied according to the viral genotypes involved. For a dual infection of AC, mortality increased above single infections at just below the LD₅₀, but fell below that of single infections at lower doses, hinting at the possibility of interference between genotypes.

Table 6.1 Summary of analysis of observed pathogenicity of *Spex*NPV dual infections against corresponding single infections and predicted values. Each genotype is only paired with another genotype from within its pathogenicity group (see Chapter 4).

Pathogenicity group	Dual infection	Model	(χ^2)
Low	AC	mix * ln(dose)	$\chi^2_1 = 6.481$, P < 0.015 (interaction)
	AF	mix + ln(dose)	$\chi^2_1 = 10.40$, P < 0.002 (mix)
			$\chi^2_1 = 52.84$, P < 0.001 (ln(dose))
	CF	mix + ln(dose)	$\chi^2_1 = 54.35$, P < 0.001 (mix)
			$\chi^2_1 = 62.77$, P < 0.001 (ln(dose))
	DF	mix + ln(dose)	$\chi^2_1 = 16.16$, P < 0.001 (mix)
$\chi^2_1 = 86.49$, P < 0.001 (ln(dose))			
EF	mix * ln(dose)	$\chi^2_1 = 4.842$, P = 0.027 (interaction)	
High	BG	mix + ln(dose)	$\chi^2_1 = 8.3$, P < 0.004 (mix)
			$\chi^2_1 = 21.69$, P < 0.001 (ln(dose))
	BH	mix + ln(dose)	$\chi^2_1 = 14.2$, P < 0.001 (mix)
			$\chi^2_1 = 49.72$, P < 0.001 (ln(dose))
	HG	mix * ln(dose)	$\chi^2_1 = 3.96$, P < 0.046 (interaction)

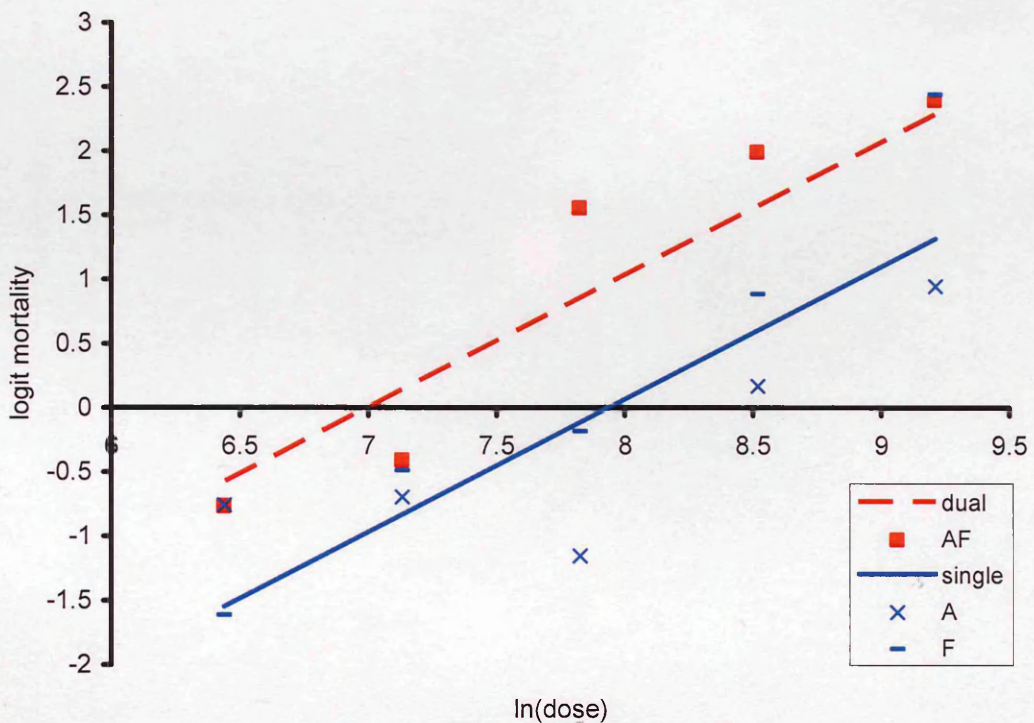


Figure 6.2 Dose-mortality curves of *Spex*NPV genotypes A and F in single (blue) and dual (red) infections. Fitted lines: A/F dual infection, $\text{logit}(\text{mortality}) = -8.187 + 1.032(\ln(\text{dose}))$; A and F single infections grouped according to level of virulence $\text{logit}(\text{mortality}) = -7.22 + 1.032(\ln(\text{dose}))$. Symbols represent observed values. Similar results were observed for DF, CF, EF, BG and BH dual infections (not shown).

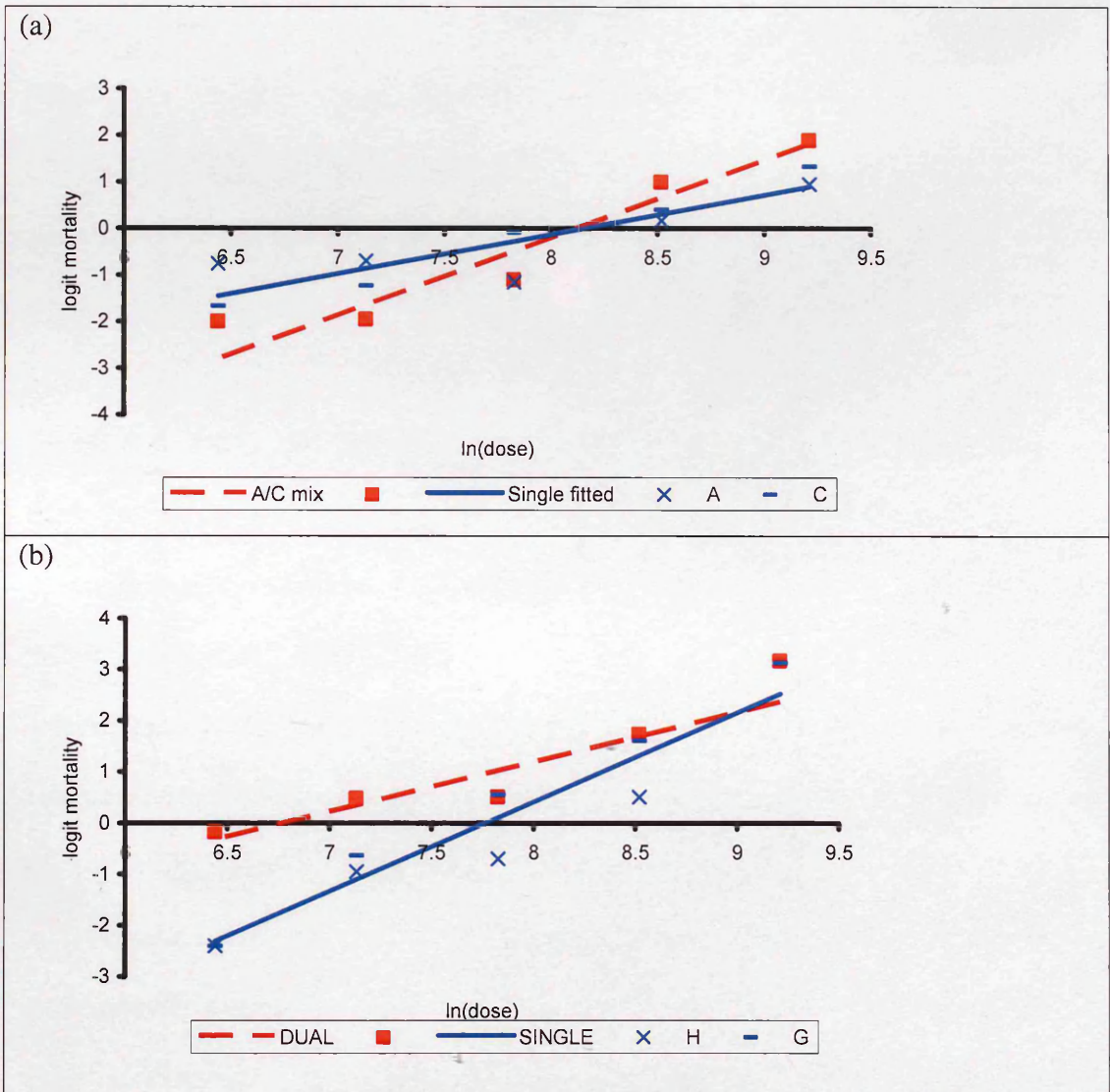


Figure 6.3 Dose-mortality curves of *SpexNPV* single and mixed infections. (a) Genotypes A and C, fitted lines: AC dual infection, $\text{logit}(\text{mortality}) = -6.867 + 0.8426(\ln(\text{dose}))$; A and C single infections (grouped), $\text{logit}(\text{mortality}) = -13.499 + 1.664(\ln(\text{dose}))$. (b) Genotypes H and G, fitted lines: HG dual infection, $\text{logit}(\text{mortality}) = -13.51 + 1.74(\ln(\text{dose}))$; H and G single infections (grouped), $\text{logit}(\text{mortality}) = -6.55 + 0.968(\ln(\text{dose}))$. Symbols represent observed values.

For mixture HG, the interaction of dose and mixture resulted in higher pathogenicity for the mixture of genotypes than for single infections at all but the highest doses, where they converge (Figure 6.3). This is perhaps explained by the fact that the genotypes H and G possess much higher individual pathogenicities than the other genotypes and consequently the elevation of pathogenicity of dual infection at high doses is restricted.

Figure 6.4 shows the difference between the observed and predicted levels of pathogenicity in dual infections and shows that, in the majority of dual infections, observed mortality exceeded predicted levels across all doses, with the exception of the AC mix, where the observed levels of mortality are much lower than the predicted levels. This confirms earlier observations that low doses appear to facilitate a degree of interference in dual infections between genotypes A and C, resulting in decreased levels of pathogenicity below single infections. In general though, this model of mixed infection and this method of prediction under-estimated the actual levels of pathogenicity observed, especially at the lower doses. At higher doses, the model was better able to predict the outcome. The exception to this was the EF mix, in which the observed and predicted values were not significantly different ($\chi^2_4 = 7.77$, $P < 0.1$).

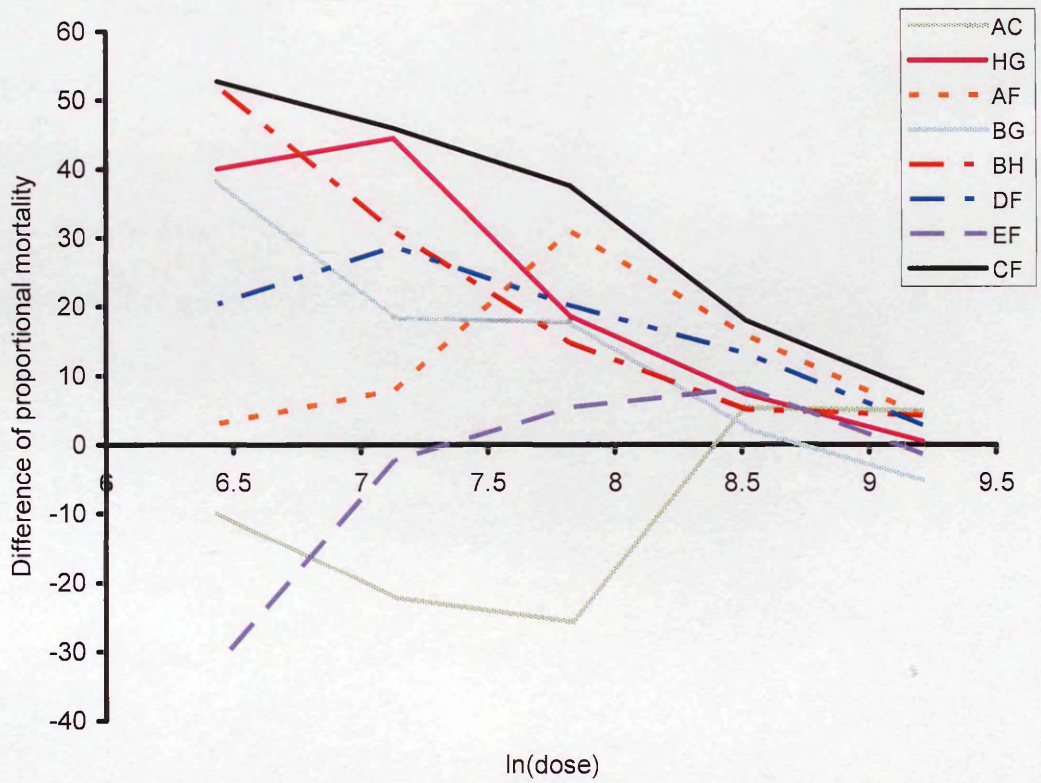


Figure 6.4 Difference between observed and predicted mortality for dual infections of *SpexNPV* genotypes using fitted mortality values for single genotype infections obtained from this experiment.

6.3.2 Speed of kill

Speed of kill, measured over intervals of between 8 and 12 hours, was calculated with zero hour taken as the time larvae were first introduced into the dosing arena. As with the mortality data, each dual infection was analysed separately and compared with its corresponding single genotype infections to determine if differences in speed of kill could be detected. The data were transformed appropriately (Table 6.2) to allow a normal error structure to be assumed and both *viral treatment* (3 levels: first single genotype, second genotype and dual infection of genotypes one and two) and the number of genotypes in the infection (*mix*) were tested in the model as factors, with the natural log of viral dose ($\ln(dose)$) treated as a covariate.

Differences between *viral treatments* were detected in all but one dual infection (ED) (Table 6.2). In the majority of cases (10/13), *mix* was also found to be a significant term in the model and allowed the single genotype infections to be combined without significantly reducing the fit of the model. This indicated that differences in speed of kill can be seen in most mixed infections in comparison to single infection of the same genotypes. However, for genotypes E and D, which have been shown to possess not only similar levels of pathogenicity, but also similar speeds of kill (Chapter 4), mixed and single infections had similar speeds of kill. In contrast, although genotypes A and C also had similar speeds of kill and pathogenicity, dual infection produced a dramatic lengthening of the speed of kill by approximately 16 hours, irrespective of dose (Figure 6.4).

Table 6.2 Speed of kill (hrs) for single and dual infections of *SpexNPV* genotypes, calculated using corresponding models at a viral dose of 10 000 OBs.

Dual infection	Transform for normality (x = speed of kill)	Minimal adequate model	Speed of kill (hrs) estimated from model at viral dose 10 000 OBs.		Outcome on infection duration
			Single infection	Dual infection	
AC	$1/(x^2)$	mix + ln(dose)	89.7	106.2	Lengthened
AD	$1/(x^2)$	mix	96.3	108.9	Lengthened
AE	$1/x$	mix	98.0	120.0	Lengthened
AF	$1/(x^2)$	mix + ln(dose)	95.2	104.8	Lengthened
CD	$1/(x^2)$	mix + ln(dose)	92.0	113.2	Lengthened
CE	$1/(x^2)$	mix + ln(dose)	87.4	102.5	Lengthened
CF	$1/(x^3)$	mix * ln(dose)	91.4	103.0	Lengthened
EF	$1/(x^3)$	mix * ln(dose)	96.2	107.5	Lengthened
BG	$1/(x^2)$	mix	108.1	112.6	Lengthened
DF	$1/(x^3)$	mix * ln(dose)	96.4	92.4	Decreased
HG	$1/x$	viral treatment	H = 117.7 G = 108.5	112.9	Intermediate
BH	$1/x$	viral treatment	B = 107.0 H = 117.4	114.1	Intermediate
ED*	$1/x$	–	E = 98.7 D = 101.4	101.0	No effect

* Terms failed to explain data, therefore estimates taken as mean speed of kill at that dose

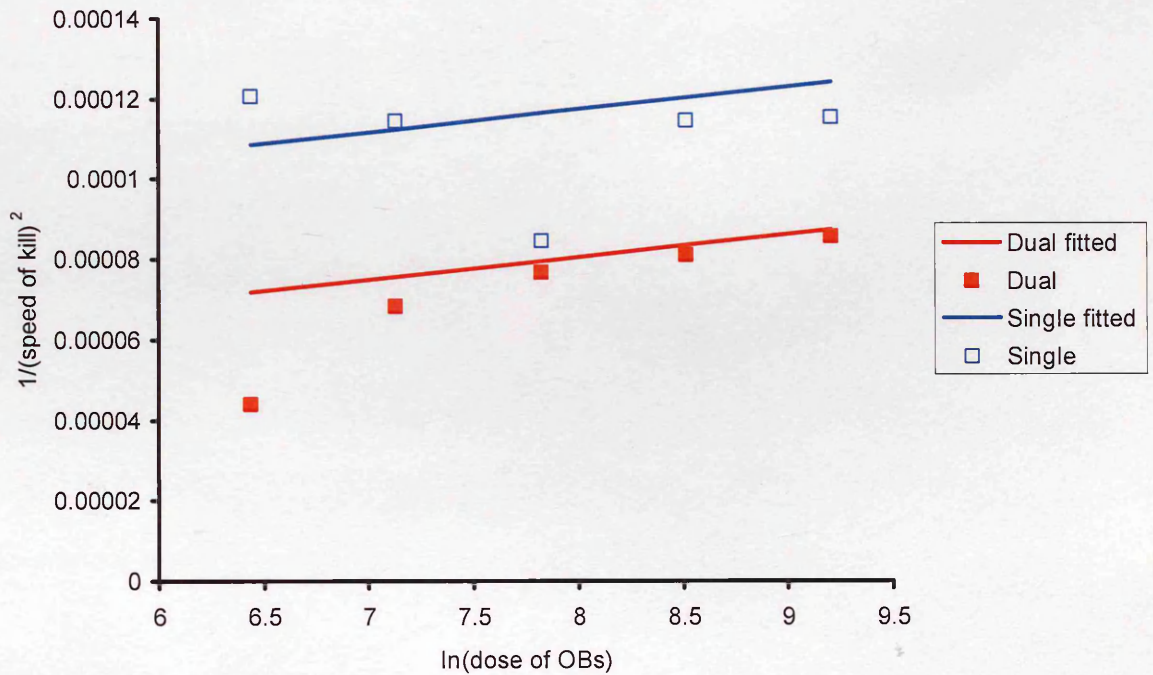


Figure 6.5 Speed of kill-viral dose relationship for single and dual infections of *SpexNPV* genotypes A and C. Fitted lines: AC dual infection, $1/(\text{speed of kill})^2 = 3.686 \cdot 10^{-5} + (5.628 \cdot 10^{-6} \cdot \ln(\text{dose}))$ and single A and C infections grouped according to speed of kill, $1/(\text{speed of kill})^2 = 7.247 \cdot 10^{-5} + (5.628 \cdot 10^{-6} \cdot \ln(\text{dose}))$. Symbols represent observed values.

In fact, in 9 out of the 12 dual infections where differences were seen, mixing of genotypes lengthened the speed of kill beyond that observed in single infections by between 4 and 22 hours (Figure 6.5).

DF was the only dual infection where speed of kill decreased below that seen in single infections. For the remaining two mixtures where differences were seen (HG and BH), the single genotypes could not be grouped and dual infections produced an intermediate speed of kill between the two single infections (Figure 6.6). This reaffirms previous observations of the unusually long speed of kill of genotype H (Chapter 4).

In addition to the number of genotypes in the infection, viral dose also proved a significant term in many of the models (Table 6.2). The lack of a dose-response in some cases may simply have been the result of using of a much narrower dose range than would usually be chosen for bioassay purposes.

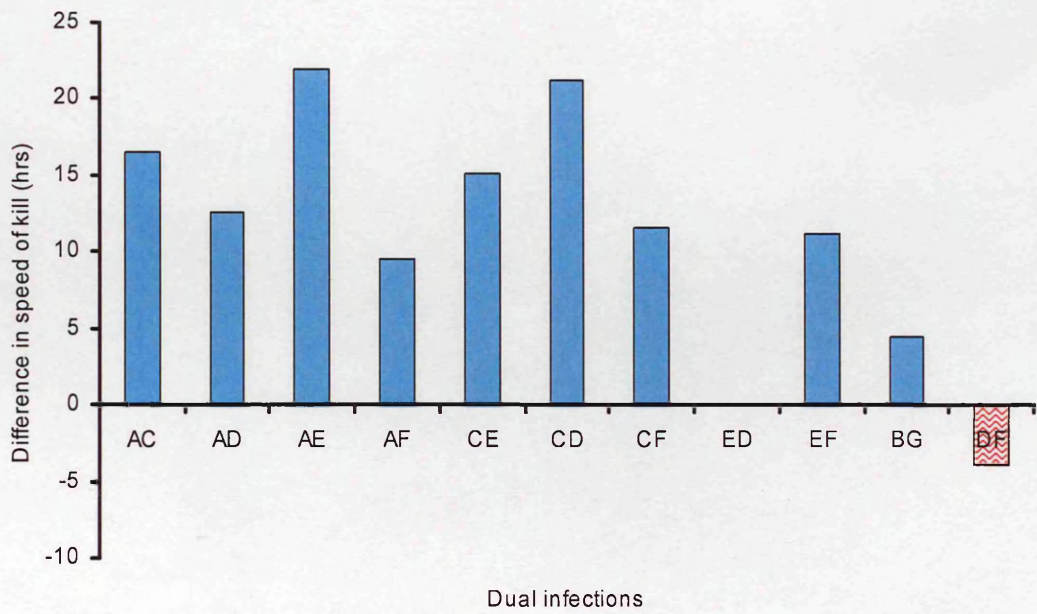


Figure 6.6 Increase in time to death (hrs) of dual infections of *SpexNPV* genotypes relative to corresponding single infections at a dose of 10000 OBs.

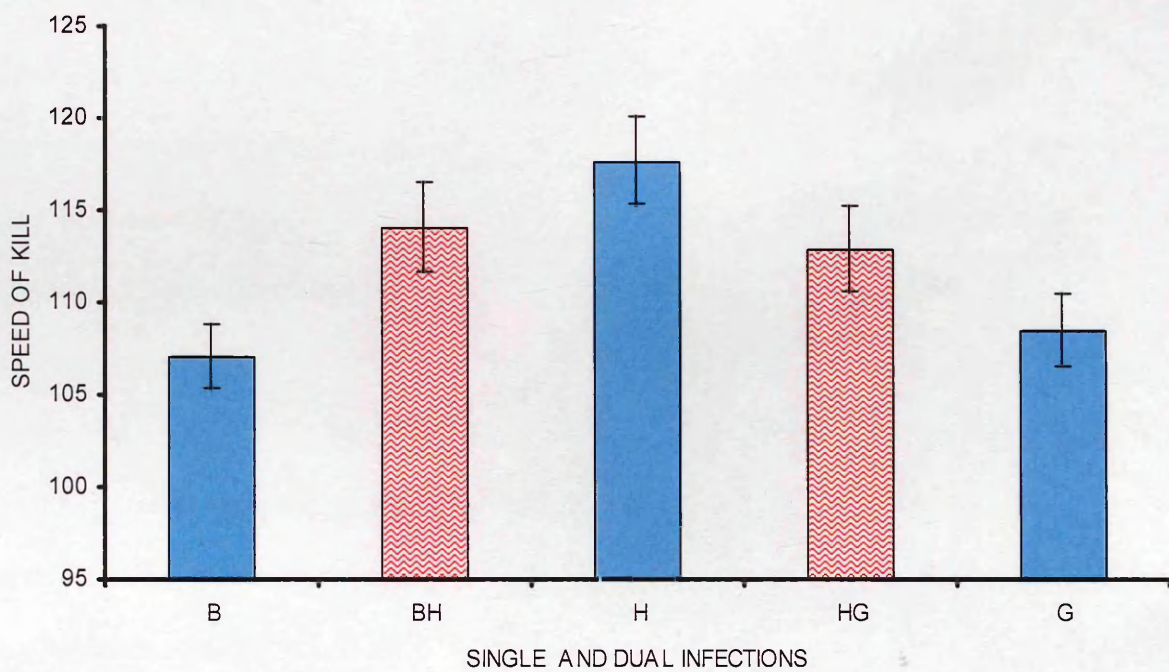


Figure 6.7 Back-transformed speed of kill (hrs) (\pm 1SE) of *SpexNPV* genotypes BH and HG dual infections and their corresponding single infections at a dose of 10000 OBs.

6.3.3 Viral yield

Following the same approach as for mortality and speed of kill data, viral yield data of dual infections were analysed separately for each mixture, with comparisons being made between the yield from mixtures and their corresponding single-genotype infections. The model comprised the terms *viral treatment* (first single genotype, second single genotype, dual infection) and *mix* (i.e. the number of genotypes in the infection) as factors in the model. The natural log of dose, $\ln(\text{dose})$ was treated as a covariate, as well as speed of kill. The interaction between these two covariates was converted into a factor in the model to allow the inclusion of two covariates in the model at the same time ($\ln(\text{dose}) * \text{speed of kill} = \text{inter}$).

Dual infection had a variable effect on yield depending on genotypes involved. For 5 out of the 13 dual infections, yields matched those found in the single infections, 4 resulted in an increase in OBs per cadaver and the remaining 4 resulted in lower yields. Yield of OBs as a measure of fitness is obviously an extremely complex biological trait to predict from single infections and is clearly influenced by many different factors including viral dose, pathogenicity and speed of kill (Table 6.3) and therefore requires closer inspection.

Table 6.3 Outcome of dual infection of *Spex*NPV genotypes on yield of OBs per *S.exempta* larva at a dose equivalent to an LD₅₀ relative to single infection.

Dual infection	Minimal adequate model	Outcome of yield estimated from model relative to single infection at LD ₅₀ .
AC	$1/\text{yield} = (\text{treat} * \ln(\text{dose})) + \text{ttd}$	Increased
AD	$\text{yield} = \text{treat} + (\text{ttd} * \ln(\text{dose}))$	No effect (Intermediate between genotypes)
AE	$\ln(\text{yield}) = \text{treat} + \text{ttd}$	Increased
AF	$\sqrt{\text{yield}} = \text{ttd} * \ln(\text{dose})$	Increased
CD	$1/\sqrt{\text{yield}} = (\text{treat} * \ln(\text{dose})) + \text{ttd}$	No effect (Same as highest yielding genotype)
CE	$1/\text{yield} = (\text{treat} * \ln(\text{dose})) + \text{ttd}$	Increased
CF	$\ln(\text{yield}) = (\text{treat} * \ln(\text{dose})) + \text{ttd}$	Decreased
DE	$\ln(\text{yield}) = (\text{treat} * \ln(\text{dose})) + \text{ttd}$	No effect (Intermediate between genotypes)
DF	$\ln(\text{yield}) = (\text{treat} + \ln(\text{dose})) + \text{ttd}$	Decreased
EF	$\ln(\text{yield}) = (\text{treat} * \ln(\text{dose})) + \text{ttd}$	Decreased
BG	$\sqrt{\text{yield}} = \text{treat} * \ln(\text{dose}) * \text{ttd}$	No effect
BH	$\ln(\text{yield}) = \text{treat} * \ln(\text{dose}) * \text{ttd}$	Decreased
HG	$\sqrt{\text{yield}} = (\text{treat} * \text{ttd}) + (\text{treat} * \ln(\text{dose}))$	No effect (Same as lowest yielding genotype)

6.3.4 Interaction between speed of kill and yield

When the interaction between speed of kill and viral yield was examined in detail, several distinct patterns appeared to emerge, as outlined below.

(i) Faster speed of kill, produces lower yields: mixture DF

DF is the only dual infection that has a faster speed of kill than its single infections. Lower yields for a given speed of kill are also seen in this dual infection and therefore this is an example of the trade-off working in the opposite direction to that predicted (Figure 6.8).

(ii) Lengthened speeds of kill, produce higher yields: mixtures AF, AE, CE and AC

For mixture AF, yield was a function of speed of kill and viral dose only (Table 6.3). By comparing yields at the same level of pathogenicity or viral dose, it becomes clearer that elevated yields are seen in dual infections but are simply the result of a lengthening of the speed of kill by approximately 10 hours beyond single infections (Figure 6.9).

Similarly, dual and single A and E infections are equally infectious but in mixture produces a dramatic lengthening of speed of kill of over 20 hours beyond single infections, irrespective of dose. AE produces higher final yields than both single infections (Figure 6.10) but again this appears to be simply the result of longer speed of kill. At any given time-point on the fitted speed of kill-yield curve dual infection produces yields intermediate between the single infections (Figure 6.11).

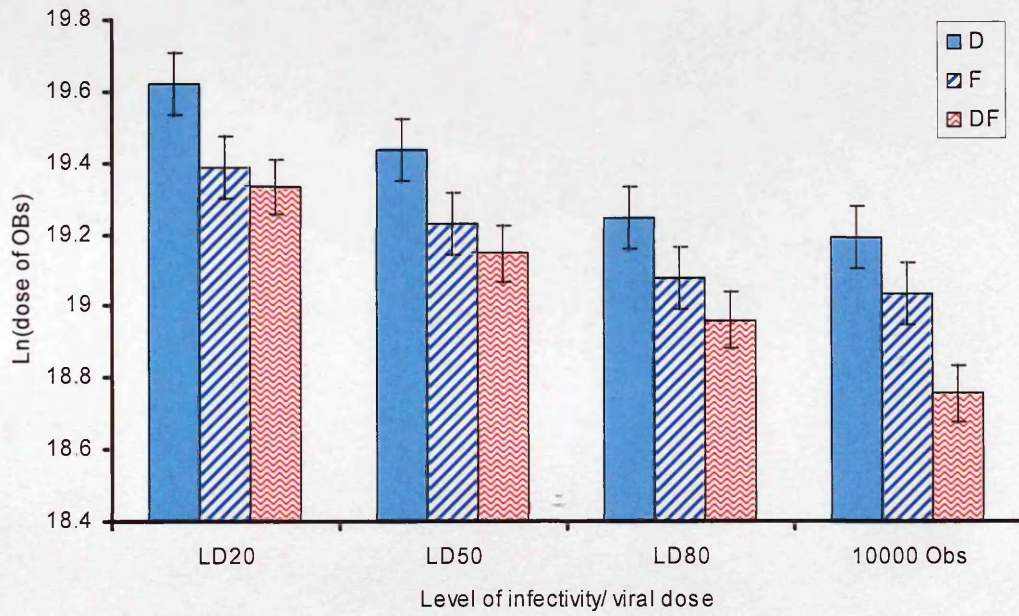


Figure 6.8 Estimated mean yield (\pm 1SE) of *SpexNPV* genotypes D and F in single and dual infection at a range of infectivity levels.

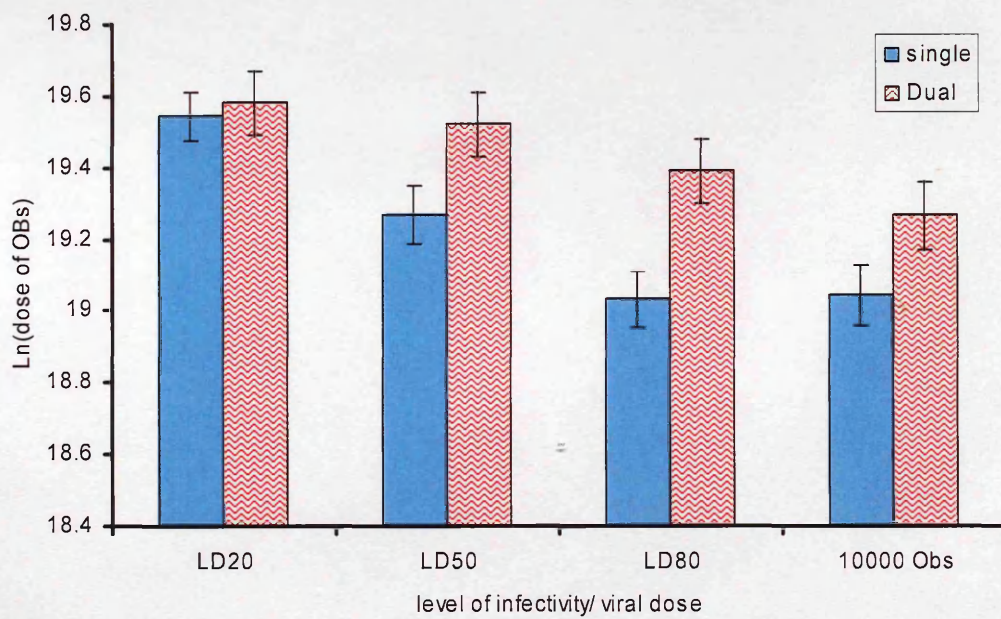


Figure 6.9 Estimated mean yield (± 1 SE) of *SpexNPV* genotypes A and F in single and dual infection at a range of infectivity levels and a dose of 10000 OBs.

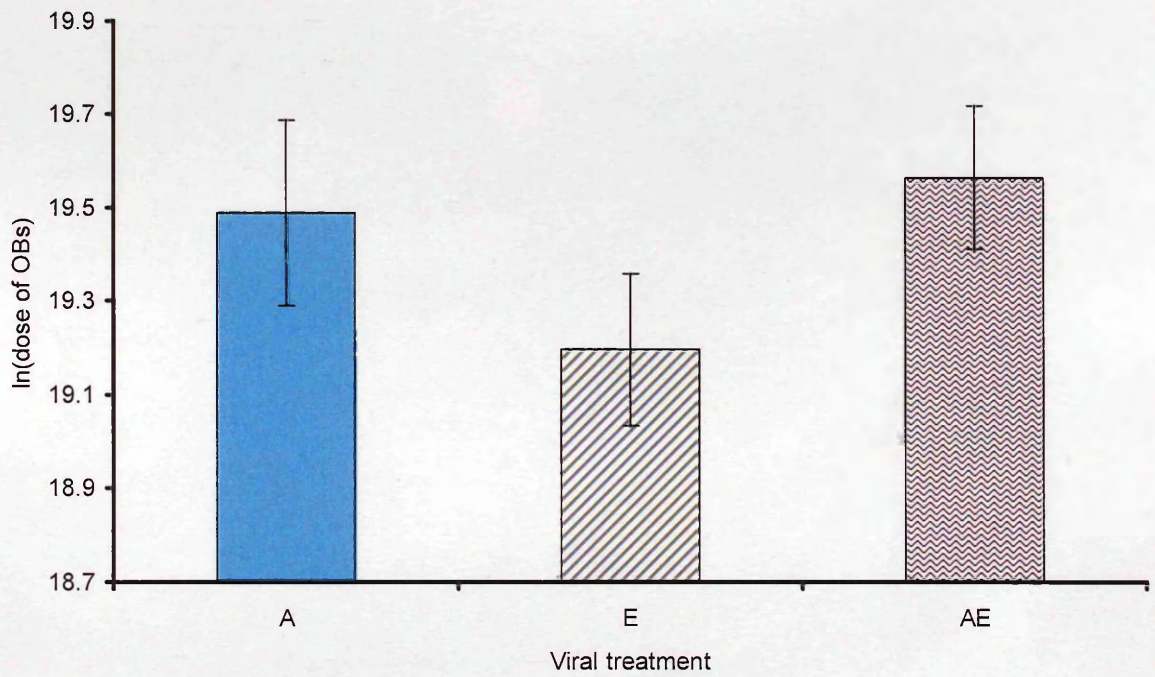


Figure 6.10 Estimated mean yield (\pm 1SE) from single and dual infections with *SpexNPV* genotypes A and E at LD₅₀.

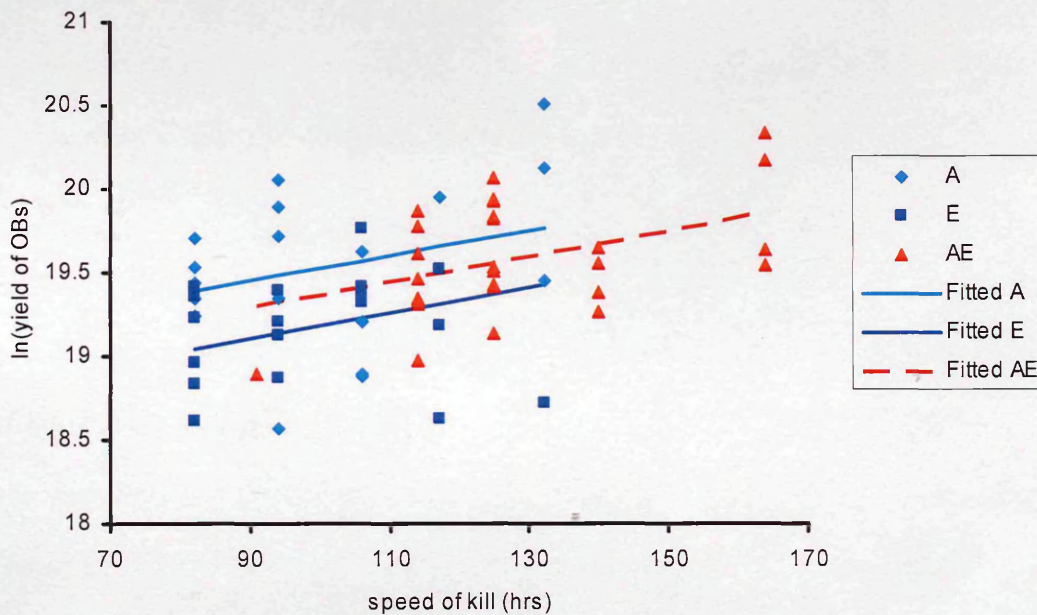


Figure 6.11 Speed of kill-yield relationship for *SpexNPV* genotypes A and E in single and dual infections at a dose of 10000 OBs. Symbols represent observed data and fitted lines: A, $\ln(\text{yield}) = 18.77 + (0.00758 * \text{speed of kill})$; E, $\ln(\text{yield}) = 18.43 + (0.00758 * \text{speed of kill})$; AE, $\ln(\text{yield}) = 18.61 + (0.00758 * \text{speed of kill})$.

For the CE mixture, single and dual infections had similar pathogenicities which were determined by viral dose only. The speed of kill for the dual infection increased by approximately 15 hours more than for single infections across all doses. Therefore, the higher yields seen at LD₂₀ and LD₅₀ in dual infection may simply be attributable to longer speed of kill in dual infection (Figure 6.12). As with the previous mixture, at any given time-point along speed of kill-yield curve, yield produced by dual infection is intermediate between the single infections (figure not shown).

At higher doses and levels of pathogenicity, although speed of kill has been lengthened by the same degree as at lower doses, yield is not significantly different to the highest of the single infections (genotype C), demonstrating that at least in this particular dual infection, the trade-off between speed of kill and yield is seen only at the lower doses (Figure 6.12).

Genotypes A and C appeared to be biologically extremely similar, with identical pathogenicity and speeds of kill and, at least at LD₈₀ levels, they produce very similar yields. Genotype C though, produces much lower yields than A at lower levels of pathogenicity and appears to respond to mortality/dose much more strongly. In terms of dual infection, although an increase in virulence and a lengthening of speed of kill are seen, and yields appear to have increased at all levels of pathogenicity, this is only significant at LD₅₀ and LD₈₀ (Figure 6.13). This increase can again be accounted for by a trade-off with speed of kill after examination the speed of kill-yield fitted curves at all doses (figures not shown).

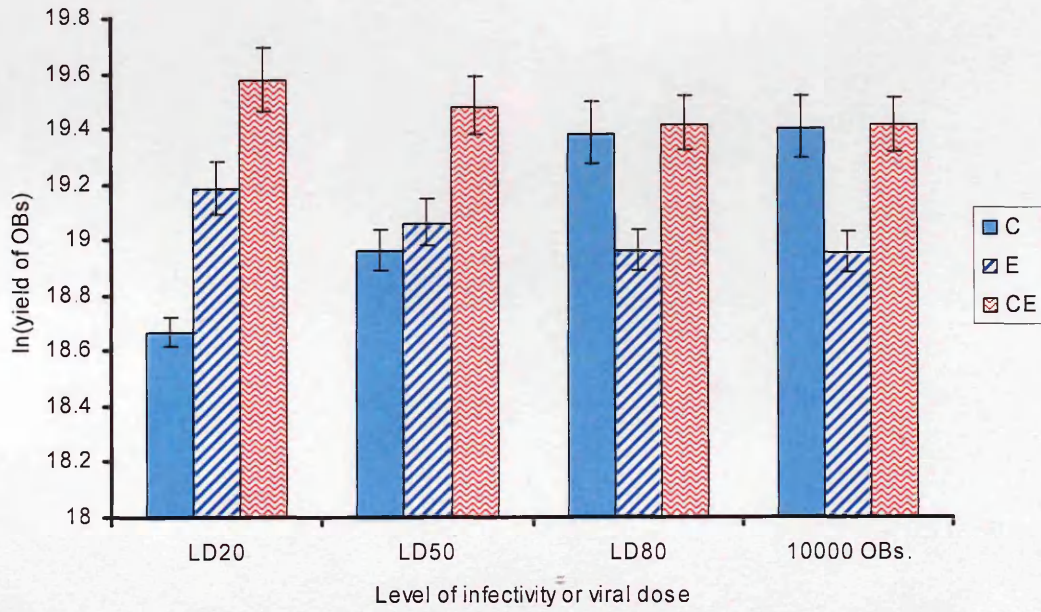


Figure 6.12 Estimated mean yield (\pm 1SE) of *Spex*NPV genotypes C and E in single and dual infection at a range of infectivity levels.

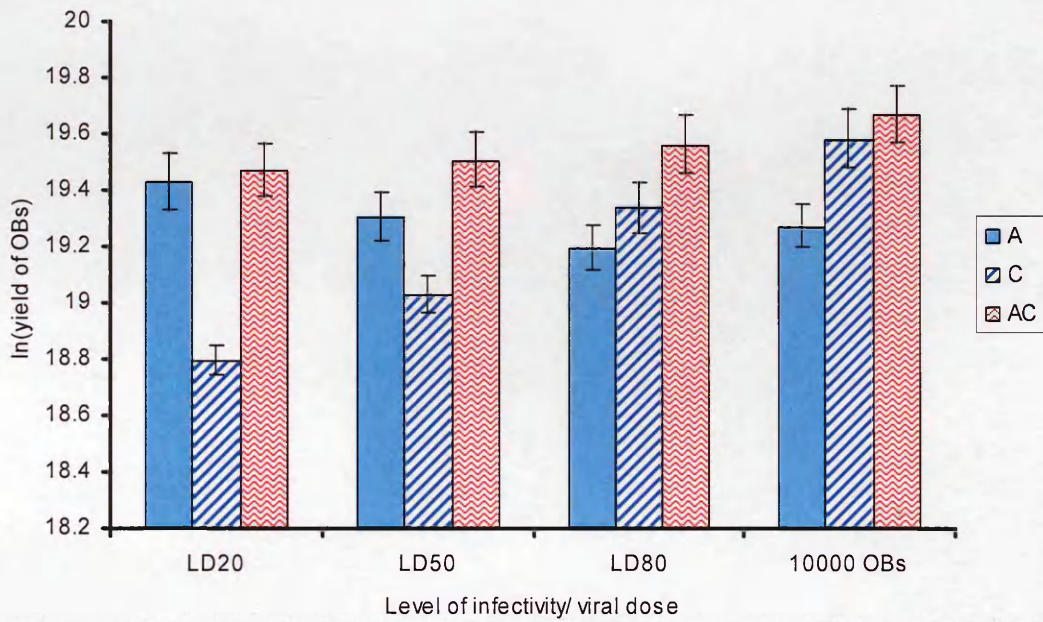


Figure 6.13 Estimated mean yield (\pm 1SE) of *SpexNPV* genotypes A and C in single and dual infection at a range of infectivity levels.

(iii) Lengthened speed of kill, reduced or unaffected yields: BG, AD, CD, CF

For the dual infection BG, although speed of kill is lengthened, yield is unexpectedly reduced dramatically (Figure 6.14). This is perhaps evidence that genotypes B and G when in a mixed infection interfere with each other. The nature of this interference is clearly not mediated at the site of initial infection in the mid-gut, since overall pathogenicity of the infection is raised. Therefore, interference is more likely to take place during the phase of within-host growth and result in competition for available host tissue.

A reduction of yields produced from dual infection of AD was similarly accompanied by a lengthening of the speed of kill and therefore represents another example of interference between the infecting genotypes. Although to a lesser degree interference could also be implicated in the dual infections CD and CF where yields are not significantly different from their single infections but speed of kill is still lengthened and conversely for BH where lower yields are produced without a lengthening of speed of kill. As a result yield per unit time and thus fitness is reduced in these dual infections relative to single infections.

(iv) Speed of kill and yield unaffected: DE and HG

The dual infections DE and HG failed to affect either speed of kill or yield, and therefore are examples of neutral interactions between co-infecting genotypes in dual infection (Table 6.4).

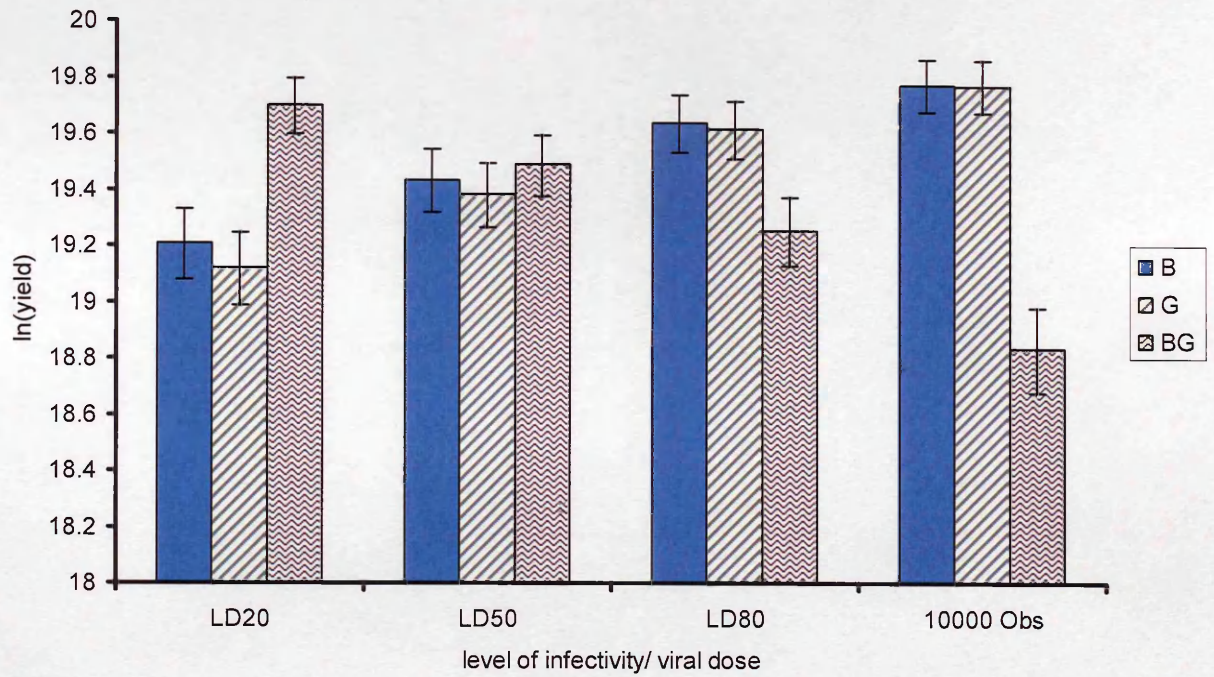


Figure 6.14 Estimated mean yield (\pm 1SE) of *SpexNPV* genotypes B and G in single and dual infection at a range of infectivity levels and a dose of 10000 OBs.

Table 6.4 Summary of the effects of dual infection of *SpexNPV* genotypes on phenotypic fitness traits.

Dual infection	Pathogenicity	Speed of kill (at 10000 OBs)	Yield (at LD ₅₀)	Trade-off (between speed of kill + yield)	Evidence of Interference
AC	Increased at high doses	Lengthened	Increased	Yes	No
AD	No effect	Lengthened	Intermediate	No	Yes
AE	No effect	Lengthened	Increased	Yes	No
AF	Increased	Lengthened	Increased	Yes	No
CD	No effect	Lengthened	Intermediate	No	Yes
CE	No effect	Lengthened	Increased	Yes	No
CF	Increased	Lengthened	Decreased	No	Yes
DE	No effect	No effect	Intermediate	No interaction	Neutral effect
DF	Increased	Shortened	Decreased	Yes	Competition
EF	Increased	Lengthened	Decreased	No	Yes
BG	Increased	Lengthened	No effect	No	Yes
BH	Increased	Intermediate	Decreased *	No	Yes
HG	Increased except at high doses	Intermediate	Intermediate *	No interaction	Neutral effect

* Calculated at 10 000 OBs rather than LD₅₀

6.3.5 Proportions of different genotypes in progeny virus

Mixed-clone viral infections were identified by identifying novel bands in restriction endonuclease profiles of individual genotypes (Table 6.5). To illustrate this approach, profiles for single and mixed infections resulting from dual inoculation of genotypes A and C are shown in Figure 6.15.

Mixed infections resulting from dual inoculation were surprisingly rare with one or the other genotypes dominating the infection in the majority of larvae (Figure 6.16). This apparent production of single infections from dual inoculation may well be an accurate representation of the actual outcome of progeny virus. An alternative view point may be that the actual level of mixed infections is much higher but the lack of sensitivity of RE profiling prevents detection of very small amounts of DNA. Still, for the majority of infections, be they mixed or single, one genotype appears to ultimately dominate.

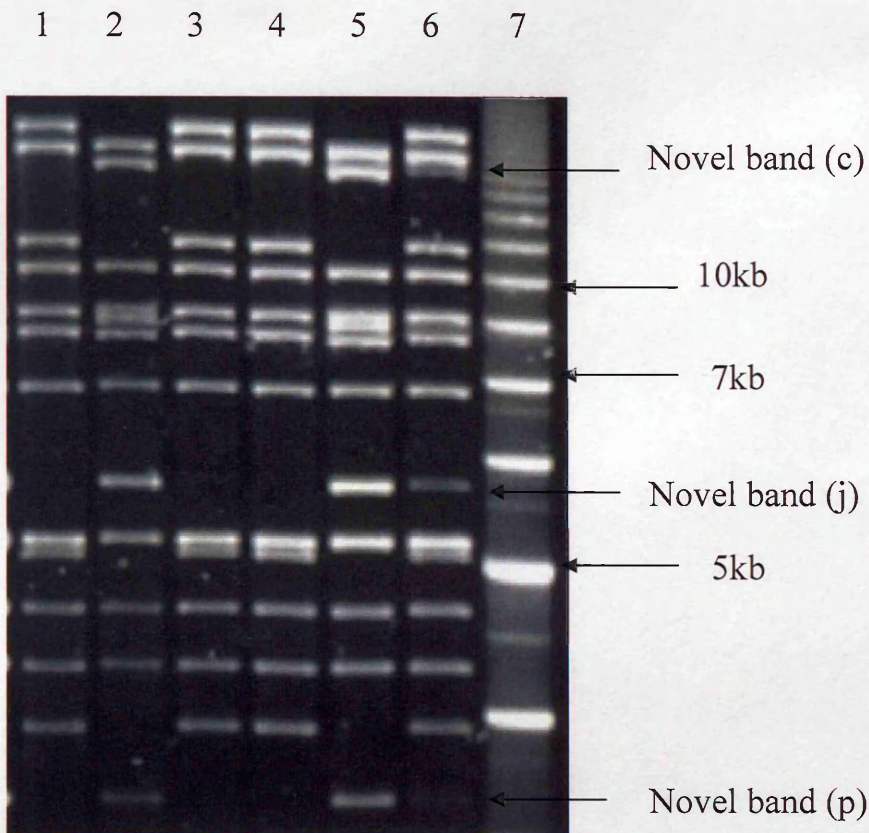


Figure 6.15 *EcoRV* profiles of DNA from virus deaths from dual inoculation with *SpexNPV* genotypes A and C at dose 10000 OBs in 3rd instar *S. exempta* larvae. Lanes 1, 3 and 4 show genotype A dominating the infection, lanes 2 and 5 shows genotype C dominating the infection and lane 6 shows a profile characteristic of a mixed infection indicated by the presence of novel bands (c, j and p) belonging to genotype C. Lane 7 molecular marker, 1Kb ruler (BioRad).

Table 6.5 Summary of characteristic novel bands in restriction endonuclease profiles used to identify mixed infections resulting from dual inoculation of *SpexNPV* genotypes at 10 000 OBs. For nomenclature of bands see chapter 3.

Dual infection	Genotype used for identification	Novel bands characteristic of genotype used for identification (present in sub-molar levels in mixed infection)
AE	A	d o
AF	A	a m o
AC	C	c g j p (see Figure 6.15)
CD	C	c g p
CE	C	c j p
CF	C	g m
AD	D	j
DE	D	d j p
DF	D	a m p
EF	F	c d j q
BG	B	a q
BH	H	p q
HG	H	p

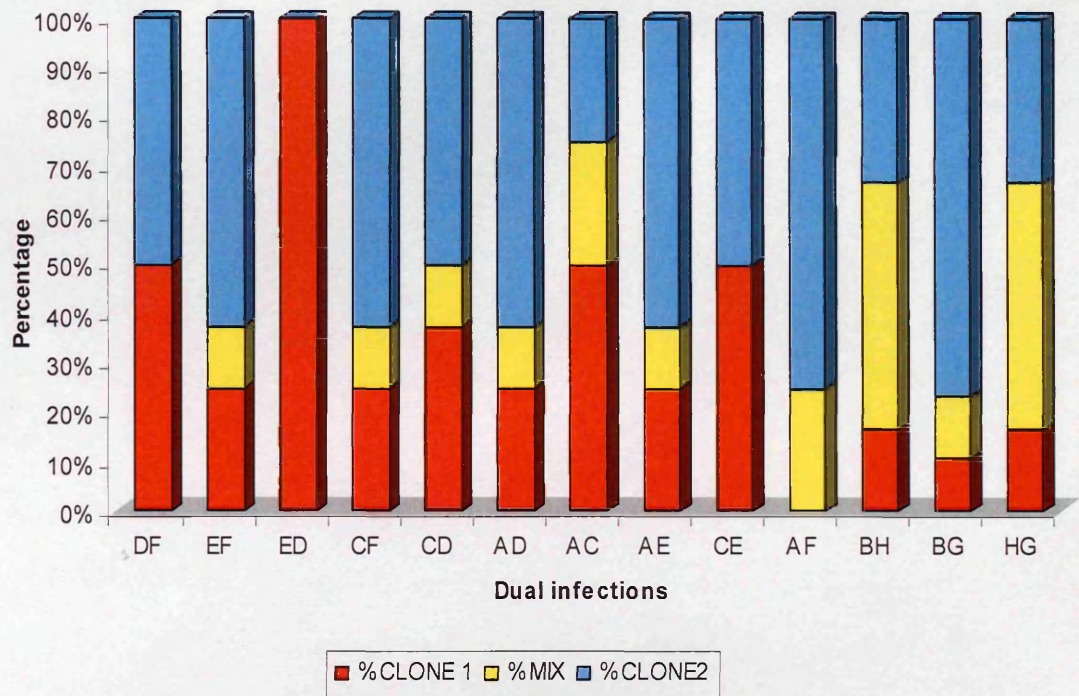


Figure 6.16 Proportion of genotypes and mixed infections resulting from dual inoculation of *SpexNPV* genotypes in a ratio of 1:1 at a dose of 10000 OBs. Labelling of genotypes in legend follows order of genotypes in dual infections on y-axis.

6.4 Discussion

We predicted that because of the obligate-killing nature of baculoviruses (Hodgson, *et al.* 2004), and the consequent severing of the link between mortality and host resource use that mortality would not necessarily be elevated in mixed genotype infections above that of single-genotype infections. The investigation of twelve different mixed-genotype infections produced a range of different effects on mortality. Four out of the twelve mixed infections yielded no significant increase in host mortality above that seen in single genotype infections (AD, AE, CD and CE). For the remaining eight (AF, CF, DF, EF, BH, BG, AC and HG), an increase in mortality was demonstrated. For all mixtures, except AC and HG, this was seen across the entire dose range. Although we did not predict an increase in mortality rate, a similar result was seen in the study by Hodgson *et al* (2004) of the dual inoculation of *Pf4* and *Pf6* NPV genotypes possessing equal pathogenicities in *Panolis falmmea* host larvae.

A simple model for predicting the mortality of a mixed infection was developed, in an attempt to explain this increased level of mortality. The model was based on the probability of infection of three possible outcomes of a dual infection, namely infection resulting from the first genotype only, infection resulting from the second only, and infection resulting from both genotypes. The predicted level of mortality was given by the sum of the mortality rates of the three possible outcomes. For all but one of the mixed infections exhibiting elevated mortality, the model failed to predict the mortality in mixture. Mixture EF was the exception, showing that for this particular mixture of genotypes the model was able to explain the level of mortality. For the majority of

cases, however, the model underestimated mortality, especially at the lower end of the dose range. The higher the dose, the closer the match between the predicted and the observed mortality rates. The observed level of mortality exhibited in the AC mixture proved much lower than predicted, indicating that genotypes A and C may exhibit a level of interference when combined.

There are several possible explanations for the inability of the model to predict the observed levels of mortality. The simplicity of the model is perhaps the most obvious explanation, since it assumes a linear relationship between dose and mortality, when a sigmoidal relationship, due to the dose-dependent nature of *Spex*NPV infections would be more realistic. Alternatively, it could simply be the result of using inaccurate fitted mortality values obtained from just a single replicate of single infections.

We predicted that speed of kill would increase (i.e. get faster) in mixed infections due to intra-host competition between co-infecting genotypes. For the majority of mixed infections investigated, speed of kill was much slower than for single genotype infections, contrary to our prediction. Dual infection of genotypes E and D was the exception to this rule and did not affect the speed of kill. Therefore, our results on the whole do not support the prediction that mixed infections result in faster speeds of kill.

One possible explanation for this may lie with the use of speed of kill as a measurement of the rate of host resource use, which assumes that parasites replicate within the host until all tissue is exploited, at which point the virus is present at such high levels that

death of the host ensues. Host resource use should, strictly speaking, be represented as replication rate. The application of real-time PCR technology could, in theory, be used to measure this. A pilot study that followed a single infection of *MbmNPV*, *AcMNPV*, *PflMNPV*, *SeMNPV* and *SpexMNPV* in *S. exigua* larvae showed that there appeared to be little correlation between within-host replication rate and time of death (J.Burden, S. White and R. Hails, unpubl. data). Thus, it seems likely that timing of death may have more to do with levels of late gene expression, and levels of chitinase and cathepsin gene products, than level of virus *per se*.

Our alternative hypothesis, based on the adaptive virulence theory, predicted that competing genotypes in mixture will attempt to gain disproportionate share of host resources, resulting in faster speeds of kill and, because of the trade-off with yield, will consequently produce lower yields. This appeared to be the case for just one of the mixed infection investigated (DF).

In four of the dual infections (AC, CE, AE and AF), a lengthening of speed of kill was apparent, and at first glance, it appears that interference between genotypes must be the cause. However, the associated increase in viral yield demonstrates that despite the mixed infection, the trade-off between speed of kill and yield is maintained. Thus, it could be argued that the lengthening of the speeds of kill, as seen in these mixed infections, simply represents a change in 'prudence strategy' in response to more than one genotype in the infection in order to maximise transmission.

For other dual infections, yield per unit time is reduced relative to single infections. For some this is due to a lengthening of the infection duration and a reduction of yields (BG, AD and EF). For others yields remained unchanged, despite lengthening of speeds (CD and CF) or lower yields are produced without a lengthening of speed of kill (BH).

Two of the dual infections (DE and HG) failed to affect speed of kill and yield and therefore appear to provide examples of neutral interactions between co-infecting genotypes in dual infection.

This investigation of thirteen dual infections of *Spex*NPV genotypes demonstrated that one single explanation is inadequate to explain the relationships between co-infecting genotypes, and that the interaction clearly depends on the specific genotypes within the mixture. Neutral and competitive interactions have been shown to have a role in some mixtures of *Spex*NPV genotypes, while for other dual infections co-infecting genotypes appear to interfere with each other. In addition, the ability to alter life-history traits in order to maintain 'prudence' have also been identified in some mixed infections.

Other possible interactions between genotypes could, in theory, result from mixed infections of other genotypes and include commensalism, parasitism, synergism. Returning to the only other study to have estimated life-history traits of single and dual genotype NPV infections, Hodgson *et al* (2004) found that speeds of kill also failed to follow adaptive virulence theory and produced speeds of kill intermediate between those seen in the two single genotype infections. In their study they found that

intermediate speeds of kill produced increased yields and suggested that this represented a degree of facilitation between the co-infecting genotypes with the production of higher yields without the compromise of speed of kill.

The use of RE analysis to estimate the relative proportion of each genotype in mixed infections, following dual inoculation and the possession of yield estimates for the same larvae could, in theory, allow the relative yield of individual genotypes to be compared. This would then allow comment on the relative fitness of genotypes when forced to share their host with the same or a different genotype. This approach was taken in the study by Hodgson *et al* (2004) who demonstrated that there was no cost associated with genotypes *Pf6* and *Pf4* sharing the host. It would be interesting to adopt a similar approach for the mixed infections of *SpexNPV* carried out in this study, but the extremely low number of mixed infections identified for each dual infection proved prohibitive. By focusing on individual dual infections of interest and repeating these mixed inoculations with sufficient replication, identification of similar patterns would support these initial findings, in addition, the number of cadavers resulting from mixed infections would be high enough to allow a thorough investigation of the potential costs associated with co-infection.

Chapter Seven

Effect of diversity of *Spex*NPV infections on virulence

Chapter 7: Effect of diversity of *Spex*NPV infections on virulence

7.1 Introduction

In the previous chapter we attempted to test the adaptive trade-off prediction that increased virulence is witnessed in mixed *Spex*NPV infections using very simple mixed infections of two genotypes in equal ratio. We predicted that speed of kill would increase as a direct result of competition between genotypes which would result in a reduced yield (as a result of the trade-off). We also postulated that mortality rate should in theory remain the same as that witnessed in a single infection because of the obligate-killing nature of baculoviruses. Although from the thirteen different dual infections a variety of different scenarios were generated, for the majority of dual infections increases in mortality and lengthening of infection duration beyond that witnessed in single genotype infections was seen. Both of these are counter-intuitive results and contrary to the predictions made by the trade-off hypothesis. In this chapter we intend to extend the investigation of mixed infections to include more complex mixtures. Although this study has not quantified the number of different genotypes present in a single larvae it can be assumed that infected-larvae from natural epizootics, where diversity and the prevalence of mixed infections have been shown to be high (chapter 5), will realistically be infected by more than just two different genotypes. In a different system, a total of 24 different *Panolis flamea* NPV genotypes have been purified from a single larva (Cory *et al.*, 2005). In this chapter we intend to estimate the same infection traits as before, namely pathogenicity, speed of kill and yield in single and mixed-genotype *Spex*NPV infections covering a range of genetic diversities (1-, 2-, 4-, 8-, and 16-

genotype infections) to see if similar counter-intuitive results as those produced in the simple dual mixtures (Chapter 6) are also witnessed with more genetic diversity. If the adaptive trade-off predictions were to hold true we would expect that increases in the number of genotypic variants within the infection (at a standard size of inoculum) will be positively correlated with an increase in the level of virulence.

7.2 Methods

7.2.1 Production of mixed genotype inoculum

Mixed genotype viral suspensions with varying levels of diversity (2, 4, 8 and 16-genotypes) were produced by mixing occlusion bodies from the individual genotypes in equal number at a concentration of 5000 OB/ μ l. A relatively high dose was chosen to increase the probability of mixed infections while still avoiding a production of 100% mortality. For the purposes of this experiment it was critical to start with extremely accurate assessments of the viral stock suspensions of the variants therefore multiple counts of the individual genotype concentrations were undertaken. In addition to possessing accurate estimates of initial viral concentrations, subsequent results also depended on the use of the correct dilution procedure. To ensure the pipetteing errors were minimised, and results did not simply reflect changes in dose all stock, viral suspensions of the individual genotypes were diluted in one step to achieve $1 * 10^6$ OBs/ μ l and mixed in the required ratios at this concentration. The mixed OB inoculum was then diluted in three steps (1:10, 1:10 and finally 1:2) to arrive at 5000 OBs/ μ l, the concentration used to inoculate the larvae consequently the number of dilution steps was standardised for all treatments irrespective of the number of variants in the mixture.

7.2.2 Replication of level of diversity

In order to replicate the level of diversity eight different genotype combinations were chosen at random for the 2 and 4 genotype mixtures from the eight *EcoRV* identified genotypes A-H (studied in detail in the chapter 3 and 4). For the 8 genotype mixtures replication four replicates were set-up from the 16 *EcoRV* identified genotypic variants identified in Chapter 3 (genotypes 1 to 16) (Table 7.1). The highest level of diversity i.e. 16-genotype mixtures was replicated twice and were created from a pool of variants identified with the enzymes *EcoRV* and *SalI*. For the wildtype a fresh aliquot of the stock taken and recounted each time.

Table 7.1 Number of replicates per block at each level of diversity of mixed variant *SpexNPV* inoculations used to infect 3rd instar *S. exempta* larvae.

Number of genotypes in mixture	1	2	4	8	16	WT
Number of replicates	8	8	8	4	2	4

7.2.3 Experimental design

Newly moulted 3rd instar larvae (25 per rep per treatment, 850 larvae per block) were challenged at a dose of 5000 OB/larvae with the wildtype virus, individual genotypes (A-H) and mixed genotype inoculations, possessing a range of levels of diversity. Mixed genotype inocula possessing 2, 4, 8 and 16 different genotypes were used to represent the various levels of inoculum diversity. An additional 25 larvae were dosed with sterile distilled water to act as controls. The experiment was repeated (2 blocks) using aliquots of the same stocks of virus re-diluted and re-mixed anew for each block. For the single genotypes, in addition to a dose of 5000 OBs a further four doses (2500, 1250, 650 and 312 OBs) were also set-up in order

to allow prediction of mortality of mixed infections from single genotype infections using a similar approach as that used in Chapter 6. Due to a limiting number of larvae available the additional four single genotype doses were only carried out for the first block. Larvae were monitored every 8-12 hours until death or pupation to produce estimates of pathogenicity and speed of kill and virus mortality was confirmed using geisma staining (see section 2.4.2). Speed of kill was calculated from the time death was recorded, with zero hour taken as the time larvae were first introduced into the dosing arena. All viral deaths were transferred to 1.5ml microtubes for storage at -20°C until yield and RFLP analysis.

7.2.4 Yield and RFLP analysis to determine the proportion of different genotypes in progeny virus

Nine cadavers per treatment, which had remained in-tact upon death, from four timepoints (chosen to span and represent the entire range of speeds of kill) were selected for yield analysis. This was carried out on all treatments at the 8 and 16 genotype level of diversity together with all replicates of the wildtype virus. At the 1, 2 and 4 genotype level four treatments were chosen at random to ensure consistency across diversity levels. Following the counting of yields, RFLP analysis was carried out on the same viral cadavers. In addition, other virus infected larvae were also genetically analysed (nine per treatment) to ensure all treatments within each level of diversity were represented. DNA from progeny cadavers was extracted and digested with the restriction endonuclease, *EcoRV*. The resultant bands were visualised by gel electrophoresis and subsequent staining with SybR Gold[®] (see section 2.3.4).

6.2.5 Data analysis

Mortality data were logit transformed ($\ln(p/(1-p))$ where p = proportional mortality) and analysed using a binomial error structure. Deviances were adjusted via the scale parameter to allow for over dispersion of the data. Speed of kill ($1/x^2$) and yield (sqrt) data were transformed and analysed using a normal error structure. In all analyses, block was treated as a factor and diversity was either treated as a factor or a continuous variable.

6.2.6 Calculating predicting mortality in dual infections

We attempted to predict the expected mortality rate when larvae are exposed to a dual infection clones in 1:1 ratio, by combining the mortality rates caused by the two clones when they infected *S. exempta* larvae singly. Thus, in order to estimate mortality at a combined dose of 10 000 OBs (5000 OBs from clone X and 5000 OBs from clone Y) we used the fitted values of mortality for each of the single infections at a dose of 5000 OBs each.

If we assume simple mass action, then if the mortality rate for clone X at 5000 OBs is x (say, 0.7) and for clone Y is y (say, 0.6) then the mortality rate from mixed infections of both X and Y is equal to xy (i.e. $0.7 \times 0.6 = 0.42$). Under this scenario, the proportion of larvae dying from clone X only would then equal $x - xy$ (i.e. $0.7 - 0.42 = 0.28$) and the proportion of larvae dying from clone Y only would equal $y - xy$ (i.e. $0.6 - 0.42 = 0.18$). Therefore, dual infection at 10 000 OBs would produce a predicted mortality of the sum of all three possible outcomes (i.e. $0.42 + 0.28 + 0.18 = 0.88$) (Figure 7.1). The same logic can be used to calculate the predicted mortality resulting from dual infection at total doses of 5000, 2500 1250 and 625 OBs. Chi-

squared analyses were used to compare observed mortality rates against these predicted values for all dual infections where differences were observed. The same logic was followed to calculate predicted mortality for all dual infections and chi-squared analysis was used to compare observed values against these predicted levels of pathogenicity.

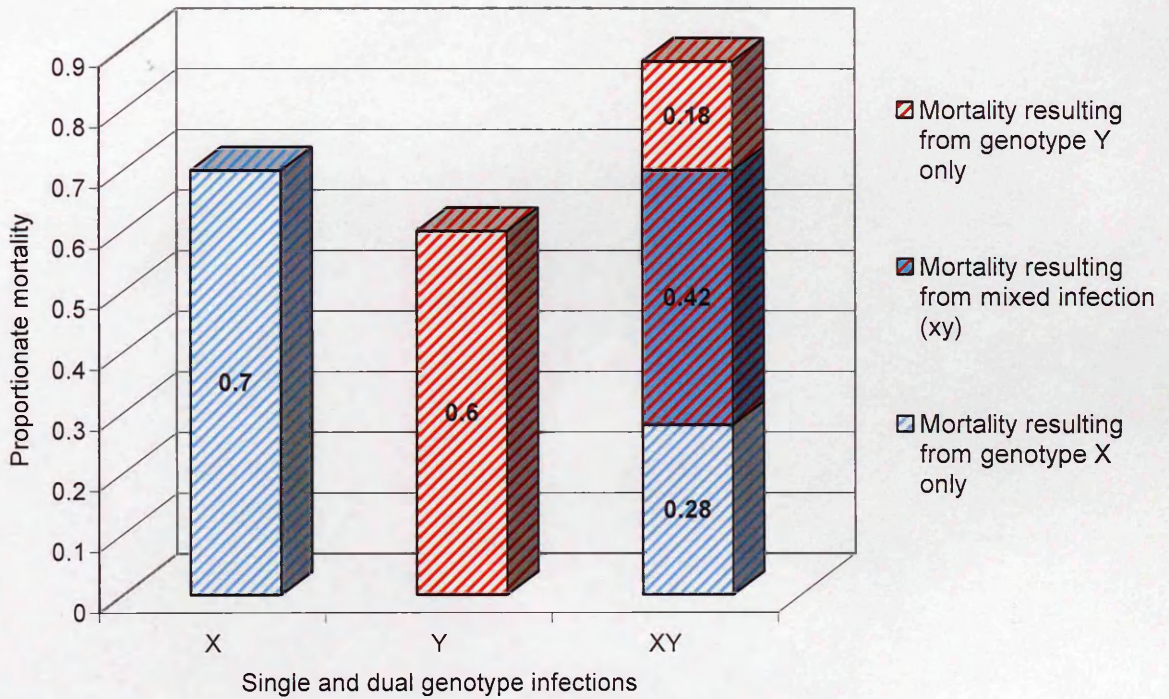


Figure 7.1 Schematic representation for predicting the proportionate mortality of a dual infection (XY) at a dose of 10000 OBs using the fitted values of single genotype infections (X and Y) at 5000 OBs.

7.2.7 Attempts to predict mortality in 4-genotype inoculations

Following success at predicting mortality of dual infections attempts were made to predict mortality from 4-genotype inoculations using the estimated mortality for individual genotype infections at a dose of 1250 OBs derived from both this experiment and the baseline bioassays from the previous chapter.

Table 7.2 Formulae used to calculate predicted mortality of 4-genotype inoculation (CDEF) at a dose of 5000 OBs, when genotypes are present in equal ratio. Proportionate mortality (X) is the sum of: mortality resulting from 4-genotype mixed infections, (P); mortality resulting from 3-genotype mixed infections, (Q); mortality resulting from dual infections, (S); and also mortality resulting from single genotype infections, (U).

Predicted mortality of inoculation with 4 genotype CDEF in equal ratio		
$X = P + Q + S + U$		
Possible outcomes	Proportionate mortality resulting from mixed infection with 4-genotypes = P	
CDEF	$C * D * E * F = P$	
	Proportionate mortality of mixed infection with 3-genotypes = Q (when $Q = \sum q$)	
CDE	$(C * D * E) - p = q_1$	
CDF	$(C * D * F) - p = q_2$	
CEF	$(C * E * F) - p = q_3$	
DEF	$(D * E * F) - p = q_4$	
	Proportionate mortality of dual infection = S (when $S = \sum s$)	
CD	$(C * D) - p = r_1$	$r_1 - (q_1 + q_2) = s_1$
CE	$(C * E) - p = r_2$	$r_2 - (q_1 + q_3) = s_2$
CF	$(C * F) - p = r_3$	$r_3 - (q_2 + q_3) = s_3$
DE	$(D * E) - p = r_4$	$r_4 - (q_1 + q_4) = s_4$
DF	$(D * F) - p = r_5$	$r_5 - (q_2 + q_4) = s_5$
EF	$(E * F) - p = r_6$	$r_6 - (q_3 + q_4) = s_6$
	Proportionate mortality of single infection = U (when $U = \sum u$)	
C	$(C - p) = t_1$	$t_1 - (q_1 + q_2 + q_3 + s_1 + s_2 + s_3) = u_1$
D	$(D - p) = t_2$	$t_2 - (q_1 + q_2 + q_4 + s_1 + s_4 + s_5) = u_2$
E	$(E - p) = t_3$	$t_3 - (q_1 + q_3 + q_4 + s_2 + s_4 + s_6) = u_3$
F	$(F - p) = t_4$	$t_4 - (q_2 + q_3 + q_4 + s_3 + s_5 + s_6) = u_4$

7.3 Results

7.3.1 Effect of diversity on pathogenicity

There were no viral deaths in the control larvae and non-viral deaths were first confirmed by Geimsa staining and removed from the dataset (3.9%). There was no significant difference between the two blocks ($\chi^2_1 = 0.06$, $P = 0.806$) which allowed their combined analysis. Virus diversity was found to be a strong predictor of mortality ($\chi^2_5 = 66.62$, $P < 0.001$) with the level of mortality increasing with increasing number of genotypes in the inoculum. Clustering together two, four and eight genotype treatments produced four groups (single; 2,4,8; 16; WT) failed to cause a significant effect on model ($F_{2,59} = 1.449$, $P = 0.243$). Combination of the 16 genotype treatment with the other mixed inoculations to produce three groups (single; 2,4,8,16; WT) also caused a non-significant increase in residual deviance ($F_{3,59} = 2.509$, $P = 0.06$), admittedly though very close to significance. The clustering into three groups, represented by the differential colouring of the bars of Figure 7.2, is the highest level of grouping possible without altering the model. The wild type virus produced the highest level of mortality (Figure 7.2a).

The number of genotypes in a mixture was then converted to a continuous variable to allow analysis of covariance of the same dataset (excluding the wildtype virus) with diversity (Figure 7.3). Virus diversity was found to be a strong predictor of mortality ($\chi^2_1 = 16.78$, $P < 0.001$; Figure 7.3) with the level of mortality increasing with increasing number of genotypes in the inoculum. The extrapolation of the fitted curve beyond 16 genotypes allowed predictions to be made about the number of genotypes present in the wildtype virus. By solving the fitted equation for 0.927,

which was the mean proportionate viral mortality (observed) for the wildtype virus, 18.8 genotypes can be predicted to be present in the wildtype virus.

The effect of treating diversity as a continuous rather than a factor can be seen by comparing the back-transformed proportionate mortality predicted by the two different models predict (Figure 7.4).

(a)

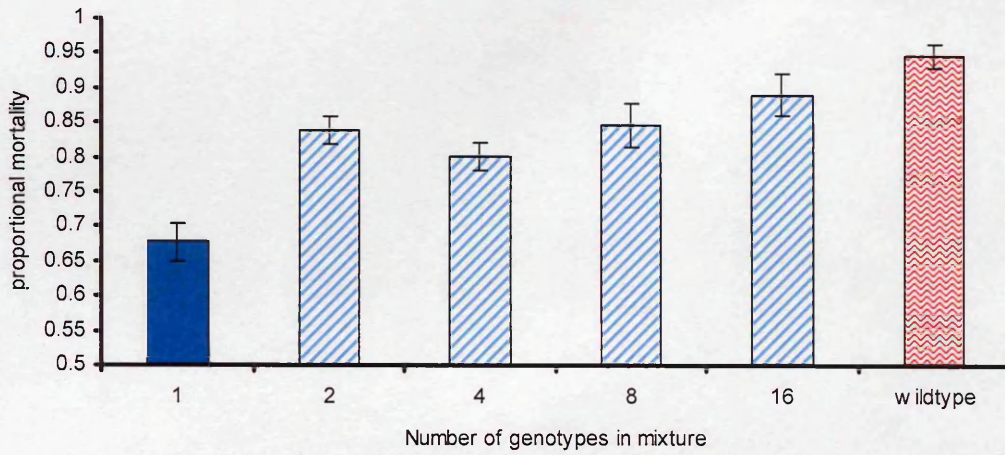


Figure 7.2 The influence of *SpexNPV* genotype diversity on fatal infection in third instar *S. exempta* larvae at a dose of 5000 OBs. Backtransformed model mean proportionate mortality (± 1 SE) of 1, 2, 4, 8 and 16 genotypes compared with the mixed parent wild type virus

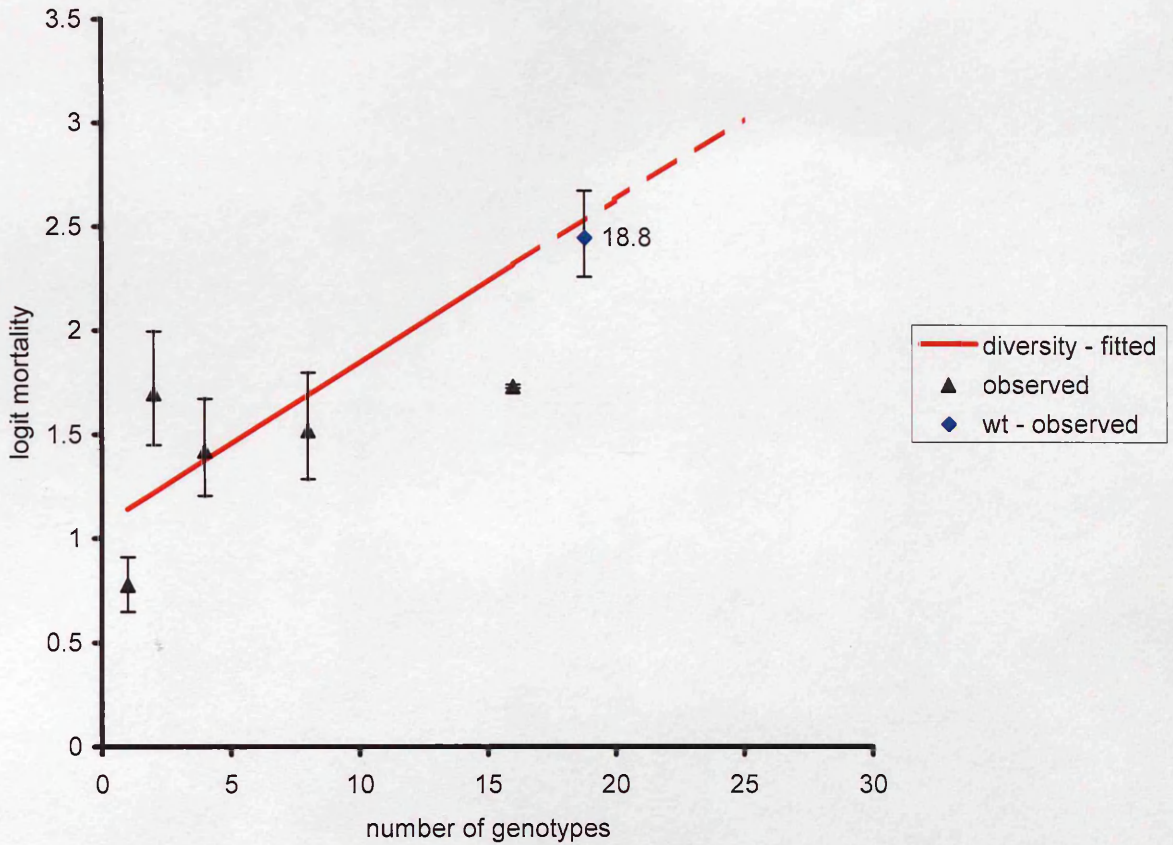


Figure 7.3 Influence of infection diversity of *Spex*NPV in 3rd instar larvae at a dose of 5000 OBs on proportional mortality. Fitted mortality curves: linear, $\text{logit}(\text{mortality}) = 1.064 + (0.0785 * \text{diversity})$. Triangular symbols represent mean observed values ($\pm 1\text{SE}$) and diamond symbol represents the estimated number of genotypes in the wildtype virus extrapolated from linear model using observed $\text{logit}(\text{mortality})$.

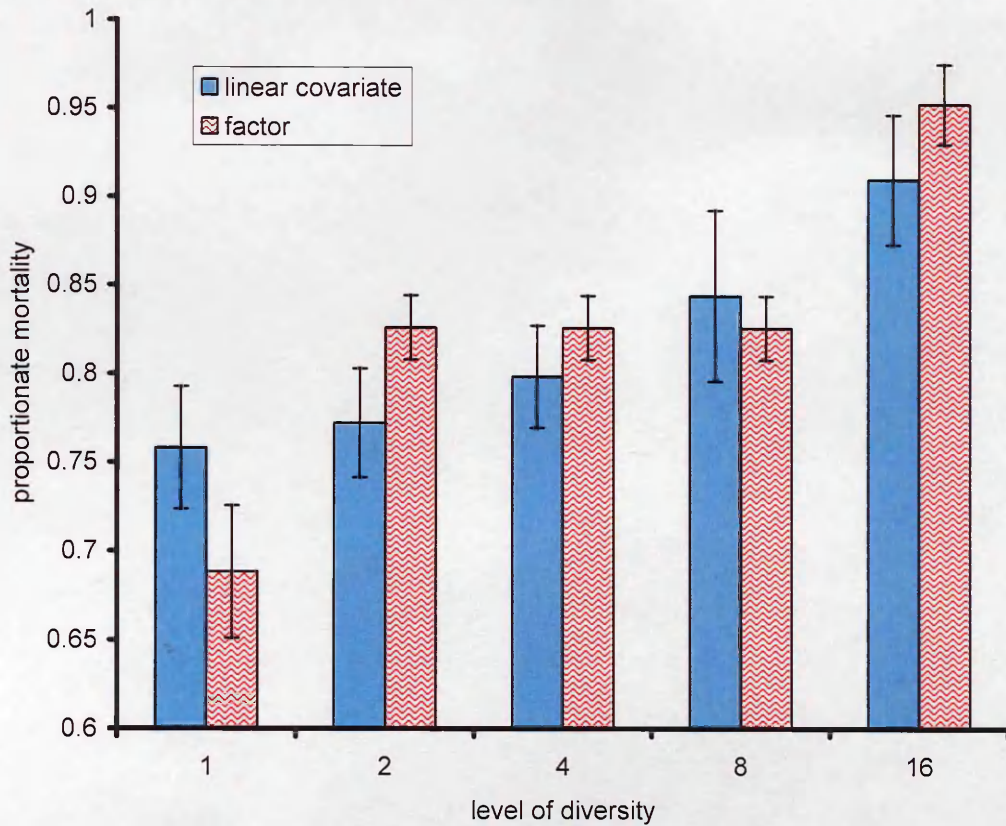


Figure 7.4 Comparison of two different statistical models which represent the influence of *Spex*NPV genotype diversity on fatal infection in third instar *S. exempta* larvae at a dose of 5000 OBs. Back transformed mean mortality (± 1 SE) estimated by assigning level of diversity as a factor or as a covariate.

7.3.2 Predicting mortality in two and four genotype infections

The mortality data for the single genotype infections were analysed treating genotype as a factor and dose as a covariate. As previously shown (Chapter 4) dose was found to have a considerable influence on pathogenicity with higher mortality seen at the higher doses (Figure 7.5). The strength of this dose effect varied between genotype (genotype*Indose, $\chi^2_8 = 27.61$, $P = 0.006$).

Significant differences were seen between observed and predicted levels of mortality when predictions of mortality were based on the single infection dose range carried out alongside this experiment ($\chi^2_7 = 21.64$, $P = 0.003$), with estimates for dual infection, in general underestimating the actual levels of mortality (i.e. predictions were too low). The exception was the dual infection of DF which produced an overestimate. When fitted values of mortality from the baseline bioassays (chapter 4) were used to make predictions about the mortality of dual infections no differences between observed and predicted mortality were seen ($\chi^2_7 = 6.4$, $P = 0.49$). Demonstrating that with enough replication and accurate estimates of the dose-response relationship of single genotype infections, it is possible to predict the pathogenicity of dual infections at least at a dose of 5000 OBs (Figure 7.6).

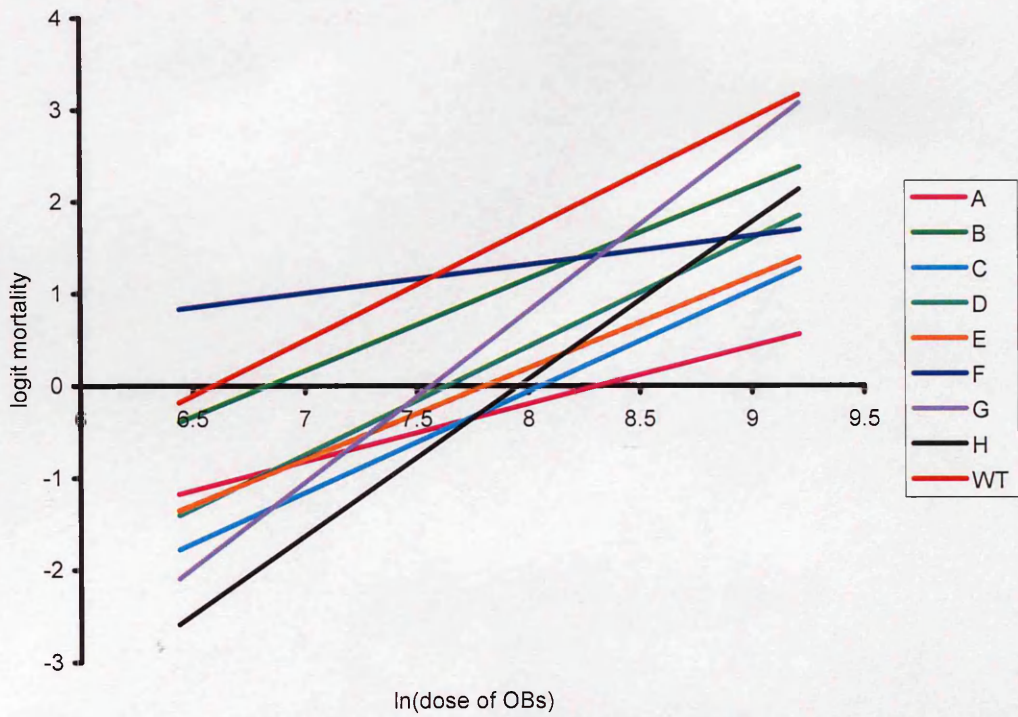


Figure 7.5 Fitted dose-response curves of *Spex*NPV genotypes and wildtype virus in 3rd instar *S.exempta* larvae.

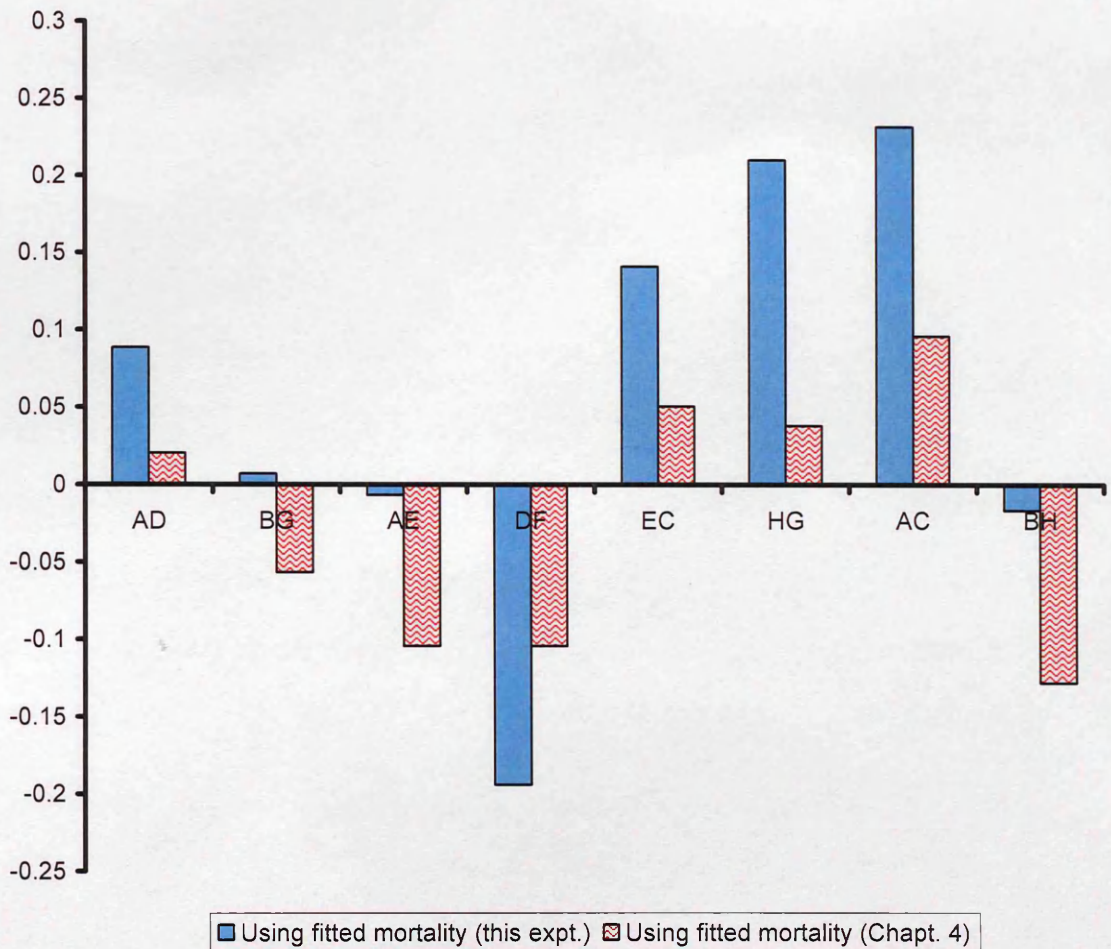


Figure 7.6 Difference between observed and predicted mortality (i.e. Observed-Expected) for dual genotype infections using fitted mortality values for single genotype infections obtained from baseline bioassays (chapter 4) and this experiment.

Following the success of predicting mortality of the dual infections, attempts were made to predict mortality in the 4-genotype infections using a similar mass action model as that used for the dual infections.

Four-genotype infection (CDEF): A worked example

Estimated mortality of single-genotype infections at a dose of 1250 OBs were taken from the single-genotype infections carried out in this experiment and also the more reliable estimates produced from chapter 4 (Table 7.3). Together with the formula set-out in the methods section (Table 7.2) these estimates were used to predict the viral mortality of 4-genotype infections when the genotypes are present in equal ratios (Table 7.4).

Four-genotype infection (CDEF): A worked example

Table 7.3 Estimated mortality of single genotype infections, at a dose of 1250 OBs, used to predict mortality of 4-genotype infection, CDEF when present in equal ratio.

Genotype		C	D	E	F
Estimated mortality	This expt.	0.267	0.357	0.339	0.740
	Chapter 4	0.448	0.448	0.448	0.448

Table 7.4 Predicted mortality of the 4-genotype infection (X), of CDEF, estimated using formula (Set-out in Table 7.2). Mortality estimates of single infections (dose = 1250 OBs) from this experiment and from chapter 4 experiments (Summarised for CDEF in Table 7.3) were used.

Predicted mortality, $x = P + Q + S + U$					
	P	Q	S	U	X
This expt.	0.02	0.164	0.385	0.346	= <u>0.920</u>
Chapter 3	0.04	0.199	0.367	0.301	= <u>0.907</u>

Mortality predictions for the majority of the 4-genotype mixtures tended to overestimate levels of pathogenicity (Figure 7.7), using either fitted mortality for single infection derived from this chapter ($\chi^2_7 = 16.0$, $P = 0.025$) or from the previous chapter ($\chi^2_7 = 22.9$, $P = 0.0018$).

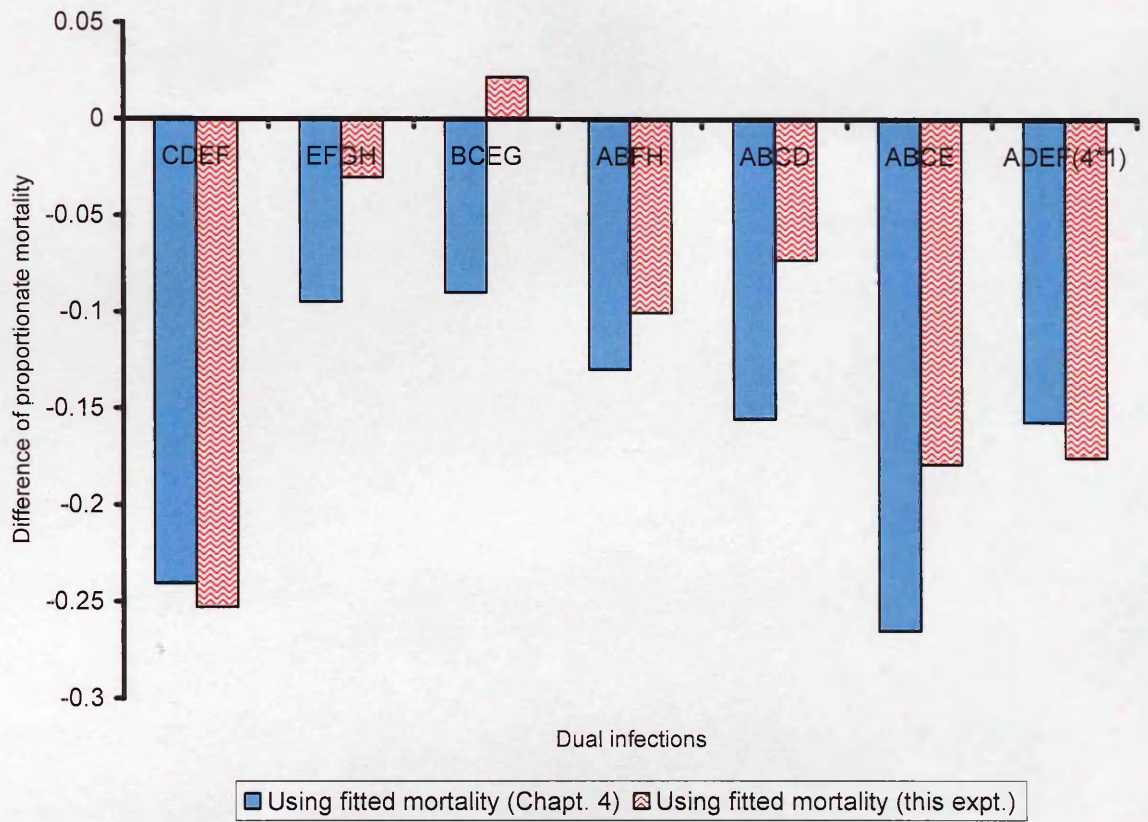


Figure 7.7 Difference between observed and predicted mortality for 4-genotype infections using fitted mortality values for single genotype infections obtained from baseline bioassays (chapter 4) and this experiment

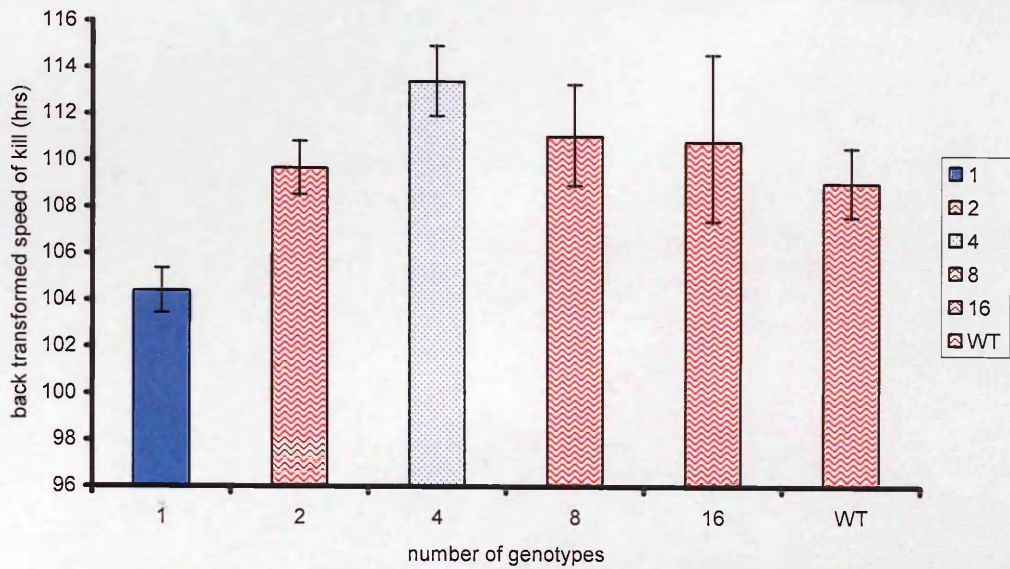
7.3.3 Speed of kill

Speed of kill data were transformed ($1/x^2$) and analysed treating the number of genotypes in the mixture as a factor and as a continuous variable. There was no significant difference between blocks and they were combined for analysis ($F_{1,935} = 1.86$, $P = 0.17$). Number of genotypes had a significant influence on speed of kill ($F_{5,966} = 12.61$, $P < 0.001$). Speed of kill reduced (lengthening time to death) with increasing diversity when the number of genotypes in the mixture was four or less. More than 4 genotypes in the inoculum resulted in increased speed of kill (shortening of time to death) with increasing levels of diversity (Figure 7.8a).

Treatments with 2, 8 and 16 genotypes and the wild type virus all possessed very similar speeds of kill and were therefore combined into a single group (Figure 7.8b). This produced three groups which when introduced into the model did not significantly increase the residual deviance ($F_{3,966} = 0.29$, $P = 0.832$).

The number of genotypes in the mixture was then converted to a continuous variable to allow the analysis of covariance (without the wild type virus). The effect of level of diversity on speed of kill, as seen in the previous analysis, did not appear to produce a linear relationship, and the best fit was for a quadratic relationship ($F_{3,969} = 29.42$, $P < 0.001$) (Figure 7.9).

(a)



(b)

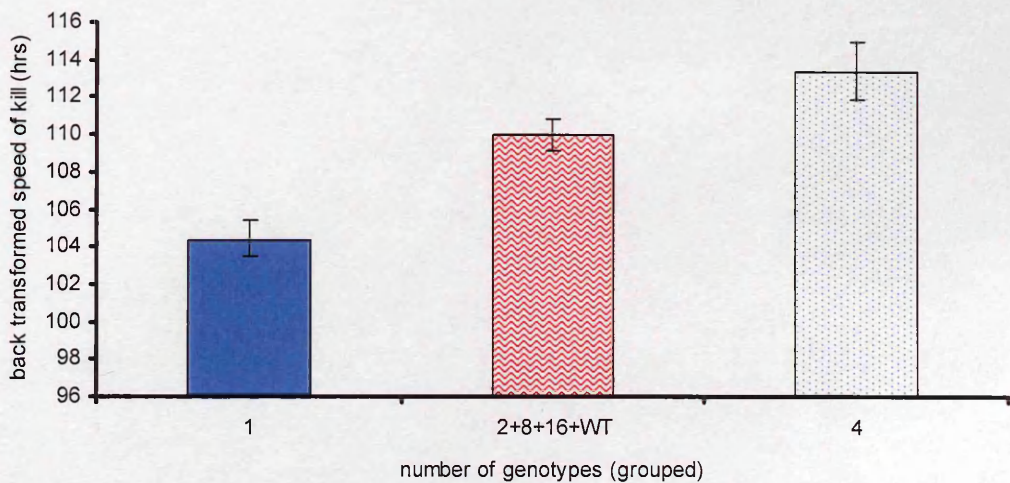


Figure 7.8 Back transformed mean speed of kill (\pm 1SE) for (a) single genotype infections, wild type virus and mixed infections at various levels of diversity and (b) virus treatment grouped according to speed of kill represented by differential colouring of bars.

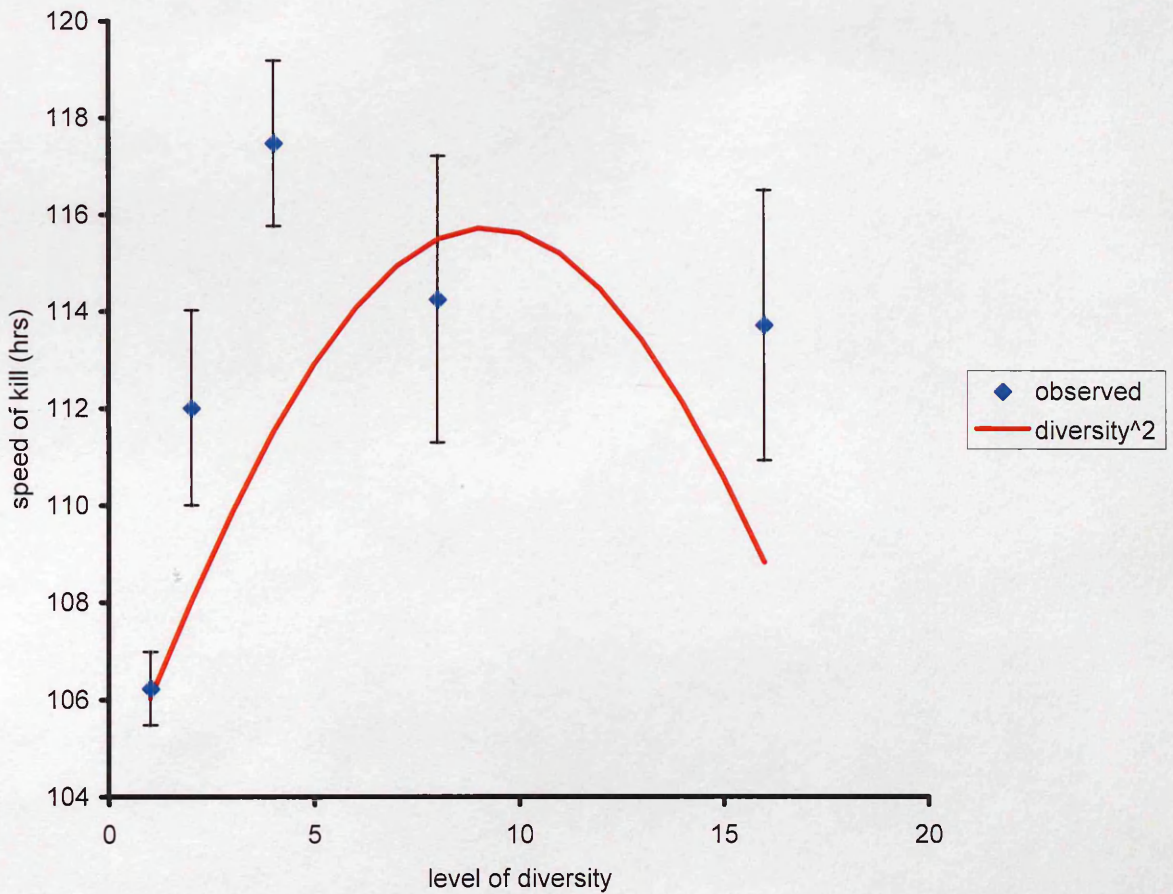


Figure 7.9 Speed of kill of mixed infections in relation to its level of diversity. Symbols represent observed mean speed of kill ($\pm 1SE$) at each level of diversity tested. Fitted lines: $(1/\text{speed of kill}^2) = 9.264e-5 + (-3.910e-6 * \text{diversity}) + (2.112e-7 * \text{diversity}^2)$. All transformations and error structures satisfied standard model checking procedures i.e. residual plots for Normal errors (GLIM version 3.77, 1985 Royal Statistical Society).

7.3.4 Yield

Yield data were transformed (square root) and modelled with a normal error structure with treatment (virus diversity) assigned as a factor. The level of infection diversity significantly influenced yield ($F_{5,199} = 2.79$, $P = 0.019$). The introduction of transformed speed of kill ($1/\text{speed of kill}^2$) proved to be a strong predictor of yield ($F_{1,198} = 45.52$, $P < 0.0001$; Figure 7.10) but did not affect the significance of diversity on yield ($F_{5,198} = 2.67$, $P = 0.023$; Figure 7.10).

Several of the treatments (levels of diversity and wildtype virus) appeared very similar and could be combined to produce two very clear cut groups consisting of single, dual and four genotype infections in one group and 8, 16 genotype inoculations and the wildtype virus in the second group. Combining the treatments in this way produced a non-significant increase in residual deviance ($F_{4,194} = 0.106$, $P = 0.98$) demonstrating the statistical validity of the grouping of the treatments (Figure 7.11).

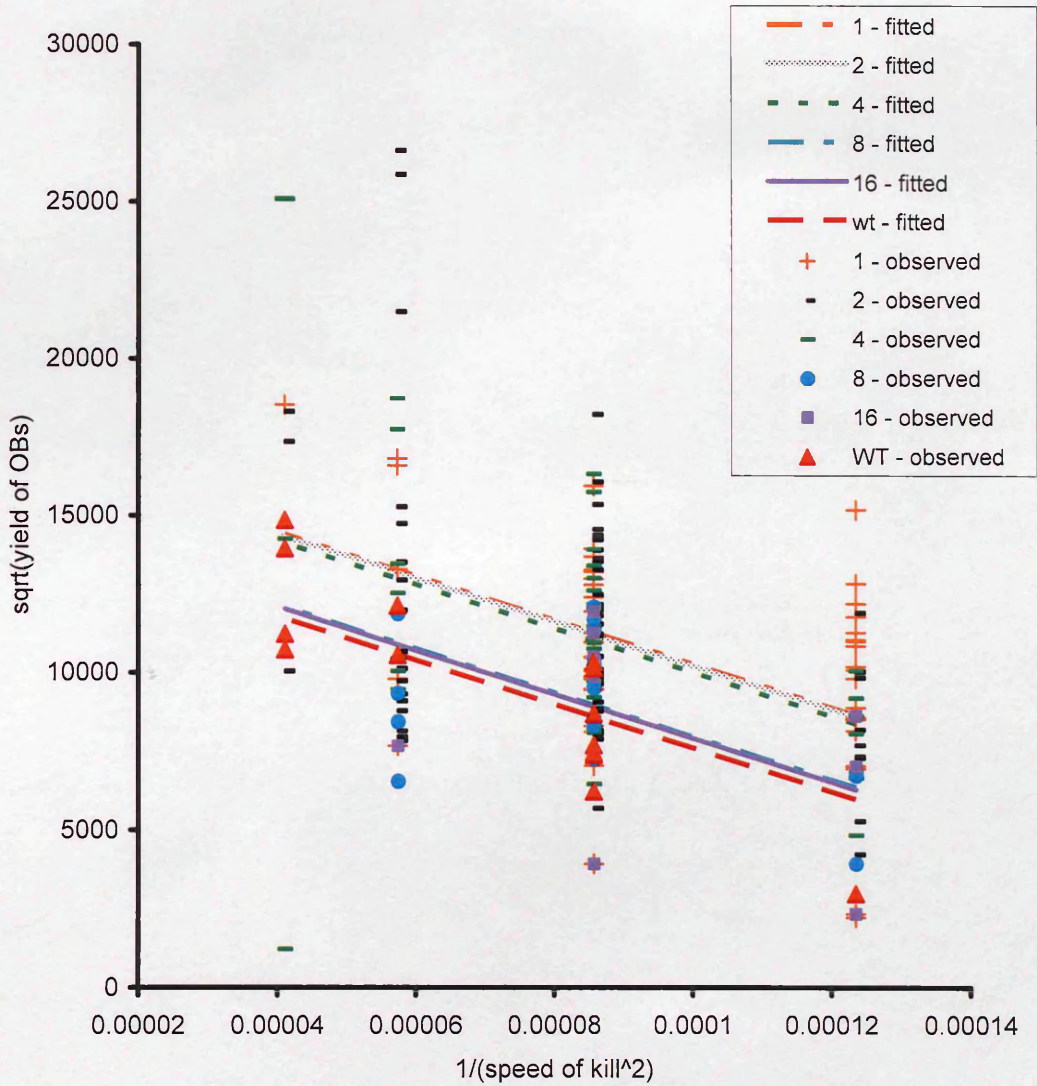


Figure 7.10 Yield-speed of kill relationship for mixed infections. Fitted lines: 1 genotype, $\sqrt{\text{yield}} = 17287 + (-69665104 * (1/\text{speed of kill}^2))$; 2 genotypes, $\sqrt{\text{yield}} = 17217.9 + (-69665104 * (1/\text{speed of kill}^2))$; 4 genotypes, $\sqrt{\text{yield}} = 17015.3 + (-69665104 * (1/\text{speed of kill}^2))$; 8 genotypes, $\sqrt{\text{yield}} = 14975 + (-69665104 * (1/\text{speed of kill}^2))$; 16 genotype, $\sqrt{\text{yield}} = 14911 + (-69665104 * (1/\text{speed of kill}^2))$; WT virus, $\sqrt{\text{yield}} = 14611 + (-69665104 * (1/\text{speed of kill}^2))$. Symbols represent observed values.

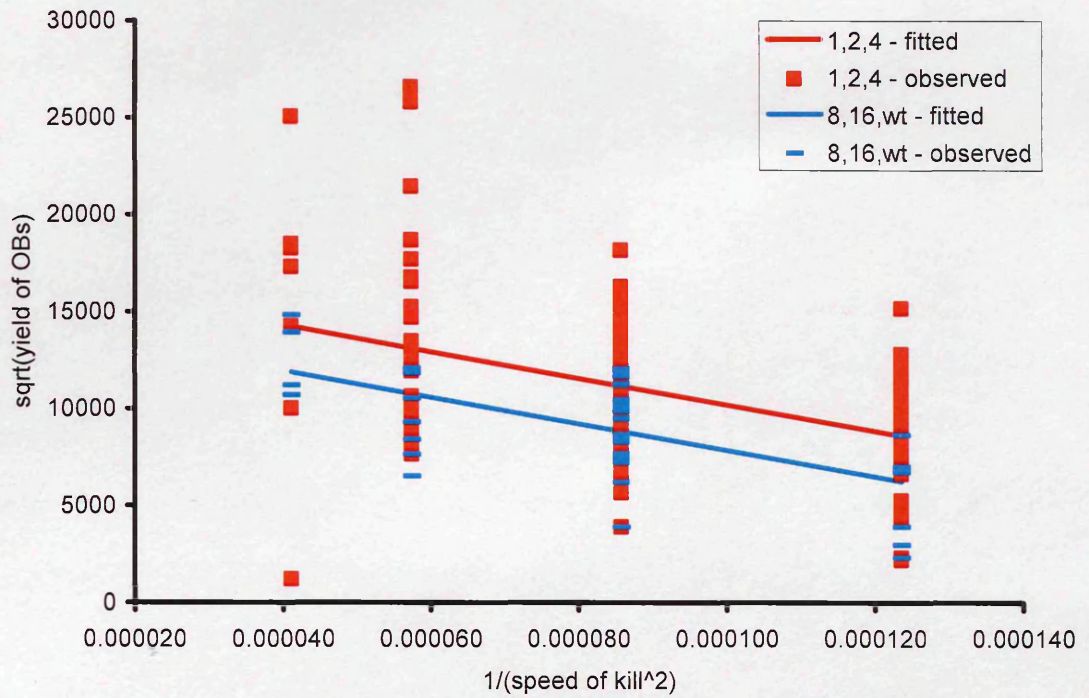


Figure 7.11 Yield-speed of kill relationship for mixed infections. Fitted lines: 1, 2, 4 genotypes, $\sqrt{\text{yield}} = 17099 + (-68589144 * (1/\text{speed of kill}^2))$; WT, 8, 16 genotypes, $\sqrt{\text{yield}} = 14745 + (-68589144 * (1/\text{speed of kill}^2))$. Symbols represent observed values.

The same dataset was then reanalysed with level of diversity converted to a covariate without the inclusion of the wildtype virus. Level of diversity when treated as a sole covariate failed to be a significant indicator ($F_{5,189} = 3.041$, $P = 0.08$), this is admittedly extremely close to significance though. Speed of kill ($1/\text{speed of kill}^2$) was then introduced into the model as a covariate alongside level of diversity. The interaction term between diversity and speed of kill was converted into a factor to allow the inclusion of two covariates into the same model. This interaction term did not prove to be a significant factor and was thus removed from the model ($F_{1,187} = 0.0128$, $P = 0.91$). The introduction of transformed speed of kill into the model was though found to be a strong predictor of yield ($F_{1,198} = 43.7$, $P < 0.001$; Figure 7.12) and in addition made level of diversity a significant covariate ($F_{1,188} = 7.22$, $P < 0.0079$; Figure 7.12).

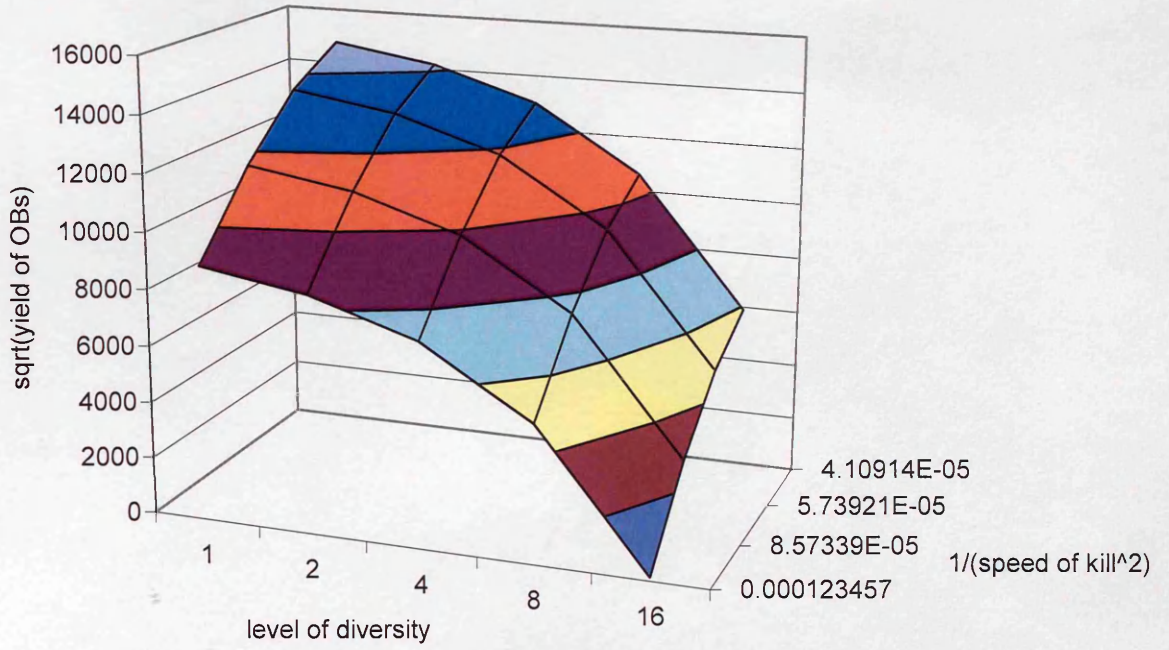


Figure 7.12 Influence of virus level of diversity and speed of kill on yield for *SpexNPV* infection of 3rd instar *S.exempta* larvae at a dose of 5000 OBs.

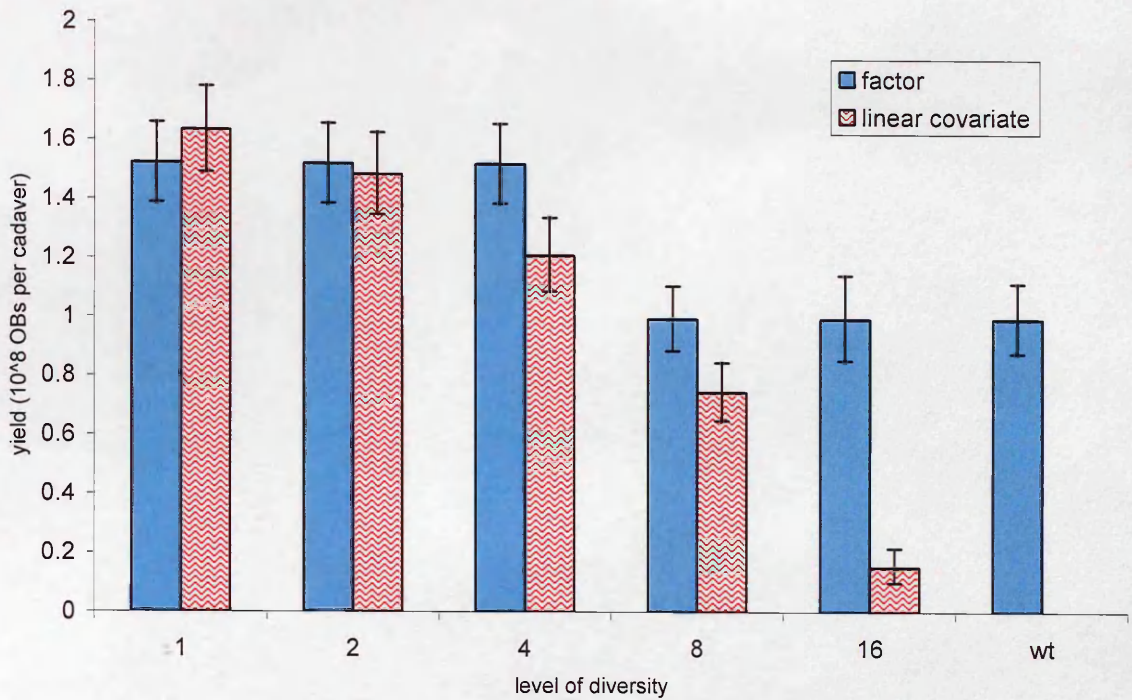


Figure 7.13 Comparison of two different statistical models which represent the influence of *Spex*NPV genotype diversity on yield (OBs per cadaver) in third instar *S. exempta* larvae at a dose of 5000 OBs. Back transformed mean yield (± 1 SE) estimated by assigning level of diversity as a factor or as a covariate. Differences between estimates of yield generated by each model can be attributed to inclusion of wild-type into the statistical analysis.

7.3.5 Proportion of different genotypes in progeny virus

Mixed-clone viral infections were identified by identifying novel bands in restriction endonuclease profiles of individual genotypes (Table 7.5). To illustrate this approach, profiles for single and mixed infections resulting from dual inoculation of genotypes A and C are shown in Figure 7.14.

Table 7.5 Summary of characteristic novel bands in restriction endonuclease profiles used to identify mixed infections resulting from dual inoculation of *Spex*NPV genotypes at 10 000 OBs. For nomenclature of bands see chapter 3.

Dual infection	Genotype used for identification	Novel bands characteristic of genotype used for identification (present in sub-molar levels in mixed infection)
AE	A	d o
AF	A	a m o
AC	C	c g j p (see Figure 7.14)
CD	C	c g p
CE	C	c j p
CF	C	g m
AD	D	j
DE	D	d j p
DF	D	a m p
EF	F	c d j q
BG	B	a q
BH	H	p q
HG	H	p

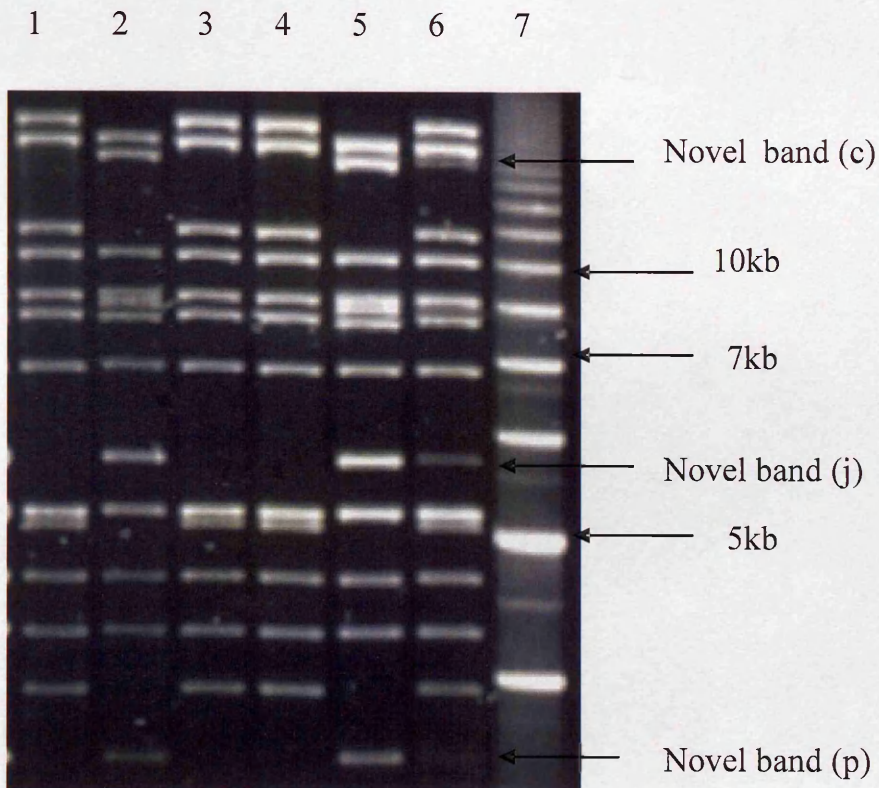


Figure 7.14 *EcoRV* profiles of DNA from virus deaths resulting from dual inoculation with *Spex* NPV genotypes A and C at dose of 5000 OBs in 3rd instar *S. exempta* larva. Lanes 1, 3 and 4 show genotype A dominating the infection, lanes 2 and 5 shows genotype C dominating the infection and lane 6 shows a profile characteristic of a mixed infection indicated by the presence of novel bands (c, j and p) belonging to genotype C. Lane 7 molecular marker, 1Kb ruler (BioRad).

The number of mixed infections detected by RE analysis was surprisingly low for the two genotype infections, except in the dual infections with genotypes BH and AC where as many as 4 out of 5 of the resulting progeny for BH and 1 in 3 for AC possessed sub-molar bands in RE profile and consequently were considered mixed infections (Figure 7.15).

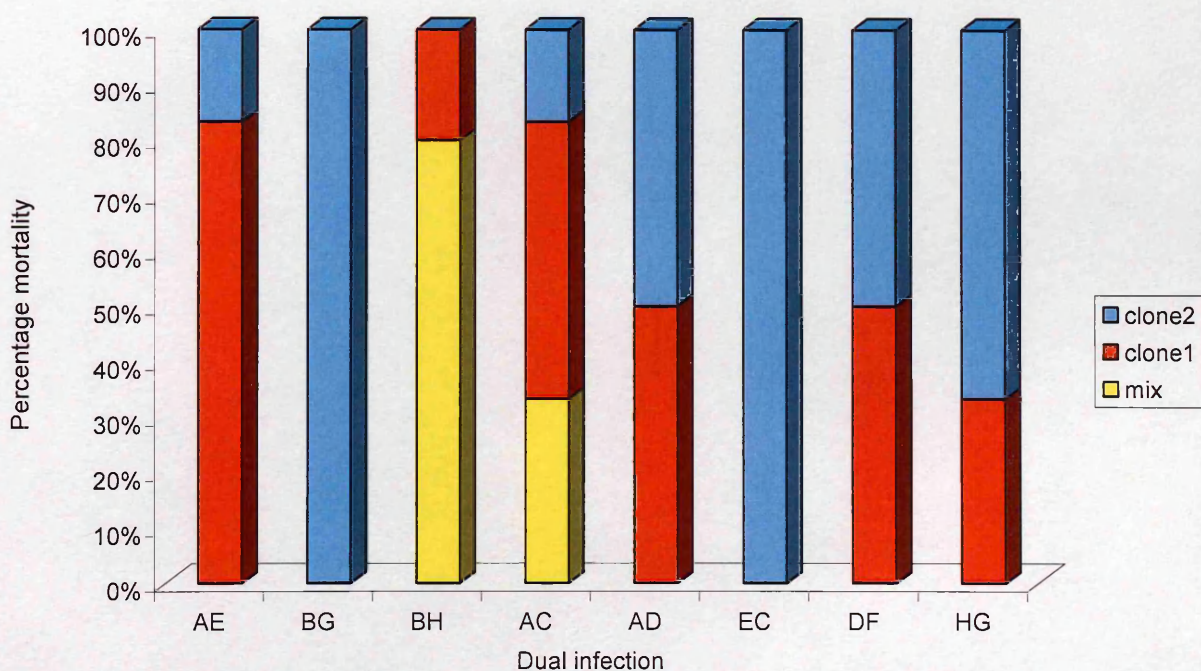


Figure 7.15 Proportion of genotypes and mixed infections resulting from dual inoculation of *SpexNPV* genotypes in a ratio of 1:1 at a dose of 5000 OBs. Labelling of genotypes in legend follows order of genotypes in dual infections on y-axis.

The number of mixed infections detected after challenge with four genotypes produced on average more mixed infections than after dual inoculation. In addition, mixed infections appeared to predominate in treatments including either B, G or H within the inoculum (Figure 7.16), interestingly the same genotypes previously shown to possess a higher level of pathogenicity in comparison to the other genotypes (Chapter 3).

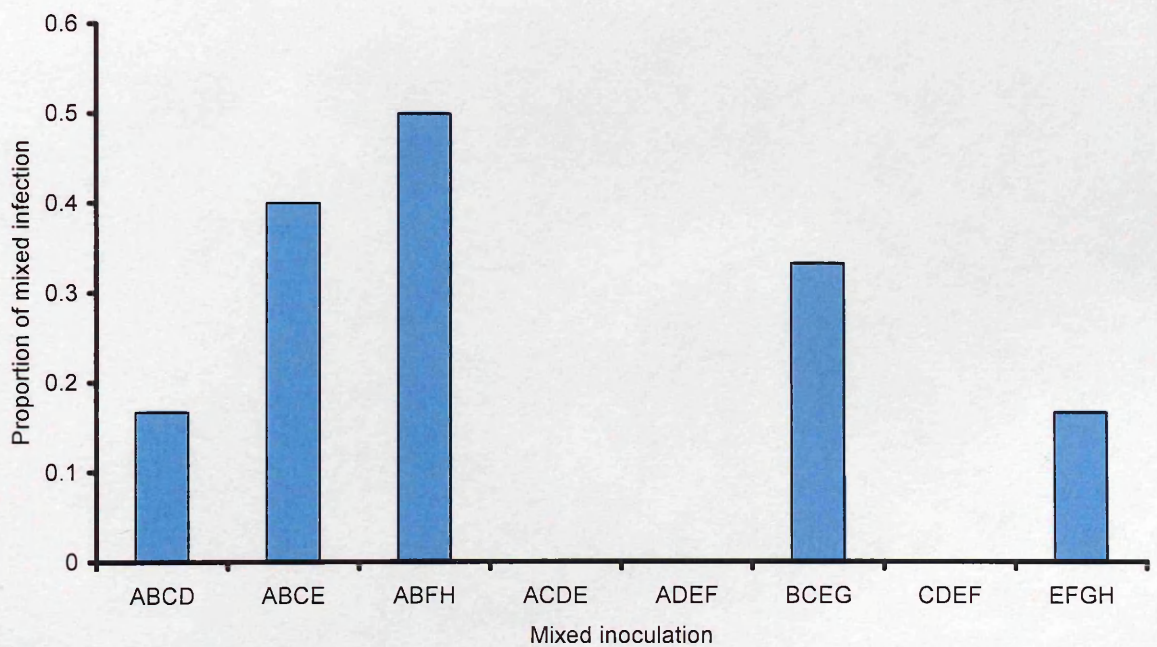


Figure 7.16 Proportion of mixed infections resulting from inoculation with four *SpexNPV* genotypes in equal ratios, at a dose of 5000 OBs per insect.

The proportion of mixed infections detected by REN analysis at each level of diversity in the progeny (excluding the wild type virus) was logit transformed ($\ln(p/1-p)$ when p = proportion of mixed infections) and analysed using a binary error structure. Deviances were adjusted via the scale parameter to allow for overdispersion of the data. Level of inoculum diversity had a large influence on the proportion of mixed infections detected with the proportion of mixed infections increasing with increasing inoculum diversity (Figure 11; $\chi^2_1 = 11$, $P < 0.001$).

The extrapolation of the fitted curve beyond 16 genotypes allows predictions to be made about the number of genotypes present in the wildtype virus. According to RE analysis, 86.3% of the progeny resulting from inoculation with the wildtype virus were mixed infections. Consequently, by solving the fitted equation for 86.3% a prediction of approximately 23 genotypes can be made.

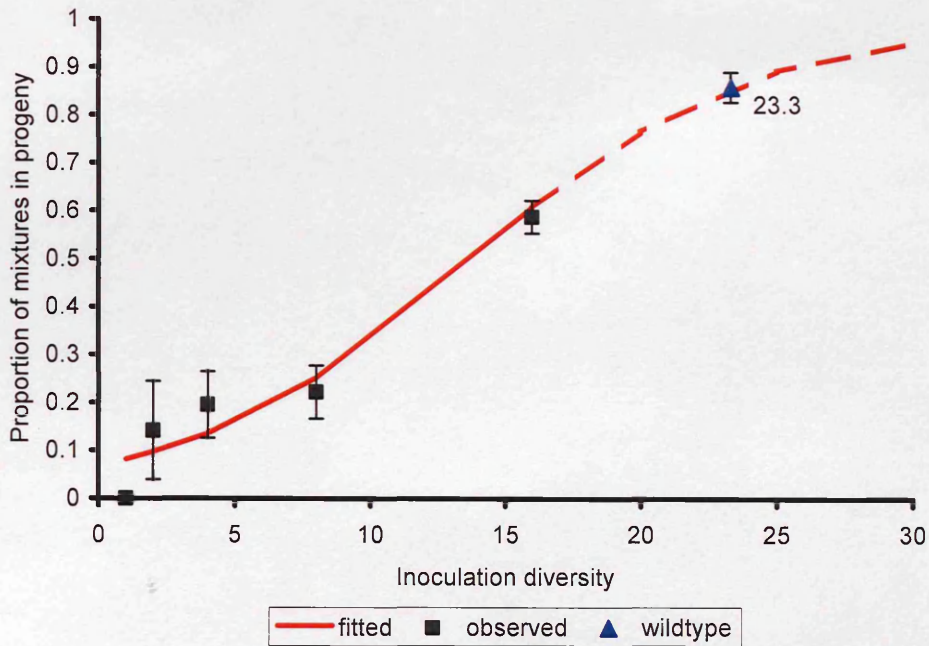


Figure 7.17 Proportion of mixtures detected in virus-killed larvae using REN analysis after inoculation with mixed *Spex*NPV variant inoculations, modelled against level of diversity within the inoculum. Fitted line is the back transformation of the minimal adequate model fitted by ANCOVA, $\text{logit}(\text{proportion of mixed infections}) = -2.608 + (0.191 * \text{mix})$ when $\text{logit} = \ln(p/(1-p))$, $p = \text{proportion of mixed infections}$ and $\text{mix} = \text{the number of genotypes in the inoculation}$. Symbols represent mean observed values ($\pm 1\text{SE}$).

7.4 Discussion

Controlled mixed-genotype infections were carried out in order to test the adaptive trade-off prediction that increasing level of diversity within an infection, due to within host competition elevates virulence above that considered 'prudent' within a single-genotype infection (Frank, 1996). We predicted that if genotypes competed for the limited host resource faster speeds of kill would be produced resulting in reduced yields. Contrary to this prediction, and consistent with the dual inoculation experiments previously carried out (Chapter 6), speeds of kill were lengthened. Therefore genotypes appear not to compete in co-infection. Other Single and mixed infection studies of the rodent malarial parasite, *Plasmodium chabaudi*, used as a model system for the highly virulent human malaria, *P. falciparum*, have demonstrated that mixed infections possess increased levels of virulence (Taylor *et al.*, 1997 and 1998). In addition, increased virulence and reproductive rate of mixed schistosome infections of snails were also found to correlate positively with the increasing heterogeneity of the infection (Davies *et al.*, 1999 and 2002). Although these two studies appear to provide evidence in support of the theoretical predictions, they fail to elucidate the exact mechanism for the observed elevation of virulence and the action of intra-host competition. Both authors postulate that the increased virulence probably has more to do with strain-specific immunity and the hosts reduced ability to clear genetically diverse infections rather than resource limitation (Taylor *et al.*, 1998; Davies *et al.*, 2002). In order to prove the existence of intraspecific competition, evidence that per capita parasite fitness is reduced by the presence of another strain is needed. Gower and Webster (2005) have very recently demonstrated this for genetic strains of *Schistosoma mansoni* and their intermediate snail host, *Biomphalaria glabrata*, using strain-specific quantitative

real-time PCR. Similar technology was used by De Roode (2005b) demonstrated that parasite strains that inhabit very similar niches inside their host compete with each other. The relative importance of resource limitation and strain-specific immunity has yet to be elucidated. The inability to detect intra-host competition between co-infecting strains of the trypanosome *Crithidia bombi* in bumblebees has been ascribed to strains inhabiting completely different niches inside their host and consequently the complete absence of ecological niche overlap (Imhoof & Schmid-Hempel, 1998; Schmid-Hempel *et al.*, 1999). Other studies have struggled to predict the phenotypic traits of mixed infections from single-genotype infections (Nakamura *et al.*, 1992; Weeds *et al.*, 2000; Cox, 2001; Hodgson *et al.*, 2004).

Although mortality of the host is not directly linked to parasite transmission (Ebert and Weisser, 1997) for baculoviruses and consequently the adaptive trade-off hypothesis does not predict increased pathogenicity (host mortality) in mixed infections, a positive correlation between level of diversity and pathogenicity was identified. Mixed-genotype infections can therefore be considered to have higher levels of fitness in comparison to single-genotype infections.

Chapter Eight

General Discussion

Chapter 8: General Discussion

In this study, I have focused on identifying genetic variation at different ecological levels, assessing whether this translates into differences in phenotype and examining the consequence of mixed infections. *Spex*NPV possesses high levels of both genetic and phenotypic variation and we have found that increased diversity results in a greater severity of infection, though it was apparent that at the lower levels of diversity the identity of the variant did have an effect.

Theory predicts various evolutionary responses to the presence of co-infecting genotypes (Van Baalen and Sabelis, 1995; Bremermann and Pickering, 1983; Frank, 1996). Phenotypic traits likely to correlate with higher baculovirus fitness include high pathogenicity (fatal infection), high yields of OBs, or faster speeds of kill (allowing for more cycles of infection). The use of controlled mixed-infection experiments have shown that the characteristics of mixed infections are difficult to predict at the two genotype level where results are dependent upon the specific genotypes within the co-infection. However, mixed infections generally resulted in elevated mortality and a positive correlation between pathogenicity and level of diversity was identified. For baculoviruses host death does not have a direct negative impact on parasite transmission and consequently the higher pathogenicity reflects increased fitness of mixed infections of *Spex*NPV genotypes. Another phenotypic trait associated with fitness is speed of kill. Contrary to predictions (Hodgson *et al.*, 2004) that intra-host competition would reduce infection duration, in general, speeds of kill were lengthened. Whether this lengthening of speed of kill translated into increased yields depended on

the specific mixed infection under study. In order to understand these differences we need to be able to monitor within host dynamics. A thorough analysis of the fitness costs incurred by a parasite that shares a host with the same or a different genotype needs to be carried out. It would also be extremely interesting to investigate the actual competitive abilities of co-infecting genotypes using genotype-specific primers, which would allow the monitoring of the genotypes' growth rate. Such studies have been recently been carried out using quantitative realtime PCR technology to determine the competitive abilities of different genotypes within mixed *Schistosoma mansoni* infections of its intermediate snail host (Gower and Webster, 2005) and mixed *Plasmodium chabaudi* in mice (de Roode *et al.*, 2005). If the fitness of mixed infections is higher than that of single infections, selection should favour within-host diversity and thus represents an important mechanism through which heterogeneity of baculovirus populations could be maintained.

Another mechanism through which diversity of *SpexNPV* infections could be maintained is through the correlation of life-history traits. A negative trade-off between speed of kill and virus yield may theoretically promote the co-existence, within a population, of fast-killing/ low yielding genotypes alongside equally fit genotypes with slow speeds of kill and high yields (Hodgson *et al.*, 2001). Although a negative trade-off between speed of kill and yield was identified for many individual *SpexNPV* genotypes, the use of mean estimates for each genotype revealed no correlation between genotypes in this study. This though does not mean that such a negative correlation may not exist and its elucidation may simply require the inclusion of more

than eight genotypes in the analysis. Other infection parameters which may potentially trade-off include persistence and transmission, with the slower release of virus and thus lower transmission of more persistent genotypes. The co-existence of infections with different phenotypes possessing equal fitness is perhaps more likely in baculovirus systems where epizootics and individual infections are commonly dominated by single genotypes and not by a mixtures of genotypes like *Spex*NPV.

Another major influence of baculovirus population diversity is host density. *Spodoptera exempta* is a migratory outbreak pest and therefore has enormous fluctuations in population densities both temporally and spatially. During the “off-season” when *S. exempta* appears in its solitary form at low host densities, the selection pressure exerted on viral genotypes will conceivably either be for increased pathogenicity, to decrease the minimum host density required for persistence by horizontal transmission (Anderson and May, 1981); or for decreased pathogenicity and vertical transmission (Bull *et al.*, 1991). During outbreaks of *S. exempta* when high host densities of the gregarious morph are seen, the ease of transmission will reduce the selection pressure exerted for high pathogenicity and theoretically allow the existence of different phenotypes. The estimation of important fitness traits of *Spex*NPV isolates from individual field-collected larvae through laboratory bioassay demonstrated that an extremely wide range of phenotypes can co-exist during an epizootic in a host population of extremely high densities. Host density can also indirectly influence diversity through a positive correlation with high viral prevalence, which in turn increases the probability of mixed infections. Preliminary data presented in this study

appears to support such a positive correlation between host and viral prevalence, as well as between host density and prevalence of mixed infections. A high prevalence of mixed infections, which was estimated for *SpexNPV* to be approximately 40%, in theory can also increase opportunities for recombination between co-infecting genotypes. Recombination has been reported to occur *in vivo* between closely related virus genotypes with high frequency (Crozier *et al.*, 1988; Crozier and Ribeiro, 1992). This will promote the creation of new genetic variants and help maintain the diversity of the population as a whole. No link between the level of mixed infections and level of diversity was detected at the high host densities sampled in this study. In order to understand the impact of host density on virus diversity, it would be valuable to carry out genetic characterization of *SpexNPV* epizootics during outbreaks of gregarious larvae at lower host densities, as well as the genetic analysis of *SpexNPV* populations of solitary larvae at extremely low host densities.

The *SpexNPV* population investigated in this study was highly diverse although no sub-structure could be identified. If it was random, the genetic variation could be considered neutral and not the result of selection. In a similar way that the Hardy-Weinberg equation is used to explain the absence of selection for sexual populations, linkage equilibrium can be used for the description of haplotype frequencies (NPV genotypes) which do not deviate from the values they would have if the genotypes combined at random. Randomisation analysis and Monte Carlo techniques could be used to verify the apparent random nature of the frequency distributions of the genotypes. Theory predicts that in the absence of selection, with random mating, the action of

recombination over time will drive the haplotypes to random frequencies where they become fixed. Such randomness appears in contrast to other natural baculovirus whose genetic populations have been studied. The dominance of individual genotypes within local *S. exigua* and winter moth populations (Gelernter and Federici, 1990; Graham *et al.*, 2004) presumably is evidence of selection favouring individual genotypes with higher fitness. Although our study and the winter moth study represent preliminary data it is interesting to compare viruses from species from different ecologies. It would seem reasonable to assume that the differences in ecology between tropical migratory pests and temperate forest insects, with one generation a year and possible cyclic population dynamics, may be responsible for the different levels of genotype diversity seen in the two natural populations of the two baculovirus systems already mentioned. In winter moth population genetics may be related to genetic bottlenecks following a move to novel host plants. If linkage disequilibrium was to be measured in these populations, high values would indicate the presence of selection acting on the genotypes. Fitness though is context-dependent and therefore different genotypes may dominate in different locations depending on the ecological and environmental conditions and therefore although genotypic diversity is low at the meta-population scale, wider scale geographical variation may be much higher. This is similar to the geographic mosaic theory of co-evolution which makes the prediction that co-evolution occurs at different sites but not necessarily with the same ecological conditions (Thompson and Cunningham, 2002). A study which measured linkage disequilibrium, diversity and levels of transmission of malaria populations in humans revealed a similar divergent range of genetic structures similar to the contrasting scenarios discussed for

baculoviruses (*OpbuNPV/ SpexNPV*). The study found strong LD, low genetic diversity, high geographic diversity in regions of low transmission, while random association, high genetic diversity and minimal geographical diversity were observed in regions of high transmission (Anderson *et al.*, 2000).

The estimation of the molecular size of the individual genotypes has shown that the genome size of *SpexNPV* variants varies considerably from 116kbp to 152 kbp (Chapter 3). It has been postulated (Hodgson *et al.*, 2001) that variants with smaller genomes possess a replication rate advantage over larger genomes. The generation of deletion mutants in cell culture is a well-documented phenomenon. Through the relaxation of selection pressure for insect to insect transmission, genotypes lacking fragments of DNA are rapidly generated and genes that are non-essential for replication, such as polyhedrin, can be lost (Piljman *et al.*, 2001). Although a model by Godfray *et al* (1997) predicted that the ‘few-polyhedra’ (FP) phenotype possessed very little, if any fitness advantage in pure infections, it has been shown that a FP phenotype is able to persist as a stable polymorphism with the wild-type via a process of frequency dependent selection (Bull *et al.*, 2003). Using similar logic, genotypic variation could potentially be maintained as a result of a trade-off between within-host and between-host transmission. Conceivably any genotypes which is able to replicate well within the host and spread may not be less occluded or perhaps be more sensitive to environmental degradation. It would be interesting to investigate if the variation of molecular size of the *SpexNPV* genotypes is related to any loss of auxillary gene expression and associated reduction in biological fitness. This would involve physically

mapping the variants and sequencing one of them in order to identify the regions of variability. On the basis of other studies we would predict that this variation will not be evenly distributed across the genome with considerable variation focused around the chitinase and *egt* gene regions (e.g. Hitchman, 2002; Hodgson *et al.*, 2001; Simon *et al.*, 2004 and 2005).

The ability of *Spex*NPV (and other NPVs) to package multiple genomes within the same occlusion body provides the opportunity for the incorporation of multiple genotypes, including defective or parasitic genotypes, and therefore represents another mechanism through which diversity can be maintained. It has been suggested that even though viruses are strictly speaking haploid, because an OB represents the relevant unit of reproduction, packaging multiple genotypes within an OB can mimic the masking of recessive alleles by diploids (Hodgson *et al.*, 2001). It is unclear to what extent each genome within the OB contributes to the production of progeny OBs, but co-infection of the same cell could allow the persistence of deleterious genotypes via a parasitic relationship with their co-infecting genotypes. Godfrey *et al.* (1997) and Bull *et al.* (2003) predict and support the finding that an average of 4 genomes will typically infect a cell at high doses. This genetic phenomenon has been referred to as 'poly-haploidy' (Hodgson *et al.*, 2001). Deleterious genotypes are maintained at low levels within any population be it haploid, diploid or poly-haploid, at a mutation/selection equilibrium, which is the allele frequency at which new mutants are produced at the same rate as they are selected against and lost from the population. It has been hypothesized that poly-haploid populations of NPVs are able to support a higher

frequency of deleterious mutants and the mutation/selection equilibrium of these defective genotypes is far greater than those seen in either haploid or diploid populations (Hodgson *et al.*, 2001). Approximately 40% of all virus-infected larvae, sampled within a natural epizootic of *Spex*NPV in Northern Tanzania, were identified as genetically diverse infections. This level is likely to represent an under-estimate of the total mixed infections actually present in nature because of the lack of sensitivity of the detection method (RE analysis). This high level of co-infection in nature coupled with the multiply occluded phenotype may promote the evolution of parasitic genotypes and their maintenance in the population (Turner and Chao, 1999; Godfray *et al.*, 1997; Hodgson *et al.*, 2001).

For sexual organisms, reproduction ensures the continual remixing of the gene pool and the maintenance of high levels of genetic variation in the population. Asexual microorganisms, such as baculoviruses also possess ways of exchanging genetic material and the co-occlusion of multiple NPVs' allows ample opportunities for recombination. Consequently, it should not be surprising that complex mixtures of parasite genotypes within individual hosts are commonly observed. Elucidation of the mechanisms that generate and maintain this variation is central to the understanding of the evolutionary ecology of host-parasite interactions. In addition, the impact and effectiveness of genetically diverse infections has important implications for microparasites, like *Spex*NPV which are utilized as bioinsecticides. A great deal of research effort has been made to improve the pathogenicity and efficacy of bioinsecticides. The wild-type *Spex*NPV represents a mixed infection of at least seventeen different genotypes, on the

basis of *in vivo* cloning. It yielded the highest level of pathogenicity relative to both single-genotype and all other mixed-genotype infections (upto 16-genotype infections) carried out in this study. Therefore in the absence of exhaustive screening for locally adapted 'fit' genotypes which match the local ecology of the host population, this study suggests that for *Spex*NPV in particular, genetically diverse sprays will be more pathogenic.

Although antigenic specificity has recently been implicated as a major determinant of the genetic structuring of some invertebrate parasite populations in vertebrates (Gupta and Anderson, 1999), not enough is known about the immune system of insects to say what role it has in disease resistance and the composition of parasite populations. The immune function usually involves the encapsulation of virions (Tradeua *et al.*, 2001) and therefore is perhaps not as specific as vertebrate immune systems but this represents an interesting area for further work. The gregarious and the solitary morphs of *Spodoptera exempta* possess different levels of resistance (Reeson *et al.*, 1998) and consequently this offers opportunities to investigate the roles melanisation, phenoloxidase and resistance and how this relates to parasite virulence within the same host species.

In this study we have found that genetic and phenotypic diversity of *Spex*NPV populations during an epizootic was universally extremely high at a range of spatial scales. Although the presence of biological diversity offers the opportunity for selection to act, the direct link between biological function and the genetic heterogeneity was not

established in this study. The apparent lack of any population structuring of *Spex*NPV appears to suggest that selection may not play a major role in the determination of the population composition of *Spex*NPV. For *Spex*NPV, within-host dynamics are perhaps the most important factor in the determination and maintenance of diversity. For mixed-genotype infections account for a large proportion of *Spex*NPV infections in the field and we have shown that co-infection can have a major influence on the infection characteristics and fitness traits.

References

References

Agnew, P., Koella, J.C. (1999) Life-history interactions with environmental conditions in a host-parasite relationship and the parasite's mode of transmission. *Evol. Ecol.* **13**, 67-89.

Ahrens, C.H., Russell, R.L.Q., Funk, C.J., Evans, J.T., Harwood, S.H., Rohrmann, G.F. (1997) The sequence of the *Orygia pseudotsugata* multinucleocapsid nuclear polyhedrosis virus genome. *Virology* **229**, 381-399.

Allaway, G.P., Payne, C.C. (1982) A biochemical and biological comparison of three European isolates of nuclear polyhedrosis viruses from *Agrotis segetum*. *Arch. Virol.* **75**, 43-54.

Anderson, R.M., May, R.M. (1980) Infectious diseases and population cycles of forest insects. *Science* **210**, 658-661.

Anderson, R.M., May, R.M. (1981) The population dynamics of microparasites and their invertebrate hosts. *Philos. Trans. R. Soc. Lond. B* **291**, 451-524.

Anderson, R.M., May, R.M. (1982) Coevolution of hosts and parasites. *Parasitology* **85**, 411-426.

Anderson, T.J.C., Haubold, B., Williams, J.T. *et al* (2000) Microsatellite markers reveal a spectrum of population structures in the malaria parasite *Plasmodium falciparum*. *Mol. Biol. Evol.* **17**, 1467-1482.

Anita, R., Levin, B.R., May, R.M. (1994) Within-host population dynamics and the evolution and maintenance of microparasite virulence. *Am. Nat.* **144**, 457-472.

Arends, H.M., Winstanley, D., Jehle, J.A. (2005) Virulence and competitiveness of *Cydia pomonella* granulovirus mutants: parameters that do not match *J. Gen Virol.* **86**, 2731-2738.

Ayres, M.D., Howard, S.C., Kuzio, J., Lopez-Ferber, M., Possee, R.D. (1994) The complete DNA sequence of *Autographa californica* nuclear polyhedrovirus. *Virology* **202**, 586-605.

Beisner, B.E., Myers, J.H. (1999) Population density and transmission of virus in experimental populations of the western tent caterpillar (Lepidoptera: Noctuidae). *Environ. Entomol.* **28**, 1107-1113.

Benz, G.A. (1986) Introduction: Historical perspective, in: *The Biology of Baculoviruses* (R.R. Granados, B.A. Federici, eds.), Vol. I: *Biological Properties and Molecular Biology*, pp.1-35, CRC, Boca Raton, FL.

Bidshi, D.K., Bigot, Y., Federici, B.A. (2000) Molecular characterisation and phylogenetic analysis of the *Harrisina brillians* granulovirus granulin gene. *Arch. Virol.* **145**, 1933-1945.

Bishop, D.H.L., Christensen, A., Jacobsen, B.L., Pastoret, P.P. (1995) Working Group-viii: Biological Pesticides (Biopesticides). *Microbial Ecology in Health and Disease* **8**, S45-S49.

Black, B.C., Brennan, L.A., Dierks, P.M., Gard, I.E. (1997) Commercialisation of baculovirus insecticides. In *The Baculoviruses*, pp. 341-387. Edited by L.K. Miller. New York, NY: Plenum Press.

Bonhoeffer, S., Nowak, M.A. (1994) Mutation and the evolution of virulence. *Proc. R. Soc. Lond. B* **258**, 133-140.

Bonning, B.C., Hammock, B.D. (1996) Development of recombinant baculoviruses for insect control. *Ann. Rev. Entomol.* **35**, 191-210.

Bonsall, M.B., Sait, S.M., Hails, R.S. (2005) Invasion and dynamics of covert infection strategies in structured insect-pathogen populations. *J. Anim. Ecol.* **74**, 464-474.

Boots, M., Norman, R. (2000) Sub-lethal infection and the population dynamics of host-microparasite infections. *J. Anim. Ecol.* **69**, 517-524.

Bremermann, H.J., Pickering, J. (1983) A game-theoretical model of parasite virulence. *J. Theor. Biol.* **100**, 411-426.

Briggs, C.J., Godfray, H.C.J. (1995) dynamics of insect-pathogen interactions in stage-structured populations. *Am. Nat.* **145**, 855-887.

Briggs, C.J., Godfray, H.C.J. (1996) The dynamics of insect-pathogen interactions in seasonal environments. *Theor. Pop. Biol.* **50**, 145-177.

Brown, D. (1982) Two naturally occurring nuclear polyhedrosis virus variants of *Neodiprion sertifer* Geoffr. (Hymenoptera; Dirrionidae). *Appl. Environ. Micro.* **43**, 65-69.

Brown, E.S., Dewhurst, C.F. (1975) The genus *Spodoptera* (Lepidoptera: Noctuidae) in Africa and the Near East. *Bull. Entomol. Res.* **65**, 221-261.

Brown, E.S., Swaine, G. (1965) Virus disease of the African armyworm, *Spodoptera exempta* (Walker) *Bull. Entomol. Res.* **56**, 95-116.

Brown, S.P., Hochberg, M.E., Grenfell, B.T. (2002) Does multiple infection select for raised virulence? *Trends in Microbiol.* **10**, 401-405.

Bulach, D.M., Kumar, C.A., Zaia, A., Liang, B., Tribe, D.E. (1999) Group II nucleopolyhedrovirus subgroups revealed by phylogenetic analysis of polyhedrin and DNA polymerase gene sequences. *J. Invertebr. Pathol.* **73**, 59-73.

Bull, J.C., Godfray, H.C.J., O'Reilly, D.R. (2001) Persistence of an occlusion-negative recombinant nucleopolyhedrovirus in *Trichoplusia ni* indicates high multiplicity of cellular infection. *Appl. Environ. Microbiol.* **67**, 5204-5209.

Bull, J.C., Godfray, H.C.J., O'Reilly, D.R. (2003) A few-polyhedra mutant and wild-type nucleopolyhedrovirus remain as a stable polymorphism during serial coinfection in *Trichoplusia ni*. *Appl. Environ. Microbiol.* **69**, 2052-2057.

Bull, J.J. (1994) Virulence. *Evolution* **48**, 1423-1437.

Bull, J.J., Molineux I.J., Rice, W.R. (1991) Selection of benevolence in a host-parasite system. *Evolution* **45**, 875-882.

Burand, J., Park, E. (1992) Effect of nuclear polyhedrosis virus infection on the development and pupation of gypsy moth larvae. *J. Invertebr. Pathol.* **60**, 171-173.

Burden, J.P., Griffiths, C.M., Cory, J.S., Smith, P., Sait, S.M. (2002) Vertical transmission of sub-lethal granulovirus infection in the Indian meal moth, *Plodia interpunctella*. *Mol. Ecol.* **11**, 547-555.

Burden, J.P., Hails, R.S., Windass, J.D., Suner, M.-M., Cory, J.S. (2000) Infectivity, speed of kill and productivity of a baculovirus expressing the itch mite toxin Txp-1 in second and fourth instar larvae of *Trichoplusia ni*. *J. Invertebr. Pathol.* **75**, 226-236.

Burden, J.P., Nixon, C.P., Hodgkinson, A.E., Possee, R.D., Sait, S.M., King, L.A., Hails, R.S. (2003) Covert infections as a mechanism for long-term persistence of baculoviruses. *Ecol. Letters* **6**, 524-531.

Burden, J.P., Possee, R.D., Sait, S.M., King, L.A., Hails, R.S. (2005) Phenotypic and genotypic characterisation of persistent baculovirus infections in populations of the cabbage moth (*Mamestra brassicae*) within the British Isles *Arch. Virol.* In Press.

Caballero, P., Aldebis, H.K., Vargas-Osuna, E., Santiago-Alvarez, C. (1992) Epizootics caused by a nuclear polyhedrosis virus in populations of *Spodoptera exigua* in southern Spain. *Biocontrol Science and Techn.* **2**, 35-38.

Chao, L., Hanley, K.A., Burch, C.L., Dahlberg, C., Turner, P.E. (2000) Kin selection and parasite evolution: higher and lower virulence with hard and soft selection. *Q. Rev. Biol.* **75**, 261-275.

Chapman, J.W., Williams, T., Escribano, A., Caballero, P., Cave, R.D., Goulson, D. (1999) Age-related cannibalism and horizontal transmission of a nuclear polyhedrosis virus in larval *Spodoptera frugiperda*. *Ecol. Entomol.* **24**, 256-275.

Cheke, R.A., Tucker, M.R. (1995) An evaluation of potential economic returns from the strategic control approach to the management of African armyworm, *Spodoptera exempta* (Lepidoptera: Noctuidae) populations in eastern Africa. *Crop Protection* **14**, 91-103.

Chen, X., Ijkel, W.F.J., Dominy, C., Zanutto, P., Hashimoto, Y., Faktor, O., Hayakawa, T., Wang, C.-H., Prekumar, A., Mathavan, S., Krell, P.J., Hu, Z., Vlak, J.M. (1999) Identification, sequence analysis and phylogeny of the *lef-2* gene of *Helicoverpa armigera* single-nucleocapsid baculovirus. *Virus Res.* **65**, 21-35.

Chen, X.W., Hu, Z.H., Jehle, J.A., Zhang, Y.Q., Vlak, J.M. (1997) Analysis of the ecdysteroid UDP-glucotransferase gene of *Heliothis armigera* single nucleocapsid baculovirus. *Virus Genes* **15**, 219-225.

Chen, X.W., Zhang, W.J., Wong, J., Chun, G., Lu, A., McCutchen, B.F., Presnail, J.K., Herrmann, R, Dolan, M., Tingey, S., Vlak, J.M. (2002) Comparative analysis of the complete genome sequences of *Helicoverpa zea* and *Helicoverpa armigera* single-nucleocapsid nucleopolyhedroviruses *J. Gen. Virol.* **83**, 673-684.

Cherry, C.L., Summers, M.D. (1985) Genotypic variation among isolates of two nuclear polyhedrosis viruses isolated from *Spodoptera littoralis*. *J. Invertebr. Pathol.* **46**, 289-295.

Clarke, E.E., Tristem, M., Cory, J.S., O'Reilly, D.R. (1996) Characterisation of the ecdysteroid UDP-glucosyltransferase gene from *Mamestra brassicae* nucleopolyhedrosis virus. *J. Gen. Virol.* **77**, 2865-2867.

Cooper, D., Cory, J.S., Myers, J.H. (2003a) Hierarchical spatial structure of genetically variable nucleopolyhedroviruses infecting cyclic populations of western tent caterpillars. *Mol. Ecol.* **12**, 881-890.

Cooper, D., Cory, J.S., Theilmann, D.A. Myers, J.H. (2003b) Nucleopolyhedroviruses of forest and western tent caterpillars: cross-infectivity and evidence for activation of latent virus in high-density field populations. *Ecol. Entomol.* **28**, 41-50.

Cory, J.S., Myers, J.H. (2003) The ecology and evolution of insect baculoviruses. *Annu. Rev. Ecol. Evol. Syst.* **34**, 239-272.

Cory, J.S., Myers, J.H. (2004) Adaptation in an insect host-plant pathogen interaction. *Ecol. Letters* **7**, 632-639.

Cory, J.S., Hails, R.S., Sait, S.M. (1997) Baculovirus ecology. *The baculoviridae* (ed. By L.K.Miller), pp. 301-339. Plenum Press, New York.

Cory, J.S., Green, B.M., Paul, R.K., Hunter-Fujita, F. (2005) Genotypic and phenotypic diversity of a baculovirus population within an individual insect host. *J. Invertebr. Pathol.* **89**, 101-111.

Cory, J.S., Hirst, M.L., Sterling, P.H., Speight, M.R. (2000) Narrow host range nucleopolyhedrovirus for control of the browntail moth (Lepidoptera: Lymantriidae). *Environ. Entomol.* **29**, 661-667.

Cory, J.S., Clarke, E.E., Brown, M.L., Hails, R.S., O'Reilly, D.R. (2004) Microparasite manipulation of an insect: the influence of the *egt* gene on the interaction between a baculovirus and its lepidopteran host. *Funct. Ecol.* **18**, 443-450.

Cory, J.S., Hirst, M.L., Williams, T., Hails, R.S., Goulson, D., Green, B.M., Carty, T.M., Possee, R.D., Cayley, P.J., Bishop, D.H.L. (1994) Field trial of a genetically improved baculovirus insecticide. *Nature* **370**, 138-140.

Cox, F.E.G. (2001) Concomitant infections, parasites and immune responses. *Parasitology* **122**, S23-S38.

Crawley, M.J. (1997) Life history and environment In: *Plant Ecology* (M.J. Crawley, ed.), pp. 73-131. Blackwell Publishers, Oxford.

Crook, N.E., Spencer, R.A., Payne, C.C., Leisy, D.J. (1985) Variation in *Cydia pomonella* granulosis virus isolates and physical maps of the DNA from these variants. *J. Gen. Virol.* **66**, 2423-2430.

Crozier, G, Ribeiro, H.C.T. (1992) Recombination as a possible cause of genetic heterogeneity in *Anticarsia gemmatalis* nuclear polyhedrosis virus wild populations. *Virus Res.* **26**, 183-196.

Crozier, G, Crozier, L., Quiot, J.M., Lereclus, D. (1988) Recombination of *Autographa californica* and *Rachiplusia* ou nuclear polyhedrosis viruses in *Galleria mellonella* L. *J. Gen. Virol.* **69**, 179-185.

D'Amico, V., Elkington, J.S., Dwyer, G., Burand, J.P., Buonaccorsi, J.P. (1996) Virus transmission in gypsy moths is not a simple mass action process. *Ecology* **77**, 201-206.

Dai, X., Hajos, J.P., Joosten, N.N., van Oers, M.M., Ijkel, W.F.J., Zuidema, D., Pang, Yi, Vlak, J.M. (2000) Isolation of a *Spodoptera exigua* baculovirus recombinant with a 10.6kbp genome deletion that retains biological activity. *J. Gen. Virol.* **81**, 2545-2554.

Davies, C.M., Fairbrother, E., Webster, J.P. (2002) Mixed strain schistosome infections of snails and the evolution of parasite virulence. *Parasitology* **124**, 31-38.

Davies, C.M., Webster, J.P., Kruger, O., Munatsi, A., Ndamba, J., Woolhouse, M.E.J. (1999) Host-parasite population genetics: a cross-sectional comparison of *Bulinus globosus* and *Schistosoma haematobium*. *Parasitology* **119**, 295-302.

Day, K. P., Koella, J.C., Nee, S., Gupta, S., Read, A.F. (1992) Population genetics and dynamics of *Plasmodium falciparum*: an ecological view. *Parasitology* **104**, S35-S52.

De Roode, J.C., Helinski, M.E., Anwar, M.A., Read, A.F. (2005) Dynamics of multiple infection and within-host competition in genetically diverse malaria infections. *Am. Nat.* **166**, 531-542.

De Roode, J.C., Culleton, R., Cheeseman, S.J., Carter, R., Read, A.F. (2004) Host heterogeneity is a determinant of competitive exclusions or coexistence in genetically diverse malaria infections. *Proc. R. Soc. Lond. B* **271**, 1073-1080.

Diffley, P., Scott, J.O., Mama, K., Tsen, T.N.R. (1987) The rate of proliferation among African trypanosomes is a stable trait that is directly related to virulence. *Am. J. Trop. Med. Hyg.* **36**, 533-540.

Doolittle, W.F. (1999) Phylogenetic classification and the universal tree. *Science* **284**, 2124-2128.

Dwyer, G. (1991) The roles of density, stage and patchiness in the transmission of an insect virus. *Ecology* **12**, 559-574.

Dwyer, G., Elkington, J.S. (1993) Using simple models to predict virus epizootics in gypsy moth populations. *J. Anim. Ecol.* **62**, 1-11.

Dwyer, G., Elkington, J.S., Buonaccorsi, J.P. (1997) Host heterogeneity in susceptibility and disease dynamics: tests of a mathematical model. *Am. Nat.* **150**, 685-707.

Dwyer, G., Elkington, J.S., Levin, S.A. (2000) Pathogen driven outbreaks in forest defoliators revisited: building models from experimental data. *Am Nat.* **156**, 105-120.

Ebert, D. (1994) Virulence and local adaptation of a horizontally transmitted parasite. *Science* **265**, 1084-1086.

Ebert, D., Herre, E.A. (1996) The evolution of parasitic diseases. *Parasitology Today* **12**, 96-100.

Ebert, D., Mangin, K.L. (1997) The influence of host demography on the evolution of virulence of a microsporidian gut parasite. *Evolution* **51**, 1828-1837.

Ebert, D., Weisser, W.W. (1997) Optimal killing for obligate killers: the evolution of life histories and virulence of semelparous parasites. *Proc R. Soc. Lond. B* **264**, 985-991.

Ebert, D., Zschokke-Rohringer, C.D., Carius, H.J. (2000) Dose effects and density dependent regulation of two microparasites of *Daphnia magna*. *Oecologia* **122**, 200-209.

Ebling, P.M., Kaupp, W.J. (1995) Differentiation and comparative activity of six isolates of a nuclear polyhedrosis virus from the forest tent caterpillar, *Malacoma disstria*, Hubner. *J. Invertebr. Pathol.* **66**, 198-200.

Eldridge, R, O'Reilly, D.R, Hammock, B.D. Milller, L.K. (1992) Insecticidal properties of genetically engineered baculoviruses expressing an insect juvenile hormone esterase gene. *Appl. Environ. Microbiol.* **58**, 583-585.

Engelhard, E.K., Kam-Morgan, L.N., Washburn, J.O. and Volkman, L.E. (1994) The insect tracheal system: A conduit for the systemic spread of *Autographa californica* M nuclear polyhedrosis virus. *Proc. Natl. Acad. Sci. USA* **91**, 3324-3227.

Evans, H.F. (1986) Ecology and Epizootiology of baculoviruses, in: *The biology of baculoviruses* (R.R. Granados and B.A. Federici, eds). Vol 2, pp 89-132, CRC Press Boca Raton, FL.

Ewald, P.W. (1994) The evolutionary ecology of virulence. *Q. Rev. Biol.* **69**, 381-384.

Ewald, P.W. (1995) The evolution of virulence- a unifying link between parasitology and ecology. *J. Parasitol.* **81**, 659-669.

Fairbairn, D.J., Reeve, J.P. (2001) Natural selection In: *Evolutionary Ecology: concepts and case studies* Eds. C.W. Fox, D.A. Roff and D.J. Fairbairn. Oxford University Press.

Faktor, O., Toister-Archituv, M., Kamensky, B. (1995) Identification and nucleotide sequence of an ecdysteroid UDP-glucosyltransferase gene of *Spodoptera littoralis* multi-capsid nuclear polyhedrosis virus. *Virus Gene* **11**, 47-52.

Fenner, F., Radcliffe, F. (1965) Myxomatosis. Cambridge University Press.

Fenton, A., Fairbairn, J.P., Norman, R., Hudson, P.J. (2002) Parasite transmission: reconciling theory and reality. *J. Anim. Ecol.* **71**, 893-905.

Flipsen, J.T.M., Martens, J.W.M., Vanoers, M.M., Vlak, J.M., Vanlent, J.W.M. (1995) Passage of *Autographa californica* nuclear polyhedrosis virus through the midgut epithelium of *Spodoptera exigua* larvae. *Virology* **208**, 328-335.

Francki, R.I.B., Faquet, C.M., Kawaoka, Y., Donatelli, I., Guo, Y., Webster, R.G. (1991) Classification and nomenclature of viruses: 5th report of the International Committee on the Taxonomy of Viruses *Arch. Virol.* **2**, 117-123.

Frank, S.A. (1996) Models of parasite virulence. *Q. Rev. Biol.* **71**, 37-78.

Fraser, M.J., Cary, L., Boonvisudhi, K., Wang, H-G.H. (1995) Assay for movement of lepidopteran transposon IFP2 in insect cells using a baculovirus genome as a target DNA. *Virology* **211**, 397-407.

Friesen, P.D., Nissen, M.S. (1990) Gene organisation and transcription of TED, a lepidopteran retrotransposon integrated within the baculovirus genome. *Mol. Cell. Biol.* **10**, 3067-3077.

Futuyama, D.J. (1998) Evolutionary biology. 3rd ed. Sinauer, Sunderland, Mass.

Fuxa, J.R. (2004) Ecology of insect nucleopolyhedroviruses. *Agric. Ecosys. Environ.* **103**, 27-43.

Fuxa, J.R., Gaegham, J.P. (1983) Multiple-regression analysis of factors affecting prevalence of nuclear polyhedrosis virus in *Spodoptera frugiperda* (Lepidoptera: Noctuidae) populations. *Environ. Entomol.* **12**, 311-316.

Fuxa, J.R., Richter, A.R. (2001) Quantification of soil-to-plant transport of recombinant nucleopolyhedrovirus: effects of soil type and moisture, air currents and precipitation. *Appl. Environ. Microbiol.* **67**, 5166-5170.

Ganusov, V.V. (2003) Evolution of virulence: adaptive or not? *Trends Microb.* **3**, 112-113.

Gelernter, W.D., Federici, B.A. (1990) Virus epizootics in Californian populations of *Spodoptera exigua*: dominance of a single viral genotype. *Biochem. Syst. Ecol.* **18**, 461-466.

Gettig, R.R., McCarthy, W.J. (1982) Genotypic variation among wild isolates of *Heliothis* spp nuclear polyhedrosis viruses from different geographical regions. *Virology* **117**, 245-252.

Godfray, H.C., O'Reilly, D.R., Briggs, C.J. (1997) A model of nucleopolyhedrovirus (NPV) population genetics applied to co-occlusion and the spread of the few polyhedra (FP) phenotype. *Proc. R. Soc. Lond. B.* **264**, 315-322.

Goulson, D. (1997) Wipfelkrankheit: modification of host behaviour during baculovirus infection. *Oecologia* **109**, 219-228.

- Goulson, D., Hails, R.S., Williams, T., Hirst, M.L., Vasconcelos, S.D., Green, B.M., Carty, T.M., Cory, J.S.** (1995) Transmission dynamics of a virus in a stage-structured insect population. *Ecology* **76**, 392-401.
- Gower, C.M., Webster, J.P.** (2005) Intra-specific competition and the evolution of virulence in a parasitic trematode. *Evolution* **59**, 544-553.
- Graham, R.I., Tyne, W.I., Possee, R.D., Sait, S.M., Hails, R.S.** (2004) Genetically variable nucleopolyhedroviruses isolated from spatially separate populations of the winter moth *Operophtera brumata* (Lepidoptera: Geometridae) in Orkney. *J. Invertebr. Pathol.* **87**, 29-38.
- Granados, R.R., Federici, B.A.** (1986) The biology of Baculoviruses Vol 2, CRC Press Boca Raton, FL.
- Granados, R.R., Williams, K.A.** (1986) *In vivo* infection and replication of baculoviruses. In: *The Biology of Baculoviruses* (Granados, R.R. and Federici, B.A., eds.) pp 89-107. Volume 1 CRC Press, Inc., Boca Raton, Florida.
- Griffiths, C. M., Barnett, A.L., Ayres, M.D., Windass, J., King, L.A., Possee, R.D.** (1999) *In vitro* host range of *Autographa californica* nucleopolyhedrovirus recombinants lacking functional *p35*, *iap1* and *iap2*. *J. Gen. Virol.* **8**, 1055-1066.
- Guarino, L.A., Xu, B., Jin., Dong, W.** (1998) A virus encoded RNA polymerase purified from baculovirus-infected cells. *J. Virol* **72**, 7985-7991.
- Gunn, A.** (1998) The determination of larval phase coloration in the thermoregulation and protection from u.v. light. *Entomol. Exp. Appl.* **86**, 125-133.

Gupta, S., Anderson, R.M. (1999) Population structure of pathogens: the role of immune selection. *Parasitol. Today* **15**, 497-501.

Haggis, M.J. (1986) Distribution of the African armyworm, *Spodoptera exempta* (Walk.) (Lepidoptera: Noctuidae), and the frequency of larval outbreaks in Africa and Arabia. *Bull. Entomol. Res.* **76**, 151-170.

Hails, R.S., Hernandez-Crespo, P., Sait, S.M., Donnelly, C.A., Green, B.M., Cory, J.S. (2002) Transmission patterns of natural and recombinant baculoviruses. *Ecology* **83**, 906-916.

Hajos, J.P., Pijnenburg, J., Usmany, M., Zuidema, D., Zavodsky, P., Vlak, J.M. (2000) High frequency recombination between homologous baculoviruses in cell culture. *Arch. Virol.* **145**, 159-164.

Ham, J.J., Styer, E.L. (1985) Comparative pathology of isolates of *Spodoptera frugiperda* nuclear polyhedrosis virus in *S. frugiperda* and *S. exigua*. *J. Gen. Virol.* **66**, 1249-1262.

Hamm, J.J., Young, J.R. (1974) Mode of transmission of nuclear polyhedrosis virus to progeny of adult *Heliothis zea*. *J. Invertebr. Pathol.* **24**, 70-81.

Harrap, K.A. 1972 The structure of nuclear polyhedrosis viruses I The inclusion body. *Virology* **50**, 114-123.

Hatfield, P.R., Entwistle, P.F. (1988) Biological and biochemical comparison of nuclear polyhedrosis virus isolates pathogenic for the oriental armyworm, *Mythimna separata* (Lepidoptera: Noctuidae). *J. Invertebr. Pathol.* **52**, 168-176.

Hawtin, R. E., Arnold, K., Ayres, M.D., Zanutto, P.M.D.A., Howard, S.C. Gooday, G.W., Chappell, L.H., Kitts, P.A., King, L.A. Possee, P.D. (1995) Identification and

preliminary characterisation of a chitinase gene in the *Autographa californica* nuclear polyhedrosis virus genome. *Virology* **212**, 673-675.

Hayakawa, T., Rohrmann, G.F., Hashimoto, Y. (2000) Patterns of genome organisation and content in Lepidoptera baculoviruses. *Virology* **278**, 1-12.

Hernandez-Crespo, P., Sait, S.M., Hails, R.S., Cory, J.S. (2001) Behaviour of a recombinant baculovirus in Lepidopteran hosts with different susceptibilities. *Appl. Environ. Microbiol.* **67**, 1140-1146.

Herniou. E.A., Olszewski, J.A., Cory, J.S., O'Reilly, D.A. (2003) The genome sequence and evolution of baculoviruses. *Ann. Rev. Entomol.* **48**, 211-234.

Herniou. E.A., Olszewski, J.A., O'Reilly, D.A., Cory, J.S. (2004) Ancient coevolution of baculoviruses and their insect hosts. *J. Virol.* **78**, 3244-3251.

Herniou. E.A., Luque, T., Chen, X., Vlak, J.M., Winstanley, D., Cory, J.S., O'Reilly, D.R. (2001) Use of whole genome sequence data to infer baculovirus phylogeny. *J. Virol.* **75**, 8117-8126.

Herre, E.A. (1993) Population structure and the evolution of virulence in nematode parasites of fig wasps. *Science* **259**, 1442-1445.

Hitchman, R.B. (2002) Pathogen variability and dynamics in insect populations. PhD Thesis. Oxford Brookes University.

Hochberg, M. (1991) Non-linear transmission rates and the dynamics of infectious disease. *J. Theor. Biol.* **153**, 301-321.

Hodgson, D.J., Vanbergen, A.J., Watt, A.D., Hails, R.S., Cory, J.S. (2001) Phenotypic variation between naturally co-existing genotypes of a Lepidopteran baculovirus. *Evol. Ecol. Res.* **3**, 687-701.

Hodgson, D.J., Hitchman, R.B., Vanbergen, A.J., Hails, S.E., Possee, R.D., Cory, J.S. (2004) Host ecology determines the relative fitness of virus genotypes in mixed-genotype nucleopolyhedrovirus infections. *J. Evol. Biol.* **17**, 1018-1025.

Hodgson, D.J., Hitchman, R.B., Vanbergen, A.J., Hails, R.S., Hartley, S.E., Possee, R.D., Watt, A.D., Cory, J.S. (2001) The existence and persistence of genotypic variation in nucleopolyhedrovirus populations. In: *Genes in the Environment* (eds. R.S. Hails, J.E. Beringer, H.C.J. Godfray) pp. 258-280. Blackwell Publishing, Oxford, UK.

Holmes, E.C., Worobey, M., Rambaut, A. (1999) Phylogenetic evidence for recombination in denuge virus. *Mol. Biol. Evol.* **16**, 405-409.

Holmes, E.C., Zhang, L.Q., Simmonds, P., Ludlam, C.A., Leigh-Brown, A.J. (1992) Convergent and divergent sequence evolution in the surface envelope glycoprotein of HIV-1 within a single patient. *Proc. Natn. Acad. Sci. U.S.A.* **89**, 4835-4839.

Hom, L.G., Volkman, L.E. (2000) *Autographa californica* M nucleopolyhedrovirus chiA is required for processing of V-CATH. *Virology* **277**, 178-183.

Hom, L.G., Ohkawa, T., Trudeau, D., Volkman, L.E. (2002) *Autographa californica* M nucleopolyhedrovirus ProV-CATH is activated during serial cell death. *Virology* **296**, 212-218.

Hood, M.E. (2003) Dynamics of multiple infection and within-host competition by the anther-smut pathogen. *Am. Nat.* **162**, 122-133.

Houle, D. (1991) Genetic covariance of fitness correlates: what genetic correlations are made of and why it matters. *Evolution* **43**, 1767-1780.

Hughes, P.R., Gettig, R.R., McCarthy, W.J. (1983) Comparison of the time-mortality response of *Heliothis zea* to 14 isolates of *Heliothis* nuclear polyhedrosis virus. *J. Invertebr. Pathol.* **41**, 256-261.

Hughes, D.S., Possee, R.D., King, L.A. (1993) Activation and detection of latent baculovirus resembling *Mamestra brassicae* nuclear polyhedrosis virus in *M. brassicae* insects. *Virology* **194**, 608-615.

Hughes, D.S., Possee, R.D., King, L.A. (1997) Evidence for the presence of a low-level persistent baculovirus infection of *Mamestra brassicae* insects. *J. Gen. Virol.* **78**, 1801-1805.

Hunter-Fujita, F., Entwistle, P., Evans, H., Crook, N. (1998) *Insect viruses and Pest Management*. John Wiley & Sons, Chichester, UK.

Ignoffo, C.M., Rice, W.C., McIntosh, A.H. (1989) Inactivation of nonoccluded and occluded baculoviruses and baculovirus-DNA exposed to simulated sunlight. *Environ. Entomol.* **18**, 177-183.

Ijkel, W.F.J., van Strein, E.A., Heldens, J.G.M., Broer, R., Zuidema, D., Goldbach, R.W., Vlak, J.M. (1999) Sequence and organisation of the *S. exigua* multi-capsid nucleopolyhedrovirus genome. *J. Gen. Virol.* **80**, 3289-3304.

Imhoof, B., Schmid-Hempel, P. (1998) Single-clone and mixed-clone infections versus host environment in *Crithidia bombi* infecting bumblebees. *Parasitology* **117**, 331-336.

James, J.W. (1974) Genetic covariances under the partition of resources model. *Aust. J. Biol. Sci.* **27**, 99-101.

Jaques, R.P. (1967) The persistence of a nuclear polyhedrosis virus in the habitat of the host insect, *Trichoplusia ni*. I. Polyhedra deposited on foliage. *Can. Entomol.* **99**, 785-794.

Jehle, J.A., Nickel, A., Vla, J.M., Backhaus, H. (1998) Horizontal escape of the novel Tc1-like lepidopteran transposon TCp3.2 into *Cydia pomonella* granulovirus *J. Mol. Evol.* **46**, 215-224.

Kang, W., Tristem, M., Maeda, S., Crook, N.E., O'Reilly, D.R. (1998) Identification and characterisation of the *Cydia pomonella* granulovirus *cathepsin* and *chitinase* genes. *J. Gen. Virol.* **79**, 2283-2292.

Kikhno, I., Gutierrez, S., Croizier, L., Croizier, G., Lopez-Ferber, M. (2002) Characterisation of *pif*, a gene required for the *per os* infectivity of *Spodoptera littoralis* nucleopolyhedrovirus. *J. Gen. Virol.* **83**, 3013-3022.

King, L.A., Possee, R.D. (1992) *The baculovirus expression system: A laboratory guide*. Chapman & Hall, London.

Kislev, N. (1985) DNA homology relationships between *Spodoptera littoralis* nuclear polyhedrosis virus and other baculoviruses. *Intervirology* **24**, 50-57.

Knell, J.D. Summers, M.D. (1981) Investigation of genetic heterogeneity in wild isolates of *Spodoptera frugiperda* nuclear polyhedrosis virus by restriction endonuclease analysis of plaque-purified variants. *Virology* **112**, 190-197.

- Knell, J.D., Begon, M., Thompson, D.J.** (1998) Transmission of *Plodia interpunctella* granulosis virus does not conform to mass action model. *J. Anim. Ecol.* **67**, 592-599.
- Knell, J.D., Summers, M.D., Smith, G.E.** (1983) Serological analysis of 17 baculoviruses from subgroups A and B using protein blot immunoassay. *Virology* **125**, 281-392.
- Kondo, A., Maeda, S.** (1991) Host range expansion by recombination of the baculoviruses *Bombyx mori* nuclear polyhedrosis virus and *Autographa californica* nuclear polyhedrosis virus. *J. Gen. Virol.* **79**, 2283-2292.
- Kukan, B.** (1999) Vertical transmission of nucleopolyhedrovirus in insects. *J. Invertebr. Pathol.* **74**, 103-111.
- Kumar, S., Tamura, K., Jakobsen, I.B., Nei, M.** (2001) MEGA2: an evolutionary genetics analysis software. *Bioinformatics* **17**, 1244-1245.
- Kunimi, Y., Fuxa, J.R., Hammock, B.D.** (1996) Comparison of wild type and genetically engineered nuclear polyhedrosis viruses of *Autographa californica* for mortality, virus replication and polyhedra production in *Trichoplusia ni* larvae. *Entomol. Exp. Appl.* **81**, 251-257.
- Kuzio, J. Pearson, M.N., Harwood, S.H., Funk, C.J., Evans, J.T., Slavicek, J., Rohrmann, G.F.** (1999) Sequence and analysis of the genome of a baculovirus pathogenic for *Lymantria dispar*. *Virology* **253**, 17-34.
- Laitinen, A.M., Otvos, I.S., Levin, D.B.** (1996) Genotypic variation among wild isolates of Douglas-Fir Tussock moth (Lepidoptera:Lymantriidae) nuclear polyhedrosis virus. *J. Econ. Entomol.* **89**, 640-647.

Lee, H.H., Miller, L.K. (1978) Isolation of genotypic variants of *Autographa californica* nuclear polyhedrosis virus. *J. Virol.* **27**, 754-767.

Lenski, R.E., May, R.M. (1994) The evolution of virulence in parasites and pathogens: Reconciliation between two competing hypotheses. *J. Theor. Biol.* **169**, 253-265.

Levin, B.R., Bull, J.J. (1994) Short-sighted evolution and the virulence of pathogenic micro-organisms. *Trends in Microbiol.* **2**, 76-81.

Levin, S.A., Pimental, D. (1981) Selection for intermediate rates of increase in a parasite-host system. *Am. Nat.* **117**, 308-315.

Li, Q., Donly, C., Li, L., Willis, L.G., Theilmann, D.A., Erlandson, M. (2002) Sequence and organisation of the *Mamestra configurata* nucleopolyderovirus genome. *Virology* **294**, 106-121.

Lipsitch, M., Moxon, E.R. (1997) Virulence and transmissibility of pathogens: what is the relationship? *Trends in Microbiol.* **5**, 31-37.

Little, T.J., Ebert, D. (2000) The cause of parasitic infection in natural populations of *Daphnia* (Crustacea: Cladocera): the role of host genetics. *Proc. R. Soc. Lond. B* **267**, 2037-2042.

Liu, W., Levin, S.A., Iwasa, Y. (1986) Influence on nonlinear incidence rates upon the behaviour of SIRS epidemiological models. *J. Math. Biol.* **23**, 187-204.

Lopez-Ferber, M., Argaud, O., Crozier, L., Crozier, G. (2001) Diversity, distribution and mobility of *bro* gene sequences in *Bombyx mori* nucleopolyhedrovirus. *Virus Genes* **22**, 247-254.

Lord, C.C., Woolhouse, M.E.J., Barnard, B, J.H. (1997) Transmission and distribution of virus serotypes: African horse sickness in zebra. *Epidemiol. Infect.* **118**, 43-50.

Lu, A., Miller, L.K. (1997) Regulation of baculoviruses late and very late gene expression. In: *The Baculoviruses*, pp. 193-216. Edited by L.K. Miller. New York: Plenum.

Lynn, D.E., Shapiro, M., Dougherty, E.M. (1993) Selection and screening of clonal isolates of the Abington strain of Gypsy moth nuclear polyhedrosis virus. *J. Invertebr. Pathol.* **62**, 191-195.

Mackinnon, M.J., Read, A.F. (1999a) Genetic relationships between parasite virulence and transmission in the rodent malaria *Plasmodium chabaudi*. *Evolution* **53**, 689-703.

Mackinnon, M.J., Read, A.F. (1999b) Selection for high and low virulence in the malaria parasite *Plasmodium chabaudi*. *Proc. Biol. Sci.* **266**, 741-748.

Maeda, S., Mukohara, Y., Kondo, A. (1990) Characteristically distinct isolates of the nuclear polyhedrosis virus from *Spodoptera littura*. *J. Gen. Virol.* **71**, 2631-2639.

Maruniak, J.E., Brown, S.E., Knudson, D.L. (1984) Physical maps of *Sf*MNPV baculovirus DNA and its genomic variants. *Virology* **136**, 221-234.

Matthews, R.E.F. (1992) Classification and nomenclature of viruses. *Interviol.* **17**, 1-199.

May, R.M., Anderson, R.M. (1983) Parasite-host co-evolution. In: *Coevolution* (Futuyma, D.J. & Slatkin, M. eds.), pp. 186-206. Sunderland, MA: Sinauer Associates.

May, R.M., Novak, M.A. (1995) Coinfection and the evolution of parasite virulence. *Proc. R. Soc. Lond. B* **261**, 209-215.

McGeoch, D.J., Dolan, A., Ralph, A.C. (2000) Toward a comprehensive phylogeny for mammalian and avian herpesviruses. *J. Virol.* **74**, 10401-10406.

Merrett, P.J. (1986) Evidence of persistent populations of the African armyworm, *Spodoptera exempta* (Walker) (Lepidoptera: Noctuidae), in Tanzania. *Bull. Entomol. Res.* **76**, 545-552.

Messenger, S.L., Molineux, I.J. & Bull, J.J. (1999) Virulence evolution in a virus obeys a trade-off. *Proc. R. Soc. Lond. B.* **266**, 397-404.

Miller, L.K., ed. (1997) *The Baculoviridae*. New York: Plenum.

Mitchell, A., Mitter, C., Regier, J.C. (2000) More taxa or more characters revisited: combining data from nuclear protein-encoding genes for phylogenetic analyses of Noctuoidea (Insect: Lepidoptera). *Syst. Biol.* **49**, 202-224.

Monsma, S.A., Oomens, A.G.P., Blissard, G.W. (1996) The GP64 envelope fusion protein is an essential baculovirus protein required for cell-to-cell transmission of infection. *J. Virol.* **70**, 4607-4616.

Munoz, D, Caballero, P. (2000) Persistence and effects of parasitic genotypes in a mixed population of the *Spodoptera exigua* nucleopolyhedrovirus. *Biol. Control* **19**, 259-264.

Munoz, D, Castillejo, J.I., Caballero, P. (1998) Naturally occurring deletion mutants are parasitic genotypes in a wild-type nucleopolyhedrovirus population of *Spodoptera exigua*. *Appl. Environ. Microbiol.* **64**, 4372-4377.

Munoz, D., Murillo, R., Krell, P.J., Vlak, J.M., Caballero, P. (1999) Four genotypic variants of a *Spodoptera exigua* nucleopolyhedrovirus (Se-SP2) are distinguishable by a hypervariable genomic region. *Virus Res.* **59**, 61-74.

Murphy, F.A., Fauquet, C.M., Bishop, D.H.L., Ghabrial, S.A., Jarvis, A.W., Martelli, G.P., Mayo, M.A., Summers, M.D. (1995) *Virus Taxonomy Sixth Report of the International Committee on Taxonomy of Viruses*. New York, Springer-Verlag.

Myers, J.H., Malakar, R., Cory, J.S. (2000) Sub-lethal nucleopolyhedrovirus infection effects on pupal weight, egg mass and vertical transmission in gypsy moth (Lepidoptera: Lymantriidae). *Environ. Entomol.* **29**, 1268-1272.

Nakamura, T., Konishi, T., Kawaguchi, H., Imose, J. (1992) Estimation of the relative fecundity in *Eimeria tenella* strains by a mixed infection method. *Parasitology* **104**, 11-17.

Nielson, C., Cooper, D., Short, S.M., Myers, J.H., Shuttle, C.A. (2002) DNA polymerase gene sequences indicate western and forest tent caterpillar viruses form a new taxonomic group within baculoviruses. *J. Invertebr. Pathol.* **81**, 131-147.

Nikaido, M., Kawai, K., Cao, Y., Harada, M., Tomita, S. (2001) Maximum likelihood analysis of the complete mitochondrial genomes of eutherians and a re-evaluation of the phylogeny of bats and insectivores. *J. Mol. Evol.* **53**, 508-516.

Nowak, M.A., May R.M. (1994) Superinfection and the evolution of parasite virulence. *Proc. R. Soc. Lond. B.* **255**, 81-89.

O'Reilly, D.R. (1995) Baculovirus encoded ecdysteroid UDP-glucosyltransferases. *Insect Biochem. Mol. Biol.* **25**, 541-545.

O'Reilly, D.R., Miller, L.K. (1989) A baculovirus blocks insect molting by producing ecdysteroid UDP-glucosyltransferase. *Science* **245**, 1110-1114.

O'Reilly, D.R., Miller, L.K. (1991) Improvement of a baculovirus pesticide by deletion of the *egt* gene. *Bio/Technology* **9**, 1086-1090.

Odindo, M.O. (1981) Dosage-mortality and time-mortality responses of the armyworm, *Spodoptera exempta* to a nuclear polyhedrosis virus. *J. Invertebr. Pathol.* **38**, 251-255.

Odindo, M.O. (1983) Epizootiological observations on a nuclear polyhedrovirus of the African armyworm, *Spodoptera exempta*. *Insect Sci. Appl.* **4**, 291-298.

Odiyo, P.O. (1981) Development of the first outbreaks of the African armyworm, *Spodoptera exempta* (Walk.), between Kenya and Tanzania during the "off-season" months of July to December. *Insect Sci. Appl.* **1**, 305-318.

Odiyo, P.O. (1984) A guide to seasonal changes in the distribution of armyworm infestations in East Africa *Insect Sci. Appl.* **5**, 107-119.

Palmieri, J.R. (1982) Be fair to parasites. *Nature, Lond.* **298**, 220.

Pang, Y., Yu, J., Wang, L., Hu, X., Bao, W., Li, G., Chen, C., Han, H., Hu, S. (2001) Sequence analysis of *S. littura* multicapsid nucleopolyhedrovirus genome. *Virology* **287**, 391-404.

Parnell, M., Grzwacz, D., Jones, K.A., Brown, M., Odour, G., Ong'aro, J. (2002) The strain variation and virulence of granulovirus of diamondback moth (*Plutella xylostella* Linnaeus, Lep., Yponomeutidae) isolated in Kenya. *J. Invertebr. Pathol.* **79**, 192-196.

Passarelli, A.L., Todd, J.W., Miller, L.K. (1994) A baculovirus gene involved in late gene expression predicts a large polypeptide with a conserved motif of RNA polymerases. *J. Virol.* **68**, 4673-4678.

Paul, R.E.L., Brockman, A., Price, R.N., Luxemburger, C., White, N.J., Looareesuwan, S., Nosten, F., Day, K.P. (1999) Genetic analysis of *Plasmodium falciparum* infections of the north-western border of Thailand. *Trans. R. Soc. Trop. Med. Hyg.* **93**, 587-593.

Payne, C.C. (1982) Insect viruses as control agents. *Parasitology* **84**, 35-77.

Pedgley, D.E., Page, W.W., Mushi, A., Odiyo, P., Amisi, J., Dewhurst, C.F., Dunstan, W.R., Fishpool, L.D.C., Harvey, A.W., Megenasa, T., Rose, D.J.W. (1989) Onset and spread of an African armyworm upsurge. *Ecol. Entomol.* **14**, 311-333.

Penner, M.P., Yerushalmi, I (1998) The physiology of locust phase polymorphism: an update. *J. Insect Physiol.* **44**, 365-377.

Pijlman, G.P., van den Born, E., Martens, D.E., Vlak, J.M. (2001) *Autographa californica* baculoviruses with large genomic deletions are rapidly generated in infected insect cells. *Virology* **283**, 132-138.

Read, A.F. (1994) The evolution of virulence. *Trends in Microbiol.* **2**, 73-76.

Read, A.F., Taylor, L.H. (2001) The ecology of genetically diverse infections. *Science* **292**, 1099-1102.

Reed, D.H., Bryant, E.H. (2004) Phenotypic correlations among fitness and its components in a population of the housefly. *J. Evol. Biol.* **17**, 919-923.

Reeson, A.F., Wilson, K., Gunn, A., Hails, R.S., Goulson, D. (1998) Baculovirus resistance in the Noctuid *Spodoptera exempta* is phenotypically plastic and responds to population density. *Proc. R. Soc. Lond. B* **265**, 1787-1791.

Reeson, A.F., Wilson, K., Cory, J.S., Hankard, P., Weeks, J.M., Goulson, D., Hails, R.S. (2000) Effects of phenotypic plasticity on pathogen transmission in the field in a Lepidopteran-NPV system *Oecologia* **124**, 373-380.

Regoes, R.R., Ebert, D., Bonhoeffer, S. (2001) Dose-dependent infection rates of parasites produce the Allee effect in epidemiology. *Proc. R. Soc. Lond. B* **269**, 271-279.

Ribeiro, H.C.T., Pavan, O.H.O., Muotri, A.R., (1997) Comparative susceptibility of two different hosts to genotypic variants of the *Anticarsia gemmatalis* nuclear polyhedrosis virus. *Entomol. Exp. Appl.* **83**, 233-237.

Richards, A., Speight, M., Cory, J. (1999) Characterisation of a nucleopolyhedrovirus from the vapourer moth, *Orgyia antiqua* (Lepidoptera: Lymantridae). *J. Invertebr. Pathol.* **74**, 137-142.

Riska, B. (1986) Some models for development, growth and morphometric correlation. *Evolution* **40**, 1303-1311.

Roff, D.A. (2002) *Life History Evolution*. Sinauer Associates, Sunderland, MA, USA.

Rose, D.J.W., Dewhurst, C.F., Page, W.W. (2000) *The African Armyworm Handbook: The status, biology, ecology, epidemiology and management of Spodoptera exempta* (Lepidoptera: Noctuidae). Second Edition Chatham, UK: Natural Resources Institute.

Rose, D.J.W., Page, W.W., Dewhurst, C.F., Riley, J.R., Reynolds, D.R., Pedgley E.D., Tucker, M.R. (1985) Downwind migration of the African armyworm moth,

Spodoptera exempta, studied by mark- and-capture and by radar. *Ecol. Entomol.* **10**, 299-313.

Rothman, L.D and Myers, J.H. (1996) Debilitating effects of viral diseases on host Lepidoptera. *J. Invertebr. Pathol.* **67**, 1-10.

Samuels, R.I, Patterson, I.C. (1995) Cuticle degrading proteases from insect moulting fluid and culture filtrates of entomopathogenic fungi. *Comp. Biochem. Physiol.* **110B**, 661-665.

Scheritz-Ponten, T., Andersson, S.G.E. (2001) Phylogenetic approach to microbial evolution. *Nucleic acids Res.* **29**, 545-552.

Schmid-Hempel, P., Pühr, K., Krüger, N., Reber, C., Schmid-Hempel, R. (1999) Dynamic and genetic consequences of variation in horizontal transmission for a microparasitic infection. *Evolution* **53**, 426-434.

Shapiro, D.I., Fuxa, J.R., Braymer, H.D., Pashley, D.P. (1991) DNA restriction polymorphism in wild isolates of *Spodoptera frugiperda* nuclear polyhedrosis virus. *J. Invertebr. Pathol.* **58**, 96-105.

Shapiro-Ilan, D.I., Fuxa, J.R., Lacey, L.A., Onstad, D.W., Kaya, H.K. (2005) Definitions of pathogenicity and virulence in invertebrate pathology. *J. Invertebr. Pathol.* **88**, 1-7.

Simon, O., Williams, T., Lopez-Ferber, M., Calablero, P. (2004) Genetic structure of a *Spodoptera frugiperda* nucleopolyhedrovirus population: High prevalence of deletion genotypes. *Appl. Environ. Micro.* **70**, 5579-5588.

Simon, O., Williams, T., Lopez-Ferber, M., Calablero, P. (2005) Functional importance of deletion mutant genotypes in an insect nucleopolyhedrovirus population. *Appl. Environ. Microbiol.* **71**, 4254-4262.

Sinervo, B., Doughty, P., Huey, R.B., Zamudio, K. (1992) Allometric engineering: a casual analysis of natural selection on offspring size. *Science* **258**, 1927-1930.

Slack, J.M., Kuzio, J., Faulkner, P. (1995) Characterisation of *v-cath*, a cathepsin L-like proteinase expressed by the baculovirus *Autographa californica* multiple nuclear polyhedrosis virus. *J. Gen Virol.* **76**, 1091-1095.

Smith, C.N. (1966) *Insect colonisation and mass production*. Academic Press, London.

Smith, H.G., Kallander, H., Nilsson, J.-A. (1989) The trade-off between offspring number and quality in the great tit *Parus major*. *J. Anim. Ecol.* **58**, 383-402.

Smith, I.R., Crook, N.E. (1988) Short Communications: *In vivo* isolation of baculovirus genotypes. *Virology* **166**, 240-244.

Smith, T., Felger, I., Tanner, M., Beck, H.-P. (1999) Premunition in *Plasmodium falciparum* infection: insights from the epidemiology of multiple infections. *Trans. R. Soc. Trop. Med. Hyg.* **93**, S59-S64.

Snounou, G., Bourne, T., Jarra, W., Virriyakosol, S., Wood, J.C., Brown, K.N. (1992) Assessment of parasite population dynamics in mixed infections of rodent plasmodia. *Parasitology* **105**, 363-374.

Stearns, S.C. (1992) *The Evolution of Life Histories*. Oxford University Press, Oxford.

Stiles, B., Himmerich, S. (1998) *Autographa californica* NPV isolates: restriction endonuclease analysis and comparative biological activity. *J. Invertebr. Pathol.* **72**, 174-177.

Swaine, G. (1966) Generation to generation passage of the nuclear polyhedral virus of *Spodoptera exempta* Wlk. *Nature, London*, **210**, 1053-1054.

Takatsuka, J., Okuno, S., Nakai, M., Kunimi, Y. (2003) Genetic and biological comparison of ten geographic isolates of a nucleopolyhedrovirus that infects *Spodoptera litura* (Lepidoptera: Noctuidae). *Biol. Control* **26**, 32-39.

Taylor, L.H., Mackinnon, M.J., Read, A.F. (1998) Virulence of mixed clone and single clone infections of the rodent malaria, *Plasmodium chabaudi*. *Evolution* **52**, 583-591.

Taylor, L.H., Walliker, D., Read, A.F. (1997) Mixed-genotype infections of malaria parasites: within-host dynamics and transmission success of competing clones. *Proc. R. Soc. Lond. B* **264**, 927-935.

Thomas, C.J., Gooday, G.W., King, L.A., Possee, R.D. (2000) Mutagenesis of the active site coding region of the *Autographa californica* nucleopolyhedrovirus *chiA* gene *J. Gen. Virol.* **81**, 1403-1411.

Thompson, C.G., Scott, D.W., Wickman, B.E. (1981) Long-term persistence of the nuclear polyhedrosis virus of the Douglas-fir tussock moth, *Orgyia pseudotugata* (Lepidoptera: Lymantriidae), in forest soil. *Environ. Entomol.* **10**, 254-255.

Thompson, J.D., Gibson, T.J., Plewniak, F., Jeanmougin, F., Higgins, D.G. (1997) The CLUSTAL_X windows interface: flexible strategies for multiple sequence alignment aided by quality analysis tools. *Nucleic acids Res.* **25**, 4876-4882.

Thompson, J.N., Cunningham, B.M. (2002) Geographic structure and dynamics of co-evolutionary selection. *Nature* **13**, 735-738.

Titterington, J.S., Nun, T. K., Passarelli, A.L. (2003) Functional dissection of the baculovirus *late expression factor-8* gene: sequence requirements for late gene promoter activation. *J. Gen. Virol.* **84**, 1817-1826.

Tradeau, D., Washburn, J.O., Volkman, L.E. (2001) Central role of haemocytes in *Autographa californica* M nucleopolyhedrovirus pathogenesis in *Heliothis virescens* and *Helicoverpa zea*. *J Virol.* **75**, 996-1003.

Tucker, M.R. (1993) Weather and epidemiology of the African armyworm (*Spodoptera exempta*). *NRI Bulletin*, No. 58 Chatham, UK: Natural resources Institute.

Turner, C.M.R., Aslam, N., Dye, C. (1995) Replication, differentiation, growth and the virulence of *Trypanosoma brucei* infections. *Parasitology* **111**, 289-300.

Turner, P.E., Chao, L. (1999) Prisoners' dilemma in an RNA virus. *Nature* **398**, 441-443.

Turner, P.E., Cooper, V.S., Lenski, R.E. (1998) Trade-off between horizontal and vertical modes of transmission in bacterial plasmids. *Evolution* **52**, 315-329.

Van Baalen, M., Sabelis, M.W. (1995) The dynamics of multiple infection and the evolution of virulence. *Am. Nat.* **146**, 881-910.

Van Beek, N.A.M., Wood, H., Hughes, P.R. (1988) Quantitative aspects of nuclear polyhedrosis virus infections in Lepidopterous larvae: The dose-survival relationship. *J. Invertebr. Pathol.* **51**, 58-63.

Vasconcelos, S.D. (1996) Alternative routes for the horizontal transmission of a nucleopolyhedrovirus. *J. Invertebr. Pathol.* **68**, 269-274.

Vasconcelos, S.D., Williams, T., Hails, R.S., Cory, J.S. (1996) Modified behaviour in baculovirus-infected lepidopteran larvae and its impact on the spatial distribution of inoculum. *Biol. Control* **7**, 299-306.

Vezina, A., Peterman, R. (1985) Tests of the role of nuclear polyhedrosis virus in the population dynamics of its host, Douglas-fir tussock moth, *Orgyia pseudotsugata* (Lepidoptera: Lymantriidae). *Oecologia* **67**, 260-266.

Vickers, J.M., Cory, J.S., Entwistle, P.F. (1991) DNA characterisation of eight geographic isolates of granulosis virus from the potato tuber moth (*Phthorimaea operculella*) (Lepidoptera, Gelechiidae). *J. Invertebr. Pathol.* **57**, 334-342.

Vlak, J.M., Smith, G.E. (1982) Orientation of the genome of the AcMNPV: a proposal. *J. Virol.* **41**, 1118-1121.

Volkman, L.E. (1997) Nucleopolyhedrosis interactions with their insect hosts. *Adv. Virus Res.* **48**, 313-348.

Volkman, L.E., Keddie, B.A. (1990) Nuclear polyhedrosis virus pathogenesis. *Semin. Virol.* **1**, 249-256.

Volkman, L.E., Blissard, G.W., Friesen, P., Keddie, B.A., Possee, R., Theilmann, D.A. (1995) Family Baculoviridae. In: *Virus Taxonomy: Sixth Report of the international Committee on Taxonomy of Viruses* (Murphy, F.A., Fauquet, C.M., Bishop, D.H.L., Ghabrial, S.A., Jarvis, A.W., Martelli, G.P., Mayo, M.A., Summers, M.D., eds.) pp 104-113. Springer-Verlag, Vienna and New York.

Wang, H.H., Fraser, M.J., Cary, L.C. (1989) Transposon mutagenesis of baculoviruses-analysis of Tfp3 lepidopteran transposon insertions at the fp locus of nuclear polyhedrosis. *Virus Genes* **81**, 97-108.

Washburn, J.O., Kirkpatrick, B.A., Volkman, L.E. (1995) Comparative pathogenesis of *Autographa californica* M nuclear polyhedrosis virus in larvae of *Trichoplusia ni* and *Heliothis virescens*. *Virology* **209**, 561-568.

Weeds, P.L., Beever, R.E., Long, P.G. (2000) Competition between aggressive and non-aggressive strains of *Botrytis cinerea* (*Botryotinia fuckeliana*) on French bean leaves. *Australas. Plant Pathol.* **29**, 200-204.

Weiss, R.A. (2002) Virulence and pathogenesis. *Trends Microbiol.* **10**, 314-317.

West, S.A., Buckling, A. (2003) Cooperation, virulence and siderophore production in bacterial parasites. *Proc. R. Soc. Lond. B* **270**, 37-44.

Willie, P., Boller, T., Kaltz, O. (2002) Mixed inoculation alters infection success of strains of the endophyte *Epichloe bromicola* on its grass host *Bromus erectus*. *Proc. R. Soc. Lond. B* **269**, 397-402.

Wilson, K.R., Reeson, A.F. (1998) Density-dependent prophylaxis:evidence from Lepidoptera-baculovirus interactions? *Ecol. Entomol.* **23**, 100-101.

Wilson, K.R., O'Reilly, D.R., Hails, R.S., Cory, J.S. (2000) Age-related effects of the *Autographa californica* multiple nucleopolyhedrovirus *egt* gene in the cabbage looper (*Trichoplusia ni*). *Biol. Control* **19**, 57-63.

Woolhouse, M.E.J., McNamara, J.J., Hargrove, J.W., Bealby, K.A. (1996) Distribution and abundance of trypanosome (subgenus *Nannonmonas*) infections of the tsetse fly *Glossina pallidipes* in Southern Africa. *Mol. Ecol.* **5**, 11-18.

Wright, S. (1978) *Evolution and the genetics of populations. Volume 4 Variability within among Natural populations.* Chicago Press, Chicago.

Zanotto, P.M.A., Kessing, B.D., Maruniak, J.E. (1993) Phylogenetic interrelationships among baculoviruses: evolutionary rates and host associations. *J. Invertebr. Pathol.* **62**, 147-164.